University of Southampton

Faculty of Medicine

Clinical and Experimental Sciences

Clinical Neuroscience

Haptoglobin as a Novel Treatment for Subarachnoid Haemorrhage

by

Matthew James Morton

Thesis for the degree of Doctor of Philosophy

September 2018

University of Southampton

Abstract

Faculty of Medicine

Clinical and Experimental Sciences, Clinical Neuroscience

Thesis for the degree of Doctor of Philosophy

Haptoglobin as a Novel Treatment for Subarachnoid Haemorrhage

Matthew James Morton

Subarachnoid haemorrhage (SAH) is a severe neurological condition caused by rupture of an intracranial aneurysm. A clot forms in the subarachnoid space and erythrocyte lysis causes haemoglobin (Hb) to accumulate in the CSF. In patients surviving the initial bleed, secondary complications such as vasospasm and delayed ischaemic neurological deficits (DIND) can result in poor long term outcome. Hb is neurotoxic through oxidative mechanisms and has also been implicated in the pathogenesis of vasospasm. Management of SAH patients is aimed at securing the aneurysm, inhibiting vasospasm and diversion of CSF to treat hydrocephalus; high morbidity means novel treatments to improve long term outcome are needed and there are none targeting Hb toxicity.

Haptoglobin (Hp) is responsible for binding to cell free Hb, facilitating scavenging by CD163-positive macrophages. Hp inhibits free Hb's pro-oxidative potential by shielding the redox active iron contained in the haem group, rendering Hb oxidatively inert. Two co-dominant HP alleles (HP1 and HP2) exist in humans as a result of an intragenic duplication event. This lead to the production of dimers in HP1 homozygotes (HP1-1), dimers and trimers in heterozygotes (HP2-1), and finally tetramers and large polymers in HP2 homozygotes (HP2-2). Hp isoforms differ in their expression levels, their ability to inhibit Hb's oxidative potential, and when in complex with Hb, their affinity for CD163 and uptake by macrophages.

In this study I hypothesized that: *haptoglobin affects outcome after subarachnoid haemorrhage through its role in haemoglobin scavenging and haptoglobin supplementation after SAH is of therapeutic benefit.* The aims were to: 1) investigate if HP genotype influences outcome after SAH via its role in Hb scavenging, 2) characterise the kinetics of Hb scavenging in the two week period after SAH, 3) establish whether Hp can reverse Hb neurotoxicity *in vitro,* and 4) establish and characterise an *in vivo* model of SAH to translate the results of the *in vitro* experiments.

Due to differential Hb scavenging function, it was hypothesized that HP genotype impacts on outcome after SAH. 1299 SAH patients were typed for their HP duplication genotype and the single nucleotide polymorphism rs2000999, the largest genetic contributor to Hp expression level. Logistic regression analysis of long term outcome identified no effect of rs2000999 but the Hp duplication affected

outcome, implying mediation through Hp function rather than expression level. HP2-2 was associated with favourable outcome in high Fisher grade patients (grades III and IV, Odds Ratio (OR): 2.4, 95% Confidence Intervals (CI) 1.4-.4.3, p=0.007).

To seek further mechanistic evidence for the effect of Hp on outcome after SAH, the kinetics of Hb and Hp was investigated in serial cerebrospinal fluid (CSF) samples from 44 Fisher grade III-IV SAH patients during a two week period post-ictus. Total Hb levels increased gradually, reaching a plateau of 11.5µM (median between days 11 and 13, interquartile range (IQR): 2.1-16.2µM); the majority of this Hb was found to be uncomplexed (median 96.3%, (IQR): 83.3-99.4%, from third day onwards). There was a trend towards an association of high uncomplexed Hb levels with worse outcome (modified Rankin Scale (mRS) at 6 months post-ictus) (OR: 0.7, 95% CI 0.5-1.0, p=0.064). Auto-oxidation of Hb can cause oxidative damage which inhibits complex formation by Hp. Exogenous Hp was added to the CSF, enough to saturate all Hb, to investigate how much Hb was still able to bind Hp; 90.6% (IQR: 65.8-96.5%) of the uncomplexed Hb was able to form complexes with exogenous Hp. The Hb scavenging ability of Hp isoforms was investigated with linear mixed modelling. Significantly lower levels of uncomplexed Hb were associated with the Hp2-2 phenotype (p=0.03, *vs* Hp1-1), in keeping with improved Hb scavenging due to Hp2-2's higher valency for Hb.

To test if Hp can protect against Hb neurotoxicity, primary hippocampal neurones from C57BL/6 mouse pups were cultured and treated with Hb, Hb+Hp, Hp or vehicle. Following a week in culture, viable neurones were counted. Hb produced a dose dependent cytotoxic effect (p<0.0001), and Hp was able to reverse this, inhibiting neuronal death (p=0.003). No adverse effects on neuronal viability were observed with Hp alone.

To translate the *in vitro* findings, I established in our laboratory an *in vivo* murine model of SAH, involving a stereotaxic injection of blood into the pre-chiasmatic cistern of C57BL/6 mice. The model was optimized to refine the technique, to prepare for future experiments testing Hp as a therapeutic agent after experimental SAH.

Table of Contents

Table of Tables

Table of Figures

Declaration of Authorship

Print name:	Matthew James Morton

Title of thesis:	Haptoglobin as a Novel Treatment for Subarachnoid Haemorrhage

I declare that this thesis and the work presented in it are my own and has been generated by me as the result of my own original research, with the exceptions described here. In Chapter 4, rs2000999 genotyping was performed externally by LGC Ltd., however their data were validated by myself using an assay set up and optimised in-house. For Chapters 4 and 5, patient recruitment and collection of samples and primary clinical data was performed by clinicians in my supervisor's research team and collaborators. In Chapter 6 experiments were conducted jointly between myself and Dr Patrick Garland for Figure 6.1, Figure 6.3, Figure 6.4 and Figure 6.6.

I confirm that:

1. This work was done wholly or mainly while in candidature for a research degree at this University;
2. Where any part of this thesis has previously been submitted for a degree or any other qualification at this University or any other institution, this has been clearly stated;
3. Where I have consulted the published work of others, this is always clearly attributed;
4. Where I have quoted from the work of others, the source is always given. With the exception of such quotations, this thesis is entirely my own work;
5. I have acknowledged all main sources of help;
6. Where the thesis is based on work done by myself jointly with others, I have made clear exactly what was done by others and what I have contributed myself;
7. None of this work has been published before submission.

Signature:		Date:	

Acknowledgements

There are a number of people who have been instrumental, without whom I would not have been able to conduct the work for this thesis. First, I must thank my supervisors: Dr Ian Galea, Professor Delphine Boche and Dr Zuby Okemefuna. Thank you for your tireless guidance, encouragement and support throughout my PhD. For all of your efforts, which have been essential for my progression, I am enormously grateful. Thank you to Dr Patrick Garland for help with experiments, technical assistance and highly useful advice!

At Bio Products Laboratory Ltd. I would especially like to thank Dr John More, Sarah Kingsland, Dr Zuby Okemefuna and Richard Chester for supporting this project, for hosting me at BPL and for facilitating this fascinating project. Thank you to Andrea Pacher and Hansraj Dhayan for technical assistance with the UPLC assay, and making my work at BPL so enjoyable.

At the University of Southampton thank you to Jon Ward and Jenny Norman in the Histochemistry Research Unit and thank you to Dave Johnston in the Biomedical Imaging Unit. Thanks to all of the staff in the Biomedical Research Facility, particularly Russ Soper and Mike Broome for all of their help, training and guidance with the *in vivo* aspects of this work. At University Hospital Southampton I thank Mr Diederik Bulters and Mr Ardalan Zolnourian for their assistance with the clinical aspects of my work including both the GOSH and HASH studies.

At University College London I would like to thank Professor David Werring and Dr Isabel Hostettler for their collaboration on the GOSH study, providing samples and clinical data. It was a pleasure working with Isabel during her work in Southampton. At the University of Bristol thank you to Dr Tom Gaunt and Dr Nabila Kazmi for collaboration and statistical support on the GOSH study. At St Michaels Hospital, Toronto thank you to Dr Loch Macdonald's research group for hosting me and training me in their *in vivo* model of SAH. Particular thanks to Dr Bert Bosche for his help and making my stay in Toronto so enjoyable!

Thank you to everyone in Southampton for all of the good times: Kathryn Jay, Alex Collcutt, Paul Ibbett, Katie Askew, Renzo Mancuso, Sarah Howard, Jay Amin, Sonja Rakic, Jo Kelly, Sofia Macari, Jordana Griffiths, Charlotte Stuart, Ellie Keeling and everyone else!

Thanks must go to the Medical Research Council and BPL for funding this work.

Finally thank you to Alison, Ralph and Sarah; without you none of this would have been possible.

Definitions and Abbreviations

ACA	Anterior cerebral artery
ADAM17	A disintegrin and metalloproteinase 17
ALSPAC	Avon longitudinal study of parents and children
ANOVA	Analysis of variance
ARE	Antioxidant response element
ASC	Apoptosis-associated speck-like protein containing a caspase recruitment domain
AUC	Area under the curve
BBB	Blood brain barrier
BCB	Blood CSF barrier
BPL	Bio Products Laboratory Limited
CARD	Caspase activation and recruitment domain
CBF	Cerebral blood flow
cGMP	Cyclic guanosine monophosphate
CI	Confidence interval
CNS	Central nervous system
CSF	Cerebrospinal fluid
CT	Computerised tomography
DAB	3,3'-Diaminobenzidine
DAMP	Danger associated molecular pattern
DAPI	4', 6-diamidino-2-phenylindole
DCI	Delayed cerebral ischaemia
DG	Dentate gyrus
DIND	Delayed ischaemic neurological deficit
DMEM	Dulbecco's modified eagle media
dNTP	Deoxynucleotide triphosphate

ET-1	Endothelin-1
EVD	External ventricular drain
FRET	Fluorescence resonance energy transfer
GCS	Glasgow coma score
GOS	Glasgow outcome scale
GOSE	Glasgow outcome scale extended
GOSH	Genetics Of Subarachnoid Haemorrhage study
GWAS	Genome wide association study
HASH	Haemoglobin After Subarachnoid Haemorrhage study
Hb	Haemoglobin
HBSS	Hank's balanced salt solution
HMGB-1	High mobility group box 1
HO	Haem oxygenase
Hp	Haptoglobin (protein)
HP	Haptoglobin (gene)
HpHb	Haptoglobin-haemoglobin complex
HPLC	High pressure liquid chromatography
Hpx	Haemopexin
HWE	Hardy-Weinberg equilibrium
I.P.	Intraperitoneal
Iba-1	Ionised calcium binding adapter molecule 1
ICA	Internal carotid artery
ICH	Intracranial haemorrhage
ICP	Intracranial pressure
IL	Interleukin
IP_3	Inositol triphosphate

IQR	Interquartile range
KASP	Kompetitive allele specific PCR
Keap1	Kelch-like ECH-associated protein-1
LD	Linkage disequilibrium
LRP1	LDL receptor-related protein-1
MAP2	Microtubule associated protein 2
MCA	Middle cerebral artery
metHb	Methaemoglobin
MMP-9	Matrix-Metalloproteinase-9
mRS	modified Rankin Scale
NO	Nitric oxide
NOII	Neurological conditions and Oncology: Immunology and Interactions study
NOS	Nitric oxide synthase
NRF2	Nuclear factor erythroid 2-related factor 2
OR	Odds ratio
oxyHb	Oxyhaemoglobin
PBS	Phosphate buffered saline
PCR	Polymerase chain reaction
PFA	Paraformaldehyde
Qalb	Albumin quotient
QHp	Haptoglobin quotient
qPCR	quantitative polymerase chain reaction
ROS	Reactive oxygen species
ROX SE	5-(6)-Carboxy-X-rhodamine, succinimidyl ester
RT	Room temperature
SAH	Subarachnoid haemorrhage

SD	Standard deviation
SEM	Standard error of the mean
SLM	Stratum lacunosum moleculare
SNP	Single nucleotide polymorphism
SR	Stratum radiatum
SRCR	Scavenger Receptor Cysteine Rich superfamily
STROBE	Strengthening of reporting of observational studies in epidemiology
TBS	Tris buffered saline
TCD	Transcranial Doppler
THBC	Total haemoglobin binding capacity
TLR	Toll like receptor
TPU	Tissue perfusion unit
TUNEL	Terminal deoxynucleotidyl transferase dUTP nick end labelling
UPLC-SEC	Size exclusion ultra performance liquid chromatography
WFNS	World federation of neurological surgeons grade

Chapter 1 Introduction

1.1 Subarachnoid haemorrhage: an introduction

Aneurysmal subarachnoid haemorrhage (SAH) is a severe neurological condition resulting from the rupture of an intracranial aneurysm within the subarachnoid space, flooding the cerebrospinal fluid (CSF) with blood[1] (Figure 1.1A). SAH causes significant neurological compromise in survivors and immediate mortality in approximately 15% of patients[1]. An aneurysm is a structural deterioration of the artery wall in which the internal elastic lamina is lost and there is disruption of the media[2]. This causes ballooning of the artery wall, which is liable to rupture.

The meninges are composed of three layers: the inner most pia mater, the arachnoid membrane and the outer dura mater. The subarachnoid space, as illustrated in Figure 1.1B, is situated beneath the arachnoid membrane and above the pia mater[3]. When an aneurysm ruptures, blood enters the subarachnoid space under arterial pressure, accounting for a rapid increase in intracranial pressure (ICP) and the characteristic *thunderclap headache* that is often reported during a SAH[1].

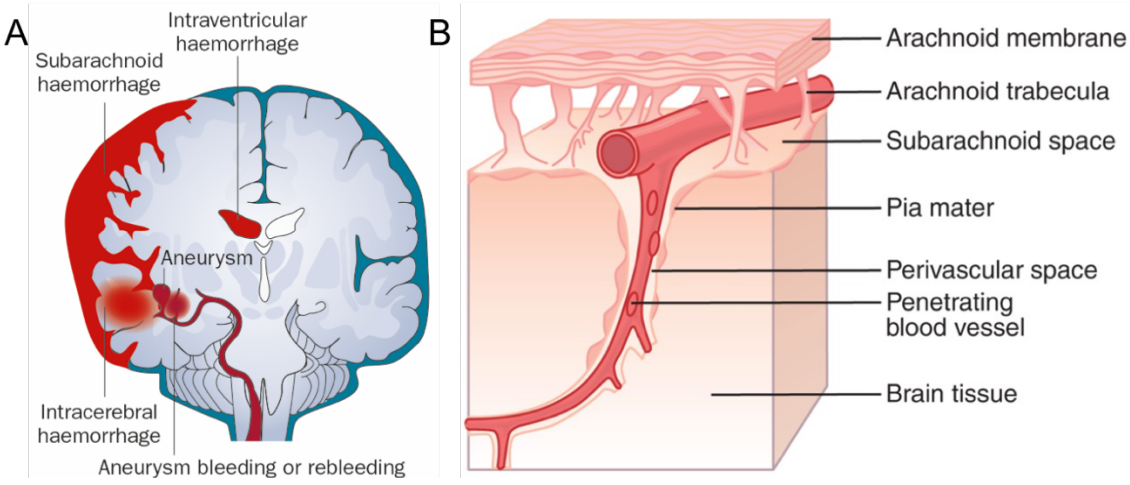

Figure 1.1 ***A)*** *Figure depicting a subarachnoid haemorrhage. Following aneurysm rupture blood fills the subarachnoid space. Figure cropped from de Oliveira Manoel et al.[4]; reproduced under a creative commons licence.* ***B)*** *The structure of the subarachnoid space. The subarachnoid space is located beneath the arachnoid membrane and above the pia mater. Figure from Guyton and Hall[3]; permission to reproduce granted by the publisher.*

Blood released during the bleed begins to clot on the surface of the brain and in contact with the cerebral vasculature. Over time, typically over the course of the first three days the clot begins to degrade, releasing its contents into the CSF[5]. The primary constituent of the erythrocytes is haemoglobin (Hb), an iron containing protein specialized for binding oxygen. The presence of oxygenated-Hb (oxyHb) has been identified in the CSF of individuals within two hours of SAH[5].

Survivors of the initial bleed can experience vasospasm (constriction of the cerebral vasculature), which reduces the vital blood supply to the brain and in up to 30% manifests as delayed ischaemic neurological deficits (DIND)[6], which contributes significantly to morbidity after SAH. While SAH itself is not considered a stroke, SAH accounts for between 5-7% of strokes worldwide[1] through the development of DIND. There is evidence implicating free Hb in contact with the vasculature as a contributor to vasospasm after SAH[7,8].

1.1.1 Demographics of subarachnoid haemorrhage patients

The prevalence of cerebral aneurysm has been reported by multinational autopsy and angiographic studies to be anywhere between 0.4%-7% in a western population[9]. The risk factors for aneurysm rupture are not dissimilar to those for developing an aneurysm and include smoking, hypertension, excessive alcohol intake, increasing age, female sex and family history of SAH. The incidence of SAH is approximately 9 per 100,000 people[10]. A recent UK audit of 14 centres conducted between 2011 and 2015 showed 3341 aneurysmal SAH patients presented during this period[11], this equates to a mean of 835 patients per year in the UK.

The median age at presentation with SAH in the UK was 55 years[11], representing the relatively low age of onset compared to ischaemic stroke. A higher proportion are female, as represented by 68.5% of patients in this audit[11]. The majority of patients initially present to hospital relatively well as defined by the World Federation of Neurosurgeon's Scale (WFNS) grades one and two[11]. These patients typically maintain their eye, verbal and motor responses but may appear confused. Despite this, 34% of patients develop moderate/severe disability or are left in a persistent vegetative state at discharge from hospital[11].

1.1.2 Current treatment methods for subarachnoid haemorrhage patients

Crucial to good outcome is early repair of the ruptured aneurysm to prevent re-bleeding which is usually a cause of mortality. There are two methods for the repair of ruptured intracranial aneurysms: endovascular coiling and neurovascular clipping[12]. Coiling is the most common and least invasive, it involves inserting a catheter into the femoral artery in the groin which is fed up to reach the aneurysm in the brain. Platinum coils are fed through the catheter to fill the

aneurysm, this induces embolization which seals the aneurysm off from the rest of circulation to prevent it re-bleeding[12]. An alternative method is neurovascular clipping[12,13]; this is a far more invasive procedure involving neurosurgery to locate the aneurysm and placing an alloy clip across the neck of the aneurysm, sealing it from the rest of the circulation[12,13].

In a seminal double blind randomised control trial in the UK it was found that nimodipine significantly reduced cerebral infarcts by 34%[14] and poor outcome by 40%[14] and as such it has become a gold standard in modern pharmacological treatment of SAH. Nimodipine is a dihydropyridine calcium channel blocker[14,15]. The rationale for testing its efficacy was to inhibit smooth muscle cell contraction[16]; however it was subsequently observed that it does not prevent vasospasm but is still neuroprotective[16].

Triple H therapy is the use of hypertension, hypervolaemia and haemodilution to improve cerebral blood flow and cerebral perfusion pressure, in an effort to prevent DIND[15]. The cerebral perfusion pressure is the difference between the mean arterial pressure and the ICP[15], and since ICP may be increased after SAH, hypertension here is beneficial to increase cerebral perfusion pressure to reduce the risk of cerebral ischaemia[15].

Despite these current medical interventions, there is still high levels of morbidity post-SAH – over 30% of patients are discharged from hospital with moderate to severe disability, requiring assistance to perform duties in the work place, unable to return to work or needing permanent daily care[11]. Therefore, new treatment modalities are required in SAH to improve patient outcomes. Notably, there are currently no treatments targeting the Hb accumulating in the CSF after SAH, the pathological consequences of which are reviewed in this introduction.

1.2 The haemoglobin insult

Erythrocytes contain a high concentration of Hb in a tetrameric conformation[17]. Hb is in equilibrium between its tetrameric and dimeric conformation, with the former being favoured at high concentrations[18]. Erythrocyte lysis in the degrading blood clot results in Hb release into the CSF, pushing the equilibrium towards the dimeric conformation at a lower concentration. Hb exists in a number of oxidation states that affect its ability to bind and transport O_2 *in vivo*.

In the oxyHb (O_2 bound) state has iron in the haem group in the Fe^{2+} (ferrous) oxidation state; however ferrous Hb undergoes a spontaneous process of auto-oxidation to methaemoglobin (metHb) when released from the erythrocyte. In the metHb form, the haem iron is in its Fe^{3+} oxidation state[19,20]; this is physiologically inactive as it is unable to bind oxygen, therefore in the

erythrocyte metHb reductase (an NADH-cytochrome b_5) is present to reduce metHb back to the functional (ie O_2 binding) ferrous Hb ($HbFe^{2+}$).

1.2.1 Haemoglobin neurotoxicity

Hb was first identified as a potent neurotoxin by Regan and Panter in 1993 through a series of *in vitro* experiments using rat primary cortical neurones[21]. They observed that exposure to a Hb solution produced a dose dependent neurotoxic effect. The addition of Trolox (a vitamin E analogue with antioxidant properties) attenuated the toxicity[21], pointing towards the suggestion that Hb's neurotoxicity is mediated via oxidative mechanisms (Figure 1.2).

Hb toxicity presents as a delayed response, with cell death occurring after 24 hours[21], whereas shorter exposures (1-2 hours) do not produce a cytotoxic response. Interestingly Hb exposure has a highly selective neuron-specific response. In mixed neuron-glia cultures exposed to Hb or blood/haemolysate products, glial cells show complete protection whereas neurons in co-culture exhibit a greater than 80% decrease in viability[21-25]. The delayed response would suggest that neurotoxicity is attributable to a product of Hb catabolism, so toxicity is not observed until Hb has begun to degrade.

Hb degradation allows haem to dissociate[26]. Unlike Hb, haem is a lipophilic molecule, so it easily crosses the plasma membrane, into the neurone. Inside the neurone, the highly constitutively expressed Haem Oxygenase (HO)-2 enzyme catalyses the reaction of haem into iron (plus carbon monoxide and biliverdin, which is subsequently converted into the anti-oxidant bilirubin). Iron as a Fenton reagent is then available to produce highly reactive protein and hydroxyl radicals that can participate in lipid peroxidation[27].

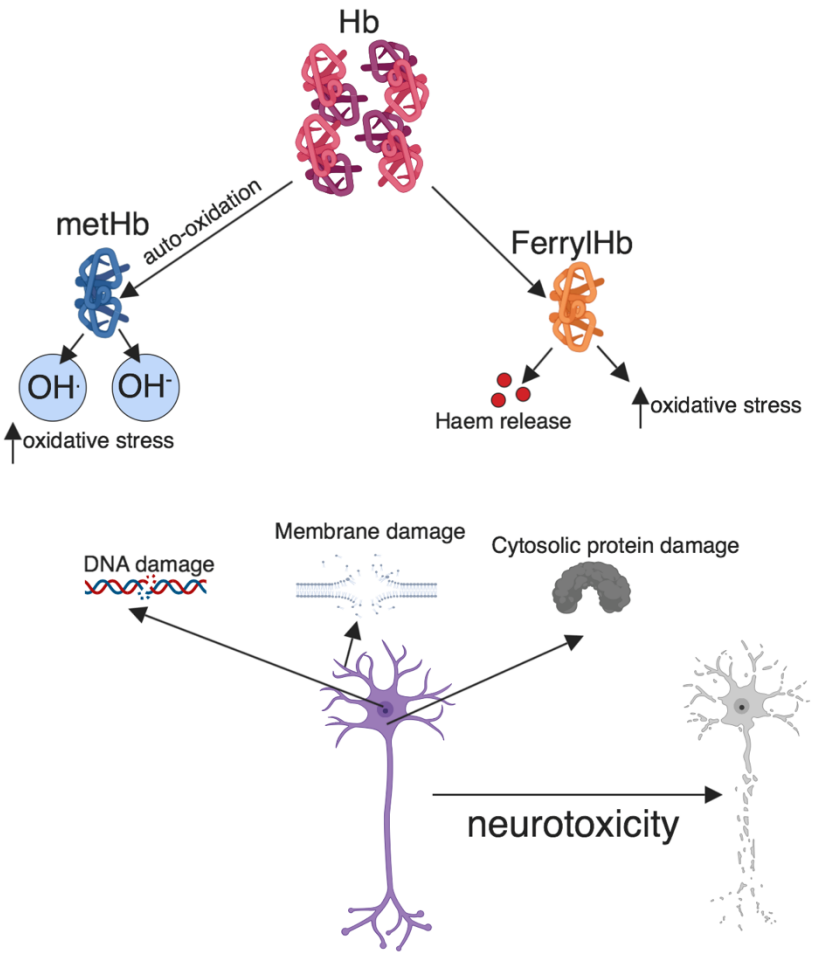

Figure 1.2 Haemoglobin is oxidized to methaemoglobin (metHb, $HbFe^{3+}$) or ferrylhaemoglobin (ferrylHb, $HbFe^{4+}$) by a process of auto-oxidation[28] (via reactions mediated by bound oxygen) or by external oxidizing agents present in pathological situations. Further degradation leads to the release of haem. MetHb and ferrylHb can extract electrons from lipids and proteins, contributing to a pro-oxidative environment responsible for neuronal cell death via DNA, protein and membrane disruption. Created with BioRender.com.

1.2.2 CNS inflammation

1.2.2.1 Inflammation in response to haemoglobin

There is a sterile inflammatory response to SAH, in that inflammation is not driven by the presence of a foreign pathogen but by an endogenous mediator acting as a damage associated molecular pathogen (DAMP)[29]. Inflammation in response to Hb in the brain after SAH contributes to the breakdown of the blood brain barrier (BBB)[29]. This facilitates the influx of cells and proteins that the environment of the CNS is normally protected from by the BBB[29]. This can further exacerbate the inflammatory response of the CNS and contribute to neuronal death.

Inflammation is an important contributor to SAH pathology; it may contribute directly to cell death through activation of neuronal apoptosis and indirectly via the production of ROS from infiltrated neutrophils.

1.2.2.2 Microglial activation

The neuronal damage from the initial bleed and effect of Hb and haem on neurones cause lysis and release of DAMPs. Microglia are the specific macrophages of the CNS, and they react to molecules released from degenerating neurons (such as DAMPs) and molecules entering the CNS from the circulation following BBB breakdown[30,31]. In the CNS, DAMPs activate microglia by binding to Toll Like Receptor (TLR) 4 homodimers or TLR4/2 heterodimers[32-35]. MetHb can activate microglia through activation of TLR 4 homodimers in a CD14 dependent manner[36]. This results in the nuclear translocation of p65 and TNFα production as observed after activation by lipopolysacharride[36], a mimic of bacterial infection and a well-established TLR 4 agonist. A study by Greenhalgh *et al.*[29] has shown that haem promotes inflammation in a perforation model of SAH *in vivo* and in an *in vitro* study of Hb exposure[29]. SAH induced a microglial interleukin 1 (IL-1) response in the cortex, hippocampus and striatum that correlated with the presence of haem (as inferred by HO-1 expression) and strongest in areas adjacent to the bleed[29].

Microglial activation in the context of sterile inflammation (in the absence of pathogen) occurs in two stages. The first involves priming of microglia in which they are activated by the DAMPs (metHb and haem in SAH) and express pro-IL-1 (α and β) through activation of the transcription factor NF-κB[37]. In the second step, the primed microglia encounter a second stimulus which results in the formation a multimeric complex known as the NLRP3 inflammasome, a cytosolic pattern recognition receptor. The inflammasome then interacts with an adaptor protein known as the apoptosis-associated speck-like protein containing a caspase recruitment domain (ASC). The ASC adaptor contains a caspase activation and recruitment domain (CARD), and as the name suggests is responsible for the recruitment of pro-caspase-1 into the inflammasome complex. It ultimately leads to the cleavage of pro-caspase 1 into its mature form. The now catalytically active caspase-1 is available to cleave pro-IL1β into its mature form. IL-1β is then secreted through a poorly defined non-classical secretion pathway as shown in Figure 1.3, below.

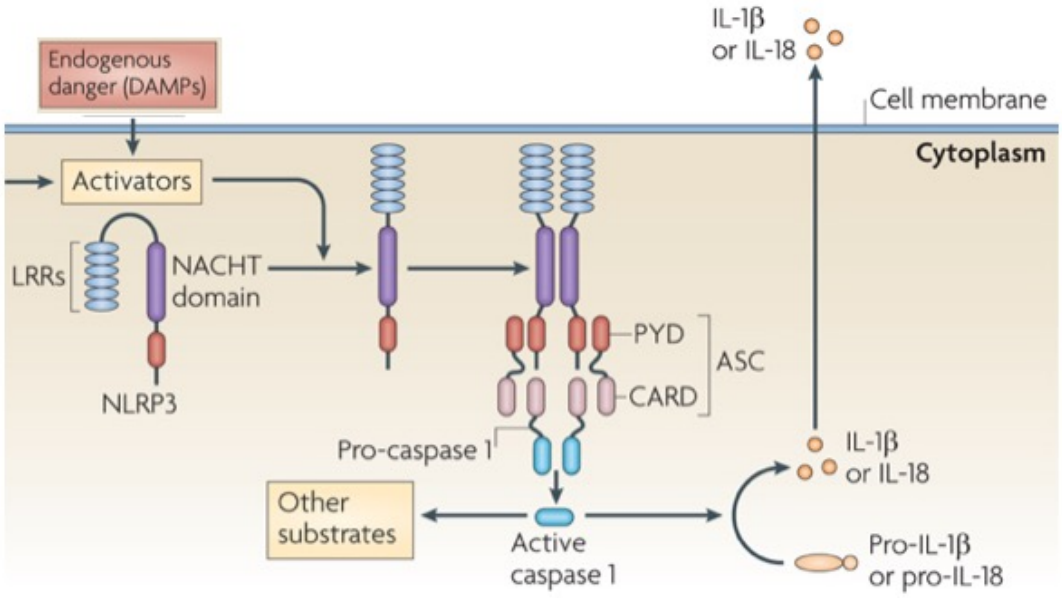

Figure 1.3 *The formation of the NLRP3 inflammasome. Under basal conditions NLRP3 is negatively regulated by an internal interaction. Activation of NLRP3 involves an interaction with the ASC (containing a caspase recruitment domain) which recruits and activates caspase-1. This in turn is able to cleave pro-IL-1β into its active form. Figure from Tschopp et al. 2010[38]; reproduced with permission from the publisher.*

1.2.2.3 IL-1β associated neurotoxicity

The production of IL-1 in the inflammatory response to SAH has deleterious neurotoxic effects[29]. IL-1β signalling through the IL-1R1 promotes Src family kinase phosphorylation and activation[39]. When active, a substrate for these kinases are the NMDA receptors on neurones; specifically the NR2A and NR2B receptors. It has been shown that phosphorylation of these subunits as a result of transient IL-1β signalling causes potentiation of the receptor allowing greater Ca^{2+} flux through the ion channel[39]. This can lead to glutamate induced excitotoxicity and cell death[39].

IL-1 can also instigate neuron specific cell death in a process that is reliant on the astrocytes[40]. IL-1β signalling induces ROS production and release by astrocytes[40], adding to the already high redox potential of the CNS following haemorrhage. *In vitro* models of neuron and glia co-cultures demonstrate that in response to IL-1β, glia produce ROS that result in neuron selective cell death (a reversal effect was observed with the use of a ROS scavenger – α-tocopheral[40]). In addition, astrocytes respond with the induction of protease synthesis, primarily Matrix-Metalloproteinase (MMP)-9[41], and work with neuron-glia co-cultures has demonstrated that MMP-9 production contributes to neuronal death[41]. It is likely that in this *in vitro* model MMP-9 is released from the astrocyte and cleaves neuronal cell surface receptors likely of the integrin family, important for cell survival signalling[41].

The release of MMP-9 also contributes to the breakdown of BBB after SAH. It is likely that in an *in vivo* setting the MMP-9 produced is responsible for the degradation of components of the basement and extracellular membrane increasing the permeability of the BBB[42,43]. Consequently, this allows greater neutrophil recruitment into the injured CNS, which can further exacerbate injury through the production of ROS and secretion of MMP proteases[44,45] leading to a vicious cycle

1.2.3 Haemoglobin driven vasoconstriction

A major aspect of SAH pathology is vasospasm of the cerebral arteries in the 14 day period subsequent to the bleed, which may lead to DIND. DIND is a prime contributor to morbidity and mortality in survivors up to 30 days[6]. Vasospasm may be a consequence of OxyHb released from the degrading erythrocytes in the blood clot[7,46] via a number of mechanisms described below.

1.2.3.1 Nitric oxide consumption by haemoglobin

Nitric oxide (NO) is a vasodilator, responsible for maintaining physiological vascular tone along with a reciprocal vasoconstriction agent, endothelin-1 (ET-1). NO functions by binding to guanylyl cyclase, functionally increasing intracellular levels of cyclic guanosine monophospate (cGMP). This increase in cGMP results in a functional blocking of release of intracellular Ca^{2+} that inhibits the contraction of smooth muscle. NO is produced by an enzyme called nitric oxide synthase (NOS) of which there are three forms: endothelial (eNOS), inducible (iNOS) and neuronal (nNOS).

Hb has a 1000x great affinity for NO than O_2 and oxyHb consumes NO in a mechanism that involves the dioxygenation of Hb[47,48].

$$OxyHb + NO \rightarrow metHb + NO_3^-$$

The consumption of NO by Hb produces Nitrate (NO_3^-), that does not retain the ability to bind to guanylyl cyclase and therefore does not have vasodilatory function[47,48]. Therefore, this conversion to NO_3^- unsettles the balance of constriction/dilation driving the equilibrium towards vasoconstriction, contributing to vasospasm.

1.2.3.2 Increased endothelin-1 synthesis

ET-1 produced by the cerebral endothelium, is a potent driver of vasoconstriction[49]. It has an opposing mechanism to the dilator function of NO. In the context of SAH where eNOS inhibition occurs and NO is sequestered by Hb, vasoconstriction may occur[50]. This imbalance is accentuated by increased ET-1 production from astrocytes in hypoxic conditions[51].

1.2.3.3 Isoprostane production

Isoprostanes are produced as a result of lipid oxidation[52] during the reduction of ferrylHb to metHb and are subsequently released from the lipids within the membrane (as described in Figure 1.4). Isoprostanes are vasoactive molecules and have been hypothesized to contribute to vasospasm following SAH, resulting from the release of Hb in close proximity to the cerebral vasculature. Indeed animals studies[53] and human observations[54] have shown that levels of F_2 isoprostanes correlate with vasospasm as measured by angiography. Furthermore, *in vivo* studies using a canine model of SAH identified significantly higher levels of F_2 isoprostanes within the basilar artery and blood clot compared to control animals[53].

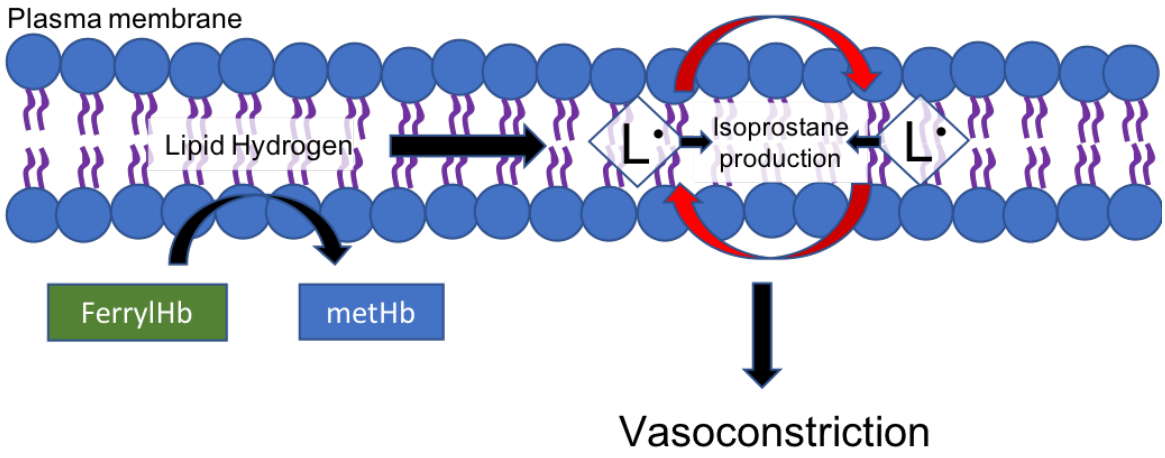

Figure 1.4 *Hb in the ferryl (Fe^{4+}) oxidation can extract a hydrogen from lipids. This process generates lipid radical species that can act in a cyclical oxidative process that generates further lipid species. The lipid radicals undergo further reactions to isoprostanes which have vasoconstrictive properties.*

1.3 The CD163-haptoglobin-haemoglobin scavenging system

1.3.1 Haptoglobin

Haptoglobin (Hp) is an acute phase plasma glycoprotein, which binds cell free Hb to detoxify its redox potential; further, it facilitates its subsequent scavenging by $CD163^+$ macrophages[55]. Under basal conditions, Hp synthesis occurs primarily in the liver but its expression has also been described in myeloid cell types[56]. Due to an IL-6 response element in the promotor of the HP gene[57], Hp synthesis is upregulated during inflammation as a result of increased hepatic synthesis

and localised release of Hp by granulocytes at sites of injury[56]. This also happens in the CNS, where oligodendroglia have been shown to synthesize Hp[58].

The crystal structure of the porcine HpHb complex has been resolved; porcine Hp retains 82% sequence homology with the human protein[59]. The Hp protein bears resemblance to a serine protease, however retains no catalytic activity[59], due to an incomplete catalytic triad[59]. Hp binds to dimeric Hb, and forms extensive interactions with both the α and β subunits of the dimeric Hb molecule[59]. Interestingly some of the interactions on the beta chain include part of the molecule involved in binding the Hb dimers together into a tetramer[59], this would explain why Hp binds exclusively to dimeric Hb[59] as opposed to Hb in its tetrameric conformation.

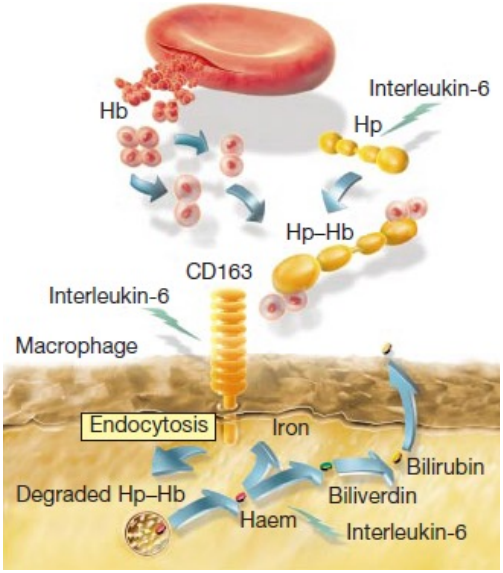

Figure 1.5 An overview of the CD163-haptoglobin-haemoglobin scavenging system. Upon release from the erythrocyte, Hb is complexed by Hp. This whole complex binds to CD163 which induces endocytosis and allows the safe recycling of the haem iron.

1.4 Haptoglobin genetics and structure

1.4.1 The *common* haptoglobin polymorphism

The basic building blocks of Hp are an α and β chain[60-62]. These two subunits together form a single monomer as illustrated in Figure 1.6. In its simplest form Hp is present as a dimer, as a result of intermolecular disulphide bond formation between two α subunits.

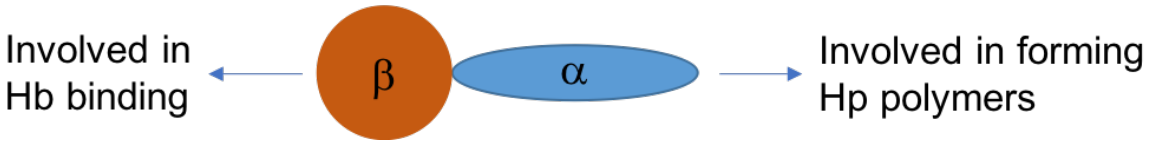

Figure 1.6 The Hp monomer. The α subunit is involved in forming intermolecular disulphide bonds between other Hp α subunits. The β subunit binds to Hb dimers.

The HP gene is composed of 5 exons (Figure 1.7), this is referred to as the HP1 allele. A duplication event of exons 3 and 4 in the HP gene has given rise to a second HP allele, and this larger allele is known as the HP2 allele[60]. The HP1 allele is the ancestral allele and the duplication event created the HP2 allele. However, the current HP1 allele is in fact a product of ancestral intragenic deletions and also recent intragenic deletions that created and continue to create the present HP1 alleles from the HP2 allele[63]. The duplication contains parts of the α chain of Hp containing the cysteine residue involved in the formation of disulphide bonds in the polymerisation of Hp. This results in an additional cysteine residue in Hp2 which allows multiple monomers to come together giving rise to trimeric, tetrameric and higher molecular weight Hp polymers in those carrying the HP2 allele.

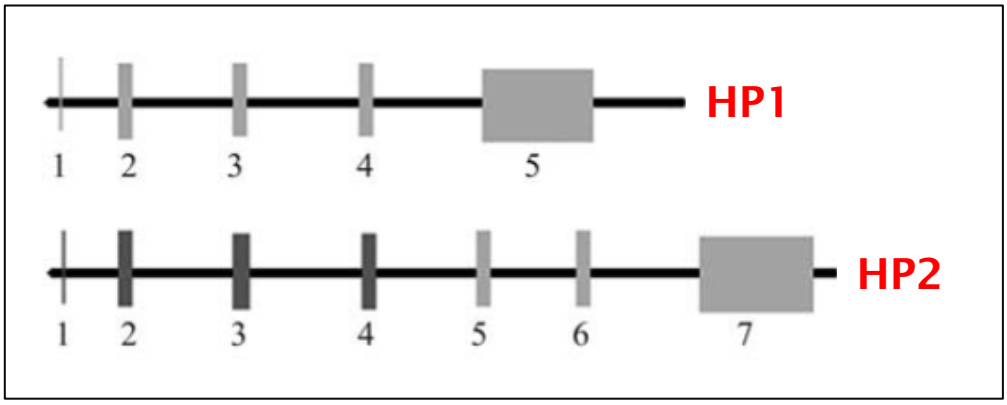

Figure 1.7 *The structure of the two HP alleles. The grey blocks represent exons within the HP gene. The HP1 allele contains 5 exons. In HP2, exons 5 and 6 are duplications of 3 and 4; the result is a final allele with 7 exons.*

There are three major genotypes: HP1-1, HP2-1 and HP2-2[62], based on different combination of HP alleles that an individual carries. HP1 homozygotes (HP1-1) only express Hp dimers. Heterozygotes (HP2-1) express Hp dimers, trimers and higher order polymers. HP2 homozygotes (HP2-2) express tetramers and higher order polymers. This is illustrated in Table 1.1.

Table 1.1 *Schematic representation of the structures of Hp encoded by the HP1 and HP2 alleles. HP1 allele encodes an α subunit with a single cysteine residue able to form a disulphide bond with another α subunit forming dimers. The duplication in the HP2 allele creates a second cysteine residue thus multiple disulphide bonds can form allowing the formation of polymers of increasing size. Heterozygotes form linear polymers whereas those homozygous for HP2 will form cyclic polymers of Hp.*

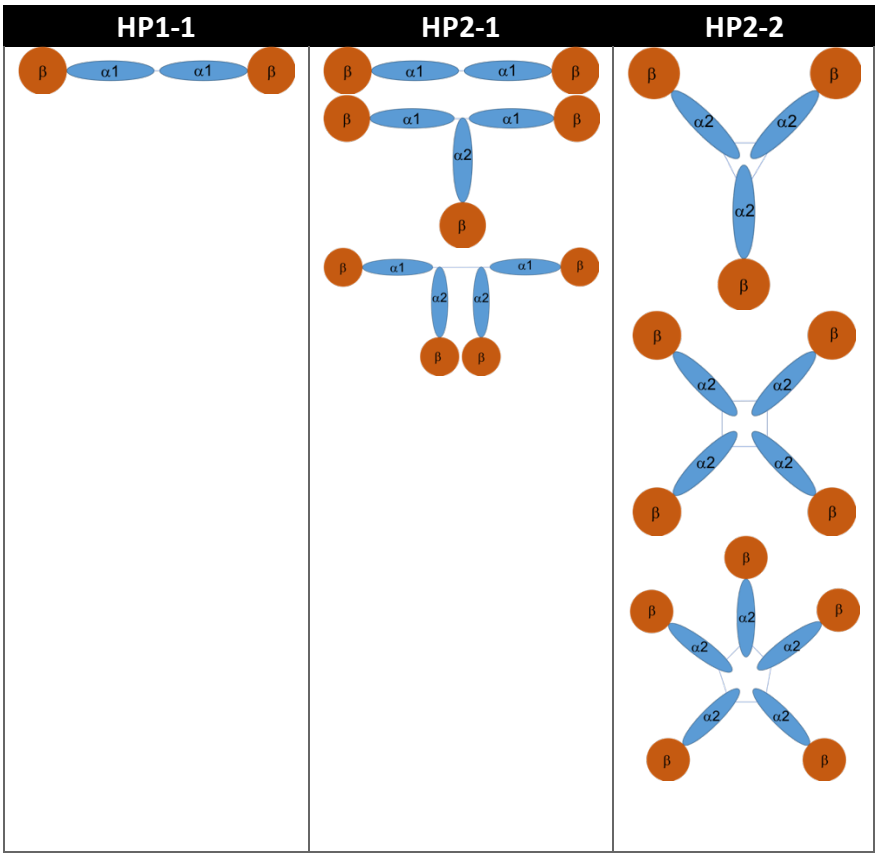

There is a deletional allelic variant referred to as the HP^{del} allele[64], in which a deletion of approximately 28kb extends from the HP promoter to the neighbouring haptoglobin-related-protein[64]. This is a mutation with low frequency amongst Asian populations, ranging between 0.1-3% and is very rare in Caucasian populations[64].

1.4.2 Single nucleotide polymorphisms in the haptoglobin gene

In addition to the duplication mutation described above, there are also a number of single nucleotide polymorphisms (SNPs) within the HP gene (or its related promoter). These polymorphisms impact on the transcription of the HP gene and therefore circulating levels of

Hp[65-67]. Mutations with lower circulating plasma levels of Hp will result in a reduced Hb scavenging capacity. These SNPs are discussed below and summarised in Table 1.2.

A genome wide association study (GWAS) by Froguel *et al.* in 2012[65] identified in a cohort of 631 children that 26% of the variance seen in circulating Hp levels was under genetic control[65]. They identified the SNP rs2000999 (G→A) was responsible for over 45% of the genetic variance HP[65], and this was backed up *in vivo* as it was found that this SNP modulated the expression of Hp mRNA within adipose tissue samples donated from non-obese individuals. This SNP is found within the intron region of the HP gene, 17 kb away from the HP duplication[65]. Every A allele of rs2000999 carried by an individual is associated with a reduction of circulating Hp levels by 0.123 g/L[65].

In complete linkage disequilibrium (LD) with rs2000999 is rs5472, an (A→G) SNP located at position -55 within the HP promoter region[66,68,69]. The LD between these two SNPs in a European population[65], provides a potential plausible biological mechanism for how rs2000999 effects circulating Hp levels[66,68,69].

Table 1.2 *Single nucleotide polymorphisms that impact on the expression of the haptoglobin gene.*

SNP	Effect Allele	Frequency	Location	Effects
rs2000999	A	0.2	Intron of neighbouring haptoglobin related protein	Strong determinant of plasma Hp levels. In complete linkage disequilibrium with rs5472[65].
rs5472	G	0.3	HP promoter region pos -55	Complete linkage disequilibrium with rs2000999 and HP2 allele[66,68,69]. Biologically plausible mechanism to explain rs2000999 action on plasma Hp levels[69].
rs5471	C	0.04	HP promoter region pos -61	Reduced induction of HP2 allele in response to IL-6[66,68]. Reduced Hp levels.[66] Association with HP^{del} allele[67].
rs5470	G	0.04	HP promoter region pos -101	Reduced Hp levels[67].
rs5469	A	0.1	HP promoter region pos -104	Reduced induction of HP2 allele in response to IL-6[66,68].

An (A→C) SNP, rs5471 sits at position -61 in one of the three IL-6 responsive regions of the HP2 promotor[68]. It strongly associates with individuals who display a phenotype known as the Hp2-1 modified phenotype (Hp2-1Mod)[68]. This is a phenotype that approximately occurs within 10% of the black American population[66,70] and appears similar to the Hp2-1 phenotype when using qualitative methods such as gel electrophoresis. However the observable difference is in the proportion of Hp1 to Hp2 when compared to a *conventional* Hp2-1 individual; there is reduced expression of the Hp2 product and greater expression of Hp1[70]. It has been postulated that the location of rs5471 within the IL-6 response element upstream of the HP2 allele is responsible for reduced expression of HP2, by interfering with transcription factor binding. In a hepatoma cell line, transfection with the rs5471 -61C SNP containing HP promoter significantly decreased HP transcriptional activity compared to the control -61A construct[68].

1.5 Haptoglobin: detoxifying haemoglobin

1.5.1 Binding to haemoglobin

Hp is an antioxidant since binding to cell free Hb decreases its redox potential and inhibits Hb's pseudoperoxidase activity[71]. In binding to and forming a complex with Hb, Hp achieves a number of aims: 1) Hp protects against the toxic Hb driven oxidative cascade, and 2) it enables the efficient clearance of cell free Hb by macrophages.

During complex formation, Hp sequesters the reactive haem group of the Hb molecule within the complex[72]. The β chains of Hp are responsible for binding Hb[59]; *in vitro* experiments with fragments of Hp identify 81 amino acids in the β chain which not only binds Hb, but is also responsible for Hp's ability to shield the pro-oxidative potential of Hb[73].

Whilst inside the HpHb complex, the iron in the haem subunit of Hb can be oxidised to the ferryl species (HbFe4+)[72] similar to uncomplexed Hb. However, whilst in complex, the ferryl ion is inert and kinetically stabilized as compared to ferryl ion in uncomplexed Hb[72,74]. Whilst Hb is in complex with Hp, oxidative reactions between the haem iron and small species (such as O_2, NO and H_2O_2) as well as globin residues can still occur within the reactive epicentre of the haem pocket[74]. Hp's anti-oxidative capacity results from Hp's ability to stabilize the resulting intermediates (the ferryl iron and globin free radical on the Hb protein), effectively decreasing the oxidative ability of both species and preventing their participation in external redox reactions. As the result, Hb is not able to cause peroxidation of lipids within the vicinity of the SAH, and the subsequent generation of lipid radicals and vasoactive isoprostane species[20]. Stabilisation of the ferryl haem decreases the oxidative modification occurring on both the globin protein chains (which is self-destructive and inhibits Hb clearance, and therefore promotes toxicity) and neighbouring molecules[72]. Instead, the Hp molecule directs the oxidative modifications onto itself in an anti-oxidative function[75].

Surface Plasmon Resonance analysis has identified that both Hp1-1 and Hp2-2 forms bind free Hb with equally high affinity (10^{-10} M)[76-78]. This has been confirmed in other techniques[73,79] including mass spectrometry[78]and spectrophotometric methods[80]. This is likely due to the fact that Hb binding to Hp is mediated via the Hp β chain which is structurally identical in all Hp forms.

However, it has been shown *in vitro* that the ability to inhibit the pro-oxidative potential of Hb is not homogenous among the different Hp phenotypes[73]. It has been demonstrated that both linolenic acid and low-density lipoprotein are oxidised by cell free Hb[73]. A series of experiments carried out by Melamed-Frank *et al.*[73] in which they measured the ability of Hp1-1 vs Hp2-2 to inhibit this pro-oxidative ability, identified that Hp1-1 had a significantly greater ability to prevent

the oxidation at equivalent protein concentrations of Hp[73]. This is because the redox active iron is stabilized more effectively by Hp1-1, inhibiting the exchange of the iron ion to other agents (such as LDL) which in turn facilitates oxidation[77]. This was observed *in vitro* by Asleh *et al.*[77] who exposed oxidation-prone hyperglycaemic Chinese Hamster ovary cell cultures to either Hp1-1Hb or Hp2-2Hb complexes in the presence or absence of an iron chelator. The authors observed a drastically increased level of intracellular oxidative stress in the Hp2-2Hb (*vs* Hp1-1Hb) incubated cultures[77], which was reversible by addition of the iron chelator[77]. The work in the literature is not unanimous however that Hp1-1 is better at inhibiting Hb's inherent oxidative capacity. Studies by Bamm *et al.*[81] who assayed the oxidation of proteins and lipids identified no differences between Hp1-1 and Hp2-2[81]. Indeed, the same was observed in 2014 by Mollan and colleagues who found that the different forms of Hp exerted similar effects in reducing Hb's redox potential using spectrophotometric methods[80].

1.5.2 CD163+ macrophages: scavenging haptoglobin-haemoglobin complexes

The scavenger receptor for the HpHb complex is CD163[55] (often referred to simply as the Hb scavenger receptor). It is expressed at a low level by circulating monocytes and highly by differentiated tissue macrophages[82]. The CD163 receptor belongs to the group B Scavenger Receptor Cysteine Rich (SRCR) superfamily[83]; its extracellular domain consists of 9 SRCR domains followed by a single transmembrane domain and a short cytoplasmic tail[83].

Whilst Hp binds and shields free Hb, this is a temporary holding measure. Clearance of these complexes is essential for a number of reasons: 1) to detoxify Hb, 2) to prevent iron loss, 3) to metabolize the complex and allow complete recycling of both amino acids and iron, and finally, 4) to remove the HpHb complex from sensitive areas such as the CNS.

1.5.3 CD163: recognition and binding to HpHb complexes

The characterisation of CD163 identified that it binds specifically to the HpHb complex in a Ca^{2+} dependent manner[55]. When the complex is formed, a neoepitope is produced, since surface plasmon resonance analysis identified that Hp alone cannot bind to CD163[55], and Hb alone has a weak affinity[55]. When HpHb complex binds to CD163, SRCR domains 1-5 (proximal to the amino tail) are critical for recognition of the HpHb complex[55]. Crystal structure of HpHb and computational modelling have indicated that the region of Hp concerned with binding to CD163 is in the serine protease like domain, that is also essential for Hb binding[59].

The functional heterogeneity of Hp phenotypes affects uptake of the HpHb complexes. The Hp2-2 phenotype exerts a higher affinity to CD163 compared to the Hp1-1 phenotype in binding assays.

The Hp1-1 molecule is a dimer, therefore is bivalent for Hb. The Hp2-2 molecule can form tetramer or higher order forms, and therefore has a higher valency for Hb, which likely explains its increased affinity for the CD163 receptor[55,84]. Hp2-2 induces a greater increase in intracellular IP_3 production compared to Hp1-1, and the lag between IP_3 production and Ca^{2+} mobilization was shorter for Hp2-2 complexes[84]. This is likely due to the higher valency of Hp2-2, which is able to crosslink the CD163 receptor more effectively.

1.5.4 Haptoglobin-haemoglobin complex internalization and signalling

Prior to its identification as the Hb scavenger receptor, work was performed investigating the effect of crosslinking the CD163 receptor with the monoclonal antibody EDHU1 and its cellular signalling pathway and subsequent effects[83]. Crosslinking results in rapid and transient production of the signalling factor inositol triphosphate (IP_3), and intracellular mobilization of Ca^{2+} culminating in the production and secretion of Il-1β and IL-6[83,84]. Activation of the CD163 receptor by HpHb complexes initiates the secretion of IL-10 in an anti-inflammatory cascade[85]. IL-10 signalling in an autocrine manner is subsequently responsible for the upregulation of downstream anti-oxidant molecules such as HO-1[85]. This was demonstrated in macrophages that were exposed to HpHb complexes. It was observed that IL-10 was increased, as was HO-1; and the use of an anti-IL-10 blocking antibody inhibited the HO-1 upregulation[85]. This autocrine signalling likely aligns Hb scavenging with anti-inflammatory signalling that results in increased HO-1 to improve Hb metabolism. Additionally, the pro-inflammatory IL-6 response also aids Hb scavenging and metabolism by increasing synthesis of acute phase proteins with an IL-6 response element (such as Hp). Therefore, these opposing anti- and pro-inflammatory process ultimately work in collaboration to improve Hb scavenging and subsequent metabolism, acting in a positive feedback loop. Internalization of HpHb complexes also results in upregulation of CD163[85], promoting Hb clearance.

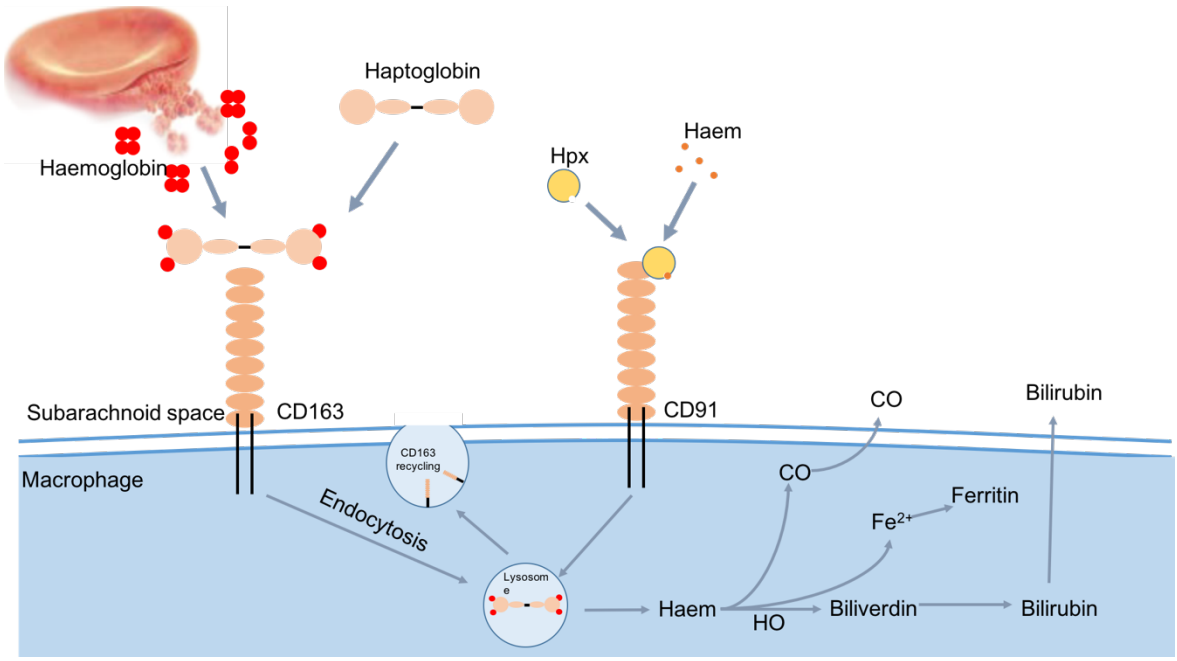

Figure 1.8 *Diagram the mechanisms of the Hp-CD163 and Hpx-CD91 system exist to scavenge free Hb and haem respectively. Hp binds to free Hb in its dimeric conformation and then this complex is internalised by binding CD163. Hpx is able to bind haem in a similar fashion and binding and internalisation is initiated through CD91. Once internalised both complexes are directed towards the lysosome where the complexes detach from their respective receptors which are then cycled back to the cell surface. HpHb and Hpx:haem complexes are degraded.*

Following internalization, the HpHb is released from the receptor when the pH falls after phagolysosome fusion. Hb is degraded, allowing recycling of the iron from the haem group and amino acids of the globin side chain. The membrane-bound CD163 molecule is recycled back to the cell surface to participate in further scavenging[86] as illustrated in Figure 1.8.

1.5.5 Scavenging of haemoglobin breakdown products

Following haemorrhage, the Hp-CD163 axis provides a method of scavenging cell free Hb. However, free Hb can begin to degrade through a series of auto-oxidation reactions that ultimately result in Hb damage and the release of the haem prosthetic group, which cannot be scavenged by the Hp-CD163 system. Therefore other scavenger systems are required.

1.5.6 Haem scavenger systems

The first source of haem scavenging is albumin, a vastly abundant serum protein with promiscuous binding capacity, in that it has the ability to bind multiple ligands with varying affinities. One such low affinity ligand is free haem, making albumin in the circulation a low affinity sink for free haem[26]. It has been suggested that under physiological conditions, albumin's ability to bind haem allows it to extract free haem that has become intercalated within the plasma membrane of the erythrocyte[87], which if not extracted would eventually lead to haemolysis. The binding to albumin is transient, and this is for several reasons. First, albumin has multiple ligands of varying affinities and thus other ligands binding albumin at the same binding site with a higher binding affinity will displace haem. Second, the affinity of haemopexin (Hpx) for haem is greater than albumin's, therefore haem will eventually be transferred to Hpx[88].

Hpx is the high affinity (Kd<1 pM) haem binding protein[89] (a Hp equivalent for haem). The affinity of Hpx for haem is very high within physiological solutions (such as plasma or CSF). However the Kd is pH dependent with weaker affinities as the pH reduces[90]. It was initially believed that Hpx deposited haem within the lysosome before recycling to the surface[90] to further participate in scavenging, but later reports disproved this[91]. It is now thought that Hpx is catabolised, similar to Hp in the context of Hb clearance[91].

Haem binds to Hpx in a pocket within the molecule by co-ordinating the iron ion with two Histidine residues: His213 and His266[92]. In doing so it forms a stable complex with the iron within the Hpx molecule, protecting it from participating in redox reactions[92] and free radical generation[93].

1.5.7 The haem scavenger receptor: CD91

The high affinity haem scavenger receptor is known as CD91, and often referred to in the literature as LDL receptor-related protein-1 (LRP1). It was identified in a similar way to CD163, through affinity purification that yielded a 600 kDa protein[91]. Interestingly, unlike the Hb receptor CD163 which is expressed on the monocyte/macrophage lineage, CD91 has a much broader pattern of expression, and in the brain is constitutively expressed on both neurons and glia[94-96]. This is likely because CD91 has many purposes outside of haem scavenging[97] and recognises multiple ligands including lipoproteins, proteases and complement[97].

Much like the Hp-Hb-CD163 system, the Hpx:haem complexes bind to CD91 in a Ca^{2+} dependent manner[91]. Experiments using surface plasmon resonance identified that haem must be in complex with Hpx to bind to CD91, and haem and Hpx separately elicit no binding response[91].

1.5.8 Haem metabolism

After internalization, HO enzymes (HO-1 and HO-2) degrade haem into iron, carbon monoxide and biliverdin. Biliverdin is subsequently converted to bilirubin by biliverdin reductase. Biliverdin is released from the cell and excreted via filtration in the kidney whilst carbon monoxide is eliminated by exhalation and oxidative metabolism. Biliverdin and low levels of carbon monoxide have anti-oxidant properties. The iron released from this reaction still has redox potential through its action as a Fenton reagent, which is prevented by complexation with ferritin. Ferritin can be exported from the cell by its transporter ferroportin. This process is illustrated in Figure 1.8.

There are two forms of HO[23], termed HO-1 and HO-2 which differ in that HO-1 is inducible and HO-2 is constitutively expressed by neurones (and at very low detectable levels in astrocytes). HO-1 becomes rapidly induced in astrocytes following Hb exposure; similar induction is not detected in neurons[98]. Under normal conditions, the HO-2 system would function to maintain free haem at levels below that of toxicity, with the aim of converting the lipophilic haem-iron into a more water soluble form of iron that can then be sequestered by ferritin[98]. This would leave biliverdin and carbon monoxide at low concentrations at which they exert an anti-oxidant function[98]. In SAH animal models, HO-1 overexpression in brain tissue protected against vasospasm[99] and suppression of HO activity increased cerebral vasospasm and neuronal apoptosis[100,101].

1.6 Haemoglobin scavenging in the brain

1.6.1 The Hp-Hb-CD163 system in the human brain

Hp concentration in the CNS is very low under physiological circumstances. The typical concentration in the CSF is approximately 800 ng/mL[102]; whereas Hp is present at a concentration of 1.36 g/L in the blood compartment[102] of a healthy individual. Therefore the CSF only has the capacity to bind 100 µg Hb[102].This is due to two factors: 1) poor ability to access the CNS across an intact BBB, and, 2) little or no local synthesis of Hp under physiological conditions. A study by Zhao *et al.*[58] investigating the role of Hp in Hb induced neurotoxicity from a similar CNS haemorrhagic disease, intracerebral haemorrhage (ICH), identified by immunohistochemistry that Hp was essentially non-existent in the naïve rat brain[58]. However following induction of ICH in their *in vivo* model, they observed a significant upregulation of Hp within the brain, specifically by oligodendroglia[58]. There is an inflammatory response to haemorrhage, and as an acute phase reactant, serum Hp levels rise after SAH, as demonstrated by our group[102].

$CD163^+$ macrophages are located in three CNS areas: the meninges, the perivascular space and in the choroid plexus[102-104]. Using the soluble form of the receptor (sCD163 – cleaved by ADAM17[105]), the presence of resident CNS macrophages expressing the receptor[102] in the non-inflamed brain is confirmed, yet the population can be dynamic with evidence of recruitment of macrophages to the CNS following SAH[102].

The capacity of the Hb-Hp-CD163 scavenging system in the brain is greatly reduced compared to that of the circulation[102]. Hp in the CSF would be able to bind and attenuate the potent redox activity of the Hb molecule in the sensitive CNS environment, prior to scavenging via CD163 on macrophages as described above. In SAH a Hb insult occurs which is vastly greater than the resident scavenger capacity is able to accommodate[102]. In a study from our group it was shown that Hp present in the CSF can bind 15 x 10^{-12} nmol/mL molecules of Hb[102] (approx. 799 ng/mL Hp), yet the Hb insult from SAH is up to 150x greater than this[102]. Also Hp is detectable in the CSF in the presence of Hb not in complex with Hp. Thus, the Hp-Hb-CD163 system is overwhelmed in its ability to detoxify cell free Hb in two ways: there is not enough Hp to bind all the free Hb and CD163 receptors are saturated[102]. It is likely that this contributes to SAH outcome, though this remains to be shown and is one of the aims of this work.

The high levels of Hb released from the blood clot generates a steep Hb concentration gradient between the CSF and the circulation across the BBB; diffusion of Hb out of the brain into the circulation following this gradient is observed as evidenced by reduction of serum Hp levels after SAH indicative of peripheral scavenging[102]. Patients with the Hp1-1 phenotype showed lower CSF Hp after SAH compared to Hp2-2, and less DIND, indicative of better HpHb complex clearance in Hp1-1 patients[102].

1.6.2 The Hpx-Haem-CD91 system in the human brain

Co-localisation and correlation of iron load with CD91 expression by immunohistochemistry, indicates an active scavenging process of haem-Hpx complexes through CD91 in the brain following SAH[106]. The study demonstrated that the majority of Hpx present within the CNS was produced locally, in contrast to the healthy brain in which most Hpx enters across the BBB[106]. The increased level of Hpx however was not sufficient to meet the overwhelming amount of haem released from degrading Hb in the CSF following SAH, and free haem was detected in addition to haem in complex with Hpx[106]. Further, it was apparent that CD91 receptors were saturated following the overwhelming haem load associated with SAH[106]. There was evidence of efflux of haem out of the CNS into the periphery[106].

1.6.3 Effect of haptoglobin genotype on outcome after subarachnoid haemorrhage

The literature suggests that the HP2 allele may confer a poorer outcome after SAH[107-111]. The results of these studies are discussed below and summarized in Table 1.3. Overall, they showed that HP2 confers a worse short term outcome (using readouts of vasospasm or DIND) or long term outcome (mRS or GOS) after SAH. Due to small samples sizes however, these studies could not provide sufficient insight into the HP2-1 heterozygous population to look for a gene dose effect with respect to HP2.

Table 1.3 *Summary of previous clinical studies investigating the relationship of HP genotype on outcome after SAH.*

Study	Size	Readout	Time point	Significance	Notes
Borsody 2006[107]	32	Vasospasm (transcranial doppler + Cerebral angiography)	TCD - Daily 2-14 days post-ictus CA - Once 3-14 days post-ictus	Significant	HP1-1 *vs* HP2-1 + HP2-2 for TCD. (HP1-1 lower incidence of vasospasm).
Ohnishi 2013[108]	95	Vasospasm (Cerebral angiography) Outcome (focal neurological deficits or 2 point GCS drop and mRS)	Twice – day of onset and between 7-10 days post-onset 3 months	Significant Not significant	HP2-2 *vs* HP1-1 + HP2-1 for CA. (HP2-2 higher incidence of vasospasm). HP2-2 *vs* HP2-1 + HP1-1 for DCI. (Trend towards higher incidence of DCI in HP2-2).
Kantor 2014[109]	193	Outcome (mRS, GOS, mortality)	3 months	Significant	HP2-2 *vs* Hp1-1 for mRS. (HP2-2 worse outcome).
Leclerc 2015[110]	74	Vasospasm (CT angiography or cerebral angiography) Outcome (mRS and GOSE)	Closest image to day 7 post-haemorrhage 6 weeks and 1 year	Significant Not significant	Hp2-2 *vs* Hp2-1 *vs* Hp1-1 for CTA and CA. (Hp2-2 higher incidence of vasospasm). Hp2-2 *vs* Hp2-1 *vs* Hp1-1 for mRS and GOSE
Murthy 2016	133	Cerebral salt wasting disease Outcome (GOS) DCI	30 days post-discharge	Significant Not significant Not significant	HP2-2 *vs* HP2-1 *vs* HP1-1. (HP2-2 higher incidence of cerebral salt wasting disease). HP2-2 *vs* HP2-1 *vs* HP1-1. HP2-2 *vs* HP2-1 *vs* HP1-1.
Kim 2018	87	DCI Vasospasm (Cerebral angiography and TCD) Outcome (mRS)	Twice - <3h and 7-10 days post-ictus 6 months	Significant Significant Not significant	Incr. α1 in Hp2-1 pts without DCI. Incr. α1 in Hp2-1 pts without vasospasm. Incr. α1 in Hp2-1 pts without vasospasm.

The first study by Borsody and colleagues with a sample size of 32 patients explored the effect of HP genotype in relation to the development of vasospasm as measured by transcranial Doppler[107]. They grouped the HP2-1 and HP2-2 together, investigating the presence of the HP2 allele *vs* HP1 alone (n=9 vs n=23, respectively)[107]. The HP2 allele was associated with a higher rate of development of vasospasm.

Ohnishi *et al.*[108] focused on the development of vasospasm, clinical deterioration due to delayed cerebral ischaemia (DCI) and functional outcome (focal neurological deficits) after SAH and their relationship to HP genotype, in a study of 95 patients. In contrast to Borsody's study[107] they grouped HP1-1 and HP2-1 individuals together and compared them to HP2-2 individuals. Their univariate analysis identified that vasospasm as measured by angiography was significantly

associated with individuals who had the HP2-2 genotype compared to HP2-1 and HP1-1 combined. A multivariate analysis identified that HP2-2 individuals showed a trend towards a higher risk of DCI *vs* the other HP genotypes combined[108].

Kantor *et al.*[109] published the largest study to date, of 193 patients, exploring the association of HP genotype and outcome after SAH[109]. They measured long term outcome, using modified Rankin Scale (mRS) scores at 3 months post-ictus. They compared HP1-1 to HP2-2 individuals and found that HP2-2 individuals had a significantly worse mRS score (and thus worse outcome). Interestingly in a second analysis they identified a similar relationship when comparing the HP2-1 group or the HP2-2 group to the HP1-1 homozygous group of patients at 3 months post-ictus. This result was not significant in their multivariate analysis.

A subsequent publication (Leclerc *et al.*)[110] confirmed previous results published by Ohnishi and colleagues[108,110]. Despite a smaller sample size (n=74), the authors attempted to address HP genotype in relation to vasospasm, short term deterioration via DCI, functional long term outcome and mortality. The previous studies have addressed these separately whereas this one was aiming at being more comprehensive. They graded vasospasm into mild, moderate and severe as opposed to simply indicating whether vasospasm occurred or not. HP2-2 was significantly associated with higher incidence of severe vasospasm[110]. With respect to DCI, no significant association was identified when comparing HP2-2 *vs* the HP2-1 and HP1-1 genotypes combined[110]. Long term outcome was measured as mRS scores and Glasgow Outcome Scale (GOS) Extended scores. A trend was found for a worse outcome with HP2-2.

Taken together the work in the literature suggests an effect of genotype on vasospasm[107,108,110] and long term outcome[108,109] and is indicative that HP1-1 is protective in both. A meta-analysis of six studies (Leclerc *et al.*[110], Murthy *et al*.[111], Kantor *et al.*[109], Ohnishi *et al*.[108], Galea *et al.*[102] and Borsody *et al.*[107]) investigating HP genotype on outcome was performed by Gaastra *et al*.[112]. The results identify that HP2-2 (vs HP1-1) imparted poor short term outcome (vasospasm/DCI) and also identified that the outcome of HP2-1 patients resembled more closely the HP1-1 patients[112]. This suggested the Hp dimer is the essential moiety that confers protection. They observed no significant effect on long term outcome in their meta-analysis. However the meta-analysis was hampered by study outcome heterogeneity and inability to correct for essential covariates. A single larger study is therefore still needed to confirm the effect of HP genotype on outcome. This will be addressed by the first hypothesis of this work in Chapter 4.

A study by Kim *et al.*[113] aimed to investigate the contribution of the HP1 and HP2 alleles to outcome by investigating Hp2-1 patient's outcome after SAH. Using western blotting to phenotype (and therefore ascertain genotype) the patients from serum, they quantified the

relative amounts of Hp dimer (HP1 allele) to higher polymers (HP2 allele) in Hp2-1 patients. Their analysis showed that Hp dimer was higher in patients who did not present with DCI or vasospasm, indicating an effect on short term outcome, however there was no effect on long term outcome (mRS at six months)[113]. This in agreement with previous studies that implicate HP2-2 in short come outcomes such as development of DCI and vasospasm[107,108,110]. The better short term outcome with higher Hp dimer concentration in Hp2-1 individuals is in keeping with the observation that the outcome of HP2-1 patients is similar to that of HP1-1 patients, and better than HP2-2, in the meta-analysis by Gaastra *et al.*[112]

1.6.4 Biological effects of haptoglobin other than Hb clearance

As reviewed above, cell free Hb is first bound by Hp and then this complex is internalised by CD163 present on macrophages in humans. In the murine system, the primary method of Hb scavenging is through the direct binding of Hb to CD163[114]. In mice, Hp exists to bind to Hb and neutralize its pro-oxidative potential, much as it does in humans, but is not required for Hb clearance[114]; the exact mechanism of Hb-Hp complex clearance in mice remains unknown. The mouse only carries a single HP allele, equivalent to the human HP1-1 genotype[115]. Chaichana *et al*. used a mouse model expressing HP2-2[115] through duplication of a number of exons of the murine HP gene, similar to human HP2-2. They induced SAH in the HP2-2 mice and wild-type HP1-1 littermates via an injection of 60 μL blood into the cisterna magna and studied activity as a measure of neurological activity, vasospasm of the basilar artery measured via histology and lymphocyte infiltration via histology. Their results showed that the HP2-2 mice exhibited a greater extent of vasospasm and worse neurological scores, suggestive of poorer outcome. Additionally, a greater number of infiltrating macrophage and neutrophils was identified into the subarachnoid space in HP2-2 mice; this was statistically significant compared to control wild-type HP1-1 animals[115].

As murine Hb clearance is not reliant on Hp[114] it is unlikely that the difference between these mouse strains was due to Hb clearance. There is evidence that Hp1-1Hb complexes are more anti-inflammatory than Hp2-2Hb complexes, so this may be the underlying mechanism in this mouse study. When cultured peripheral blood mononuclear cells were exposed to Hp1-1 or Hp2-2 in complex with Hb, it was observed that the Hp1-1 cultures exhibited a significantly greater increase in production of both IL-10 and IL-6 compared to Hp2-2 (which did not differ significantly from controls)[116].

It is possible that Hp exerts its effects via another target, not just Hb. Hp has been shown to bind to HMGB1, a DAMP released during tissue injury[117,118]. Hp-HMGB1 complexes stimulate

production of anti-inflammatory enzymes such as HO-1 and anti-inflammatory enzyme cytokines such as IL-10, in a CD163-dependent manner. However it is not yet known whether HP genotype impacts on this pathway.

1.7 *In vivo* models of subarachnoid haemorrhage

There are a number of considerations that must be made when designing and selecting an animal model of disease. First it must recapitulate the essential clinical features of the disease that it is modelling. Second it must be experimentally suitable to test the hypothesis under investigation. Finally, it must be an ethically approved procedure, and the knowledge gained from the interpretation of results outweighs any suffering caused during the experimental procedures. Consideration must be made to the principle of the 3Rs (Replacement, Reduction, Refinement) which promotes high standards of welfare in animal research and aims to reduce the numbers of animals used in research. Therefore a good model of SAH would produce the following:

- Blood entering the subarachnoid space and subsequent clot formation.
- Increase in ICP.
- Lysis of clot and release of Hb.
- Hb neurotoxicity.
- Spasm of large cerebral arteries proximal to the clot.
- High repeatability and low variability between experimental animals.

In vivo models of SAH have been developed in several experimental animals, including mouse, rat, rabbit, and dog[119]. Due to reasons of cost, and availability of transgenic animals, more groups are moving towards the use of small rodent models (mouse and rat). In this project, I planned to set up and characterize a mouse model of SAH[120]. Current models available will be summarized (for comprehensive review of all animals models see Titova *et al.* 2009[119]).

Models of SAH can broadly be divided into two categories based on the method of introducing blood into the subarachnoid space: the injection model or the endovascular perforation model. Further variations exist within the injection model such as site of injection or single *vs* double injections which allows modelling of re-bleeding, a common complication of aneurysmal SAH.

1.7.1 Small rodent models: SAH in the mouse

One of the first murine model of SAH was a perforation model described by Kamii et al 1999[121], during which the anterior cerebral artery (ACA) was perforated near the anterior communicating artery by feeding a blunted nylon suture up the internal carotid artery (ICA) and through the left

ACA. When resistance was felt, the suture was advanced a further 5mm and immediately withdrawn to perforate the artery wall[121]. For sham surgeries, the suture was advanced through the internal carotid artery but stopped when resistance of the artery wall was felt, so as not to damage the wall and cause haemorrhage. The authors recorded a mortality of 29% in their wild-type animals within the first 72 hours, and they observed heterogeneity of SAH between experimental animals; those with severe SAH died within the first 72 hours. A cast of the cerebral vasculature was produced by perfusing with a gelatin and carbon black (to stain the gelatin) solution to quantify vessel diameter. They observed significant vasospasm at day three, which by day seven was almost resolved[121].

Another study concentrated on a knockout of superoxide dismutase and its effects on the induction of vasospasm after SAH; as such no data were available on neuronal injury in this model. In this model they perforated the right middle cerebral artery (MCA) at the bifurcation with the ACA[122]. Using a similar casting protocol of India ink stained gelatin, they quantified vasospasm at day 3 and observed results in agreement with Kamii *et al.*[121] In this study however, they also performed basic motor and sensory neurological scoring, demonstrating deficits correlating with vasospasm.

A study by Matz *et al.* in 2000[123] explored the effects of DNA fragmentation with regard to apoptosis following exposure of redox-active oxyHb after SAH. They injected 50 µL of haemolysate into the cisterna magna in a mouse brain (a common injection site in rat models of SAH). They observed a very high level of mortality (50%) and regurgitation of blood from the cisterna magna in survivors[123]. They concluded that, unlike the rat cisterna magna injection model, this was not an appropriate model of SAH in mice[123]. Therefore, they injected the haemolysate into the subarachnoid space over the right neocortex through a burr hole, over the coronal suture, 2 mm to the right of the midline, slowly injecting 50µl over one minute. While not strictly aligned to human SAH as a clot does not form with haemolysate and there is no ICP rise, it recapitulates the Hb exposure aspect of SAH. In their experimental group, they observed a 16% mortality rate. Using TUNEL staining, they identified apoptotic neurons , worse on the injected side, and the expression of HO-1[123].

The injection model is by far the most widely used to induce SAH in a wide range of experimental animal models. While the perforation model closely mirrors the rupture of an intracranial aneurysm, as occurs in the disease, it leads to heterogeneity in blood volume, thus variability amongst animals. The use of, an injection model standardizes the volume of blood, the location of the blood, and the rate of injection. Perforation and injection models also differ in how the experiments are controlled. A perforation model is controlled with the use of sham surgery –

inserting the suture but not perforating the vessel. The injection model can be controlled with sham surgery plus a saline injection, incorporating an increase in ICP and allowing one to determine the specific contribution of Hb to the pathology of SAH.

The first time an injection model in the mouse was published was by Lin *et al.* in 2003[124] who injected autologous blood into the cisterna magna in a development of the rat cisterna magna injection model. Their pilot studies used a varied injection volume ranging from 40 – 90 µL. They identified that volumes above 60 µL caused efflux of blood from the burr hole and were associated with higher rates of mortality, which was 3.4% at 60 µL[124]. *Post-mortem* examination showed a clot formed mostly over the ACA, basal artery and proximal branches of the MCA[124]. Significant vasospasm was observed in blood injected animals in the ACA that peaked up to day three and persisted until day seven at which point it approached baseline levels[124]. Significant vasoconstriction was present also in the MCA, within the same time frame as the ACA however to a lesser degree – which is to be expected as it is further from the injection site and therefore subject to less insult from Hb[124]. Constriction of the basilar artery was also identified, however this was very short term. Vasospasm in this artery peaked at the six hour time point and was not significant after this[124]. Modifications have been made to this method such as placing animals head down for a period of time post-injection to confine the injected blood to the intracranial cisterns, to encourage clot formation in these areas[115].

In 2009 Sabri *et al.*[120] published a similar injection model in the mouse, where the injection was into the prechiasmatic cistern. Their model had a mortality rate of 10%. Vasospasm was identified in both the MCA and ACA following blood injection. Other groups using the same model have identified that vasospasm is biphasic, with maximal spasm at days three and 10[125]. Furthermore, the Sabri model[120] identified neuronal apoptosis in the cortex and hippocampus of animals receiving blood injections which was not detected in control saline animals.

1.8 Previous investigation of haptoglobin treatment for SAH

1.8.1 Clinical studies

In 1979, Nonaka and colleagues investigated the clinical application of Hp to the arteries surrounding the aneurysm for two days during and following clipping of the ruptured aneurysm[126]. They focused on longitudinal angiographic measurement of vasospasm as a readout, since there was no control group. At the time, it was thought that the ability to prevent vasospasm would translate into improved long term outcome. However it is now known that there is a lack of correlation between neurological outcome and vasospasm[127]. This Japanese

study focused on 27 patients, a relatively small number, that was then subdivided into four groups depending on the timing of surgery and vasospasm. In patients whose vasospasm was changing (increasing or decreasing), 14/17 patients responded with improvement in vessel diameter; of these, in 5/7 improvement was noted in patients whose vasospasm was deteriorating prior to surgery, and 9/10 improvement was noted in patients whose vasospasm was already improving prior to surgery. In patients who were recruited early (when vasospasm is not expected) or whose vasospasm was static, there was no response (2/10), with only one patient responding from each group. A lack of control group, small sample size and further subgrouping make it difficult to draw solid conclusions from this study, but it is suggestive that in some patients the administration of Hp was beneficial in improving vasospasm. More work is required to determine if Hp supplementation improves long term outcome after SAH.

1.8.2 Experimental studies

There are no experimental studies of Hp supplementation in SAH animal models. However a study by Zhao *et al.*[58] investigated the role of Hp in ICH. Depletion of systemic Hp before induction of experimental ICH in rats resulted in greater levels oxidative damage and worsened oedema associated with the bleed, when compared to ICH in rats with normal systemic Hp levels[58]. Additionally, after ICH in a mouse Hp knock out model, they observed greater neurological dysfunction on behavioural testing. Finally, a transgenic mouse model overexpressing the human HP2 allele subjected to ICH showed better outcome in terms of neurological dysfunction and neuronal loss[58].

There are innumerable studies on the therapeutic benefit of systemic Hp supplementation during intravascular haemolysis. Some of these studies have demonstrated that the mechanism of action of Hp might be relevant to application in SAH. Intravascular haemolysis causes hypertension due to systemic arterial wall vasoconstriction, akin to vasospasm of cerebral arteries after SAH. In a canine model, Boretti *et al.*[128] administered prednisone (a glucocorticoid) to upregulate endogenous Hp[128], and found that it reversed hypertension induced by intravenous Hb. In a guinea pig model, intravenous administration of exogenous Hp reversed non-haem iron deposition and 4-hydroxynonenal–modified protein (a marker of oxidative tissue damage) in the kidneys after intravenous Hb challenge[128]. Since vasospasm and oxidative stress are major pathological features after SAH, these observations suggest that Hp supplementation may be therapeutic after SAH.

Chapter 2 Hypotheses and aims

The overarching hypothesis of this thesis is:

> **Haptoglobin affects the clinical outcome after subarachnoid haemorrhage through its role in haemoglobin scavenging.**

In this thesis I address the following sub-hypotheses:

1) **Hypothesis:** An individual's HP genotype affects outcome after SAH. Specifically, 1) In SAH patients, a HP genetic variation driving Hb clearance (HP duplication) affects outcome after SAH; 2) in SAH patients, a HP genetic variation driving serum Hp concentration (rs2000999) affects outcome after SAH.

Aim: Aneurysmal SAH patients from the Genetics of Subarachnoid Haemorrhage (GOSH) study will be genotyped for their HP duplication status using in house genotyping assays and typed for their rs20009999 status with commercial KASP genotyping technology (LGC Genomics, Hertfordshire, UK). Associations between HP genotype and outcome after aneurysmal SAH will be sought using logistic regression analysis.

2) **Hypothesis:** Hb released from the lysing blood clot into the CSF, overwhelms the resident Hb scavenging system and impacts on functional outcome after SAH.

Aim: Serially collected CSF samples from aneurysmal SAH patients from the Haemoglobin after Subarachnoid Haemorrhage (HASH) study will be analysed by Size Exclusion Ultra Performance Liquid Chromatography (UPLC-SEC) to quantify the amount of free Hb, the amount of scavengeable Hb and Hp level. The Hp phenotype of the patients will be determined by UPLC analysis of serum and Western blotting and logistic regression analysis employed to investigate the contribution of these analytes in the CSF to functional outcome. Additionally, linear mixed modelling analysis will be used to make inferences on how the Hp phenotype impacts on Hb scavenging in the CSF.

3) **Hypothesis:** Hp can ameliorate the neurotoxicity of cell free Hb *in vitro*.

Aim: Primary murine hippocampal neurones will be prepared and treated with either haemolysate alone to model chronic exposure to Hb, or a mix of haemolysate plus Hp at an equimolar concentration to the Hb content. Other control groups will include vehicle and Hp alone. Neuronal viability will be assessed morphologically after MAP2 immunocytochemistry.

4) **Hypothesis:** Characterizing a mouse model of experimental SAH, intended to test the hypothesis that Hp supplementation can rescue neurological deficits after SAH.

Aim: A mouse model of SAH, based on an injection of blood into the prechiasmatic cistern, will be optimised to provide a tool to test the efficacy of Hp *in vivo*. The model will be characterised for behavioural readouts, vasospasm, histological markers of tissue injury and iron deposition.

Chapter 3 Materials and Methods

3.1 Clinical study ethics approvals

3.1.1 Genetics Of Subarachnoid Haemorrhage (GOSH) study

In Chapter 4, DNA samples and clinical data of aneurysmal SAH patients from the GOSH study were used for HP genotyping. This study was co-ordinated by Professor David Werring at University College London and samples were donated for this collaborative study. The Research Ethics Committee approval number was 09/H0716/54.

3.1.2 Haemoglobin After Subarachnoid Haemorrhage (HASH) study

In Chapter 5, CSF and serum samples and clinical data of aneurysmal SAH patients from the HASH study were used for UPLC analysis of Hb analytes. This study was co-ordinated by Dr Ian Galea at University Hospital Southampton. The Research Ethics Committee approval number was 12/SC/0666.

3.1.3 Neurological conditions and Oncology: Immunology and Interactions (NOII) study

In Chapter 5, CSF and serum samples and clinical data of patients with non-haemorrhagic and non-inflammatory neurological conditions from the NOII study were used as controls for the UPLC analysis of Hb analytes. This study was co-ordinated by Dr Ian Galea at University Hospital Southampton. The Research Ethics Committee approval number was 11/SC/0204.

3.2 Clinical variables: Definitions

Table 3.1 *Definitions of variables used in clinical studies in this thesis.*

Delayed Ischaemic Neurological Deficit (DIND)	The occurrence of a focal neurological impairment as defined by Vergouwen et al.[6] A patient was determined to develop DIND if any of the following occurred: hemiparesis, dysphasia, a clear new focal deficit 72 hours post-SAH or a GCS drop of 2 or more.
Fisher Grade	A radiological grade to classify SAH based on amount of blood clot present on a CT scan[129]. The full scale is detailed in Appendix A.
Glasgow Coma Score (GCS)	A clinical scale used to assess the level of consciousness in a person following neurological injury[130]. The scale ranges from 3 (good response) to 15 (no response) and takes into account eye, motor and speech responses to stimulation. The full scale is detailed in Appendix A.
Glasgow Outcome Score (GOS)	A clinical scale used to assess the functional outcome following neurological injury[131]. The scale ranges from 1 (death) to 5 (good recovery). The full scale is detailed in Appendix A.
modified Rankin Scale (mRS)	A clinical scale used to assess the functional outcome following neurological injury. The modified version[132] of the Rankin Scale[133] was used, ranging from 0 (no symptoms at all) to 5 (severe disability); a grade of mRS 6 (death) was added to include mortality[134]. The full scale is detailed in Appendix A.
Vasospasm as assessed by transcranial Doppler (TCD)	Where assessed by TCD, vasospasm was deemed present when a velocity of >200 cm/s was recorded[135].
World Federation of Neurological Surgeons grade (WFNS)	A clinical scale used to assess the severity of injury after SAH based on the GCS combined with the presence or absence of focal deficits[136]. The scale ranges from 1 (GCS 15 with no motor deficits) to 5 (GCS 3-6, with or without deficit). The full scale is detailed in Appendix A.

3.3 Haptoglobin genotyping

The patients from the GOSH study were typed for their HP duplication genotype initially by a high throughput qPCR method described in detail below. The patients were typed for the SNP rs2000999 using commercial KASP technology. These two protocols were followed by validation by the gold standard of conventional Polymerase Chain Reaction (PCR) for the HP duplication and a Taqman qPCR assay for rs2000999.

3.3.1 Polymerase chain reaction protocol

A PCR protocol[137] was used to qualitatively determine HP genotype. The protocol involves two separate reactions with different sets of primers (A&B and C&D) (see Table 3.2). 25 µL reactions were prepared as in Table 3.3. The reactions contained 10x PCR buffer (Qiagen, USA), deoxyribonucleotide triphosphate (dNTP) mix with 2.5 mM of each nucleotide (Applied Biosystems, USA), **either** primers A & B **or** C & D (10 µM) (Eurofins Genomics, Germany), HotstarTaq DNA Polymerase (Qiagen, USA), $MgCl_2$ (Qiagen, USA) and DNase and RNase free H_2O (Gibco, Life Technologies).

Table 3.2 *Primers for PCR method HP genotyping.*

Name	Sequence (5'-3')	supplier
Primer A	GAGGGGAGCTTGCCTTTCCATTG	Eurofins Genomics (Germany)
Primer B	GAGATTTTTGAGCCCTGGCTGGT	Eurofins Genomics (Germany)
Primer C	CCTGCCTCGTATTAACTGCACCAT	Eurofins Genomics (Germany)
Primer D	CCGAGTGCTCCACATAGCCATGT	Eurofins Genomics (Germany)

Table 3.3 *Mastermix prepared for PCR reaction to determine HP genotype.*

	Primers A and B	**Primers C and D**
	Per reaction (22µl + 3µl DNA)	Per reaction (23µl + 2µl DNA)
10x buffer	2.5	2.5
dNTP mix (2.5each)	8.0	8.0
Forward primer (10 µM)	2.5	2.5
Reverse primer (10 µM)	2.5	2.5
HotstarTaq polymerase	0.5	0.5
$MgCl_2$	4.0	4.0
H_2O	2.0	3.0
DNA per reaction	3.0	2.0

Primers A and B were used to generate an HP1 allele specific product of 1757 bp in size and an HP2 allele specific product of 3481 bp. Primers C and D produced only a 349 bp HP2 allele specific product. Primer binding positions and products are illustrated in Figure 3.1 and expected allele specific PCR products are summarised in Table 3.4.

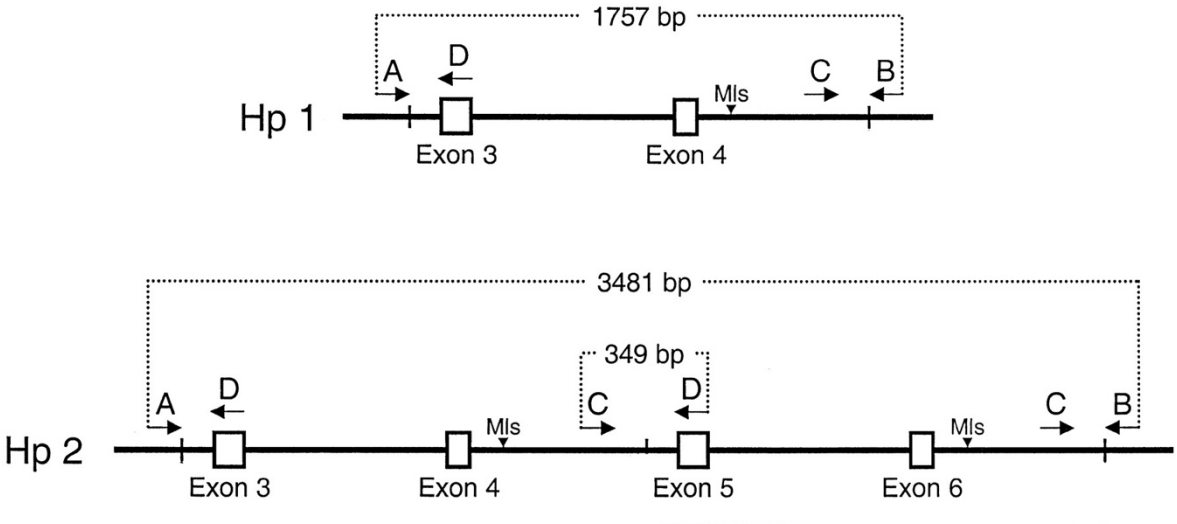

Figure 3.1 *PCR products generated from reactions with primers A&B and C&D. The top schematic shows the relative binding locations of Primers A and B and the 1757 bp HP1 allele specific product produced. The bottom schematic shows the relative binding position of primers A and B and the 3481 bp HP2 allele specific product and the binding position of primers C and D and the 349 bp HP2 specific products. Figure from Koch et al. 2002[137]; reproduced with permission from the publisher.*

Reactions with **primers A and B** were subject to an initial Hotstart activation step of 95°C for 15 minutes. Following this, a denaturation step at 94°C for 1 minute, an annealing step at 71°C for 1 minute and an extension step at 72°C for 3 minutes was cycled for 35 cycles. A final extension step at 72°C for 10 minutes was performed.

Reactions with **primers C and D** were subject to an initial Hotstart activation step of 95°C for 15 minutes. Following this, a denaturation step at 94°C for 1 minute, an annealing step at 71°C for 1 minute and an extension step at 72°C for 1 minute was cycled for 35 cycles. A final extension step at 72°C for 10 minutes was performed.

The resulting PCR products were run on a 1% agarose gel and stained with GelRed (Biotium, CA, USA) to visualise bands. A 1 kB plus DNA ladder (ThermoFisher Scientific, USA) was run alongside to identify product sizes.

Table 3.4 *The expected allele specific product sizes for each primer pair during PCR identifies the HP duplication genotype.*

Genotype	Expected products A+B	Expected products C+D
HP1-1	1757	-
HP2-1	1757 + 3481	349
HP2-2	3481	349

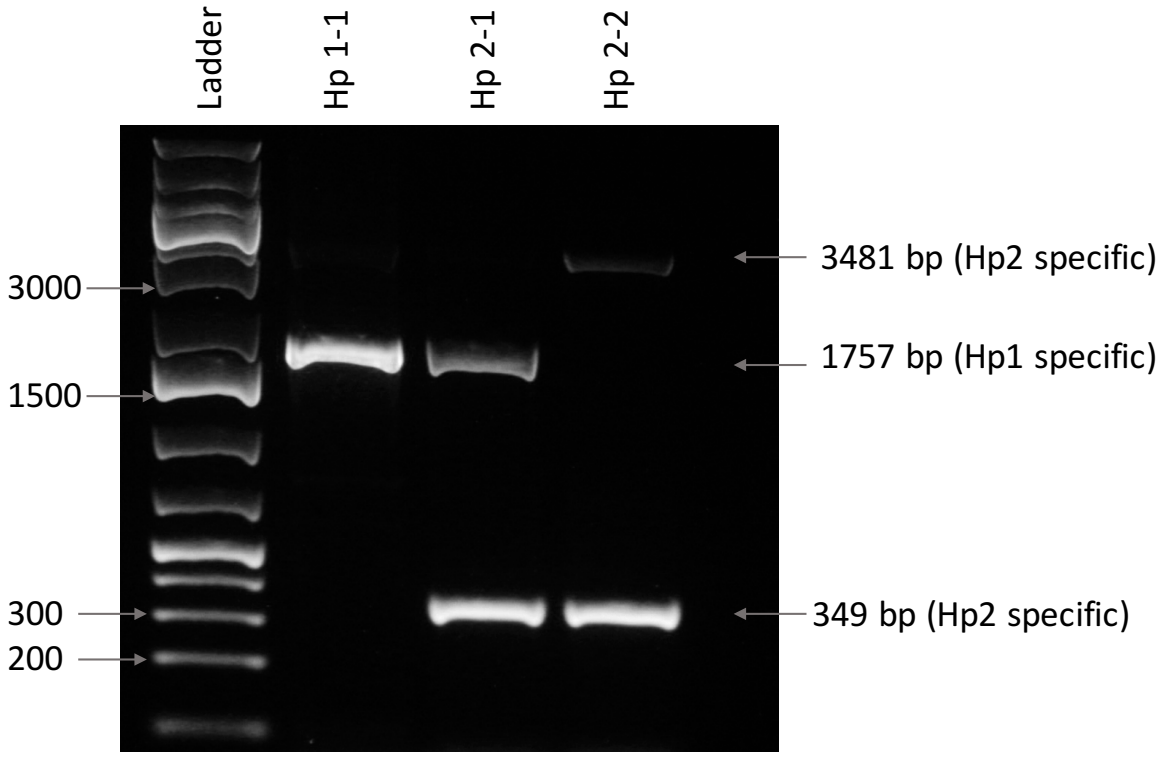

Figure 3.2 *Representative agarose gel image showing PCR products used to genotype individuals. PCR was performed on patient DNA in separate reactions with Primers A & B and C & D. Both reactions for each patient were pooled before loading onto a 1% agarose gel. Lane 1 is a GeneRuler 1 kb plus ladder (ThermoFisher Scientific, USA), lane 2 is the PCR product from a HP1-1 individual, lane 3 shows the products from a HP2-1 individual and lane 4 shows products from a HP2-2 individual.*

In the first instance the protocol from the original Koch *et al.*[137] publication was followed, however this was initially unsuccessful and resulted in no amplification products. As the first optimisation step, DNA concentration and $MgCl_2$ concentration titration experiments were performed. If the DNA concentration is too low there is not enough substrate for the DNA polymerase whilst if too high, this can sterically inhibit the enzyme. $MgCl_2$ is a co-factor for the polymerase enzyme and therefore an optimal concentration is required for the polymerase reaction. These steps resulted in the production of amplification products; the best conditons were 0.6 µg/µL and 0.4 µg/µL DNA for primers A&B and C&D respectively, and 4 mM $MgCl_2$ in both reactions.

However the reaction was non-specific, producing multiple PCR products in addition to the desired HP specific products. A common cause is non-specific binding at room temperature, occurring between preparation of the mixture and thermal cycling. Therefore to improve specificity, the taq DNA polymerase was substituted with Hotstart taq DNA polymerase. The latter enzyme is non-active until it has been through a 10 minute heat-activation phase at 95°C, thus inhibiting non-specific binding during preparation of the reaction mixtures. This was not successful in preventing non-specific amplification, and therefore experiments were performed titrating the annealing temperature. The temperature of the annealing phase of the PCR reaction can result in non-specific products if the primers are able to bind to similar but not fully complimentary sections of DNA. This optimisation step worked well, with an annealing temperature of 72°C, producing sufficient HP specific amplification with minimum non-specificity, to allow accurate HP duplication genotyping.

3.3.2 Quantitative polymerase chain reaction protocol

To enable high throughput, a multiplex quantitative PCR (qPCR) protocol developed by Soejima *et al.*[138] was used to amplify two regions within the HP gene: a 5' internal control region and a region between exons 4 and 5; this is the duplication junction present only in the HP2 allele.

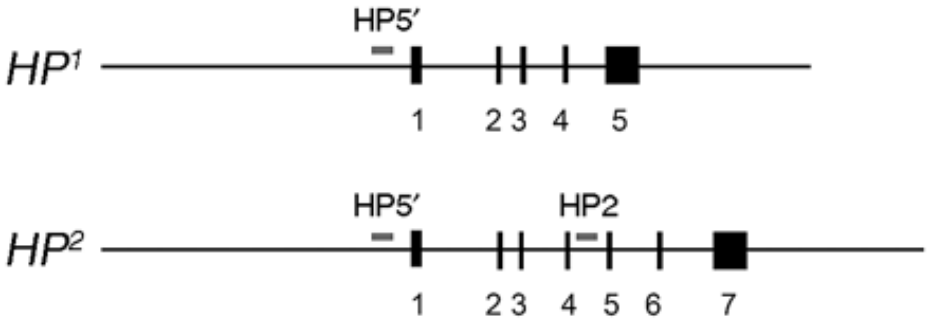

Figure 3.3 S*chematics of both the HP1 and HP2 gene. Exons are numbered and the location of the primer binding sites are identified. Figure from Soejima et al. 2008; reproduced with permission from the publisher.*

10 μL reactions were prepared as described in Table 3.5. Each reaction constituted: Taqman Universal PCR Mastermix (Applied Biosystems, USA), 3 μL of template DNA (5 ng/μL) plus the following primers and probes: Hp5' Forward (150 nM), Hp5' Reverse (150 nM), Hp5' probe (42 nM), Hp2 Forward (300 nM), Hp2 Reverse (300 nM), Hp2 probe (83 nM). Primer and probe sequences are detailed in Table 3.6.

Table 3.5 *Preparation of mastermix for qPCR to type the HP duplication*

	Per sample in triplicate
Taqman Universal PCR mastermix II	15 μL
HP5' Forward primer (150 nM)	0.5 μL
HP5' Reverse primer (150 nM)	0.5 μL
HP5' probe (42 nM)	2.0 μL
HP2 Forward primer (300 nM)	0.5 μL
HP2 Reverse primer (300 nM)	0.5 μL
HP2 probe (83 nM)	2.0 μL

Table 3.6 *Primer and probe sequences used in multiplex qPCR to type the HP duplication.*

Name	Sequence (5'-3') + modifications	Supplier
HP5' Forward	CAC ATT TAC TGA TTT CAG GCT GGA	Eurofins Genomics (Germany)
HP5' Reverse	CCT TTT CAC AGT AAT TTT CTC CAC CT	Eurofins Genomics (Germany)
HP5' Probe	VIC-AGC TTT TAA GCA ATA GGG AGA TGG CCA CA-BHQ2	Applied Biosystems (USA)
HP2 Forward	GGA GCT GCT CTG CAC ATC AA	Eurofins Genomics (Germany)
HP2 Reverse	CCC TTT CAA TGA ATT TCA GGG A	Eurofins Genomics (Germany)
HP2 Probe	FAM-ACC CCG AAT AGA AGC TCG CGA ACT GTA-BHQ1	Eurofins Genomics (Germany)

Raw data were analysed using the ΔΔCt method:

$$1)\ \Delta\text{Ct} = HP5Ct - HP2Ct$$

$$2)\ \Delta\Delta Ct = sample\Delta Ct - Reference\Delta Ct$$

$$3)\ Ratio = 2^{-\Delta\Delta Ct}$$

The reference ΔCt (as used above) was selected from 116 healthy control patients (from the Analysis of the role of inflammation and HLA genotype in age related macular degeneration study, donated by the Vision Sciences group, University of Southampton) whose genotype had been previously established using gold standard PCR genotyping method. Of these, the ΔCt values of the HP2-2 patients were compared. The reference value was selected as the smallest ΔCt (expected result for an HP2-2 individual).

The ranges of ratios for each HP2-1 (0.2-0.46) and each HP2-2 (0.77+) sample were identified from this subset of samples. These ranges were used to type the HP duplication in GOSH. Cases in an intermediate range (0.46-0.77), between the HP2-1 and HP2-2 genotypes, were typed by traditional PCR (see section 3.3.1[137]).

3.3.2.1 Quality control

To ensure accurate typing, 10% of the samples that had been subject to qPCR alone were randomly selected and their genotype assayed via the PCR approach. 151 patients from the GOSH study were selected and genotyped. It was observed that 149 samples had concordant genotypes in both methods, and two samples were discordant; therefore, HP duplication typing had an accuracy of >98%. The discordant samples were retested with both qPCR and PCR. In these repeat assays results were concordant, and matched the first PCR. Therefore these two errors likely arose due to pipetting errors during preparation of the qPCR plates.

3.3.3 SNP genotyping by KASP

Individuals were typed for the rs2000999 SNP genotype by LGC Genomics Ltd. using their commercially available Kompetitive Allele Specific PCR (KASP) genotyping service.

Briefly, KASP is a PCR based Fluorescence Resonance Energy Transfer (FRET) assay. The assay mix contains a forward primer, unique to each SNP and a single common reverse primer. Each forward primer contains a tail sequence which: 1) is unique for each allele 2) is complimentary with, and will compete with, corresponding universal FRET cassettes. One of the strands of the FRET cassette is composed of a sequence complementary to the unique tail sequence on the primer attached to a fluorophore, but this fluorophore is quenched by virtue of FRET from the quencher on the opposite strand.

Throughout the PCR reaction, the allele specific forward primers will anneal to the DNA template depending on the SNP genotype of each individual. This primer will elongate as the polymerase uses the primer to synthesize a new strand; the unique tail region becomes incorporated into the newly synthesized strand.

In second and subsequent rounds of PCR the complementary sequence to the unique tail sequence is synthesized and it is to this that the fluorophore-labelled strand of the FRET cassette is able to bind. The quenching FRET cassette strand and the template DNA compete for the fluorophore-labelled strand of the FRET cassette during each melting round; whilst the fluorophore-labelled strand of the FRET cassette is bound in the FRET cassette no fluorescence is emitted but a signal specific to the SNP genotype is emitted when binding to the DNA template occurs. Genotypes were called automatically by SNPviewer v4.0 (LGC Genomics Ltd., Hertfordshire, UK).

3.3.4 SNP genotyping by Taqman

Cases marked equivocal by SNPviewer after KASP (n=51) were typed using a Taqman assay. Each 5 µL reaction, in triplicate, contained 2.5 µL Taqman genotyping mastermix (ThermoFisher, USA), 0.25 µL 20x assay solution containing primers and probes (C__11439054_10, ThermoFisher, USA) and 2.25 µL genomic DNA. A 7900 HT Fast Real-Time PCR system (Applied Biosystems, USA) was used for thermal cycling (as per kit instructions) and fluorescence reading. Baseline pre-PCR fluorescence data was subtracted from post-PCR data and cluster plots were observed using Taqman genotyping software (v1.4, Applied Biosystems, USA) to call genotypes.

3.3.5 Quality control

30 other cases typed by the KASP assay and successfully called by SNPviewer were cross-checked with the Taqman assay and 100% concordance was observed. Nine out of 1299 samples failed to be called by both KASP and Taqman methods, resulting in a 99.31% call rate.

3.4 Ultra Performance Liquid Chromatography

3.4.1 UPLC analyte measurement

Size Exclusion Ultra Performance Liquid Chromatography (UPLC-SEC) was used to separate the components of patient CSF samples by size. This protocol makes use of the fact that haem absorbs light at 415 nm, therefore monitoring this wavelength facilitated the measurement of haem-containing species only. The molecular species was identified by its retention time on the chromatogram and quantified by measuring the peak's area against a Hb standard curve.

The Hb standard curve was constructed from lyophilized Hb (Sigma-Aldrich, UK). Nine concentrations ranging from 0 to 1 mg/mL were measured at 415 nm on the UPLC. The construction of the Hb standard curve was performed by Dr Zuby Okemefuna, Bio Products Laboratory Ltd. (BPL) whilst developing this in-house Hb binding assay for use at BPL.

Each patient sample was prepared and run on the UPLC in three ways:

1. 60 µL neat CSF.
2. 57 µL CSF + 3 µL 5 mg/mL Hb (Sigma-Aldrich, UK).
3. 57 µL CSF + 3 µL 5 mg/mL Hp (BPL, UK).

50 µL of each sample was injected onto the UPLC column (ACQUITY BEH size exclusion column, Waters, USA) in running buffer (50 mM Tris and 150 mM NaCl, pH 7.5) and absorbance monitored at 415 nm wavelength (as depicted in Figure 3.4). The area of the peak on the chromatogram was calculated using proprietary Empower software (Waters, USA) and this was read against the Hb standard curve.

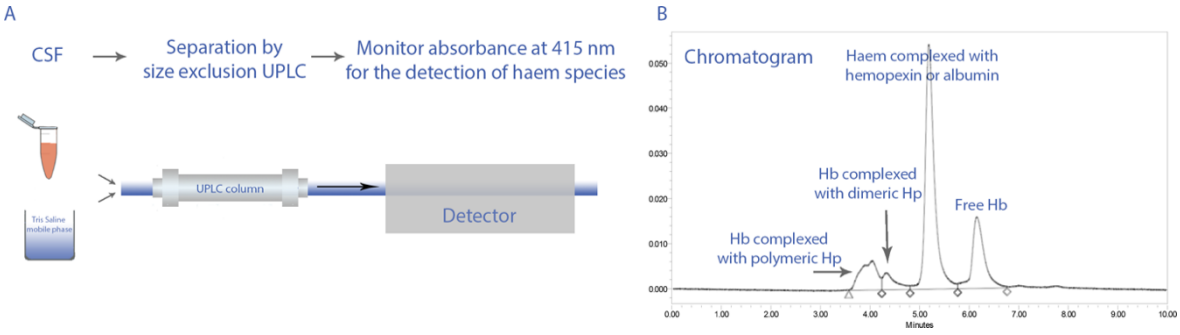

Figure 3.4 *The UPLC-SEC process in which CSF (or CSF+Hp/Hb) were separated on a size exclusion column in a Tris-saline running buffer. Following elution from the column, the separated components of the CSF were detected by spectrophotometric absorbance measurement at 415nm to identify haem containing species.*

3.4.2 UPLC haptoglobin quality controls and run acceptance criteria

3.4.2.1 Haptoglobin controls

UPLC runs were quality controlled using three in-house Hp (BPL, UK) controls of 200 µg/mL (High CSF Control), 10 µg/mL (Low CSF Control) and 1 µg/mL (UltraLow CSF Control) to cover the dynamic range of the assay. Each Hp control was saturated with Hb at the same ratio of sample to Hb as the samples during preparation. These controls were included at the start and end of each UPLC run comprising a maximum of 19 sample injections. Representative chromatograms of these controls can be seen in Figure 3.5.

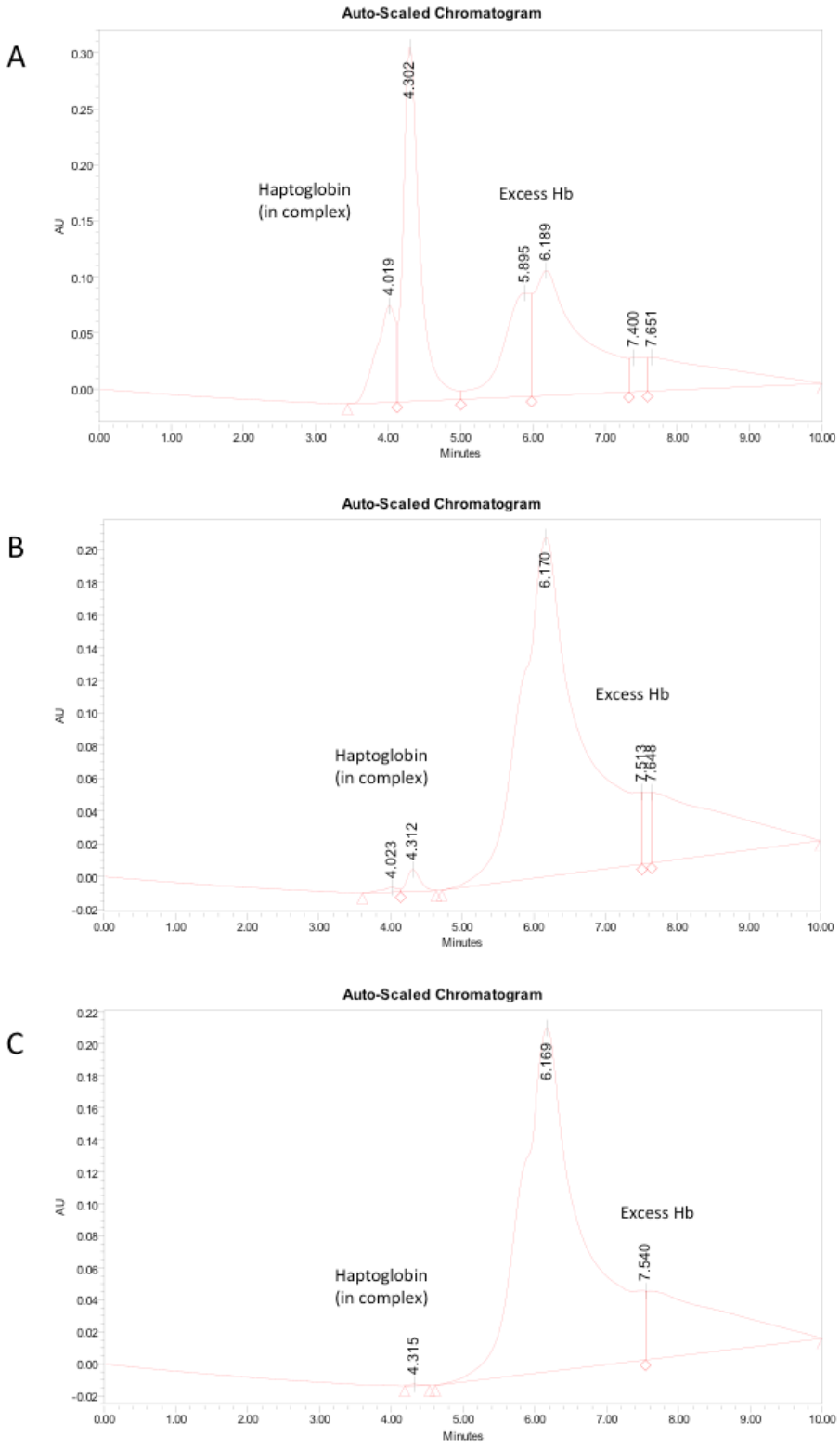

Figure 3.5 *Representative UPLC chromatograms of Hp controls: A) CSF High Control, B) CSF Low Control, C) CSF UltraLow Control*

3.4.2.2 Acceptance criteria

To accept the results for a particular UPLC run, each control had to fall within an acceptance range. For each quality control (High, Low and UltraLow), this range was defined as two

standard deviations either side of the mean, determined from multiple separate runs. These limits are shown in Table 3.7. If the controls were outside these limits the samples in that run were rejected and prepared and run again on the UPLC.

Table 3.7 *Established acceptance criteria for UPLC runs based on variability in Hp control runs.*

	Mean (µg/mL)	**CV**	**N**	**Upper limit**	**Lower limit**
Hp High CSF (200 µg/mL)	180.09	4.18%	61	195.14	165.05
Hp Low CSF (10 µg/mL)	5.74	15.32%	77	7.50	3.98
Hp UltraLow CSF (1 µg/mL)	0.34	27.72%	35	0.52	0.15

3.4.3 Derivations of each analyte

3.4.3.1 Analytes measured from the UPLC chromatograms

The following analytes were measured directly from UPLC chromatograms: total Hp, complexed Hb, total free Hb and non-scavengeable free Hb. Table 3.8 describes how these were derived. Figure 3.6 below shows a representative UPLC chromatogram to identify each aspect described in Table 3.8.

Table 3.8 The derivation of analytes that were measured directly from the UPLC chromatograms.

	Analyte	Derivation
A	**Total Hp**	The area under the **HpHb complex peak** on the chromatogram when CSF + excess Hb are run on the UPLC.
B	**Complexed Hb**	The area under the **HpHb complex peak** on the chromatogram when neat CSF is run on the UPLC.
C	**Free Hb**	The area under the **Hb peak** on the chromatogram when neat CSF is run on the UPLC.
D	**Non-Scavengeable free Hb**	The area remaining under the **Hb peak** on the chromatogram when CSF + excess exogenous Hp are run on the UPLC.

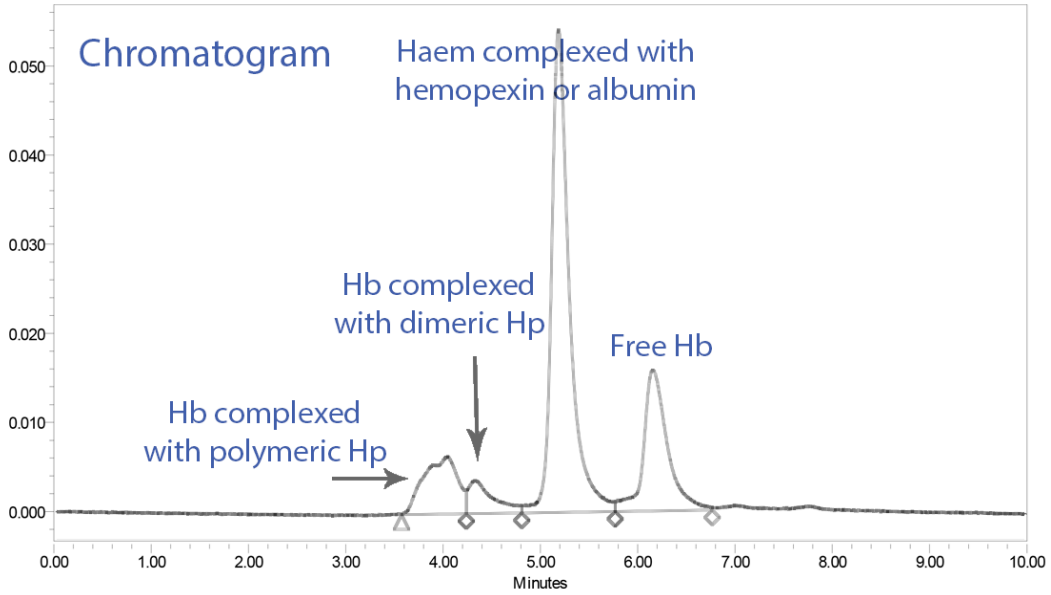

Figure 3.6 *A representative CSF chromatogram demonstrating peaks of Hb complexed to dimeric and polymeric Hp, haem complexed to Hpx and albumin, and free Hb. Peak area-under-the-curve was quantified using a Hb standard curve.*

3.4.3.2 Analytes derived from data

Some analytes were inferred from those derived directly from the chromatograms. These are presented in Table 3.9 with a description of how each was calculated. A schematic of how scavengeable Hb was derived is shown in Figure 3.7.

Table 3.9 *How each analyte is derived from other analytes previously derived in. Letters refer to labels in Table 3.8.*

Analyte	Derivation
Total Hb	**C + B**
Scavengeable Free Hb	**C - D**

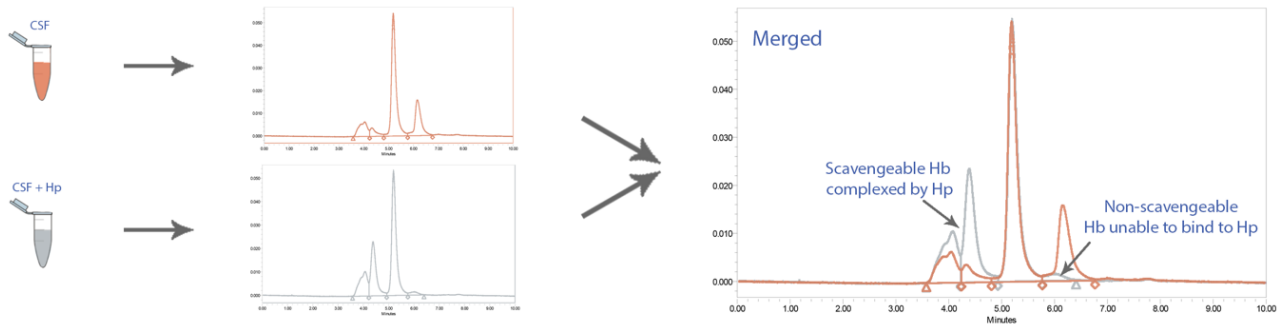

Figure 3.7 *The process by which endogenous Hp was added to CSF samples to identify Hb that was able to be bound to Hp, termed scavengeable Hb. The orange trace represents when a CSF sample is run neat, and the grey trace represents when the same sample is run with exogenous Hp added. Note the shift of Hb (on the right) to HpHb on the left. As the concentration of Hp added was super-saturating, the remaining grey peak on the right of the trace represents Hb that cannot be bound to Hp.*

3.4.3.3 Non-scavengeable Hb correction

The BPL Hp preparation used to spike CSF samples in order to assay non-scavengeable Hb contained small amounts of non-scavengeable Hb. This was quantified to enable correction of non-scavengeable Hb values obtained using this reagent. Five stock tubes of the BPL Hp preparation were prepared for the UPLC, each in triplicate (3 µL 5 mg/mL Hp + 57 µL sample diluent consisting of 0.9% NaCl and 100 mM EDTA. The area under the free Hb curve was measured against the Hb standard curve, as had been done previously for CSF analysis. It was reasoned that, as this was a Hp solution, any free Hb must be non-scavengeable Hb. The data are shown in Figure 3.8.

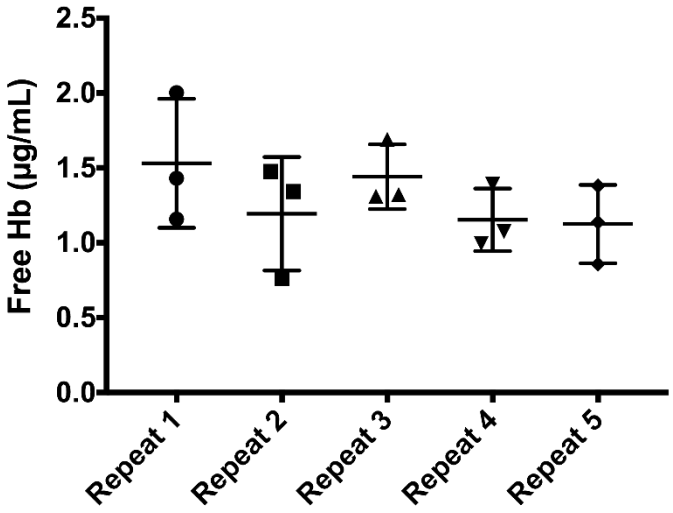

Figure 3.8 *Non-scavengeable free Hb measured in the BPL Hp preparation as measured by UPLC. Data are presented as mean ± SD.*

The mean non-scavengeable Hb value was 1.289 µg/mL. To correct for the carry over into CSF samples, the mean + 2 SD (1.918 µg/mL) was subtracted from each non-scavengeable Hb value to achieve a 5% Type I error tolerance.

3.4.4 Serum THBC measurements

In Hp1-1 patients, matching serum collected at the same timepoint as the CSF was assayed for total Hb binding capacity (THBC) by UPLC to enable calculation of intrathecal Hp synthesis by calculation of the Hp index. The UPLC protocol for differs from CSF due to its higher protein content. The serum samples were diluted 1:2 with either sample diluent (0.9% NaCl, 10 mM EDTA) or 5 mg/mL Hb solution and 5 µL of each preparation was injected onto the UPLC column (ACQUITY BEH size exclusion column, Waters, USA) in running buffer (50 mM Tris and 150 mM NaCl, pH 7.5) and absorbance monitored at 415 nm wavelength. The area of the peak on the chromatogram was calculated using proprietary Empower software (Waters, USA) and this was read against the Hb standard curve.

3.4.5 Albumin quotient, haptoglobin quotient and haptoglobin index analysis

Albumin is not synthesized within the CNS, and the albumen quotient (Qalb = CSF albumin/serum albumin) was used to quantify BBB impairment after SAH. Only samples from day four onwards were to exclude albumin entering the CSF through the bleed. Temporal analysis of Hp in the CSF indicated that by this time point bleed-derived excess of plasma proteins were cleared from the CSF. Since Hp1-1 has a similar molecular weight to albumin, the Hp intrathecal index (Hp index =

QHp/Qalb) was used to quantify intrathecal Hp1-1 synthesis in Hp1-1 individuals. Matched CSF and serum samples from day four onwards were measured for albumin by NHS clinical biochemistry using a spectrometric assay run on a Beckman Coulter clinical chemistry analyser. The assay relies on the reaction of albumin with Bromocresol Purple to form a coloured complex; absorbance is then measured at 600 nm to obtain an albumin measurement.

3.4.6 Calculation of bleed size volume

The volume of the blood clot in the subarachnoid space was calculated to control for the size of the bleed between patients in statistical analysis of effects of Hb in the CSF. CT imaging of the head was available for 38 patients of the HASH study and volumetric blood clot volume was calculated using Medical Image Processing, Imaging and Visualization v7.2 software. To ensure standardisation, all CT images were acquired using the same protocol within the first three days post-ictus, using contiguous slices. The radiodensity threshold of CT images was set between 50 and 80 Hounsfield units, and converted to binary mask. Regions of interest representing SAH and total blood clot were drawn manually on each slice, and grouped into single 3D volumes.

3.5 Primary hippocampal cell culture

3.5.1 Statement of ethics

All animal experiments were approved by the University of Southampton Ethics committee and conducted in accordance with the United Kingdom Home Office Animals (Scientific Procedures) Act 1986. The work in this section was performed under Schedule 1 of the act: appropriate methods of humane killing.

3.5.2 Culture protocol

Hippocampal and cortical cultures were prepared from post-natal day 0 (P0) C57BL/6 mice. Mice were culled via Schedule 1 cervical dislocation and were subsequently decapitated. The brain was dissected and transferred to Hank's Balanced Salt Solution (HBSS) (Gibco, Life Technologies). Under the dissection microscope the midbrain was removed and the two hemispheres were separated. The hippocampus was identified in each hemisphere and carefully removed by cutting away the surrounding cortical tissue. Once isolated, the hippocampi and cortex were collected in separate 15 mL centrifuge tubes (Corning, USA) containing HBSS.

The hippocampal and cortical neurones were dissociated using a kit designed for post-natal neurons (Miltenyi, Germany). 2 mL of enzyme mix 1, as detailed in Table 3.10 was added to each

neuronal preparation. The tissue was incubated at 37°C for 15 minutes on a shaker. 30 µL of enzyme mix 2 as described in Table 3.10 was next added to each preparation and the tissue was gently agitated by pipetting up and down 10 times before further incubation at 37°C for 10 minutes on a shaker. An additional 15 µL of enzyme mix 2 was added followed by trituration until a cell suspension had formed. The suspension was filtered through a 100 µm cell strainer and the enzymatic activity of the neural dissection kit stopped by dilution with 10 mL BSA solution. The cells were pelleted by centrifugation at 130 g for 10 min and the resulting pellet was resuspended in 1 mL filter sterilized neuron media (Table 3.11).

Table 3.10 *Enzyme mixtures from Miltenyi neuron dissociation kit used for the digestion of brain tissue to produce a cellular suspension. Enzymes and buffers in the Miltenyi kit are proprietary information.*

Enzyme mix 1			**Enzyme mix 2**	
Enzyme P (sol 1)	Buffer Z (sol 2)	B-mercaptoethanol 1:1000	Buffer Y (sol 3)	Enzyme A (sol 4)
10 µl	1950 µl	10 µl	30 µl	15 µl

Table 3.11 *Constituents of Neuron Media.*

Volume	Reagent
1 ml	50 x Neurobrew
500 µl	GlutaMAX
48.5 ml	Neurobasal media

12 well culture plates were prepared with a circular glass cover slip in the centre of each well. The cover slip and outer ring of the well were coated in poly-D-Lysine. Hippocampal cells were seeded onto the central glass coverslips at a density of 5000 cells/well and cortical cells were seeded around the perimeter of each well at a density of 200,000 cells/well. Cultures were maintained at 37°C and 4% CO_2 for one week to allow the establishment of neuronal networks.

3.5.3 Assessment of viable cells

Cells were fixed in 4% Paraformaldehyde (PFA) for 30 minutes and the glass coverslips removed. Immunocytochemistry for Microtubule-associated Protein 2 (MAP2) with 4', 6-diamidino-2-phenylindole (DAPI) counterstaining was performed on coverslips to enable visualization of viable neurones. Following staining, coverslips were mounted onto slides and viewed at x40 magnification. Moving in a linear direction from top of the coverslip to the bottom, viable cells were counted and compared to controls. Viable neurones were defined as MAP2-positive cells with clearly defined dendritic processes and well defined healthy nuclei.

3.5.4 Haptoglobin neurotoxicity experiment

Established neuronal cultures were allowed to mature for 7 days and then the culture media was supplemented with either vehicle (saline), Hp5911 (BPL Hp preparation) or a purified fraction of Hp5911. Hp fractions were loaded at equivalent amounts to their proportion in the original Hp5911 preparation. Cultures were maintained for 14 days and treatment of each condition was re-treated during the media change.

3.5.5 Haemoglobin neurotoxicity experiment

Established neuronal cultures were allowed to mature for seven days and then the culture media was treated with a mouse haemolysate prepared as detailed in Section 3.5.8 containing the following range of Hb concentrations: 0.1 µM, 1 µM, 10 µM, 25 µM, 50 µM. The cultures were maintained for a further 7 days and re-treated with each condition during the media changes.

3.5.6 Haptoglobin efficacy experiment

The established neuronal cultures were treated with a pre-mixed solution of mouse haemolysate (as above) and an equimolar concentration of Hp (Bio Products Laboratory, UK). The cultures were maintained for a further seven days and re-treated with each condition during the media change.

3.5.7 Hp5911 dialysis

5 mL of BPL Hp5911 Hp preparation was added to dialysis tubing with a 20 kDa size cut off and placed in 1L 0.9% Saline on a stirrer plate. The solution was dialysed for seven days and the 0.9% saline solution changed twice a day. During the day the dialysis vessel was stored at RT and at 4°C overnight.

3.5.8 Production of a murine haemolysate

Adult C57BL/6 mice were terminally anaesthetised by intraperitoneal (I.P.) administration of 50 µL pentobarbital. The peritoneal cavity was opened and the diaphragm removed to expose the heart. Blood was collected via cardiac puncture and transferred to heparinized Eppendorf tubes.

4 mL of collected blood was combined with 14 mL endotoxin-free PBS (Gibco, ThermoFisher Scientific, USA) and centrifuged at 475x g for 15 minutes. The supernatant and a buffy coat was removed and replaced with 14 mL endotoxin-free PBS. This process was repeated until the supernatant was colourless. Deionised water was added to the collected erythrocytes at a ratio of 4 mL of dH_2O per 1 mL of cells to lyse them. Following this the solution was centrifuged at 13000 RPM for 30 minutes to removed ghost membranes of the lysed erythrocytes. The resulting pellet was discarded leaving a haemolysate solution (the supernatant).

3.6 *In vivo* methods

3.6.1 Statement of ethics

All animal experiments were approved by the University of Southampton Ethics committee and conducted in accordance with the United Kingdom Home Office Animals (Scientific Procedures) Act 1986 under project licence 30/3057. All animal experiments were performed at the University of Southampton Biomedical Research Facility. Animals were housed in conditions with a 12 hours light/dark cycle with food and water available *ad libitum*.

3.6.2 Experimental subarachnoid haemorrhage model

An injection model of SAH in mice developed by Dr R. Loch Macdonald's group was used here[120]. Competency in the technique was achieved through a period of training in their laboratory in April 2015. C57BL/6 males aged either 2 months or 3-4 months were anaesthetised with isoflurane (5-3%), or a ketamine (Bayer) and xylazine (Pfizer) mixture (100 and 10 mg/kg, respectively) (as detailed Chapter 7). The head was shaved and then fixed in a stereotaxic frame. A burr hole was drilled 4.5 mm anterior of bregma and 1 mm laterally. Visual landmarks of the vasculature crossing between the eyes was used to identify the site of drilling. The drill was angled at 40° and the hole was filled with bonewax (Covidien, NHS supply chain) to prevent leakage of blood during injection and maintain ICP. A laser Doppler probe was positioned flat on the surface of the skull, as posterior to the burr hole as possible, ensuring it was not directly above a major blood vessel.

A blood donor animal was anaesthetised with 5% isoflurane or a ketamine (Bayer) and xylazine (Pfizer) mixture (100 and 10 mg/kg, respectively) (as detailed Chapter 7). The peritoneal cavity was opened and the diaphragm removed to expose the heart and approximately 300 µL of blood was collected via cardiac puncture using a glass syringe (Hamilton, USA). Once collected the animal was immediately sacrificed via cervical dislocation.

A 27 gauge spinal needle with a Whitacre tip was attached and the Hamilton syringe was fitted to a syringe driver on the arm of the stereotaxic frame. The needle was inserted through the burr hole at a 40° angle until the base of the skull was reached; the needle was withdrawn slightly so the tip was in the prechiasmatic cistern. Either 100 µL or 60 µL of blood was injected with the syringe driver at a rate of either 300 µL/minute or 200 µL/minute using a syringe driver (as detailed Chapter 7). Cerebral tissue perfusion was monitored by laser Doppler. The needle was left in place for 5 minutes to allow sufficient time for clot formation and to prevent reflux up the needle tract. Following removal, the burr hole was closed with bonewax and the incision sutured. Control animals received an injection of sterile saline in the prechiasmatic cistern as opposed to blood.

3.6.3 Behavioural assessment

3.6.3.1 T maze spontaneous alternation

Spontaneous alternation in mice was assessed using a T maze as a measure of working spatial memory[139]. Within the maze, a 0.5 mm layer of bedding was placed at a ratio of 70:30 clean to soiled bedding. The addition of soiled bedding from another cage separate to the animal's home cage provided motivation for the animals to run the maze and promoted spontaneous activity.

The mouse was placed in the start arm, facing away from the goal arms and the time taken for it to enter a goal arm was measured. The goal arm entered (right or left) and the time taken to enter was recorded. Upon entering a goal arm, the guillotine door was closed and the mouse allowed to explore the goal arm for 30 seconds. The mouse was classed as entering the start arm once the tip of its tail had passed the guillotine door of that arm. The central partition was removed and the mouse was again placed in the start arm of the maze, facing away from the goal arms and allowed to run the maze a second time. The time taken to enter a goal arm and the goal arm entered (left or right) on the second run was recorded. A cut off time of 90 seconds was used; if the mouse failed to enter a goal arm within this time then it was recorded as a failed run attempt. Four trials were performed per day, typically two in the morning and two in the afternoon equalling 20 trials per week. Repeat trials of each animal were separated by a minimum of 10 minutes.

If animals alternated the arm chosen they received a score of 1, if they failed to alternate they would receive a score of 0. The scores were summed and expressed as a percentage of the total number of trials (20 trials). Failed run attempts were not included in analyses. For example if across 20 trials an animal successfully alternated 10 times, then its rate of alternation can be calculated as 10/20=0.5.

3.6.3.1.1 T Maze habituation

Animals were run through the T Maze for 20 trials, spread over the course of one week, prior to SAH surgery. This was to acquire baseline pre-surgery data for each animal. The average of blocks of four trials were plotted to investigate habituation of the mice to the test. This can be seen in Figure 3.9; there is consistently 60-70% spontaneous alternation, even from the first attempts at the maze indicating there is no requirement for a habituation or learning phase of the task.

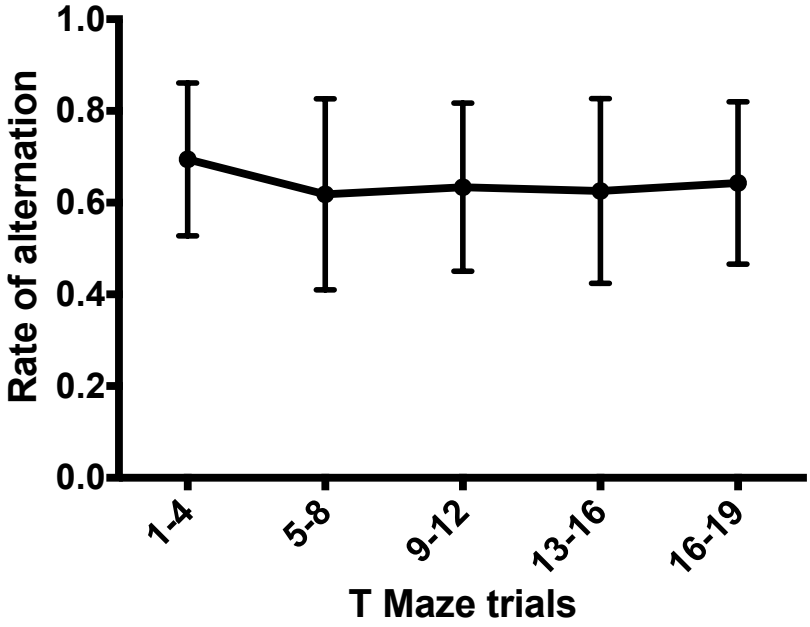

Figure 3.9 *The average spontaneous alternation behaviour. Data show the average of block of four trials to investigate habituation to the behaviour test. There is uniform alternation occurring across the 20 trials, indicating that there is no requirement for a habituation stage. Data are expressed as mean ± SD.*

3.6.3.2 Burrowing behaviour

Burrowing behaviours in the mouse were assayed as described in Deacon *et al.* 2006[140]. Prior to assessment of burrowing ability, animals were habituated to the assay. This involved placing a burrowing tube (made in-house) filled with food pellets into the cage of group housed animals overnight. The following evening animals were individually housed with a burrowing tube filled with food pellets placed in their cage. The burrowing tubes were inspected the following morning. If all of the animals had successfully burrowed the contents of the tube then they had become habituated or they had *learnt* the assay. If an animal was found not to have completely burrowed the entire tube of pellets, the habituation process was repeated until all the animals burrowed; this allowed the other animals to *teach* the mice that failed.

Assessment of burrowing was made at baseline (pre-surgery) and at days 7 and 14 post-surgery. Burrowing tubes filled with food pellets were weighed and left in the animal's cage overnight. Tubes were recovered the following morning and weighed to assess the weight of pellets burrowed.

3.6.3.3 Open field arena

Behaviour was assessed using the open field behaviour paradigm. Mice were placed in the centre of a laser-monitored behaviour arena (Med Associates, USA). Recording began automatically and continued for a five minute period. Habituation occurred for three days prior to surgery, and the final session was recorded as a baseline score of behaviour. Post-surgery, mice were assessed daily from day two onwards. Testing was performed in the same room and at the same time each day, under the same light conditions, by the same operator.

Measurements were made of ambulatory distance, ambulatory velocity, number of ambulatory counts, number of vertical counts, number of stereotypic counts, number of jump counts and duration resting.

The preference for a mouse to spend time in the periphery close to the walls of the arena (as opposed to venturing into the centre of the open field) is termed thigmotaxis and is often interpreted as an anxious phenotype[141]. Therefore a zonal analysis was performed in which the arena was divided into the centre zone and a peripheral zone.

3.6.4 Tissue harvesting

Animals were euthanized with 50 µL pentobarbital and transcardially perfused through the left ventricle with heparinised-10mM glucose-PBS followed by 20 mL 20µM 5-(6)-Carboxy-X-rhodamine, succinimidyl ester (ROX SE) dye in 10mM glucose-PBS prior to perfusions with 4% PFA (in PBS). Brains were extracted and post-fixed in 4% PFA in the dark at 4°C for 24 hours before being transferred to PBS.

3.6.5 Fluorescent imaging of circle of Willis to assess vasospasm

Brains were assessed for vasospasm by fluorescent imaging of the major arteries of the circle of Willis in a technique established by the Zipfel group[142]. Arteries were visualised by staining with ROX SE during perfusion fixation (see Section 3.6.4). This is a rhodamine analogue dye that forms NHS esters with amine side chains of proteins on the surface of endothelial cells.

Brains were placed *en bloc* on a glass coverslip and gently covered in PBS before placing on the stage of an SP8 confocal laser scanning microscope (Leica, Germany). Vessels were imaged at 1024 x 1024 pixel resolution with four line averaging, 10x magnification and 0.75 zoom using an excitation laser wavelength of 561 nm and monitoring emittance between wavelengths of 572 – 699 nm. Z stacks were generated through the entire vessel with spacing of 10 µm. The z stack data were visualized in two dimensions using the maximum projection function.

Photomicrographs were acquired of the Anterior Cerebral Artery (ACA), Middle Cerebral Artery (MCA) and the Posterior Communicating Artery. Measurements of vessel thickness were made in ImageJ (National Institute of Health, USA) using the line tool and measure function by drawing from one wall of the vessel to the other in a perpendicular direction. Measurements were made at the narrowest point across the first 1 mm of the vessel.

3.6.6 Histology

Sections were dewaxed in xylene and rehydrated through graded concentrations of ethanol. Protocols for each marker or stain are described below.

3.6.6.1 Iba-1

Endogenous peroxide activity was quenched with 3% H_2O_2 in methanol for 10 minutes. Antigens were retrieved by incubating slides in citrate buffer in a pressure cooker for two minutes. Sections were then blocked in medium containing DMEM, fetal calf serum and bovine serum albumin for 20 minutes at RT. Primary antibody was incubated at 4^{o}C overnight (1:5000 anti-rabbit iba1, Wako). Following three washes in TBS, sections were incubated with biotinylated goat anti-rabbit secondary antibody (1:1000, Vector Labs) for 30 minutes at RT. Sections were washed three times in TBS and then incubated in ABC solution for 30 minutes at RT. Sections were washed three times followed by development by 0.05% w/v 3,3'-Diaminobenzidine (DAB) and 0.015 v/v hydrogen peroxide for two minutes. Sections were counterstained in haematoxylin, dehydrated through increasing concentrations of ethanol and cleared in xylene prior to mounting using DPX mounting medium.

3.6.6.2 Synaptophysin

Antigens were retrieved by incubation at 65^{o}C in 0.2M boric acid (pH 9) for 30 minutes. Endogenous peroxide was quenched using 0.3% hydrogen peroxide in PBS. Sections were then blocked in 10% normal goat serum for one hour at RT in PBS before incubation with primary antibody (anti-synaptophysin, 1:2000, Millipore) in the same blocking solution at 4^{o}C overnight. Sections were washed three times in PBS then were then incubated in biotinylated anti-mouse secondary antibody (Vector Labs) in PBS for one hour at RT. Sections were washed three times for five minutes each in PBS prior to incubation in ABC solution for 45 minutes. Sections were developed with 0.05% w/v DAB and 0.015% v/v hydrogen peroxide in 0.1M phosphate buffer for three minutes. Sections were washed again for a final three times in PBS and mounted in DPX mounting medium.

3.6.6.3 Perls' staining

Perls' reagent consists of potassium ferrocyanide and hydrochloric acid. The hydrochloric acid denatures iron-binding proteins (such as haemosiderin and ferritin) releasing ferric iron. Potassium ferrocyanide then reacts with ferric iron to produce ferric ferrocyanide which is an insoluble blue pigment. The staining is amplified by development with DAB.

Sections were incubated in 7% w/v potassium ferrocyanide and 2% v/v hydrochloric acid (mixed in a 1:1 ratio) at 40^{o}C. Following a wash in distilled water, endogenous peroxidase activity was quenched in 0.3% v/v hydrogen peroxide in TBS for 30 minutes at RT. Sections were developed in 0.05% w/v DAB and 0.015% v/v hydrogen peroxide in 0.1M phosphate buffer for seven minutes. Of the two sections per slide, only one was counterstained with haematoxylin; the unstained section was used for Perls' quantification. Sections were dehydrated through graded ethanol/water solutions and cleared in xylene prior to mounting with DPX mounting medium.

3.6.7 Imaging and analysis

To ensure blinding, all samples were coded prior to image capture and analysis. Images were captured using a DM4B microscope (Leica, Germany).

3.6.7.1 Iba-1

Sections were viewed under x20 magnification of the striatal region proximal to the blood clot and at 40x magnification of the hippocampus. Iba-1 positive cells, whose nuclei were clearly visible were counted using a 10 mm reticule with a 10 x 10 grid. In the striatum cells were counted in two non-overlapping regions: 1) the basal surface of the brain, encompassing the ventral striatum on the ipsilateral side of injection, and 2) more superiorly, in a central region of the striatum. In the hippocampus, cells were counted in a region encompassing the molecular layers of the stratum radiatum (SR) and stratum lacunosum moleculare (SLM). Two sections per animal were counted and means were calculated for striatal and hippocampal regions. Representative images were captured at 20x magnification in both regions.

3.6.7.2 Synaptophysin

Images were taken at x10 magnification in order to image multiple strata of the hippocampus ipsilateral to the injection site. Staining was quantified according to a method established by Cunningham *et al*[143], to quantify staining as a ratio between regions normalised to the background staining intensity. Hippocampal strata pixel densities were measured using ImageJ software (NIH, USA. The dentate gyrus (DG) granular cell layer (the area of highest transmittance) was used as an

internal control for each section and other strata transmittances were adjusted by subtraction of the DG transmittance from this layer's transmittance. A ratio was then calculated using the adjusted transmittances for the SR and the SLM: Ratio = $(T_{DG} - T_{SR})/(T_{DG} - T_{SLM})$. One section per animal was analysed.

3.6.7.3 Perls' staining

Brightfield images of non-counterstained sections were obtained at x20 magnification. Using ImageJ, images were converted to 8 bit format, and were subjected to the same thresholding. The area fraction of staining in the whole ipsilateral hippocampus was then quantified to represent the degree of non-haem iron deposition.

3.7 Statistical analysis

Normality was routinely determined across all data sets using the Kolmogorov-Smirnov test. Where necessary, log(10) or Ln transformation was used to normalise data. Results were considered significant at p=0.05. Two-tailed hypotheses were considered throughout. Statistical analysis and graph creation was carried out using SPSS (v24) and GraphPad Prism (v7.01), with data expressed as mean ± standard deviation (SD), mean ± standard error of the mean (SEM), or median ± interquartile range (IQR), as stated in relevant figure legends. Detailed methods of statistical modelling are explained in detail in Chapter 4 and Chapter 5 where relevant.

Chapter 4 Haptoglobin genotype and clinical outcome after aneurysmal subarachnoid haemorrhage

4.1 Introduction

After SAH, erythrocyte lysis results in high concentrations of free Hb in the CSF. There is evidence that cell free Hb is a contributor to pathology after SAH, causing direct neuronal death[21] and contributing to vasospasm and DCI. It has recently been shown that the brain has a limited capacity to clear this Hb[102].

Extracellular Hb and its clearance by Hp may be an important modifier of outcome after SAH. Six studies have suggested an association between HP genotype and outcome; these studies were relatively small in size and only looked at the HP duplication (HP1 vs HP2)[107-111,113].

The mechanistic basis for the difference in outcome between HP1 and HP2 is not yet clear. These include:

1) Hp expression level. This is a fairly consistent finding in the literature. Serum Hp levels are higher in HP1-1 > HP2-1 > HP2-2.
2) Hb clearance. There are multiple points in Hp's mechanism of Hb scavenging where differences between isoforms may reside, as listed below. Multiple studies in the literature have investigated these isoform differences, and reports are not always in agreement, as summarized in Appendix B.
    I. affinity for Hb
    II. inhibition of Hb's oxidative potential
    III. inhibition of haem release from Hb
    IV. inhibition of NO scavenging by Hb
    V. affinity for CD163
    VI. uptake by $CD163^+$ macrophages

In distinguishing between 1) and 2), above, a study of the association between clinical outcome and Hp level (in CSF and/or serum) may be considered. However such a study would be challenging for a number of reasons. First, an opportunity to sample CSF in SAH patients only occurs in high-grade patients requiring external ventricular drainage (EVD), leading to a biased patient population. Second, the Hp level is not an accurate reflection of Hb scavenging since it does not take into account the rate of Hp recycling. Also, Hp level is influenced by a variety of

other factors. For instance, Hp expression increases during inflammation[144], because of an IL-6 response element in the promoter region of the gene. Additionally, a number of CNS-resident cell types are able to express Hp during inflammatory processes; for example oligodendroglia are able to express Hp during CNS haemorrhage[58]. Further, during SAH Hp levels in the periphery are observed to decrease due to scavenging of HpHb complexes by CD163+ macrophages[102].

In view of these complexities, a genetic approach was considered. The SNP rs2000999 is the strongest known determinant of Hp expression[65], so can be used as a proxy to investigate the relationship between Hp expression capacity and outcome after SAH. A genetic approach facilitates a large study sample size, since DNA is more readily available than CSF. rs2000999 is a G→A SNP which explains up to 45% of the genetic variation in Hp circulating levels[65]. It is located 17 kb downstream of the HP duplication mutation, in an intronic region of the haptoglobin-related protein gene. A number of cohorts have been used to replicate the effects of rs2000999 on Hp levels and these are presented by Froguel *et al.* 2012[65]. The use of the rs2000999 polymorphism would enable me to work out whether the difference in outcome with HP duplication genotype was due to differences in 1) Hp expression level, or 2) Hb scavenging efficiency, between the HP isoforms.

The over-arching hypothesis in this chapter is that an individual's HP genotype affects outcome after SAH. Specifically, I hypothesize that 1) In SAH patients, a HP genetic variation driving Hb clearance (HP duplication) affects outcome after SAH; 2) In SAH patients, a HP genetic variation driving serum Hp concentration (rs2000999) affects outcome after SAH.

In order to address these hypotheses, aneurysmal SAH patients from the Genetics of Subarachnoid Haemorrhage (GOSH) study were genotyped for their HP duplication status using in house genotyping assays and typed for their rs20009999 status with commercial KASP genotyping technology (LGC Genomics, Hertfordshire, UK). GOSH was a study investigating the genetics of aneurysmal rupture risk, and therefore recruited patients with ruptured and unruptured aneurysms; clinical outcome was also recorded using mRS and GOS at the time of recruitment.

A missingness analysis was conducted to determine whether the HP genotype or rs2000999 affected early mortality after SAH, by comparing the frequency of genotypes in the GOSH cohort with that of a control cohort. The latter cohort was a subset of the ALSPAC (Avon Longitudinal Study of Parents and Children) study, previously genotyped for the HP duplication and rs2000999 (n=927)[145]. This population of young adult (18-20 year old) mixed-gender community dwellers in England, was ideal to determine genotype frequencies with minimal bias as a result of disease, country of origin, gender and healthcare, in a population relevant to the GOSH study.

In the outcome analysis, the *a priori* planned primary outcome was long term outcome on follow up as measured by mRS. Secondary outcomes included GOS at follow up, mRS and GOS scores at discharge, TCD confirmed vasospasm, DIND and length of time from ictus to discharge from hospital.

4.2 Results

4.2.1 The effect of the HP duplication and rs2000999 on Hp expression level in healthy individuals

Both the HP duplication and rs2000999 have been reported to influence serum Hp in a number of non-British ethnic groups[62,65,69,146-154]. In this study, it was important to assess the contribution of the HP duplication and rs2000999 to serum Hp levels in a British population, similar to the GOSH SAH population. To this end, I studied individuals from the ALSPAC study in whom both HP genetic variations and Hp serum concentration were available (n=325). Association of HP duplication and rs2000999 type with Hp serum level was investigated using multiple regression with Hp level as outcome and the HP duplication, rs2000999 and gender as explanatory variables. Age was not included as a covariate as all participants were around 20 years old, and age does affect Hp serum level[65]. It was found that the HP duplication and rs2000999 influenced Hp serum levels to a similar extent: the HP2 allele and the rs2000999 A allele were associated with a decrease in serum Hp of 0.26 and 0.14 g/L, respectively (Table 4.1). An effect of male gender was also found to associate with a 0.14 g/L reduction in serum Hp level.

Table 4.1 *Multivariate linear regression of Hp serum level vs the HP duplication and rs2000999 in an ALSPAC subpopulation (n=325) (model fit: r squared = 0.23, p = 2.2×10^{-16}).*

	Coefficient	SE	Lower 95% CI	Upper 95% CI	p value
HP duplication	-0.2641	0.0354	-0.334	-0.195	**8.46×10^{-13}**
rs2000999	-0.1356	0.041	-0.217	-0.054	**0.00124**
Gender (male)	-0.136	0.046	-0.227	-0.045	**0.0037**

4.2.2 SAH population: demographic and patient characteristics

This analysis utilized aneurysmal SAH patients from the GOSH study. A flow diagram of participants from the GOSH study used in this analysis is shown in Figure 4.1 in accordance with the STrengthening of Reporting of OBservational studies in Epidemiology (STROBE) guidelines[155].

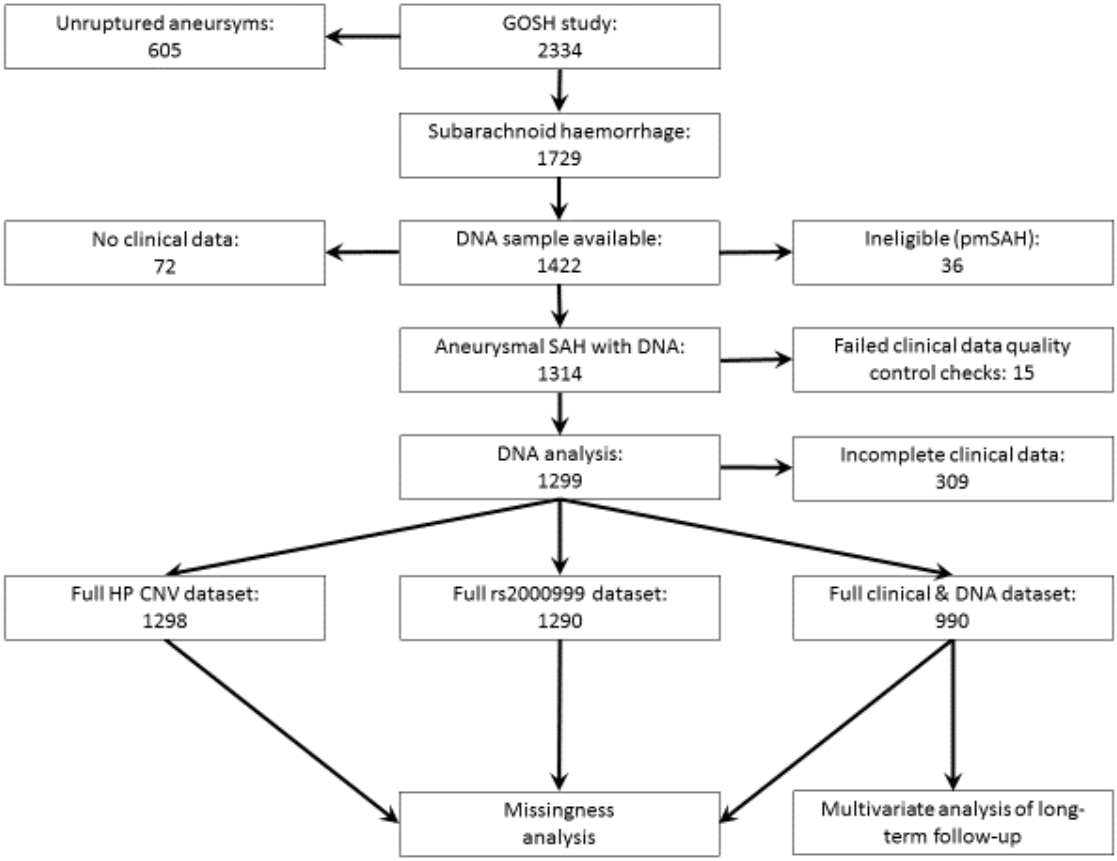

Figure 4.1 *STROBE (strengthening the reporting of observational studies in epigenetics initiative) flow diagram detailing progress of selection of patients from the GOSH study for analysis.*

The demographics and clinical characteristics of the GOSH study population are presented in Table 4.2, for the two types of analyses conducted: 1) missingness analysis, and 2) outcome analysis. This is because clinical data were not available for all patients who were genotyped, who therefore could not be entered into the outcome analysis. GOSH was a study of long term outcome in SAH survivors, since patients were assessed after recovery from the acute phase of SAH, with a median time from ictus of 18 months (IQR: 27 months). In fact 68% of patients in GOSH had a good outcome at discharge (by mRS score) and a significant higher rate of lower

Fisher grades (I-II), compared to a recent multicentre study recruiting mostly from the UK[156] (39% *vs* 16% respectively, χ^2=120.8, p<0.0001). This is because patients who died after admission or experienced significant morbidity would not have been recruited to the GOSH study, due to its retrospective design.

The cohort is mostly women (70%); incidence of SAH is higher in women and other study populations have a similar gender ratio[107-110,157,158]. The mean age was 53 years; this is within the expected age range of SAH patients and similar to other SAH populations[107,109,110,157,159].

Hydrocephalus occurred in approximately one third of the cohort (35%) which is in line with the expected rate of hydrocephalus[108,160] and there was no significant difference in the incidence of hydrocephalus between the three HP duplication genotypes. Hypertension was slightly more frequent in the HP1-1 group, however this was not statistically significant. The prevalence of hypertension in this study was 29.7%, and was similar to the rate of those taking blood pressure medication (22.4%). This is low, compared to a recent UK SAH audit (35.6%)[11]. The majority of patients received an aneurysm coiling procedure (76%), followed by aneurysm clipping (20%). This is in line with modern clinical practice[161], which prioritises coiling over clipping due to better expected outcome[162]. 1.1% of patients received no aneurysmal treatment.

Transcranial Doppler (TCD) to assess large vessel vasospasm was only performed regularly at a subset of centres (King's College Hospital, National Hospital for Neurology and Neurosurgery, Newcastle, Royal Preston, University Hospital Southampton and James Cook University Hospital). Of the patients from these centres who were assessed with TCD, 23.2% had vasospasm; this is lower than expected[163]. DIND[6] occurred in 20.6% of cases, similar to that observed in SAH studies in the literature[164].

Table 4.2 *Demographics and clinical characteristics for GOSH participants included in the missingness analysis[a] and clinical outcome dataset[b]. Notes: Mean & range[c], number and %[d], median & range[e], % is of available data[a] or of total data[b].*

	Missingness analysis[a]	**Outcome analysis[b]**
Number	1299	990
Age (years)[c]	53, 16-92	54, 19-92
Gender[d]		
male	385, 30%	288, 29%
female	914, 70%	702, 71%
Hypertension[d]		
Yes	383, 29%	291, 29%
No	916, 71%	699, 71%
WFNS[d]		
1	711, 56.9%	549, 55.5%
2	278, 22.3%	228, 23.0%
3	54, 4.3%	49, 4.9%
4	129, 10.3%	97, 9.8%
5	77, 6.2%	67, 6.8%
Fisher grade[d]		81, 8.2%
1	94, 8.0%	296, 29.9%
2	363, 30.8%	227, 22.9%
3	266, 22.5%	386, 39.0%
4	457, 38.7%	
Hydrocephalus[d]		
Yes	459, 35%	362, 37%
No	840, 37%	628, 63%
Aneurysmal management[d]		
Coiled	991, 78%	784, 79%
Clipped	265, 21%	198, 20%
Supportive	14, 1%	8, 1%
Aneurysm location[d]		
Anterior circulation	1087, 84%	840, 85%
Posterior circulation	177, 14%	142, 14%
Not classified	35, 3%	8, 1%
Nimodipine[d]		
Yes	1211, 93%	948, 96%
No	88, 7%	42, 4%
Time since ictus (months)[e]	18, 0-519	18, 0-96
HP duplication genotype[a]		
HP1-1	205, 16%	155, 16%
HP2-1	612, 47%	467, 47%
HP2-2	481, 37%	368, 37%
rs2000999 genotype[a]		
AA	57, 5%	41, 4%
AG	379, 29%	290, 29%
GG	854, 66%	659, 67%

4.2.3 Genotype missingness analysis

In the GOSH cohort, 205 patients (16%) had the HP1-1 genotype, 612 (47%) had the HP2-1 genotype and 481 (37%) had the HP2-2 genotype. For the rs2000999 SNP, 854 (66%) of patients had the GG genotype, 379 (29%) had the GA genotype and 57 (5%) had the AA genotype.

Missingness is the absence of individuals from a genotype group compared to what is expected. Reasons for missingness include errors in the genotyping technique or bias due to clinical ascertainment which relates to a genotype[165] (such as higher rates of mortality relating to a specific genotype). Missingness in a genotype-association study such as this, may result in biased or erroneous outcomes. To test for missingness in the GOSH study, two analyses were performed: 1) genotype frequencies were checked for Hardy-Weinberg equilibrium (HWE); 2) comparison was made with genotype frequencies in a control population, a subset of the ALSPAC cohort (n=927). The survivor characteristic of the GOSH cohort was used to determine whether Hp impacts on early mortality or morbidity after SAH; missingness observed in the above comparisons would indicate a genotype is implicated in early mortality or morbidity after SAH.

4.2.3.1 Hardy-Weinberg equilibrium

HWE is achieved when genetic variation in a population remains constant from one generation to the next in the absence of disturbing factors such as selection pressures. Therefore the frequencies of genotypes will remain the same between generations. To assess missingness using HWE, an online calculator[165] was used. The hypotheses are stated below:

Null Hypothesis (H_0): There is **no significant difference** between frequencies of the genotypes in the GOSH cohort compared to the expected frequencies (**GOSH is in HWE**).

Alternative Hypothesis (H_1): There is a **significant difference** between frequencies in the GOSH cohort compared to the expected frequencies (**GOSH is not in HWE**).

The observed and expected frequencies of the HP duplication in the GOSH cohort are shown in Table 4.3. Using the online HWE calculator[165], the allele frequencies were identified as: HP1 (p)=0.39; HP2 (q)=0.61 and the chi-squared test against expected frequencies was not significant (χ^2=0.2, p>0.05). **The null hypothesis is accepted**, therefore this cohort is in HWE with respect to the HP duplication.

Table 4.3 *The observed frequencies of HP duplication genotypes in the GOSH cohort. Expected frequencies derived from chi-squared calculation of HWE.*

Genotype	Expected numbers	Observed Numbers	Frequency
HP1-1	201 (15%)	205	16%
HP2-1	620 (48%)	612	47%
HP2-2	477 (37%)	481	37%
Total	**1298**	**1298**	**100%**

The observed frequencies of each genotype for the SNP rs2000999 are shown in Table 4.4. Using the online HWE calculator[165] the allele frequencies of rs2000999 in the GOSH cohort were identified as: G (p)=0.81; A (q)=0.19 and the chi-squared test against expected frequencies was not significant (χ^2=3.18, p>0.05). **The null hypothesis is accepted**, therefore this cohort is in HWE with respect to rs2000999.

Table 4.4 *The observed frequencies of rs2000999 SNP genotypes from the GOSH cohort. Expected frequencies derived from chi-squared calculation of HWE.*

Genotype	Expected Numbers	Observed Numbers	Frequency
GG	844 (65%)	854	66%
GA	399 (31%)	379	29%
AA	47 (4%)	57	5%
Total	**1290**	**1290**	**100%**

4.2.3.2 Comparison to a healthy control cohort

The chi-squared (χ^2) test was used to assess missingness by comparison to the control ALSPAC population[145]. The HP duplication genotype frequencies are presented in Table 4.5; these were not significantly different in GOSH *vs* the ALSPAC population (χ^2=2.36, p>0.05). The rs2000999 frequencies are presented in Table 4.6; once again no difference was observed between the GOSH and ALSPAC populations (χ^2=0.10, p>0.05).

Table 4.5 *HP duplication genotype frequencies in GOSH vs ALSPAC.*

	HP1-1	HP2-1	HP2-2	Total	χ^2 *vs* GOSH
GOSH	205 16%	612 47%	481 37%	1298 100%	
ALSPAC	137 15%	418 45%	372 40%	927 100%	χ^2=2.19 NS p=0.335

Table 4.6 *rs2000999 genotype frequencies in GOSH vs ALSPAC.*

	rs2000999 GG	rs2000999 AG	rs2000999 AA	Total	χ^2 *vs* GOSH
GOSH	854 66%	379 29%	57 5%	1290 100%	
ALSPAC	485 65%	229 31%	34 4%	748 100%	χ^2=0.39 NS p=0.822

The presence of HWE and lack of missingness of the HP duplication and rs2000999 when compared to a healthy control population indicated that these HP genetic variations do not impact on early morbidity or mortality after SAH. It also provides confidence in the accuracy of the genotyping technique.

4.2.4 Linkage Disequilibrium estimation

Linkage Disequilibrium (LD) is the non-random association of alleles at different loci; it represents the non-independence of inheritance of alleles at different loci ie how often the two alleles are coinherited. The CubeX online tool[166] was used to estimate LD between the HP duplication and the SNP rs2000999. The frequencies of the nine possible genotype permutations from both genetic polymorphisms are shown in Table 4.7. The results indicate that the two polymorphisms are in LD but this is not complete (D'=0.92, R^2=0.13). The high D' value indicates that alleles are inherited together 92% of the time. The R^2 value takes into account the frequency of alleles, and the low value means that they do not provide identical information; ie one polymorphism cannot substitute the other. R^2 is heavily influenced by the complete absence of the coinheritance of the two rare alleles (Hp1-1:AA) making this number low.

Table 4.7 *Frequencies of the 9 possible haplotypes in the GOSH cohort.*

	HP1-1			HP2-1			HP2-2		
	GG	**GA**	**AA**	**GG**	**GA**	**AA**	**GG**	**GA**	**AA**
No. of patients	199	7	0	415	200	2	241	185	56
Frequency	15.2	0.5	0	31.8	15.3	0.2	18.5	14.2	4.3

4.2.5 Association of HP genetic polymorphisms with outcome

4.2.5.1 Primary outcome

The effect of HP genotype on long term outcome in GOSH cannot be assumed to be the same as that in previous studies examining the association between HP genotype and outcome[107-111]. Important differences are that 1) GOSH is a study of long term, not short term outcome, since patients were followed up with a median time since ictus of 18 months; 2) GOSH represents a population of patients who performed well in conventional terms, such that only 15% had an unfavourable follow up mRS of 3-6. The longer duration of follow up in this study of SAH survivors may be expected to minimize the effect on outcome of variable recovery from acute pathological factors such as increased ICP, mechanical stretch injury, ischaemia and inflammation.

The *a priori* planned primary outcome was long term outcome after SAH as measured by the follow up mRS. Logistic regression modelling was employed to assess the effect of the two HP genetic variations on follow up mRS, while controlling for covariates. The sample size was smaller in the outcome analysis (n=990), compared to the missingness analysis (n=1299), due to lack of complete clinical data for some samples. However there was no missingness of any genotype compared to ALSPAC within these 990 patients (data not shown). Also, the baseline clinical characteristics of the missingness and outcome analysis populations were similar (Table 4.2).

Modelling was performed for the two long term outcomes: mRS and GOS scores at follow up; although the latter was a secondary outcome, results are presented here since it is a long term outcome. mRS and GOS scores were dichotomised into favourable (mRS 0-1, GOS 5) and unfavourable (mRS 2-6, GOS 1-4). Usually favourable mRS is classified as 0-2 and GOS 4-5, but this dichotomization resulted in two groups which were highly asymmetric in size, such that 16% of patients would have been classed as unfavourable, which is undesirable due to the potential for

statistical bias. However, using mRS 0-1, 32% were classed as unfavourable; this dichotomization is still meaningful in terms of disability. Preplanned covariates were HP duplication genotype, rs2000999 genotype, age, sex, admission WFNS, admission GCS, Fisher grade, time to follow up, hypertension pre-ictus, anti-hypertensive medication use pre-ictus, hydrocephalus, method to secure the aneurysm and nimodipine treatment. Admission GCS and anti-hypertensive medication were excluded from the model due to collinearity (with admission WFNS and hypertension, respectively). Since the biology of Hp is intricately associated with blood, interaction terms between the HP genotypes and Fisher grade (indicative of blood clot volume) were included in the model. In order to simplify contrasts between different HP genotypes at different Fisher grades, the Fisher grade was dichotomized into low (grade I-II) and high (grade III-IV) Fisher grades.

Inclusion of the interaction between HP duplication genotype and Fisher grade improved the model fit (p=0.001). For the primary outcome follow up mRS, the model explained 27% of the variance observed (Nagelkerke pseudo R^2). The Hosmer and Lemeshow test to assess the goodness of fit of the model was acceptable (p=0.239). Lower age, lower WFNS, absence of hydrocephalus, and coiling (*vs* clipping) predicted a better outcome (Table 4.8). There was a Centre effect. The HP duplication predicted long term outcome, but this depended on Fisher score. At high Fisher grade, HP2-2 predicted a favourable long term outcome *vs* HP1-1; (OR = 2.2, 95% CI 1.2-3.9, p=0.007). At low Fisher grade, there is a visual trend suggesting that the reverse might be happening (ie that HP1-1 confers a favourable outcome *vs* HP2-2, (Figure 4.2A), but this was not significant (OR=2.3, 95% CI 0.84-6.1, p=0.106). For rs2000999 similar trends were observed, but results were not significant (Figure 4.2B). This indicates that Hp expression does not exert a major influence on long term outcome.

Table 4.8 *Multivariate logistic regression analysis for primary outcome (favourable mRS 0-1). Logistic regression model fit excellent (log-likelihood chi-squared test $p<10^{-25}$; Hosmer & Lemeshow test p=0.239). The model explained 27% of the variance.*

	p (overall effect)	OR	95% C.I.		Contrast	p (contrast)
Age	**0.044**	0.987	0.974	1.000		
Gender	0.303	1.195	0.851	1.678	Female *vs* male	0.303
Hypertension	0.761	1.055	0.746	1.493	Absent *vs* present	0.761
WFNS	**<0.001**	4.355	2.335	8.121	WFNS 1 *vs* 5	**<0.001**
Hydrocephalus	**<0.001**	1.846	1.310	2.601	Absent *vs* present	**<0.001**
Aneurysmal Rx	**0.041**	1.633	1.105	2.413	Coiling *vs* clipping	**0.014**
Nimodipine	0.282	1.486	0.722	3.061	Given *vs* not given	0.282
Follow up time	0.121	1.007	0.998	1.015		
Centre	**<0.001**					
rs2000999	0.286	1.754	0.809	3.802	GG *vs* AA	0.154
Fisher x Hp	**0.015**					
Fisher	**0.004**	4.318	1.589	11.735	Low *vs* high Fisher in Hp1-1	**0.004**
Hp	**0.027**	2.206	1.238	3.930	Hp2-2 *vs* Hp1-1 at high Fisher	**0.007**

The different outcomes at higher Fisher grade could be due to a biological reason or could be mediated by lack of case ascertainment of HP2 patients with high Fisher scores and poor outcome. However there was no evidence of missingness within high or low Fisher grade groups that could have biased the results, as shown by several analyses: 1) HP duplication genotype frequency was not significantly different between low and high Fisher grade groups (χ^2=1.23, p=0.54); 2) HP duplication genotype frequency in the high and low Fisher grade groups was not significantly different from the ALSPAC control cohort (χ^2=1.1, p=0.58 and χ^2=2.181, p=0.34 respectively); 3) HP duplication genotype frequency of patients excluded from the regression due to data availability was not significantly different from that of the included patients (HP duplication: χ^2=0.06, p=0.97 and rs2000999: χ^2=0.82, p=0.66, respectively) or the ALSPAC control cohort (HP duplication: χ^2=1.22, p=0.54 and rs2000999: χ^2=0.34, p=0.84, respectively). A sensitivity analysis was performed with favourable mRS defined *post hoc* as 0-2 and this showed the same results (data not shown). Additional sensitivity analyses included decreasing follow up

intervals and results remained robust until losing significance at one year as sample size decreased (data not shown).

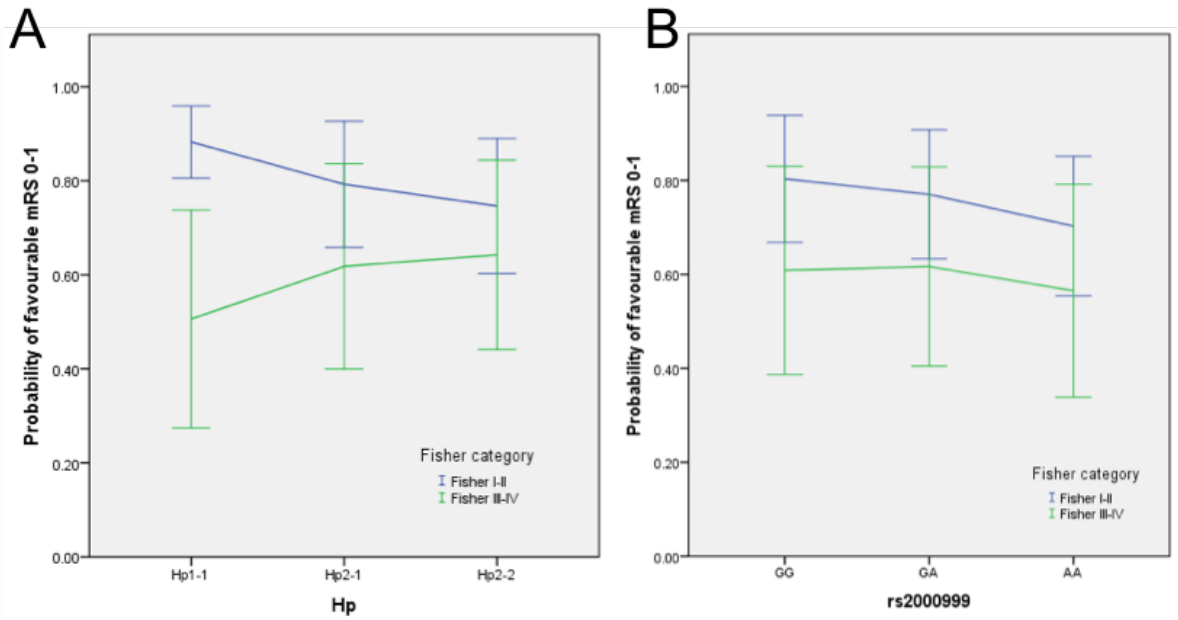

Figure 4.2 *Regression lines of mean predicted probabilities (± 1 SD) of favourable outcome by dichotomised mRS score are plotted by* ***(A)*** *HP duplication genotype and (****B****) rs2000999, for patients with high (green) and low (blue) bleed size.*

Although the follow up GOS was a secondary outcome, results are presented here as it is also a long term outcome. The same pattern was seen for both the HP duplication and rs2000999 (Table 4.9).

Table 4.9 *Multivariate logistic regression analysis of secondary outcome (favourable GOS 5). Logistic regression model fit excellent (log-likelihood chi-squared test $p<10^{-19}$; Hosmer & Lemeshow test p=0.808). The model explained 25% of the variance.*

	p (overall effect)	OR	95% C.I.		Contrast	p (contrast)
Age	**0.043**	0.985	0.971	1.000		
Gender	0.396	1.174	0.811	1.698	Female *vs* male	0.396
Hypertension	0.485	1.142	0.787	1.658	Absent *vs* present	0.485
WFNS	**<0.001**	3.996	2.133	7.487	WFNS 1 *vs* 5	**<0.001**
Hydrocephalus	**<0.001**	2.127	1.464	3.089	Absent *vs* present	**<0.001**
Aneurysmal Rx	0.073	1.631	1.073	2.478	Coiling *vs* clipping	**0.022**
Nimodipine	0.378	1.411	0.656	3.037	Given *vs* not given	0.378
Follow up time	0.313	1.005	0.995	1.014		
Centre	**0.001**					
rs2000999	0.546	1.585	0.686	3.661	GG *vs* AA	0.281
Fisher x Hp	**0.004**					
Fisher	**0.003**	7.015	1.933	25.458	Low *vs* high Fisher in Hp1-1	**0.003**
Hp	**0.016**	2.386	1.309	4.350	Hp2-2 *vs* Hp1-1 at high Fisher	**0.005**

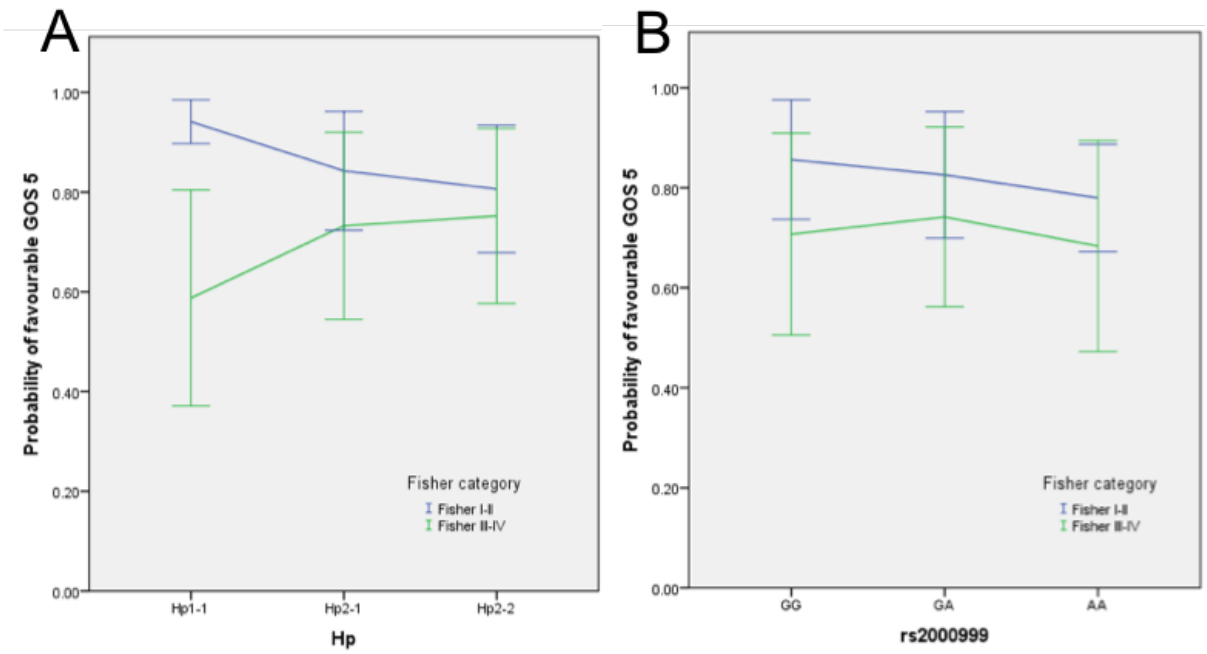

Figure 4.3 *Regression lines of mean predicted probabilities (± 1 SD) of favourable outcome by dichotomised GOS score are plotted by (A) HP duplication genotype and (B) rs2000999, for patients with high (green) and low (blue) bleed size.*

4.2.5.2 Secondary outcomes

The following secondary outcomes (which are all short term outcomes) were examined but no trend or significant effect was found:

1. Discharge mRS, including all covariates as above but substituting follow up time with time from ictus to discharge.
2. Discharge GOS, including all covariates as above but substituting follow up time with time from ictus to discharge.
3. Incidence of large vessel vasospasm in patients from centres where transcranial Doppler is employed regularly to monitor for this event.
4. Incidence of delayed ischaemic neurological deficit.
5. Time from ictus to discharge in those patients were this was less than 1 month (in order to exclude patients who stayed in hospital longer due to problems with placement in the community).

4.3 Discussion

This investigation of 1299 aneurysmal SAH patients from the GOSH study is the largest HP genotype association study to date. It provides a number of novel insights into the role of Hp in Hb scavenging after SAH.

The GOSH cohort is biased towards *better outcome patients* due to recruitment of survivors (ie excluding mortality in the first weeks and months). This can be observed in the demographics table in the results section of this chapter which shows that the median mRS scores at discharge and follow up are 1. The mRS scale (see Appendix A for details) ranges from 0 (good outcome) to 6 (poor outcome) demonstrating the favourable outcomes of the patients in this cohort. Patients who had largely adverse outcomes that resulted in death would not have been included in the study as they would have died prior to recruitment and DNA collection. This bias is a strength of this investigation as it has provided a cohort of patients in which the confounding effect of severe early brain injury (vascular due to sudden surge in ICP, and sheer mechanical stretch), is minimised. The indirect effect of HP genotype on short term outcome was studied by examining HWE, and by comparison with a control cohort. No evidence for such an effect was found. This is unsurprising since Hb scavenging is not thought to be related to the major determinants of early mortality ie mechanical and ischaemic early brain injury, and re-bleeding.

The HP duplication and rs2000999 in the GOSH population were identified to be in LD, however it was not complete. LD is the non-independent inheritance of alleles; this phenomenon occurs due to the lack of recombination between loci of the two polymorphisms. Some studies have identified LD between the HP duplication and rs2000999, whereas others have not[65,145]. When polymorphisms are in complete disequilibrium, one can completely predict the other. This has two implications. First, the phenomenon of complete LD may be used to the advantage of genetic association studies; this is because typing one polymorphism is sufficient, since it acts as a surrogate of the other. Second, LD has a disadvantage in that the effect of the two polymorphisms cannot be separated in genetic association studies. In this study, the lack of complete LD between the HP duplication and rs2000999 meant that both genetic variations could be investigated and included as covariates in a multivariate regression.

Logistic regression analysis was employed to investigate if HP genotype influences long term outcome after SAH. Previously Kantor *et al.*[109] identified that HP2-2 (*vs* HP1-1) was significantly associated with worse outcome (by mRS score at 3 month follow up) after SAH in a small study of 193 patients. However other authors (Ohnishi *et al.*[108] and Leclerc *et al.*[110]) failed to find a significant association with worse long term outcome. A meta-analysis of all published studies also failed to identify an association between HP duplication and long term outcome[112], and an individual patient level data re-analysis of these studies has also shown no effect of the HP duplication on long term outcome (manuscript under review, personal communication, Dr I Galea). In all these studies, outcome was assessed at six months or less after ictus. In contrast this study examines outcome on a significantly longer time scale.

A striking outcome of this investigation is that the effect of HP duplication genotype on outcome depended on the size of the SAH. At high Fisher grade, HP2-2 predisposed to better outcome compared to HP1-1, whereas this effect was not observed at low Fisher grade. It has been shown that the difference in HpHb complex scavenging rate between Hp1-1 and Hp2-2 depends on the concentration of HpHb complexes[78], such that the performance of Hp1-1 and Hp2-2 starts to diverge at a HpHb complex concentration above 10μg/ml (0.13μM). It is possible that the effects of the HP2 alleles at different Fisher grades are a reflection of this biochemical fact, with Hp2-2 conferring better Hb scavenging at higher Hb concentrations, compared to Hp1-1. An important clinical implication of the Fisher grade dependency of the HP prognostic effect relates to clinical trials. Since most trials recruit SAH patients with Fisher grade III-IV, and it is in this subgroup of patients that HP duplication is an important covariate, HP duplication typing may be considered as an essential covariate.

The only known effect of rs2000999 is to influence circulating levels of Hp[65]; the HP duplication is also known to affect circulating levels but there are also functional differences in the proteins encoded by the HP1 and HP2 alleles. The effects of the HP duplication and rs2000999 on Hp expression were confirmed in a British population (the ALSPAC cohort). Since rs2000999 does not impact significantly on long term outcome after SAH, circulating levels of Hp are less likely to be important after SAH. This demonstrates that amongst the two main ways in which the HP duplication may affect long term outcome, ie Hp expression level or Hb scavenging, the latter is the predominant mechanism of action of the HP duplication.

There is controversy regarding the relative efficacy of Hp1-1 and Hp2-2 in human CD163-mediated Hb scavenging. In complex with Hb, Hp2-2 has a high binding affinity to CD163 compared to Hp1-1, using two different experimental approaches[167,168]. Although one study suggested that CD163-mediated cellular uptake of HpHb complexes is better with Hp1-1[167], two subsequent studies have reported that Hp2-2 is better[150,169]. It is possible that the differences between the clinical effects of HP1 and HP2 alleles are amplified in the brain where the low CD163 expression level is a limiting factor in Hb scavenging[170,171], especially in the presence of a high Hb concentration. In this situation it could be hypothesized that the higher valency of Hp2-containing complexes means that more Hb can be scavenged per Hp molecule. Also higher valency is likely to be associated with improved clustering of CD163 receptors, since small angle X-ray scattering and *ab initio* structural modelling of human HpHb complexes incubated with soluble CD163 fragments has shown that CD163 can bind simultaneously to each β chain of the HpHb complex[59]. This will be explored further in the next Chapter of this thesis, in which I present data on differences in CSF Hb, according to Hp phenotype, in Fisher III-IV SAH patients.

The finding that HP genotype influences long term outcome after SAH supports the therapeutic potential of Hp supplementation. The novel finding that HP2-2 imparts a favourable prognosis after high-grade SAH argues that supplementation of an Hp2-2 enriched preparation would be superior to Hp1-1. The finding that increased Hp expression does not impact long term outcome (the lack of rs2000999 effect) does not argue against the use of Hp supplementation, which would aim to achieve supra-physiological levels of Hp.

From a manufacturing point of view, delivering Hp preparations of specific types (ie Hp1-1 or Hp2-2) has cost implications, since plasma would need to be collected from individuals with specific HP genotypes, as opposed to pooled plasma as is current practice across the plasma purification industry. The administration of Hp2-2 to HP1-1 patients and vice versa may result in toxicity due to immunological rejection in the CSF, an area of the brain which is not immunologically privileged[172]. The important issue of which Hp preparation is best to use (Hp1-1, Hp2-2 or mixed) must be addressed using *in vivo* models of SAH, such as the one described in Chapter 7 of this thesis.

A strength of this study is its sample size, making it the largest study associating HP genotype with outcome after SAH. Furthermore, this is the only study investigating rs2000999, which has provided mechanistic insight into how Hp influences outcome after SAH. In addition, this study has stringently tested for missingness by comparing to a British young age control group, to avoid the confounding effects of modifiable risk factors such as smoking, high fat diet and diseases that may influence genotype frequencies later in life. Therefore a younger control population is much closer to the expected gene frequencies at the point of assignment of alleles. Comparison with a control population of this nature, enables a more stringent study of missingness, compared to assessment of HWE. The findings that HP2-2 imparted a good prognostic outlook and the interaction of HP genotype with Fisher grade, are novel. The analysis was robust to two clinical outcome measures (mRS and GOS), and survived multiple sensitivity analyses.

A limitation of the work is the retrospective study design. Also, the study recruitment process meant that data capture was opportunistic, so follow up time varied. GOSH was originally designed to study the genetics between individuals with ruptured *vs* unruptured aneurysms, but I took advantage of the fact that long term outcome was assessed in aneurysmal SAH patients in GOSH. In summary, due to these limitations, a prospective study would be required to confirm the results presented here.

Chapter 5 Haemoglobin scavenging kinetics in the cerebrospinal fluid after subarachnoid haemorrhage

5.1 Introduction

Following SAH, blood from the ruptured aneurysm enters the CSF and a clot is formed on the surface of the brain which begins to degrade. Erythrocyte lysis releases free Hb which would likely result in high concentrations of Hb in the CSF. Previous studies from our group have identified that the Hp-Hb-CD163 system is active in the brain[102]. However, the concentrations of Hp in the CSF are 50,000 times lower than in the blood[102]; thus the CNS is much less equipped to manage Hb clearance by Hp after haemorrhagic events. It is likely then, that the concentrations of Hb accumulating in the CSF will far exceed its capacity to scavenge it.

There is evidence in the literature, implicating Hb in 1) direct neurological damage[21] and, 2) vasospasm[7,46]. This can have neuropathological consequences by driving the development of DIND and influencing long term outcome. Understanding the kinetics of Hb accumulation and its scavenging in the CSF, therefore will help the understanding of how Hb contributes to these pathologies. Additionally, it would be beneficial to understand the Hb scavenging *deficit* and identify a window of opportunity for Hp treatment against Hb neurotoxicity after SAH.

This chapter addresses the second hypothesis set out in the Hypothesis and Aims chapter of this thesis, that: **haemoglobin released from the lysing blood clot into the cerebrospinal fluid, overwhelms the resident Hb scavenging system and impacts on functional outcome after subarachnoid haemorrhage.**

The Haemoglobin After Subarachnoid Haemorrhage (HASH) study was undertaken at University Hospital Southampton to understand the kinetics of Hb release and degradation in the CSF after SAH. CSF and serum were serially collected over the 14 day period post-ictus as described in Figure 5.1. CSF collections were made via an external ventricular drain (EVD). This is a drain inserted into the lateral ventricle used to control hydrocephalus in SAH cases with a high Fisher grade[173]. Additionally, it provides a point of access to sample the CSF and in many instances it is used to provide therapeutic compounds directly to the CNS such as antibiotics[173].

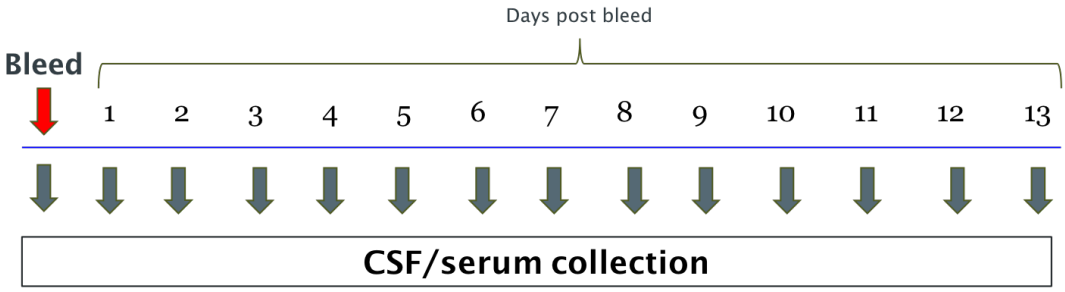

Figure 5.1 *Schematic depicting the daily paired serial collection of CSF and serum from HASH patients each day after their haemorrhage. CSF was collected from an indwelling EVD and serum samples were taken at corresponding time points. Due to patient care considerations and protocol restraints, the maximum number of samples was eight and CSF samples were not taken at each time point in each patient. Therefore not all patients had samples taken every day, and some patients did not have samples taken up to day 13 (for example if the EVD was removed prior to this).*

In this work, a size-exclusion Ultra Performance Liquid Chromatography (UPLC-SEC) method was used to separate the components of the CSF samples. Monitoring absorbance at 415 nm allowed the visualization and quantification of total, complexed and free Hb and Hp. Methodology is described in detail in Chapter 3.

5.2 Results

5.2.1 Demographic and clinical characteristics

The demographic and clinical characteristics of the SAH patients in the HASH study are shown in Table 5.1. The mean age was 59.8 years and there was a higher proportion of females in this cohort; this is not unusual for those presenting with SAH in the UK based on figures from a recent multicentre UK audit[11]. The majority of patients' Fisher grade was IV; only two patients had SAH of Fisher grade III. While this was part of the eligibility criteria as these patients were those requiring CSF diversion via EVD placement to control hydrocephalus, it does represent a bias towards *worse grade* SAH. This is reflected in the patients' WFNS score, such that there were fewer patients with Grade 1 (best outcome) and slightly more patients with Grade 4. When compared to the UK SAH demographic from a large multicentre UK audit of SAH patients[11], the frequencies of WFNS scores were found to be significantly different (χ^2=36.0, p<0.0001). The Hp phenotypes were observed at frequencies expected of a UK population and were found to be in HWE (X^2=0.57, p>0.05).

Control individuals were patients presenting to a neurology clinic with non-inflammatory or non-haemorrhagic conditions who received a lumbar puncture and were observed to have normal CSF with respect to protein, glucose, cell count, cytology, albumin CSF/serum quotient and isoelectric focusing for oligoclonal bands. Their conditions included normal pressure hydrocephalus, idiopathic intracranial hypertension and headache.

In the control group there was a prevalence of females although frequencies were in fact similar to the SAH population (χ^2=0.53, p=0.47); similarly, ages of the groups were not significantly different (Mann-Whitney, p=0.946). The Hp phenotypes for the control group (Table 5.1) were found to be in HWE (χ^2=0.03, p>0.05).

Table 5.1 *The demographic characteristics of the SAH cohort and the two control cohorts.*

	HASH patients	Control patients
Number	44	20
Age (years)[a]	59.8 ± 12.3	53.7 ± 25.1
Gender[b]		
Male	15 (34%)	5 (25%)
Female	29 (66%)	15 (75%)
Hp Phenotypes		
Hp1-1	9 (21%)	3 (15%)
Hp2-1	19 (43%)	10 (50%)
Hp2-2	16 (36%)	7 (35%)
Hypertension[b]		
Yes	23 (52.3%)	
No	21 (47.7%)	
WFNS[b]		
1	5 (11.4%)	
2	10 (18%)	
3	6 (13.6%)	
4	15 (29.5%)	
5	8 (13.6%)	
Fisher grade[b]		
3	2 (4.5%)	
4	42 (95.5%)	
Aneurysmal management[b]		
Coiled	32 (72.7%)	
Clipped	5 (11.4%)	
Supportive	6 (13.6%)	
Aneurysm location[b]		
Anterior circulation	32 (72.7%)	
Posterior circulation	7 (15.9%)	
Non-aneurysmal	4 (9.1%)	
Unknown	1 (2.3%)	

Notes: Mean & SD[a], Percentage[b]

5.2.2 Kinetics of haemoglobin and its scavenger mechanism in the cerebrospinal fluid

CSF samples were analysed using UPLC-SEC for analytes involved in the Hb scavenging pathway. The UPLC process and a representative chromatogram are presented in Figure 5.2. Data were organised into day post-ictus using time points available from clinical records of sample collection. Data were tested for normality using the Kolmogorov-Smirnov test in Prism (v7.0, GraphPad Software, USA) and were observed to be non-parametric and therefore are presented as median ± IQR.

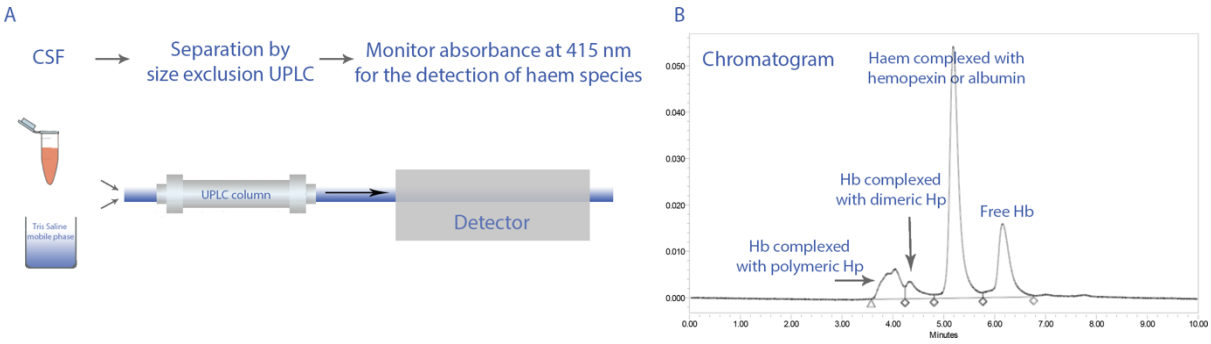

Figure 5.2 *Hb and Hp levels were assayed via UPLC-SEC* ***(A)*** *The UPLC process: CSF was injected onto the UPLC column in a tris saline mobile phase. Separation of the components was achieved by a size exclusion UPLC column and the elution absorbance was monitored at 415 nm to detect only haem containing species.* ***(B)*** *A representative chromatogram from running neat CSF on the UPLC. On the left, complexed with both polymeric and dimeric Hp peaks are seen, followed by haem bound to Hpx and albumin, and finally free Hb.*

5.2.3 Haemoglobin in the CSF after SAH

Hb was classified into three major forms:

1. Free Hb: this is Hb that has is not in complex with Hp.
2. Complexed Hb: this is Hb that has been complexed by Hp.
3. Total Hb: the total amount of Hb, both free and in complex with Hp.

5.2.3.1 Free haemoglobin

Free uncomplexed Hb in the CSF after SAH (Figure 5.4A) was measured directly from the area under the curve for Hb on the UPLC chromatogram when neat CSF was run on the UPLC. This is the peak labelled *free Hb* in Figure 5.2B.

Minor amounts of free Hb were detected up to the third day, after which levels increased, peaking at day 11 (8.5 µM). Figure 5.4B shows the levels of free Hb (expressed as a percentage of total Hb (ie all of the Hb present, both free and in complex with Hp). It can be observed that by day five, approximately all of the total Hb in the CSF after SAH is free and not in complex with Hp.

When Hb is free and released from the confines of the erythrocyte, it can undergo oxidative modifications including intermolecular crosslinking of the α chain[174] and as such can no longer be bound by Hp. Hb that has undergone this process was termed *non-scavengeable Hb*. This process of autoxidation can occur spontaneously, and initiates a detrimental process that ultimately results in the release of haem[26]. Non-scavengeable Hb was measured in the CSF as the area remaining under the Hb peak on the UPLC chromatogram after the addition of excess Hp. This derivation can be observed in Figure 5.3; note the reduction in the uncomplexed free Hb curve as it is bound by Hp that is added to the CSF. The remaining free Hb is non-scavengeable Hb.

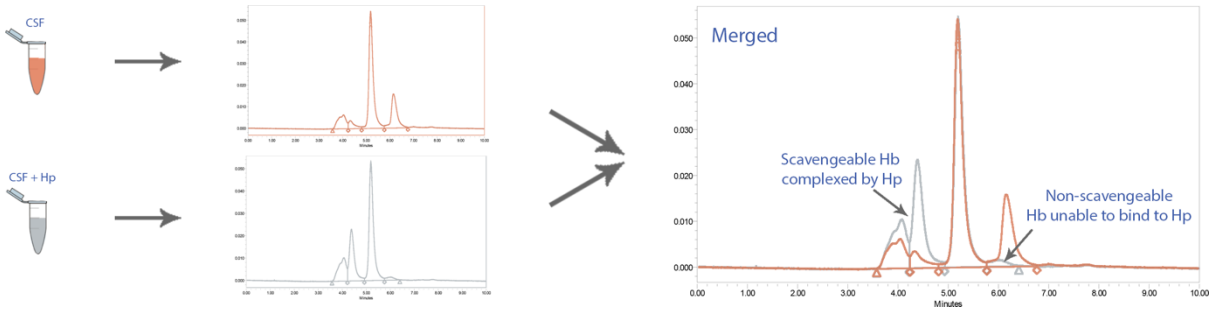

Figure 5.3 *Non-scavengeable free Hb was measured by running CSF either neat or spiked with saturating Hp. The remaining free Hb peak represented non-scavengeable Hb. Note how upon addition of saturating Hp, the majority of uncomplexed Hb is transferred to complexed Hb.*

Scavengeable free Hb is the proportion of free Hb that has not been damaged by the redox environment and is therefore still able to be bound by Hp. Scavengeable free Hb in the CSF was calculated as the difference between total free Hb and non-scavengeable free Hb, at each time point for each patient. These data are shown in Figure 5.4C: scavengeable free Hb begins to rise steadily up to day 11 (7.4µM).

Non-scavengeable Hb is present at considerable levels from the seventh day. When the data for scavengeable and non-scavengeable free Hb are expressed as a percentage of total free Hb in the CSF (Figure 5.4D&F), it is clear that from days 2-7, considerable levels of Hb are able to be scavenged by Hp. However, a substantial level of non-scavengeable Hb is also present in some

cases as shown by the interquartile range. Figure 5.4F suggests that initially 100% of the free Hb is non-scavengeable, however these levels are in fact very low (<1 μM, Figure 5.4E) until day three when larger quantities of Hb build up in the CSF.

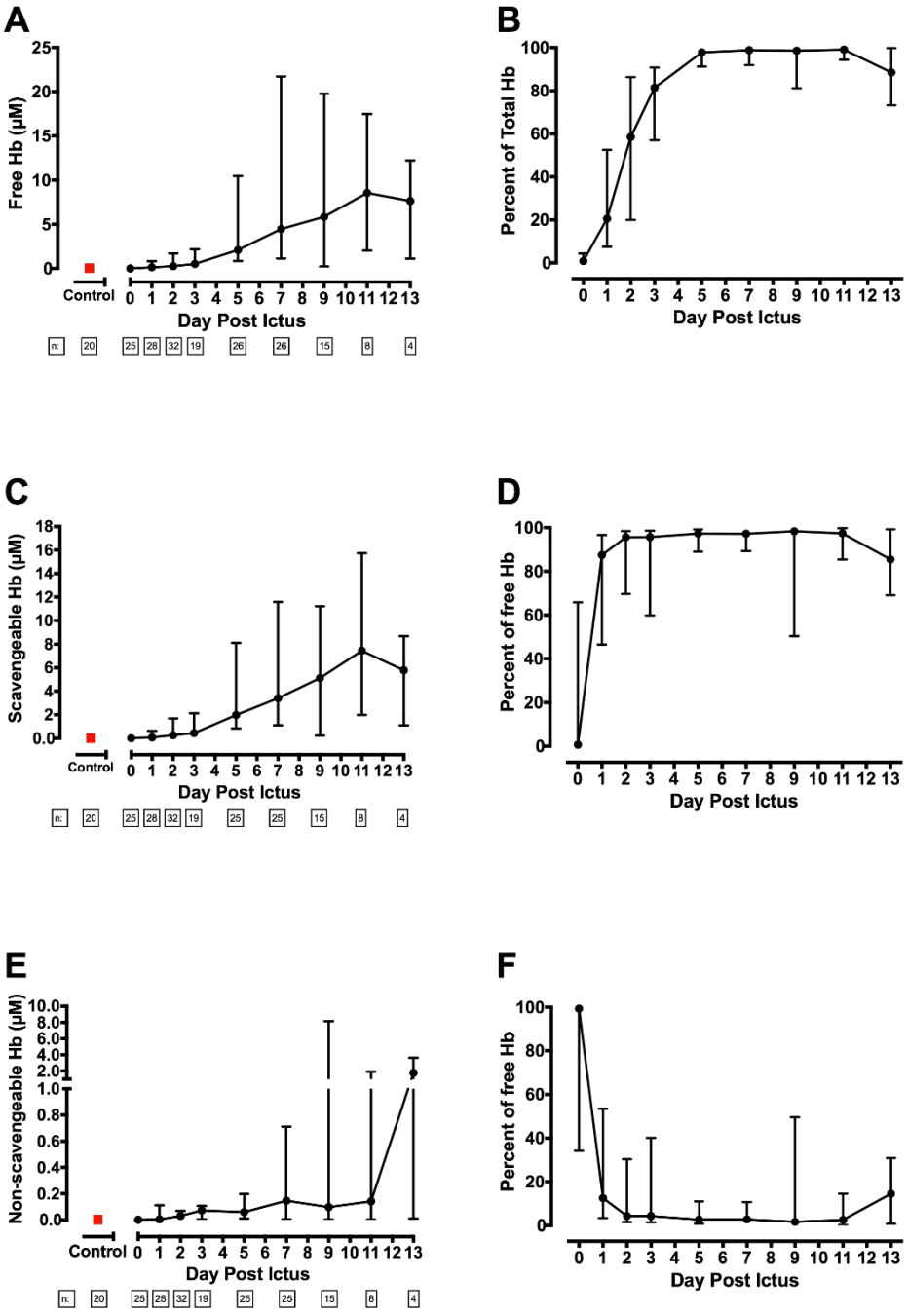

Figure 5.4 *Levels of Hb analytes in the CSF after SAH as measured by UPLC. Data presented as median ± IQR.* ***(A)*** *Levels of total free Hb in the CSF* ***(B)*** *total free Hb expressed as a percentage of the total amount of Hb,* ***(C)*** *levels of free Hb in the CSF that is able to be scavenged by Hp,* ***(D)*** *scavengeable free Hb expressed as a percentage of total free Hb,* ***(E)*** *levels of non-scavengeable free Hb, and* ***(F)*** *non-scavengeable expressed as a percentage of total free Hb. The error bars on the control values on* ***(A)***, ***(C)*** & ***(E)*** *are smaller than the size of the symbol would be therefore are not displayed.*

5.2.3.2 Complexed haemoglobin

Levels of Hb complexed to Hp are presented in Figure 5.5A, in which highest levels of 0.6 µM are seen at day one, which then decrease to 0.1 µM by day five and then remain steady. In control patient CSF, complexed Hb was detectable at low levels (median 0.03 µM), however this is likely to be an artefactual figure, due to the effect of *in vitro* haemolysis. A lumbar puncture is known to be a traumatic procedure, frequently with blood contamination of CSF; any Hb were released in this process would very rapidly be bound to free Hp, therefore producing artefactual complexed Hb. It is likely that CSF complexed Hb *in vivo* is present at even lower concentration, or more likely absent. Figure 5.5B shows complexed Hb presented as a percentage of total Hb. This shows that on day zero all of the free Hb is complexed by Hp, but this percentage falls, such that most Hb is uncomplexed by day five. Interestingly levels do not drop to absolute zero and are mostly observable even up to day 13, indicating the presence of HpHb complexes throughout. This may represent the saturation of scavenging and/or drainage pathway of HpHb complexes.

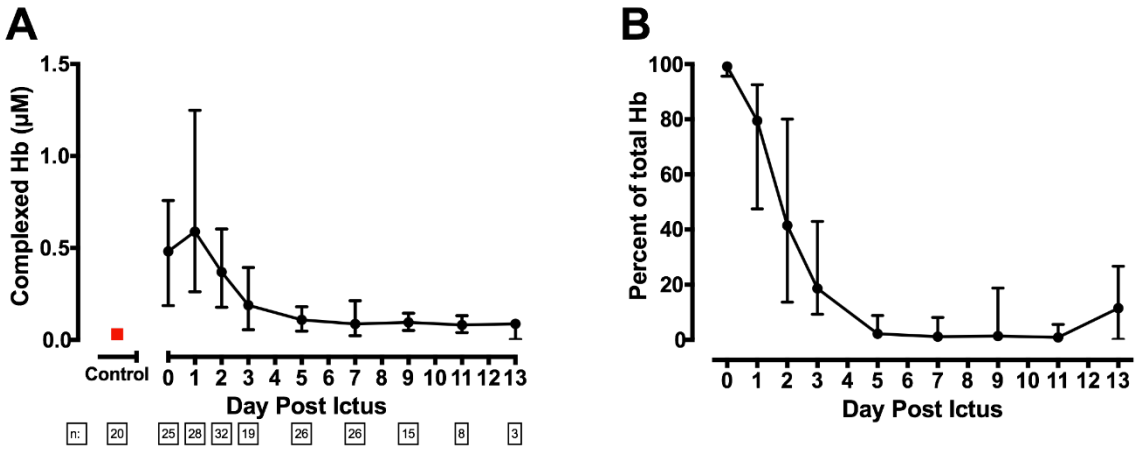

Figure 5.5 *Levels of Hb in complex with Hp in the CSF after SAH as measured by UPLC.* ***(A)*** *Levels of Hb complexed to Hp presented in terms of µM of Hb.* ***(B)*** *Amount of Hb complexed presented as a percentage of total Hb. Data presented as median ± IQR. The error bars on the control values on (A) are smaller than the size of the symbol would be therefore are not displayed.*

5.2.3.3 Total haemoglobin

Total Hb levels (Figure 5.6) in the CSF were calculated as free Hb plus the amount of Hb complexed to Hp for each patient at each time point. In control patients, Hb was observed at very low levels, the median for these individuals was 0.06 µM. The total Hb level in SAH patients remained similar to that in control individuals until day three post-ictus. After day three, total Hb level increased to a median of 8.6 µM on day 11 and remain around this level to day 13.

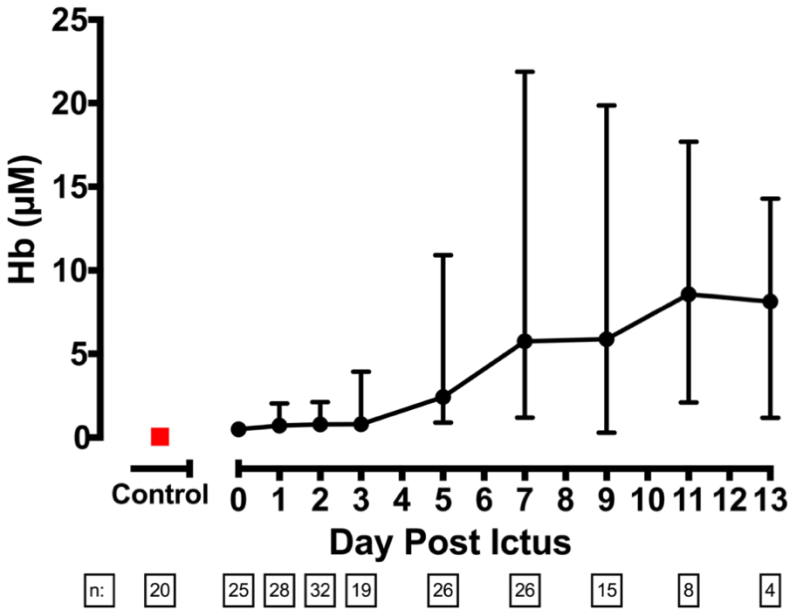

Figure 5.6 *Levels of total Hb in the CSF after SAH as measured by UPLC. Data presented as median ± IQR. The error bars on the control values are smaller than the size of the symbol would be therefore are not displayed.*

5.2.4 Total haemoglobin scavenging capacity of the CSF after SAH

Total Hp in the CSF at each time point was measured from the area under the HpHb complex curve on the UPLC chromatogram after addition of excess Hb to ensure all the available Hp was in complex with Hb (and therefore visible when measuring absorbance at 415nm). Calculating the exact molarity of Hp is challenging due to the presence of multiple isoforms of Hp of increasing molecular weight in Hp2-1 and Hp2-2 individuals. In light of this, Hp was expressed as total Hb scavenging capacity (THBC) - the amount of Hb it is able to bind.

Figure 5.7A shows that THBC in control patient CSF is low (median of 0.04 μM Hb). In SAH patients the largest THBC of 1.2 μM Hb is observed on the day of ictus. These levels then consistently decrease until day three, at which they fluctuate around control levels for the remaining days. To highlight the Hb scavenging deficit in the CSF after SAH, the total Hb curve is overlaid on Figure 5.7 to illustrate the fact that total Hb levels can reach up to five times the Hb scavenging capacity. It is interesting to note that there is enough Hb scavenging capacity to deal with Hb seen during the first three days post-ictus. This is likely due to two factors: the low levels of CSF Hb in the first few days and the entry of Hp into the CSF with the blood injection accompanying the aneurysmal rupture.

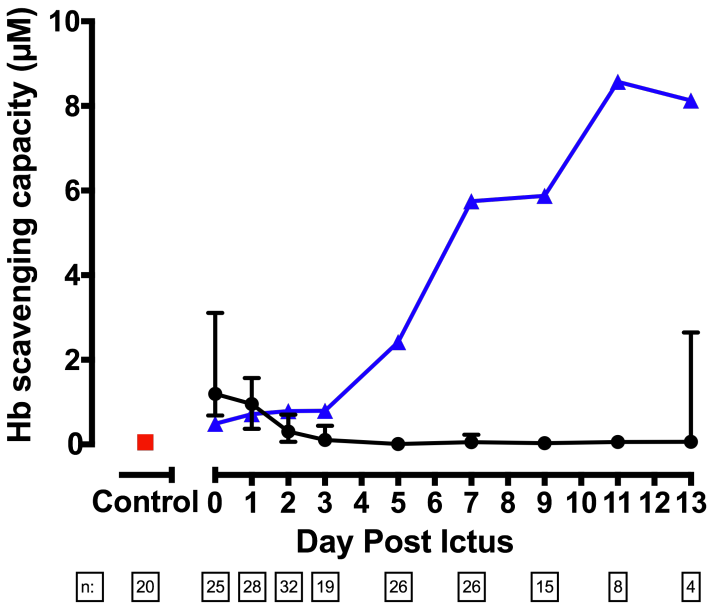

Figure 5.7 *Levels of THBC in the CSF after SAH as measured by UPLC (black curve). These data are presented as the amount of Hb that Hp is able to bind in molar terms. Data are presented as median ± IQR. For comparison, total Hb (from Figure 5.6) is overlaid (blue curve) to highlight the Hp deficit in the CSF after SAH.*

5.2.5 A sustained increase in blood-brain barrier permeability after SAH

There is evidence that there is breakdown of the BBB after SAH[102,175-177]. This may lead to adverse clinical outcome such as by leakage of plasma components[29,30] that usually would not be present at such high levels in the CNS. Conversely however, within the context of SAH it may be beneficial as the increased permeability may facilitate a clearance route for Hb, HpHb complexes or both.

Albumin is a protein that is abundant in the serum but not synthesized in the CNS, therefore any albumin present in the CSF is as a result of entry across the blood-CSF barrier (BCB). Thus, the albumin quotient (Qalb) between the CSF and serum can be used as a proxy for the permeability of the BBB, a component of which is the BCB[178]. An increase in this ratio indicates that there is increased BCB permeability to molecules of similar size to albumin.

To investigate changes in BCB permeability, paired CSF and serum samples from SAH patients taken at day four or later were assayed for albumin by colorimetric Bromocresol purple assay (NHS clinical biochemistry). Time points earlier than day four were excluded since analysis at these time points would have been confounded by albumin that had entered the CSF with the bleed, based on observations of the removal of other plasma proteins (ie Hp, Figure 5.7).

The Qalb data from the SAH patients and the control individuals are presented in Figure 5.8. From day five onwards, it appears that there is an increase in the albumin ratio between the CSF and serum compared to that of a healthy cohort. Qalb was significantly higher than control levels on days five, seven, nine and 13 ($p<0.0001$, $p=0.0002$, $p=0.0177$, $p=0.00285$ and $p=0.0228$ respectively, Mann-Whitney tests). This finding was robust to Bonferroni correction for multiple comparisons (adjusted significance level: 0.01) at days five and seven.

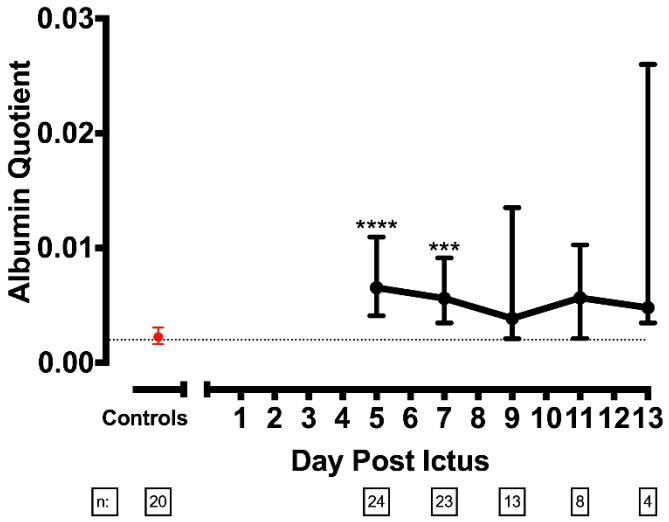

Figure 5.8 *The BCB permeability is increased after SAH. Median ± IQR Qalb ratios for healthy control individuals (red) and SAH patients (black) at days 5,7,9,11 and 13 after ictus. Dotted line represents control patient level. Multiple Mann-Whitney tests with Bonferroni correction for multiple comparisons indicated that days 5 ($p<0.0001$) and 7 ($p=0.0002$) were significantly elevated from control levels. Error bars for the control data are smaller than the size of the symbol therefore not shown.*

5.2.6 Absence of intrathecal synthesis of haptoglobin after SAH

During SAH there is an inflammatory response in the brain[29]. Hp is an acute phase reactant[57], and it is released by activated neutrophils[56]. Whilst most Hp is synthesized by the liver, there is evidence of expression at other sites including the brain in experimental models of intracranial haemorrhage[58]. Here, it was hypothesized that intrathecal synthesis contributes significantly to the concentration of Hp present in the CSF in humans after SAH.

To test this hypothesis, the Hp quotient (QHp = CSF Hp/serum Hp) was first calculated. This then allowed the Hp index to be calculated as QHp/Qalb. This is a measure of intrathecally produced Hp in the CSF, having controlled for Hp entering by diffusion across the BCB (Qalb). An increased Hp index compared to controls, would be therefore indicative of increased intrathecal synthesis of Hp. Because albumin is here being used as a proxy for BCB permeability, only molecules of comparable size can be used; this limited the analysis to the Hp dimer, therefore QHp and Hp index were only calculated in Hp1-1 control and HASH individuals. As can be seen in Figure 5.9, the Hp index of the Hp1-1 patients is significantly lower than controls ($p=0.0049$), excluding a significant contribution of intrathecal synthesis to CSF Hp concentration in these patients. The lower Hp index after SAH could be consistent with HpHb complex uptake by macrophages, and/or clearance of HpHb complexes to the systemic circulation.

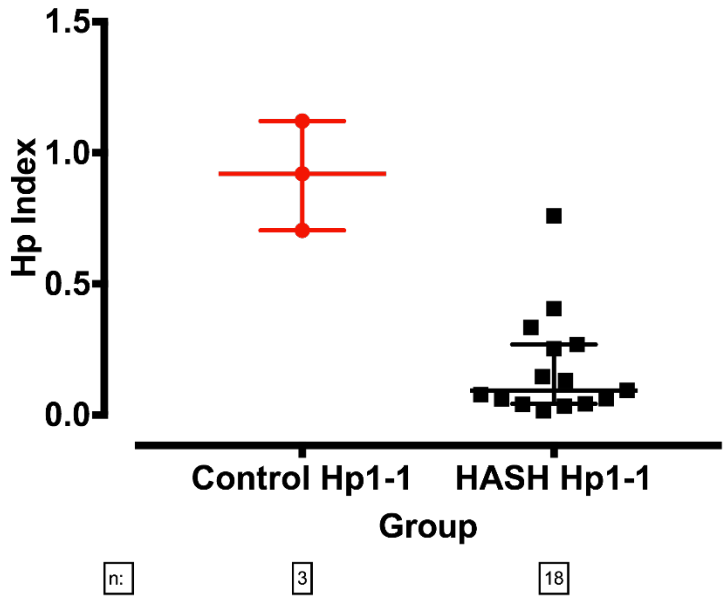

Figure 5.9 *The Hp index of three Hp1-1 control and 18 Hp1-1 HASH patients. There is a decreased index compared to controls. Data are presented as median ± IQR (Mann Whitney test p=0.0049).*

5.2.7 Preferential scavenging of Hb by the Hp2-2 phenotype

In the previous Chapter, it was observed that HP2-2 individuals have better long term outcome compared to HP1-1 individuals who have high Fisher grades (ie large haemorrhages). Based on these observations, it was hypothesized that this may be due to more efficient Hb scavenging by the higher polymers of Hp compared to the dimeric form, due to their higher valency for Hb. It was hypothesized that Hp2-2 patients would have lower levels of complexed Hb in the CSF after SAH, compared to Hp1-1 patients. Although the Hp2-1 patients would be expected to behave in a manner which is intermediate between Hp1-1 and Hp2-2 patients, this may not happen since the ratio of expression of the dimer and higher polymeric forms is variable amongst Hp2-1 patients[113].

Linear mixed modelling was employed to investigate Hp phenotype differences in the HASH cohort; this is an extension of a generalized linear model that allows for repeated effects. In this instance it allows me to model repeated measurements of Hb over time (the repeated measure) without violating the assumption of independence in linear regression.

In the linear mixed model a first order ante dependence covariate structure was used to model correlated terms. Within-subject random effects were modelled using random intercepts. Model comparison was assessed using the log-likelihood ratio and the Akaike information criterion. All variables were tested for normality and Ln or $\log_{10}$ transformation was used to normalise data where required. The dependent variable was complexed Hb and the covariates entered into the

model were Hp phenotype, time post-ictus, clot volume (to control for bleed size) and EVD drainage volume (to control for the effect of different drainage volumes on metabolite level).

Variables that significantly predicted complexed Hb level were the Hp2-2 phenotype (*vs* Hp1-1), time and blood clot volume. To understand the effect of Hp phenotype on complexed Hb level, the predicted complexed Hb values from the model were saved. As Hb data were Log_{10} transformed to normalise data for linear mixed modelling analysis, the inverse of the log_{10} - operation (base 10 raised to the power of each Hb value) was applied to the saved predicted values, and data are presented by phenotype in Figure 5.10.

Table 5.2 *Linear mixed model to predict complexed Hb levels.*

			95% Confidence Interval	
Parameter	Estimate	Sig.	Lower Bound	Upper Bound
Intercept	.238130	.813	-1.783813	2.260072
Hp2-2 (*vs* Hp1-1)	-.406905	.033	-.777970	-.035840
Hp2-1 (*vs* Hp1-1)	.076756	.658	-.274301	.427813
Hp1-1 (reference)	0	.	.	.
Time	-.077733	.000	-.108447	-.047020
Clot volume	.471654	.024	.066611	.876696
EVD drainage volume	.151809	.414	-.214632	.518250

As can be seen in Figure 5.10, the median complexed Hb values are lower for the Hp2-2 patients, whereas no significant difference was observed between Hp1-1 and Hp2-1 patients. Re-adjusting the contrasts in the analysis identified that Hp2-1 also had significantly higher levels of bound Hb than Hp2-2 (p=0.002). Figure 5.10A shows the predicted values at each day, whereas in Figure 5.10B the median complexed Hb from all time points is presented by phenotype.

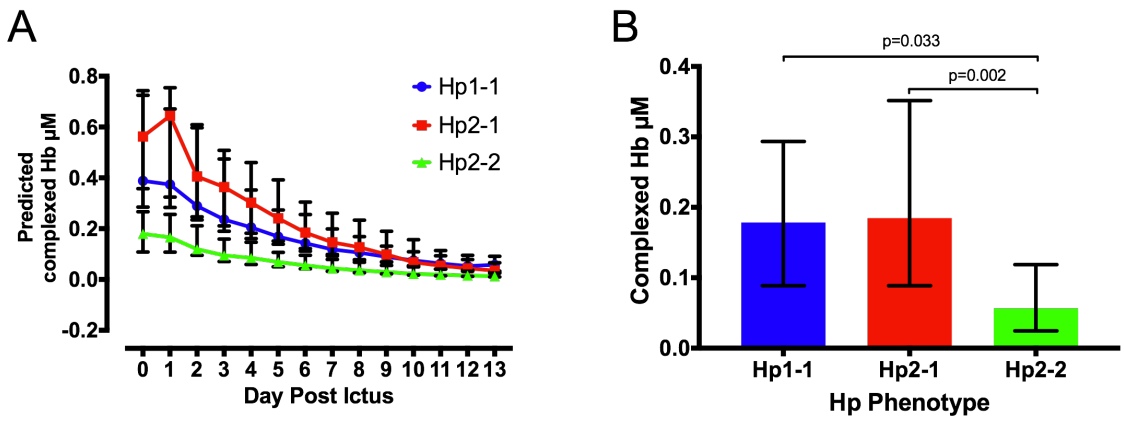

Figure 5.10 *Lower levels of complexed Hb is observed in Hp2-2 individuals.* ***(A)*** *the predicted levels of complexed Hb in patients of each Hp phenotype from the linear mixed modelling analysis. Hp2-2 individuals can be seen to show lower levels of Hb complexed to Hp2-1 and Hp1-1 patients across the entire 13 day period according to the linear mixed model.* ***(B)*** *A summary of predicted complexed Hb levels in patients from all three phenotypes across all 13 days. Data are presented as median ± IQR.*

5.2.8 The contribution of Hb to clinical outcome

Logistic regression modelling was used to investigate the hypothesis that Hb contributed to clinical outcome in this cohort of patients. The *a priori* planned short term outcome was development of DIND and long term outcome was mRS score at 6 months.

5.2.8.1 Delayed Ischaemic Neurological Deficits

DIND is the presence of a focal neurological deficit after SAH and was defined here as a drop by two points on the GCS, or any focal deficit in the absence of the usual causes of deterioration (eg hydrocephalus, infection, seizure or re-bleed)[6]. Five patients presented with DIND. A multivariate logistic regression model was used to predict the development of a DIND. Covariates included Hp phenotype, blood clot volume and the maximum free Hb value.

The model explained 25.6% of the variation (Nagelkerke pseudo R^2) and correctly predicted DIND in 85.6% of cases. Goodness of fit of the model was assessed by the Hosmer and Lemeshow test and was acceptable (p=0.788). The Hp2-2 Hp phenotype (*vs* Hp1-1) showed a trend (p=0.086) of increased likelihood for developing DIND, however this was not significant. No other covariates showed a significant effect contributing to the development of DIND (Table 5.3).

Table 5.3 *Logistic regression model for the development of a Delayed Ischaemic Neurological Deficit.*

	B	S.E.	df	Sig.	OR
Hp Phenotype			2	.218	
Hp Phenotype (Hp1-1 vs Hp2-1)	-1.504	1.275	1	.238	.222
Hp Phenotype (Hp1-1 vs Hp2-2)	-2.597	1.512	1	.086	.074
Clot volume (Ln transformed)	-.993	.732	1	.175	.370
Total Free Hb Max (Ln Transformed)	.348	.265	1	.188	1.416
Constant	2.401	2.466	1	.330	11.031

5.2.8.2 Long-term outcome (6 month mRS)

To predict the effect of Hb on long term outcome by mRS score at 6 months post-ictus, the mRS score was dichotomised into favourable (mRS 0-1) and unfavourable (2-6). More commonly in the literature, a favourable mRS is defined as 0-2, however this dichotomization resulted in two asymmetric groups. By defining favourable mRS as 0-1, dichotomization was more balanced, this minimizing statistical bias, compared to defining favourable mRS as 0-2 (63% *vs* 47%, respectively).

The logistic regression model was the same as previously used for DIND and included Hp phenotype, blood clot volume and free Hb as covariates. The model successfully predicted long term outcome 82.9 percent of the time and explained 41.3% of the variation (Nagelkerke pseudo R^2). The Hosmer and Lemeshow test for goodness of fit was acceptable (p=0.52). Clot volume significantly predicted unfavourable outcome at 6 months (p=0.025, OR=4.7, Table 5.4) indicating that a larger bleed would have a worse outcome. There was also a trend for free Hb to predict unfavourable outcome that was verging on significance (p=0.064, OR=0.7).

Table 5.4 Logistic regression model for the development of unfavourable long term outcome (6 month mRS 2-6).

Variables in the Equation

	B	S.E.	df	Sig.	OR
Hp Phenotype			2	.461	
Hp Phenotype (Hp1-1 vs Hp2-1)	.145	1.109	1	.896	1.157
Hp Phenotype (Hp1-1 vs Hp2-2)	-.977	1.135	1	.389	.376
Clot volume (Ln transformed)	1.561	.697	1	.025	4.765
Total Free Hb Max (Ln Transformed)	-.332	.179	1	.064	.718
Constant	-4.660	2.447	1	.057	.009

5.3 Discussion

This chapter presents observations of Hb accumulation in the CSF after SAH from serially collected CSF samples from the Haemoglobin After Subarachnoid Haemorrhage study.

It was observed that after SAH, there is an accumulation of Hb in the CSF over the first 13 days. CSF Hb concentration is low in the first two days after SAH, but subsequently increases from day three onwards. This delay in its increase is likely due to the time taken for breakdown of the blood clot and lysis of erythrocytes dispersing their Hb content into the subarachnoid space.

It was observed that a significant proportion of the Hb that was not in complex was able to be bound by Hp (ie it is scavengeable Hb). Hb becomes non-scavengeable due to oxidative modifications that occur as a result of Hb's pseudoperoxidase activity[174]. Through this process, H_2O_2 is consumed and ferric Hb is converted to oxo-ferryl Hb (Fe^{4+}=O) via a radical intermediate[174]. During this redox cycling process, radicals are generated at the reactive haem group and migrate outward onto the protein chains[179]. Both the oxo-ferryl (which is highly reactive and radical-like) and the protein radical are required to initiate crosslinking, and during ferric-ferryl redox cycling haem-protein adducts are formed[179]. It was recently identified that these redox reactions of Hb in the presence of H_2O_2 generate Hb molecules that crosslink on their

alpha chains at serine 138[174]. This means that these crosslinked Hb molecules become fixed in a tetrameric conformation, hiding the neo-epitope required for Hp and hindering HpHb complex formation[174].

From the second day post-ictus it was observed that almost all of the unbound Hb is able to be scavenged by Hp. Appreciable levels of non-scavengeable Hb were seen at day 7, however despite this, between days 2-13 the median scavengeable Hb was 89% (IQR 60.4-96.7) of all free Hb; therefore a window of opportunity exists in which Hb can be targeted by Hp based therapeutics.

It was seen here, and in previous work from our group[102] that the baseline level of THBC in the CSF of a control population was extremely low. Following SAH, the THBC is seen to peak to its highest level on the day of ictus. As Hp is a serum protein, this increase on the day of the bleed is likely due to a bolus delivery of Hp from the circulation accompanying the bleed. There is experimental evidence to show that Hp can be synthesized in the CNS during inflammatory conditions[58] however if this increase in Hp was to be attributed to this it would be expected to be a more prolonged increase. In these patients we found no evidence of substantial intrathecal Hp synthesis, as assessed by Hp index from day 4 onwards.

The THBC peak on the day of ictus is followed by a decrease in THBC and by day 3 it has returned to control levels. This, combined with the observation that levels of complexed Hb decrease, indicates that there is a removal of complexes from the CSF once they are formed; this could be through scavenging by microglia and cerebral macrophages in the choroid plexus, meninges or perivascular space expressing the Hb scavenger receptor CD163[55] or alternatively, these complexes may be diffusing out of the brain across a compromised BBB. As the Hp index corrects for BBB permeability, the lower Hp index suggests that Hp is being removed from the CSF via a different process to leakage across a permeable BBB. This is likely to be scavenging of HpHb complexes, such as via CD163, a mechanism known to be active in the CSF after SAH[102].

One of the hypotheses of the work in this chapter is: **haemoglobin is released from the lysing blood clot into the cerebrospinal fluid, overwhelming the resident Hb scavenging system.** These data clearly support this hypothesis since 1) there is a high concentration of free uncomplexed Hb, and 2) the THBC of the CSF is very low and becomes depleted within a few days after ictus. The finding that the majority of Hb is able to be scavenged by Hp, in combination with the observation that there was a trend towards worse long term outcome with increased Hb supports the notion that Hp supplementation would be of therapeutic benefit.

These observations have also provided insight into the amount of Hp required to provide therapeutic benefit. Based on the area under the curve of free Hb in the CSF it was possible to

calculate the required amount of Hp to suitably bind and detoxify this amount of Hb, as demonstrated in Figure 5.11.

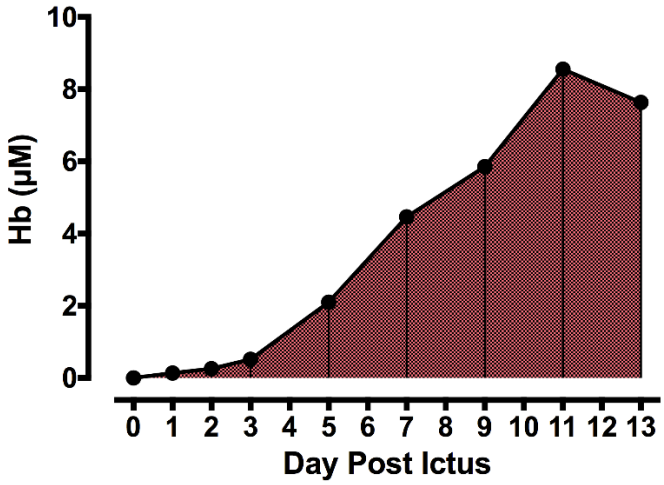

Figure 5.11 *The Hp deficit in the CSF after SAH. The area under the curve for scavengeable free Hb represents the required Hp in the CSF to deal with the Hb insult. Vertical lines represent the 2-3 day blocks in which AUC were calculated to establish the daily Hp requirement to fulfil the Hp deficit.*

The area under the curve for epochs of 2-3 days was calculated, these data are presented in Table 5.5 as daily Hb loads that are required to be detoxified. The binding ratio of Hb to BPL's current preparation has been calculated to be 1:1.2 (Hp:Hb, proprietary data on file, BPL). Therefore the amount of Hp required to detoxify this amount can be calculated.

However this does not reflect cycling of Hp in a kinetic system, so almost certainly the required amount of Hp is likely to be lower in a clinical setting where CSF Hb is measured on a daily basis, and the equimolar amount of Hp administered in a tailored fashion. This requires investigation in future empirical studies.

Table 5.5 *The area under the curve in 2-3 day segments from the scavengeable free Hb graph was used to calculate daily Hp requirements to fulfil the Hp deficit in these patients.*

	Days 0-3	**Days 3-5**	**Days 5-7**	**Days 7-9**	**Days 9-11**	**Days 11-13**
Hb AUC (µM x day)	7.67	11.17	22.68	23.71	22.1	18.71
Daily Hb load (µM day^{-1})	1.92	5.59	11.34	11.86	11.05	9.36
Required daily Hp (µM)	1.60	4.66	9.45	9.88	9.21	7.80

This work has a number of strengths. It is the first longitudinal study of CSF to provide temporal insight into the release of Hb and the kinetics of its scavenger mechanisms following a SAH. Previous work has made observations of Hb in the CSF[102], however no kinetic analysis has been performed over a two week period. This has provided a unique insight into how Hb levels accumulate and the Hp scavenging deficit. A limitation of this work was the lack of standardisation of day of sample collection. This would have strengthened the longitudinal data, with more samples on specific days. Additionally, a greater number of a patients would have reduced the error associated at each time point.

This work is representative of a group of patients with a large haemorrhage (Fisher grade III & IV). Whilst this is a biased cohort, it characterises a worst case scenario and likely represents the highest level of Hb that would be observed in the CSF of those surviving an initial haemorrhage. It would be interesting to further investigate the state of the Hp deficit in individuals with a smaller SAH. However, these samples are more difficult to obtain as typically these patients do not require the placement of an EVD. In the previous Chapter, it was found that at low Fisher grades clinical outcome was not substantially different between HP1 and HP2, suggesting that high Fisher grade patients are likely to benefit the most. Methods of Hp supplementation are discussed in greater detail in the final chapter of this thesis.

Chapter 6 Neurotoxicity of haemoglobin can be ameliorated by haptoglobin *in vitro*

6.1 Introduction

Hb has been demonstrated to be neurotoxic *in vitro*[21] through pro-oxidative mechanisms. Previous reports and observations from our laboratory have demonstrated that the addition of a Hb solution to neuronal cultures causes a reduction in the number of viable neurones (unpublished results, Dr Patrick Garland).

Hp exists as a Hb scavenger that in the first instance binds to free Hb. Through sequestering of the haem group, Hp inhibits Hb's pro-oxidative potential and therefore inhibits its cytotoxic effects, while it is cleared. In addition, this complex formation prevents degradation of Hb to iron and therefore the accumulation of redox-active iron and oxidative tissue damage. This is largely apparent in peripheral tissues such as the kidney where renal filtration of cell free Hb causes iron accumulation and kidney damage. Following SAH, the free Hb in the CNS is left uncomplexed[102] and is toxic to the delicate brain tissue. It is here hypothesized that supplementation of Hp will ameliorate the toxic effects of free Hb to neurons *in vitro*.

BPL purify Hp from human plasma (containing multiple isoforms of Hp); this preparation (named Hp5911) is over 98% pure. Preliminary *in vivo* studies from our group using Hp5911 identified that this preparation induced inflammation in the brains of C57BL/6 mice (unpublished results, Dr Patrick Garland). Subsequently, members of our laboratory undertook further purification steps using HPLC that separated Hp5911 into individual fractions containing the different Hp isoforms (dimer, trimer and higher forms). The contents of the resulting fractions are shown in Table 6.1.

Table 6.1 *The content of each fraction of Hp5911 following HPLC separation. (HPLC separation performed by Dr Patrick Garland).*

Fraction	Constituents
I	60% Higher polymers + Impurities
II	4.2% Trimer + 86% Higher polymers + Impurities
III	34% Trimer + 62% Higher polymers + Impurities
IV	19% Dimer + 64% Trimer + 7% Higher polymers + Impurities
V	93% Dimer + 6.2% Trimer + 0.1% Higher polymers (High protein concentration- 15 mg/mL)
VI	94% dimer + 1.3% Trimer + Impurities (Low protein concentration – 5 mg/mL)
VII	Impurities

This chapter addresses the third hypothesis of this thesis set out in Chapter 2: **haptoglobin can ameliorate the neurotoxicity of cell free haemoglobin *in vitro*.**

Using *in vitro* cultures of primary murine hippocampal neurons, a model of chronic Hb exposure to neurons has been established, that shows results similar to those in the literature[21]. Using these *in vitro* hippocampal cultures I will investigate 1) the neurotoxicity of the HPLC-purified Hp preparation (Hp5911) and 2) the effect of Hp supplementation on the neurotoxicity associated with chronic Hb exposure.

6.2 Results

This work was performed working in collaboration with Dr Patrick Garland, post-doctoral scientist working in this laboratory whilst I trained in this *in vitro* technique. All experiments were designed, analysed and discussed collaboratively; Hp fraction toxicity testing, Hp dialysis toxicity testing, Hb toxicity and Hp treatment experiments were performed jointly.

6.2.1 Haemoglobin is toxic to hippocampal neurons *in vitro*

The exposure of primary murine hippocampal neurons to a murine haemolysate (the primary constituent of which is Hb) produced a dose dependent neurotoxic effect (Figure 6.3). Significant reduction in the number of viable neurons was observed at Hb concentrations above 10 µM ($p=0.0027$), which is comparable to the level of Hb in the CSF of patients following SAH[102] (see Chapter 5 of this thesis).

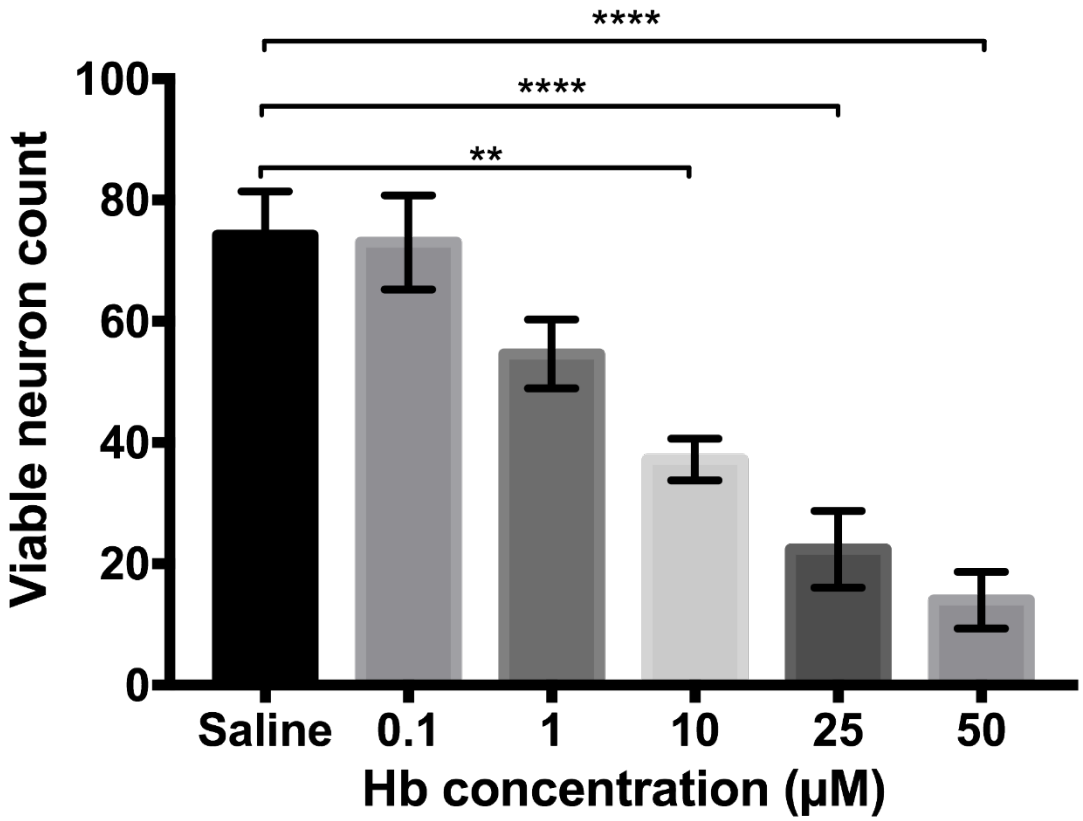

Figure 6.1 *Titration of murine Hb (haemolysate) shows a dose-dependent toxic effect to primary hippocampal murine neurones. Data are expressed as counts of viable neurons (mean ± SEM). 10, 25 and 50 µM were significantly toxic, compared to saline vehicle, in a one-way ANOVA with Tukey's correction for multiple comparisons. Vehicle vs 10 µM p = 0.0027; vehicle vs 25 & 50 µM p <0.0001.*

6.2.2 Purified BPL haptoglobin is not toxic to hippocampal neurons *in vitro*

It has previously been established by our group that the Hp5911 preparation of Hp was toxic and produced neuroinflammation following intracerebroventricular infusion *in vivo* (unpublished results, Dr Patrick Garland). Hp5911 is 98% pure (Figure 6.2) and contains a mixture of different isoforms of Hp (dimer, trimer plus higher polymers). Further purification by members of our group (Dr Patrick Garland) separated Hp5911 into seven fractions. This produced fractions that contained the specific isoforms (Table 6.1 in the introduction to this chapter).

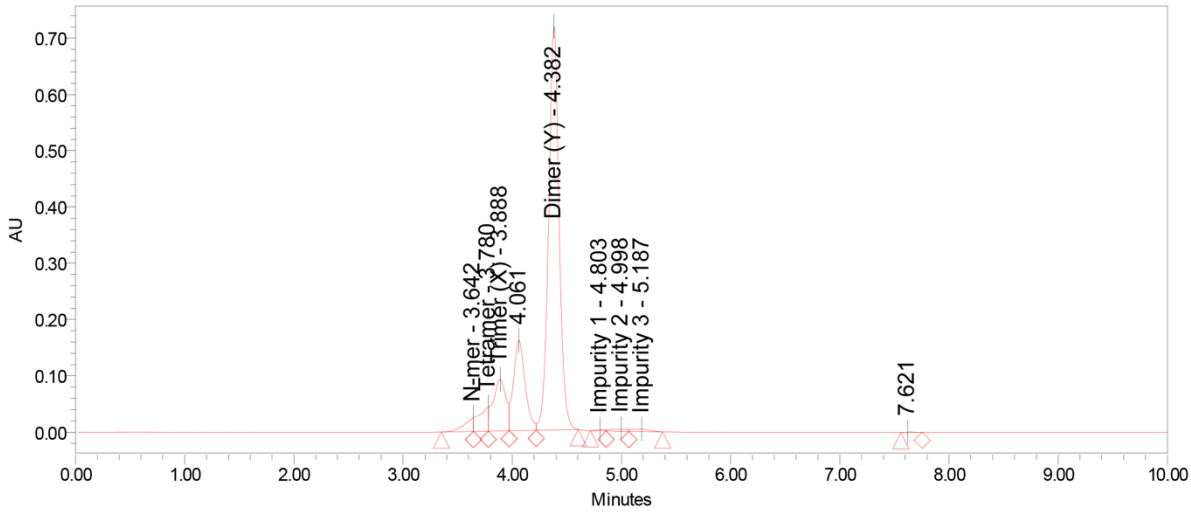

Figure 6.2 *UPLC chromatogram showing absorbance at 280 nm when BPL Hp5911 was run on the UPLC. Each peak represents a different isoform of Hp. The primary constituent is the Hp dimer with other isoforms making up the other major constituents. Smaller impurities are also present.*

Before commencing an investigation into the ability of Hp to inhibit the neurotoxicity by haemolysate exposure, it was important to establish which fraction of Hp5911 contained the neurotoxic constituent. To test this, primary hippocampal neurons were treated with all of the various fractions that were collected during the HPLC purification process. 50µL of 10 µg/µL Hp5911 was added to cultures to achieve a final weight of 500 µg of Hp. This was calculated to achieve equimolar binding of Hp to 10 µM Hb. The fractions of Hp were loaded by weight in equivalent amounts to which they are present in the original Hp5911 preparation; for example, the weight of dimer from fraction V (see Table 6.1 for details of each fraction) added to the cultures was the same as the weight of dimer present in Hp5911 when added to cultures.

Following one week in culture, the fractions were added to cultures and maintained for a further week. Cultures were re-treated with fractions during regular media changes. After treatment, cultures were stained with a MAP2 antibody to visualise neurones and counterstained with DAPI

to identify non-apoptotic nuclei. Cover slips were observed under a fluorescent microscope at x40 magnification; viable neurones were counted, starting at the top of the coverslip and moving vertically down the coverslip. The results can be seen in Figure 6.3. As previously observed, Hp5911 produced significant neurotoxicity as compared to the saline treated control cultures (one-way ANOVA, $p<0.0001$). Surprisingly, no toxicity was observed with any of the seven fractions.

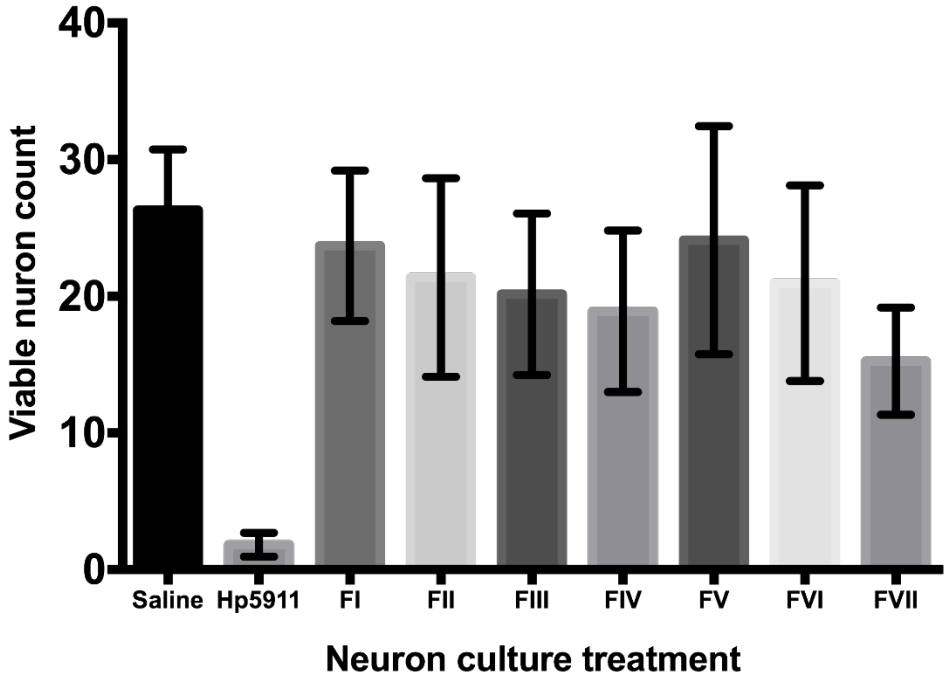

Figure 6.3 *The neurotoxicity of the Hp fractions. Data are presented as counts of viable neurons (mean ± SEM). No significant toxicity was observed with the fractions collected from the HPLC purification process of Hp5911.*

6.2.3 Dialysed BPL Hp5911 is not toxic to neurons

As no toxicity was associated with any of the fractions, it was hypothesized that the toxic constituent in Hp5911 was lost during the fractionation process, and might therefore be of low molecular weight. To test this hypothesis Hp5911 was dialysed across a membrane with a cut off size of 20 kDa, as this would allow clearance of the putative low molecular weight toxic molecule(s). Figure 6.4 shows the effect of this dialysis step. As before, Hp5911 had inherent cytotoxicity (one-way ANOVA, $p<0.0001$), however the dialysed solution showed no significant difference to the vehicle control. This indicates the molecular weight of the toxic component is less than 20 kDa and can effectively be removed (or reduced to non-neurotoxic levels) by dialysis.

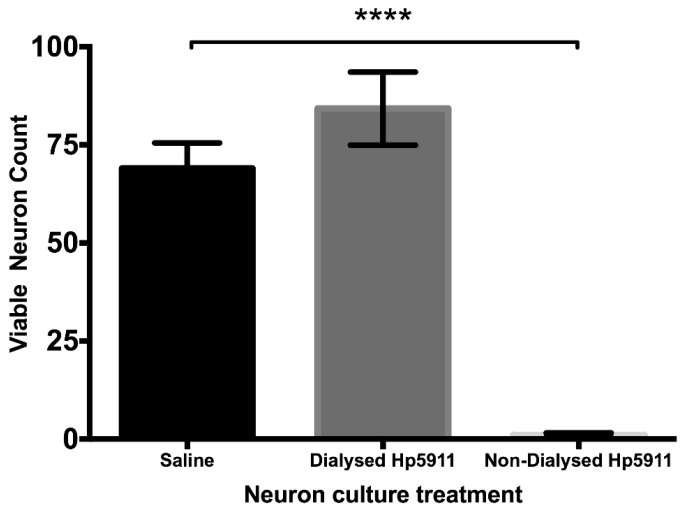

Figure 6.4 *The neurotoxicity of dialysed Hp5911 and non-dialysed Hp5911 compared to vehicle (saline) control. Non-dialysed Hp5911 showed significant neurotoxicity compared to controls (one-way ANOVA, p<0.0001, Tukey's correction for multiple comparisons). Data are presented as mean ± SEM.*

6.2.4 BPL Hp5911 binds to mouse haemoglobin

Prior to testing the ability of BPL's preparation of Hp to rescue the neurotoxicity of chronic Hb exposure in the *in vitro* assay (Figure 6.1), it was essential to ensure that the BPL (human) Hp can bind to murine Hb. Mouse Hb (from haemolysate) was added in increasing concentrations to a BPL Hp5911 concentration of 1 mg/mL. HpHb complexes were measured using the UPLC Hb binding assay, as described in Chapter 5 of this thesis. Figure 6.5 shows HpHb complex concentration plotted against the Hb concentration; it is clear that the BPL Hp5911 binds to murine Hb. Saturation was observed at 1.2 mg/mL Hb, identical to the known binding ratio of Hp5911 to human Hb which had previously been established to be 1:1.2 (proprietary data on file, BPL).

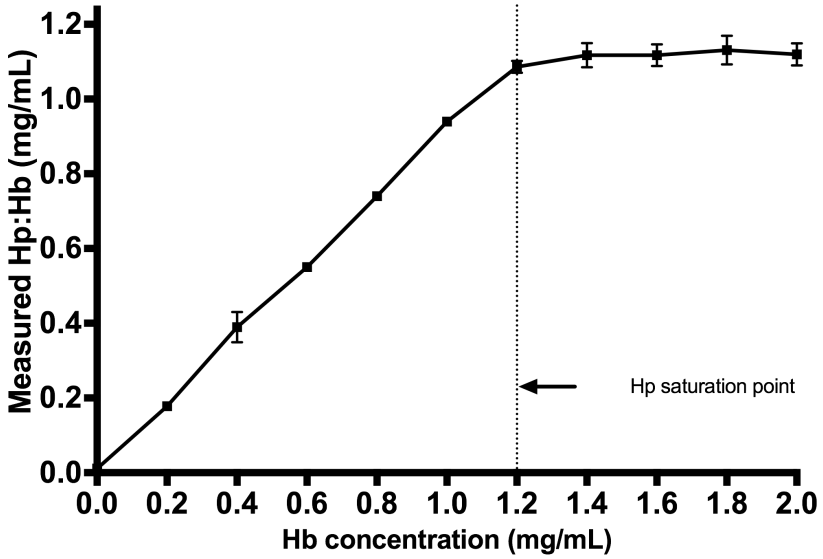

Figure 6.5 *The binding curve of BPL Hp to mouse Hb (from haemolysate). Murine Hb was added at increasing concentrations (0 to 2 mg/mL) to 1mg/ml BPL Hp. Mixtures were run on the UPLC and absorbance monitored at 415 nm to measure haem containing species. Samples were prepared in triplicate and data are presented as mean ± SD; data points with no error bars are due to the error bar being smaller than the data symbol itself.*

6.2.5 Haptoglobin can rescue haemoglobin neurotoxicity *in vitro*

To test the hypothesis that dialysed Hp inhibits cell death due to chronic Hb exposure, primary hippocampal neurons were treated for 1 week with either vehicle, 15 µM Hb, dialysed Hp5911 Hp, or 15 µM Hb + dialysed Hp5911 Hp at either 1:1, 1:2 or 1:3 equimolar ratios. The results in Figure 6.6 show that when in complex with Hp, the neurotoxic effect of Hb to primary neurons is reversed. In a one way ANOVA, no significant difference in viable neuron counts is observed with Hp compared to vehicle control (saline), a significant difference was observed between Hb and HpHb (1:1) ($p=0.028$), HpHb (1:2) ($p=0.011$) and HpHb (1:4) ($p=0.003$). These analyses are without corrections for multiple comparisons however and only Hb *vs* HpHb (1:4) was robust to Dunnett's correction for multiple comparisons ($p=0.021$).

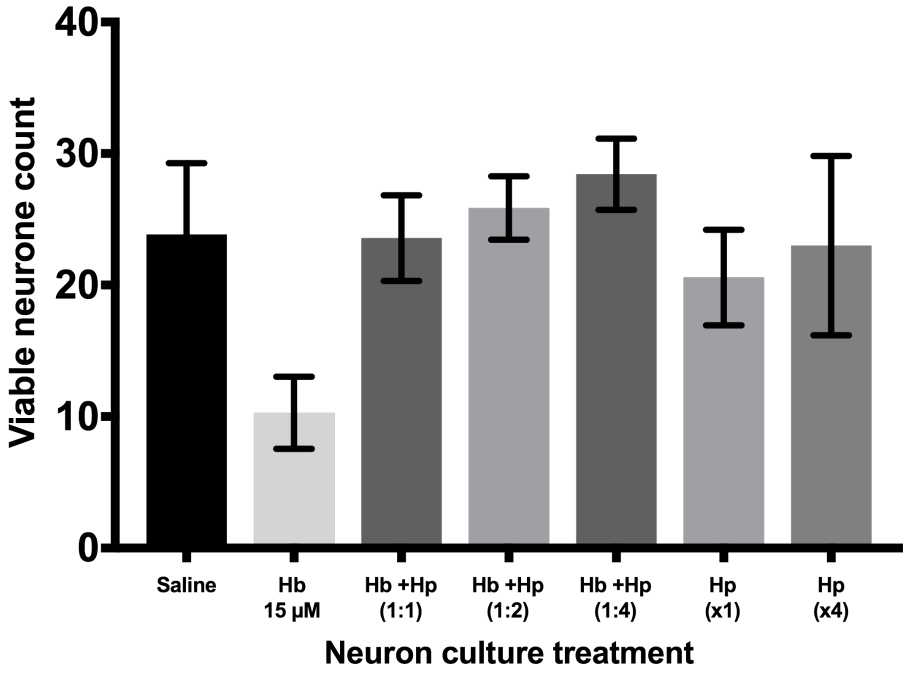

Figure 6.6 *The treatment of primary murine hippocampal neurons with either vehicle (saline), 15 µM Hb, 15 µM Hb + Hp at 1:1, 1:2 or 1:4 equimolar amounts, or equivalent amounts of Hp alone.*

6.3 Discussion

In this chapter it has been demonstrated that 1) Hb causes dose-dependent neurotoxicity, 2) fractionation of BPL Hp5911 Hp produces a series of preparations of individual Hp isoforms that are not toxic to neurons *in vitro*, 3) dialysis of BPL Hp5911 is sufficient to remove neurotoxicity, 4) Hp5911 is able to bind to mouse Hb, and finally 5) dialysed Hp can effectively inhibit Hb neurotoxicity.

Interestingly, none of the seven fractions of Hp5911 show a difference compared to vehicle control (saline); in other words, the toxicity observed with the original Hp5911 does not associate with a specific fraction (and therefore it is not a single isoform of Hp that is toxic). The purification process was achieved using Size Exclusion High Performance Liquid Chromatography (HPLC-SEC). In this method, during the mobile phase of the chromatography, analytes interact with an adsorbent material within the chromatography column. This interaction slows the passage of the analyte through the column and the strength of the interaction is a function of the molecular size of the analyte. Smaller particles are retained in the column longer and larger particles pass through quicker, thus separation of the constituents occurs by size. It is likely that a low molecular weight component of Hp5911 eluted from the column later and was not collected in any of the fractions. Although the identification of the neurotoxic component was not pursued, it is possible

that haem may contribute to some or all of it, since Hp5911 was visually xanthochromic and this xanthochromia disappeared after dialysis.

These results demonstrated that primary murine hippocampal neuron cultures are sensitive to Hb exposure in a dose-dependent manner, with significant neuronal death occurring above 10 µM Hb. Low density neuronal cultures were employed to enable visualization of individual neurons and a robust assessment of their integrity, whereas this would have been impossible in more traditional high density neuronal cultures. High density is usually needed to maintain longevity in culture, possibly through secretion of the right concentration of soluble trophic factors. Therefore in this work high density neurones were displaced to a ring of *trophic support* neurons (200,000 cells), which were seeded around the perimeter of the well. This facilitates the growth of the hippocampal neurons on coverslips in the middle of the culture wells at low density (5,000 cells).

Due to the low density of neurones on the coverslip, technical variability in cell number becomes easy to detect, as can be seen by comparing Figure 6.1 and Figure 6.3. Variability likely arises during tissue processing and counting of cells prior to seeding. To ensure that this variability is controlled for, it was essential that each plate from each preparation accommodated replicates of all the multiple conditions being tested e.g. vehicle, Hb, Hp and Hb + Hp.

In these experiments it was important to use the same Hb concentration as that observed after human SAH (Chapter 5, median 11.5 µM total Hb in ventricular CSF, ± IQR of 2.1-16.2 µM Hb). Amongst different cultures, variability was observed in neuronal survival after exposure to 10 µM Hb (data not shown); hence it was decided to use 15 µM Hb in subsequent experiments which consistently demonstrated significant and less variable decreased neuron counts. Both 10 and 15 µM are representative of the Hb concentration after human SAH. It can be argued that the Hb concentration experienced by neurones close to the blood clot may be higher than the Hb concentration measured in ventricular CSF.

In vitro, Hb resulted in injury to isolated hippocampal neurones directly, while *in vivo*, there could be additional injury to cells such as oligodendrocytes and astrocytes which provide neuronal support. While the culture system included an outside ring of cortical neurones, these were located in the periphery of the well, distant from the hippocampal neurones on the coverslip located centrally in the well, and this supporting ring of cells was absent of glia. Mixed neuronal glial culture, or organotypic hippocampal culture, would have more closely modelled the *in vivo* arrangement, though the *in vitro* nature would still necessitate in vivo experiments. For instance Hb can cause vasospasm by scavenging nitric oxide, which can lead to neuronal damage through ischaemia, but this cannot be modelled by any of the *in vitro* systems mentioned above.

Direct damage to Hb *in vitro* would have been mediated via oxidative mechanisms; the strong pro-oxidative potential of Hb is mediated by the redox active iron in the haem prosthetic group. Previous publications which have reported that the neurotoxicity of Hb is reversed by addition of an antioxidant (Trolox: a vitamin E derivative)[21] or the ferric iron chelator deferoxamine[24]. This is further demonstrated by the temporal occurrence of markers of oxidative stress when Hb is added to neuronal cultures and the timing of neuronal cell death, and the fact that antioxidants are equally effective if treatment is delayed is consistent with a redox-mediated mechanism of injury[24].

Hp rescued neurotoxicity after Hb exposure, such that neuronal density was comparable to vehicle controls (saline). Visual inspection of Figure 6.6 suggests a dose-dependency, but this was not significant. After binding to Hb, Hp renders the haem ferryl iron thermodynamically[74] and kinetically inert[72]. In doing so it alters its redox potential such that it is less able to participate in downstream radical generating reactions[72,74]. It will be interesting to compare the relative efficacy of Hp, Trolox and deferoxamine, and combinations, in future *in vitro* and *in vivo* experiments.

There is a body of work in the literature which details mechanistic differences in the ability of different isoforms of Hp to bind or clear Hb[55,77,84] (summarised in Appendix B). As purified fractions containing specific isoforms of Hp have been generated it would be interesting to repeat the experiment using Hp dimer, Hp trimer and higher order polymeric Hp forms separately. If a certain Hp species was better or worse at scavenging Hb, this will have implications for clinical trials and Hp purification strategies in the pharmaceutical industry.

Having established that Hp can successfully prevent the cellular neurotoxicity of Hb *in vitro*, the next step is to reproduce this finding *in vivo* following an experimental model of SAH. Hb-mediated toxicity is not the only mechanism underlying the pathogenesis of poor long term outcome after SAH; other mechanisms include mechanical damage, ischaemia and inflammation. It is therefore important to investigate the relative contribution of Hb-mediated neurotoxicity to overall outcome in the *in vivo* setting after experimental induction of SAH.

While the effect here has been described *in vitro*, the effect of Hb within the complexity of the CNS parenchyma may well be different. In this *in vitro* model, neurones are surrounded in media containing a high concentration of Hb. This is similar to the situation *in vivo* where the CSF and interstitial fluid contains Hb released from the lysing blood clot and the Hb concentration *in vitro* was matched to that observed *in vivo* after human SAH. Although the culture medium was changed regularly during *in vitro* culture, this is not the same as the continuous flow of CSF and interstitial fluids *in vivo*. While Hb was replaced with media changes, any toxic breakdown products of Hb would have been in contact with neurones for a prolonged period of time *in vitro.*

This is likely to be associated with a greater and/or different type of damage. Also, neurones were isolated in culture, which is quite different from the situation *in vivo*, where neurones are surrounded by glia designed to provide immediate tropic support to neurones, and clear toxins. As an example, the situation could be quite different *in vivo*, where perivascular and meningeal macrophages expressing CD163 which can scavenge Hb and Hb-containing complexes, are situated close to neurones.

An *in vivo* study examined intrastriatal injection of whole blood lysate and demonstrated damage to surrounding tissue consistent with Hb associated oxidative damage[58]. While this work closer resembles intracranial haemorrhage, rather than SAH it showed that oxidative Hb mediated neurotoxicity occurs *in vivo*, and therefore findings from the culture model in this chapter are likely to be relevant *in vivo.* A model of intraventricular haemorrhage, in which 7 day old rat pups were intraventricularly injected with an Hb solution, is much more comparable to SAH, with exposure to high Hb concentrations in the CSF and subarachnoid space[180]. The investigators reported that in the hippocampus, a region proximal to the lateral ventricles, there were significantly fewer neurones, and an increased number of degenerating neurones (as assessed by fluorojade C) compared to non-Hb injected controls[180].

In the next chapter, I describe my efforts to establish and characterise an *in vivo* model of SAH in our laboratory. This model could be used as a tool to test the effect of Hp interventions for Hb toxicity in a model of SAH. The hypothesis of this work is that Hp-based can ameliorate Hb neurotoxicity. The approach taken in this chapter was to supplement culture media with purified exogenous Hp. It would be possible to directly supplement Hp in the CSF in SAH patients by administration via an indwelling EVD, similar to when patients need intrathecal antibiotics for ventriculitis. This would limit treatment to patients with high-grade SAH, as it is these patients who require an EVD to manage their condition. Also there may be immunogenicity issues when Hp1-1 is administered to HP2 homozygous patients and *vice versa*, so this needs further study. Finally, there will be a limit to how much protein can be administered intrathecally, without causing adverse events as a result of osmotic shifts and increased CSF viscosity. Another method, however would be to upregulate local Hp synthesis using pharmacological methods. Hp expression is under the control of the transcription factor nrf2, and therefore nrf2-activating drugs upregulate Hp expression[181]. However the effect of these drugs on Hp expression is modest (as an example sulforaphane upregulates Hp mRNA 1.6-fold[182]) and high-grade SAH patients are likely to need much more Hp. As discussed in Chapter 5, the Hp concentration in CSF is around 0.04μM in both controls and after SAH (in terms of Hb binding capacity), and CSF Hp levels will need to rise 100-fold (to between 2 and 10μM) to be able to neutralize a mean concentration of 10μM Hb in the subarachnoid space.

Chapter 7 An *in vivo* model of subarachnoid haemorrhage

7.1 Introduction

A clinically relevant animal model of SAH is essential to translate the *in vitro* efficacy of Hp against Hb toxicity observed in Chapter 6, to the *in vivo* setting. A murine model of SAH has been developed in Loch Macdonald's laboratory[120] at St Michael's Hospital, University of Toronto, which I have established in our laboratory in Southampton following a period of time spent training at their institution.

As previously discussed in the introduction to this thesis, there are a number of different types of *in vivo* SAH models, involving either perforation of a major cerebral artery or injection of blood. The model used in the Macdonald lab[120] uses an injection of whole blood into the prechiasmatic cistern, and reproduces aspects of human SAH including increased ICP, development of large artery vasospasm[120,125] and neuronal death[120].

The use of a controlled injection (rather than artery perforation) results in greater reproducibility, reduced variability[29,183] and allows the use of saline injection as control (only sham surgery control is available with the perforation models[29,121]). Therefore, this model can effectively be used to disentangle the mechanical effects of increased pressure from the effects of Hb in the brain.

There are distinct anatomical differences between the anatomy of the meninges in man and mouse which are worth considering. The arachnoid membrane encompasses the CSF filled subarachnoid space[184]. In the human, the subarachnoid space contains arachnoid trabeculae which extend from the arachnoid membrane down to the pia mater on the surface of the brain[184], but these are absent in the mouse[185]. In the rodent CNS, the subarachnoid space is shallower than in the human, and in places occluded, due mainly due to the smoothness of the mouse cortex, without the presence of sulci as in the human brain[185].

Following a period of training in the Macdonald lab in Toronto, I established the murine prechiasmatic model in our laboratory in Southampton. This chapter describes my efforts to refine and characterise this model.

7.2 Results

7.2.1.1 The Macdonald lab method

In the first instance, the model was performed as per protocol detailed in the original Sabri *et al.* 2009[120], taught during a period of training in their laboratory. This involves an injection of 100 µL of saline or blood into the prechiasmatic cistern at a rate of 300 µL/minute, under aseptic technique. General anaesthesia was delivered by isoflurane inhalation and animals were given buprenorphine subcutaneously as post-surgery analgesia. Further experimental detail is available in Chapter 3. Surgery was performed across three experiments in 8-10 week old mice as detailed below:

1. Assessment of T maze alternation and burrowing behaviour (survivors sacrificed at 14 days, n=6 saline, n=6 SAH).
2. Assessment of light/dark preference (survivors sacrificed at 14 days, n=7 saline, n=8 SAH).
3. Assessment of locomotor activity in the open field arena and vasospasm (survivors sacrificed at three days, n=5 saline, n=6 SAH).

7.2.1.2 Morbidity and mortality

The mortality rate of mice undergoing surgery (saline n=19, SAH n=31) was 24% (12 of 50 animals, 1 saline animal, 11 SAH animals). Death occurred immediately following injection. There were two animals showing signs of sickness behaviour that had to be sacrificed at one day post-surgery. These were both animals which had received saline injections. This was not attributable to the intracranial injection, and might have been a post-operative infection.

7.2.1.3 Cerebral blood flow changes

Throughout surgery the cerebral blood flow (CBF) of mice was monitored with a laser Doppler flow probe placed contralaterally on the surface of the skull, circa 6 mm caudal to the site of injection. This allowed monitoring of cerebral perfusion during surgery, important to confirm the rise in ICP during the injection. Arbitrary tissue perfusion units (TPU) were normalized by expressing as a percentage of mean pre-injection CBF values. It was observed that during anaesthesia the cerebral blood flow was relatively stable and the two minutes prior to injection was averaged and this taken as baseline. Subsequent to injection there was a decrease in CBF (Figure 7.1), as increased ICP caused cerebral hypoperfusion.

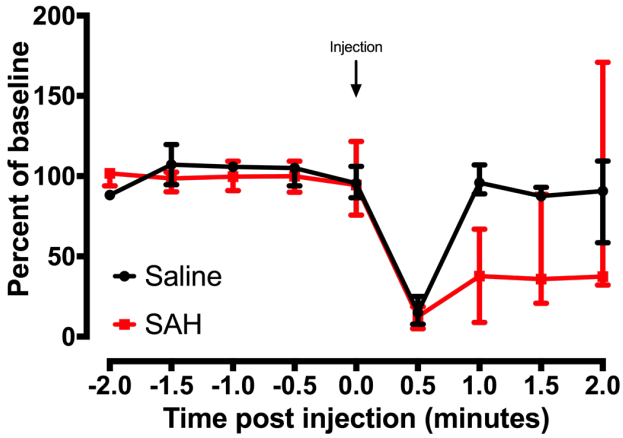

Figure 7.1 *Representative CBF changes as measured by laser Doppler flowmetry during injection of either 100 µL blood or 100 µL saline at a rate of 300 µL/minute (n=3 saline, n=6 SAH). TPU were normalized by expressing as a percentage of mean pre-injection CBF values. Data are presented as median ± IQR.*

Saline and blood injections showed a decrease in CBF to 15.1% and 12.4% of baseline, respectively. The CBF of blood injected animals appeared to remain low for a longer period of time, *vs* saline injected animals. This is likely to be due to 1) the increased viscosity of blood compared to saline and, 2) the presence of a blood clot in blood injected animals.

7.2.1.4 Body weight

The general health of all animals undergoing surgery was monitored by visual inspection and daily weight measurements. Other than the two animals referred to above, there was no obvious sign of abnormal or sickness behaviour in either blood or saline injected survivors as a result of the intracerebral injection. Weight data are presented in Figure 7.2 as percent of baseline weight. Saline injected mice lost weight up to day one, after which they start putting on weight again. SAH animals showed a decrease in weight which was more prolonged in duration, such that weight did not start to increase again until day three. This was not statistically significant (multiple t tests with Bonferroni correction, ANOVA was not applicable due to missing data points).

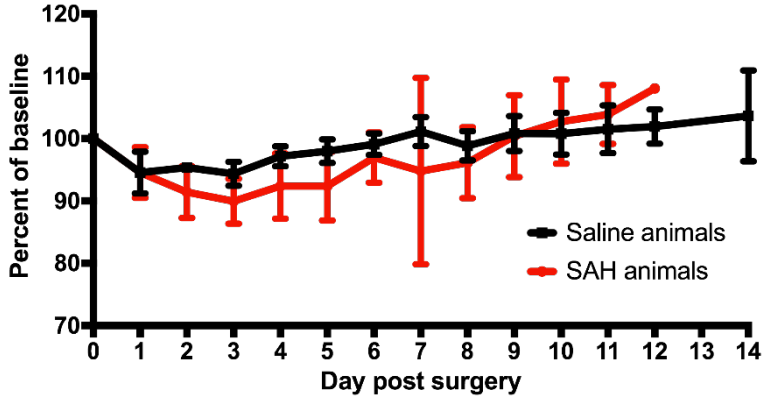

Figure 7.2 *Mouse body weight following injection of 100 µL blood or saline presented as change from baseline (pre-surgery) weight (n=6 saline, n=6 SAH). Data are presented as mean ± SD. Not statistically significant (multiple t tests with Bonferroni correction, ANOVA was not applicable due to missing data points).*

7.2.1.5 T maze spontaneous alternation

The T maze is a short term memory test used to assess hippocampal function in rodents[139]. It relies on the animal's innate desire to investigate new areas (in search of food or shelter). It is expected that an animal with functioning short term memory remembers previously investigated areas and thus explores new grounds. In this test the mouse is placed in a T shaped maze and allowed to run through the maze, during which it will investigate one of the two arms. Following a period of time exploring that arm, the mouse is placed back at the starting point in the maze. It would be expected to alternate to the other arm on the second run. Twenty trials were performed across a week, during a trial, if the animal alternated it received a score of 1, and if it failed to alternate then would receive a score of 0. The scores were then summed and expressed as a percentage of the total number of trials (20) (Figure 7.3).

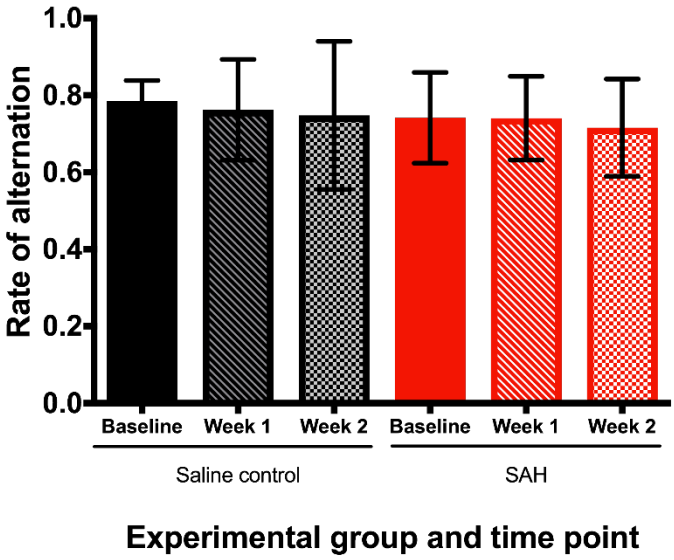

Figure 7.3 *Rates of alternation observed in the T maze behavioural test for saline control and SAH animals pre-surgery, and one and two weeks post-surgery (n=3 saline, n=6 SAH). High rates of alternation are observed in both groups before surgery, which did not change post-surgery.*

High rates of alternation (~80%) were observed in the mice prior to injection of blood or saline. This is in line with what is expected in healthy wild type animals[139]. No change in the rate of alternation compared to baseline levels was observed following injection of either saline or blood (Figure 7.3).

7.2.1.6 Burrowing behaviour

Burrowing is an innate behaviour in rodents which may be compromised in many models of neurodegeneration, and a deficiency in burrowing is a reliable sign of dysfunctional behaviour[140,186]. An assessment of burrowing, as described in Chapter 3, was performed prior to surgery as a habituation exercise to obtain baseline readings, and then reassessed once per week post-surgery for two weeks (Figure 7.4).

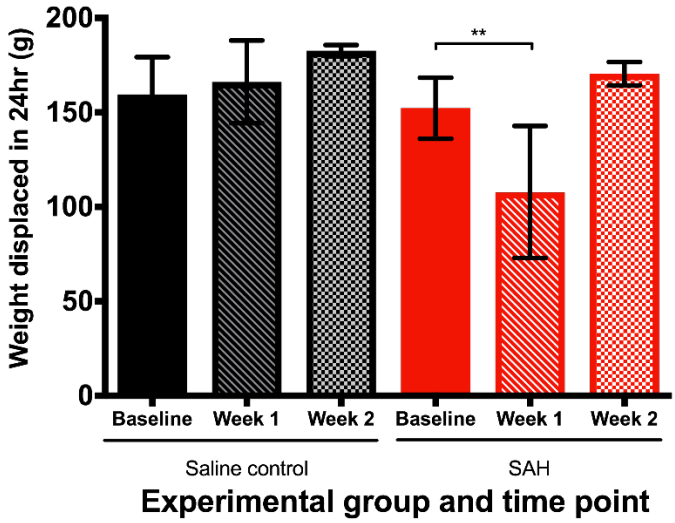

Figure 7.4 *Burrowing as assessed by the weight of material burrowed from a hollow tube in a 24 hour period (n=6 saline, n=6 SAH). SAH animals burrowed significantly less material at one week compared to baseline (p<0.01).*

No change was detected in the animals' burrowing at any time points in the saline injected animals. A statistically significant reduction in burrowing was observed at one week post-surgery in the blood injected animals (one way ANOVA, with Tukey's multiple comparisons post hoc test, $p<0.01$). This behaviour returned to baseline levels in the second week following surgery.

7.2.1.7 Light/dark preference

SAH patients often report photophobia, thought to be secondary to meningeal irritation[187]. It was therefore hypothesized that SAH animals may also show an aversion to light. A dark box test was used here to assess light/dark preference in the animals. The open field arena (see section 7.2.1.8 below) was modified using a cardboard box to completely cover the sides of one half of the arena. A cardboard divider between the two halves of the arena blocked as much light as possible, but still allowed the mouse to travel freely between light and dark areas, while not obstructing the lasers for motion detection. The test involved placing the mouse in the light area of the arena where it would be tracked by laser detection for five minutes. To test for photophobia, the duration spent in the dark area was measured; this is presented in Figure 7.5. No significant difference was observed between saline and SAH animals (t test, $p=0.381$).

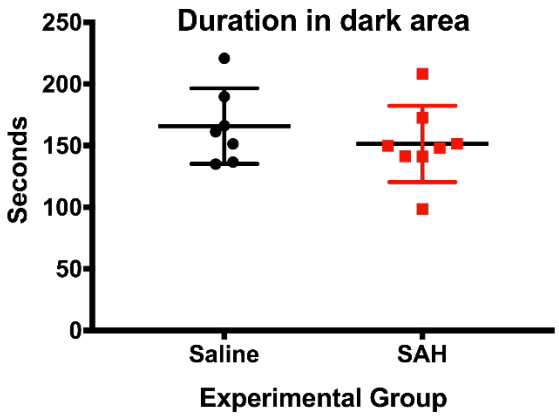

Figure 7.5 *The duration of time spent by SAH and saline injected mice in the dark area of the open field arena. No significant difference was seen between groups (p=0.381). Data are presented as mean ± SD.*

Although there was no difference in the duration of time spent in the dark area between the two groups, their activity in the area was investigated. It was reasoned that whilst both groups spent equivalent times in the dark area, SAH animals displaying aversion to light may spend more time immobile whilst in the dark area. The time animals spent moving and the distance travelled in the dark area are presented in Figure 7.6. SAH animals showed a trend towards increased activity which was not statistically significant (p=0.085 for time and p=0.096 for distance, t tests).

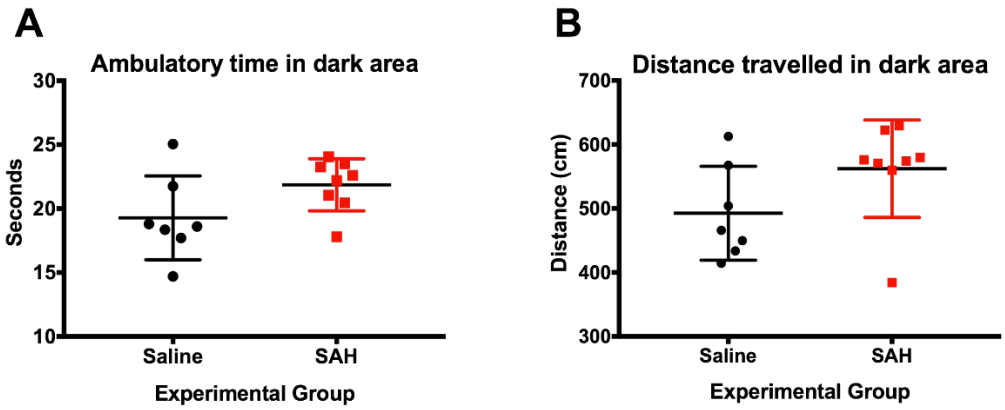

Figure 7.6 ***(A)*** *Time mice spent moving in the dark area of the open field arena, and* ***(B)*** *the distance travelled by mice in the dark area of the open field arena. Data are presented as mean ± SD.*

7.2.1.8 Locomotor activity assessment

Locomotor activity was assessed in the mice using the open field paradigm. This is a square arena with high Perspex walls preventing escape. The animal is placed in the centre of the arena at the start of the assay, and its ambulation is tracked throughout the arena by laser detection over a

five minute period. Animals were habituated to the arena for three days prior to induction of SAH, with the final session recorded as baseline, and then re-tested on day three post-surgery.

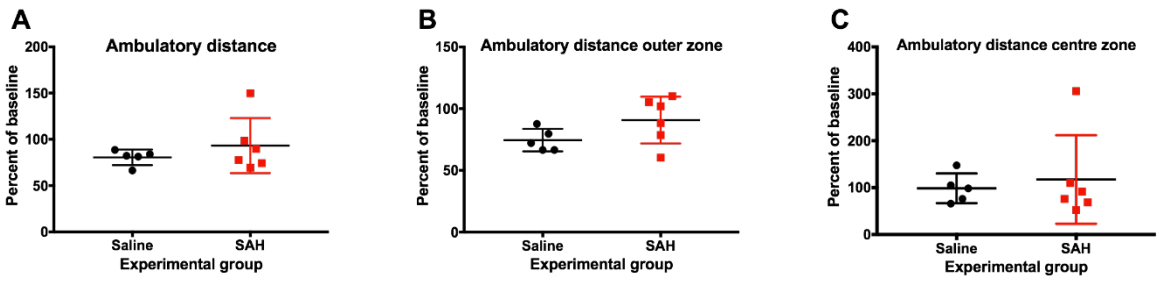

Figure 7.7 *Ambulatory assessment in the open field arena.* ***A)*** *the total ambulatory distance travelled by mice throughout the whole arena* ***B)*** *the ambulatory distance travelled in the outer zone of the arena,* ***C)*** *the ambulatory distance travelled in the centre zone of the arena. Dara are presented as mean ± SD.*

The ambulatory distance travelled across the whole arena is presented in Figure 7.7A. The saline injected animals moved less after surgery, yet the SAH group did not show a significant change (p=0.007 & p=0.599 respectively, one sample t test against the baseline value of 100%). The change in ambulation from baseline was not significantly different between the two groups (p=0.384, t test). The variance in the SAH group was high.

It has been proposed that the open field arena can be used as a measure of anxiety. Thigmotaxic behaviour, the preference to stay close to the perceived safety of the wall, as opposed to the open centre of the arena, has been proposed to characterise the anxious phenotype[141]. Therefore it was hypothesized that while the total distance travelled may not have increased, their choice of exploratory area within the arena may be different between groups. This was assessed by investigating the ambulatory distance in both the outer and centre zone (Figure 7.7B&C) and the duration spent in both areas (Figure 7.8A&B). There was no significant difference in the distance travelled (p=0.114, t test) or the duration spent (p=0.999, t test) in the outer zone between SAH animals and controls.

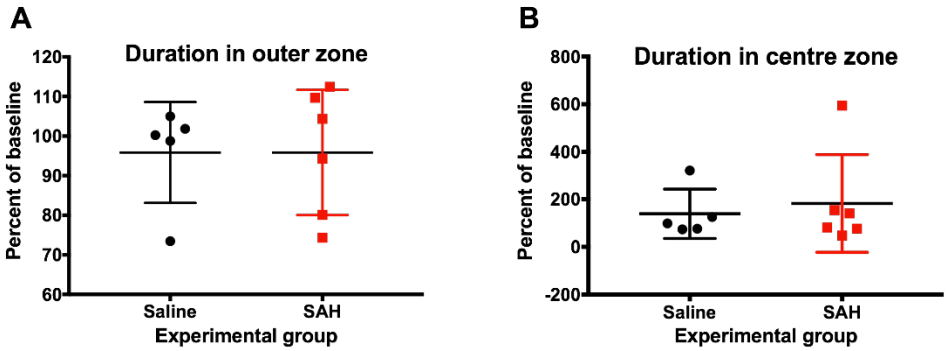

Figure 7.8 *The duration of time spent in **A)** the outer zone or **B)** the centre zone of the open field arena. Dara are presented as mean ± SD.*

7.2.1.9 Vasospasm

Vasospasm was assessed at three days post-ictus by visualising the cerebral arteries of the circle of Willis after perfusion with the fluorescent dye ROX SE (5,6-Carboxy-X-Rhodamine, Succinimidyl Ester) during the perfusion fixation procedure[142]. ROX SE forms succinimidyl esters with side chains of proteins on endothelial cells of the arteries allowing their fluorescent visualisation after laser excitation with light in the yellow-green range of the spectrum. Confocal photomicrographs were taken of the MCA ipsilateral to the side of blood injection and the maximum projection processing method used to construct two-dimensional images from the z stack. In some instances, the vessel was found to be either missing or damaged such it could not be reliably quantified, and these specific animals were excluded from analysis.

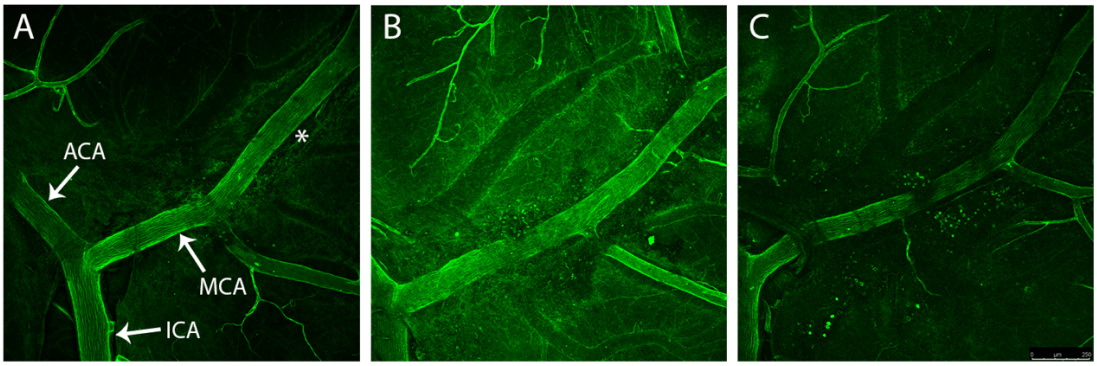

Figure 7.9 *Representative confocal photomicrographs of the ipsilateral MCA from mice undergoing surgery.* ***A)*** *MCA from a naïve mouse,* ***B)*** *MCA from a saline injected animal, and* ***C)*** *MCA from a blood injected animal. Vasospasm was quantified by measuring the narrowest part of the artery along the first millimetre (*) of the ipsilateral MCA after its bifurcation from the ACA; data presented in Figure 10. Labelled are the Anterior Communicating Artery (ACA), Middle Cerebral Artery (MCA) and Internal Carotid Artery (ICA).*

Representative photomicrographs of the ipsilateral MCA can be seen in Figure 7.9. The MCA of a naïve mouse is shown for comparison. Vasospasm was quantified by measuring the narrowest part of the artery along the first millimetre of the ipsilateral MCA after its bifurcation from the ACA. These data (Figure 7.10) showed a single SAH animal and a single saline injected animal with considerably reduced vessel diameter but most were comparable.

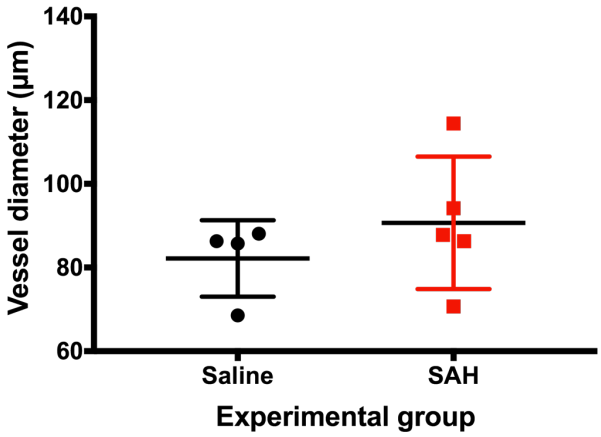

Figure 7.10 *Quantification of MCA ipsilateral to the injection in mice receiving an injection of 100 µL saline or blood at 300 µL/minute. Data presented as mean ± SD. Mice are from the same experiment as* Figure 7.7 *and* Figure 7.8*, but there are less data points since the MCA was either missing or damaged in some brains.*

7.2.2 Refinement of the model I

Modifications were made to refine the model in efforts to reduce mortality, and reproduce a rate of vasospasm similar to that in human SAH survivors. The following adjustments were made, and their rationale is described below:

1. Use of older animals, as the 8-10 week old mice used previously were equivalent in biological age to a young human in their teenage years. Three month old mice were used since these are equivalent to a human age of around 30 years. Whilst this is still young for a SAH, it is closer to the median age of around 50[11].
2. A slower injection rate of 200 µL/minute. This slower rate of injection, in combination with the larger cranium in older mice, was aimed at reducing mortality by lowering the sudden ICP rise; this is in keeping with the recommendations of the 3R's. It was reasoned that the extra survivors may represent a population of mice more susceptible to developing vasospasm.
3. Use of injectable ketamine/xylazine anaesthesia for surgery. Previously, isoflurane had been used to anaesthetise animals for induction of SAH, however isoflurane has hypotensive and cytoprotective effects[188]. Consideration was given to the fact that these anaesthetic factors may have affected vascular tone.

7.2.2.1 Mortality and morbidity

The mortality rate of all mice undergoing this modified surgery (saline n=8, SAH n=11) was reduced, at 26% (5 of 19 animals, two saline animals, three SAH animals). Death occurred immediately following injection in animals receiving blood, except for one saline injected animal. This animal showed an unusual CBF pattern, with prolonged reduction in flow following the removal of the needle that was accompanied with reflux of blood from the burr hole. This indicated that an artery on the circle of Willis had been perforated. A single SAH animal lost weight more rapidly than other SAH animals, was observed huddled in the corner of its cage and exhibited circling behaviour. This animal had to be sacrificed early, and therefore the SAH group in this section of the Chapter consisted of either seven or eight animals.

7.2.2.2 Cerebral blood flow

As in the previous experiment, there was a demonstrable drop in CBF as measured by laser Doppler flowmetry. Saline and blood injections resulted in a decrease in CBF to 34.9% and 6.0% of baseline, respectively (Figure 7.11). In the previous version of the method, CBF had decreased to 15.1% and 12.4% of baseline previously. The substantial improvement in CBF in the saline group

was probably secondary to the slower injection rate. In SAH animals a lower CBF nadir was observed, and CBF took longer to recover than previously (as appreciated by comparing Figure 7.1 and Figure 7.11). This decrease in median CBF was probably due to the older age of the mice; the different anaesthetic agent may also have contributed.

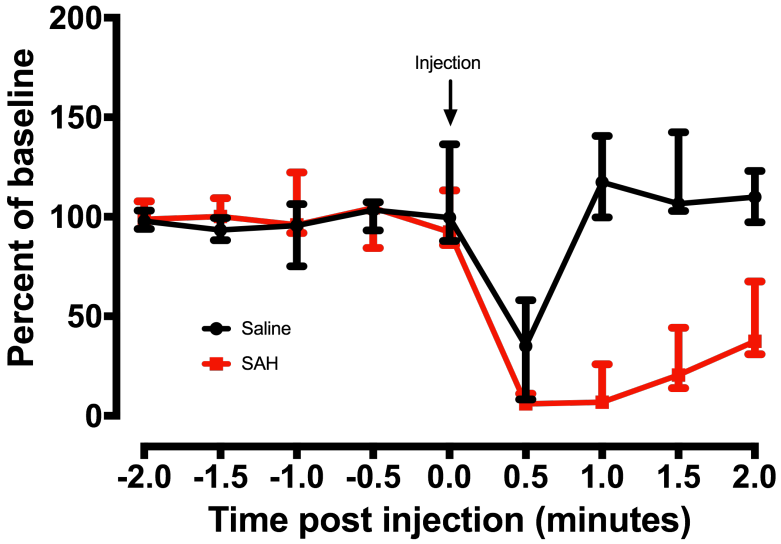

Figure 7.11 *Representative CBF changes as measured by laser Doppler flowmetry during injection of either 100 µL blood or 100 µL saline at a rate of 200 µL/minute (n=6 saline, n=7 SAH). TPU were normalized by expressing as a percentage of mean pre-injection CBF values. Data are presented as median ± IQR.*

7.2.2.3 Locomotor activity assessment

Ambulatory distance data are presented in Figure 7.12. As was observed in the previous experiment, there were no significant differences between saline and blood injected animals, however variance was higher in the SAH group.

Figure 7.12 *Ambulatory assessment in the open field arena.* ***A)*** *the total ambulatory distance travelled by mice throughout the whole arena* ***B)*** *the ambulatory distance travelled in the outer zone of the arena,* ***C)*** *the ambulatory distance travelled in the centre zone of the arena. Data are presented as mean ± SD.*

7.2.2.4 Vasospasm

Blinded visual examination of vasospasm by ROX SE fluorescent imaging revealed instances of vasospasm that was either focal (Figure 7.13A) or present across the entire length of the vessel (Figure 7.13B), and this data was collected. Focal vasospasm, which is seen after human SAH, had not been seen in the previous experiment.

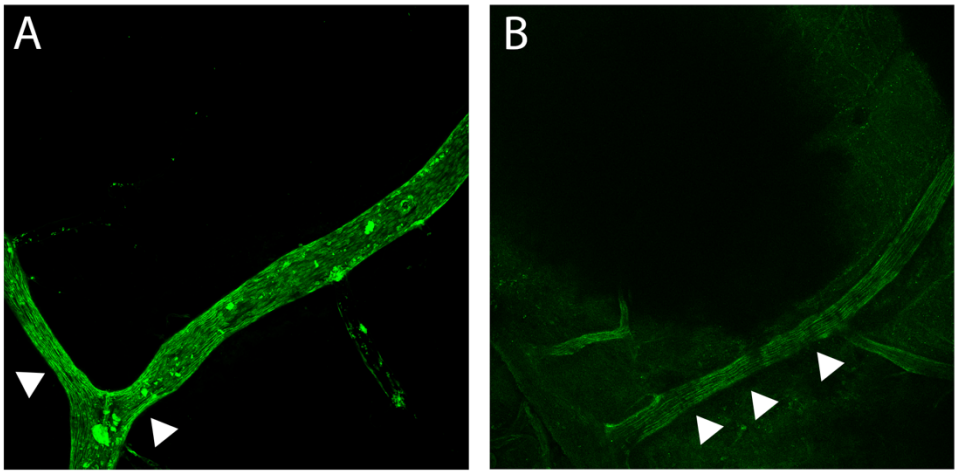

Figure 7.13 *Representative confocal photomicrographs of the ipsilateral MCA from mice undergoing SAH surgery.* ***A)*** *the MCA of an animal exhibiting focal vasospasm (white arrow heads),* ***B)*** *the MCA from an animal exhibiting vasospasm across the whole length of the vessel (white arrow heads).*

Unblinding of images revealed that 50% (4 of 8) of the SAH animals and a single saline injected animal had vasospasm as assessed angiographically using ROX SE. A trend towards a higher rate of

vasospasm in SAH animals compared to saline animals was not significant (Table 7.1, χ^2= 1.66, p=0.198). Representative images of all four groups in Table 7.1 are presented in Figure 7.14.

Table 7.1 *Number of experimental saline and SAH animals with vasospasm after examination of ROX SE fluorescent photomicrographs.*

	No vasospasm	Vasospasm	
Saline	5	1	
SAH	4	4	χ^2=NS

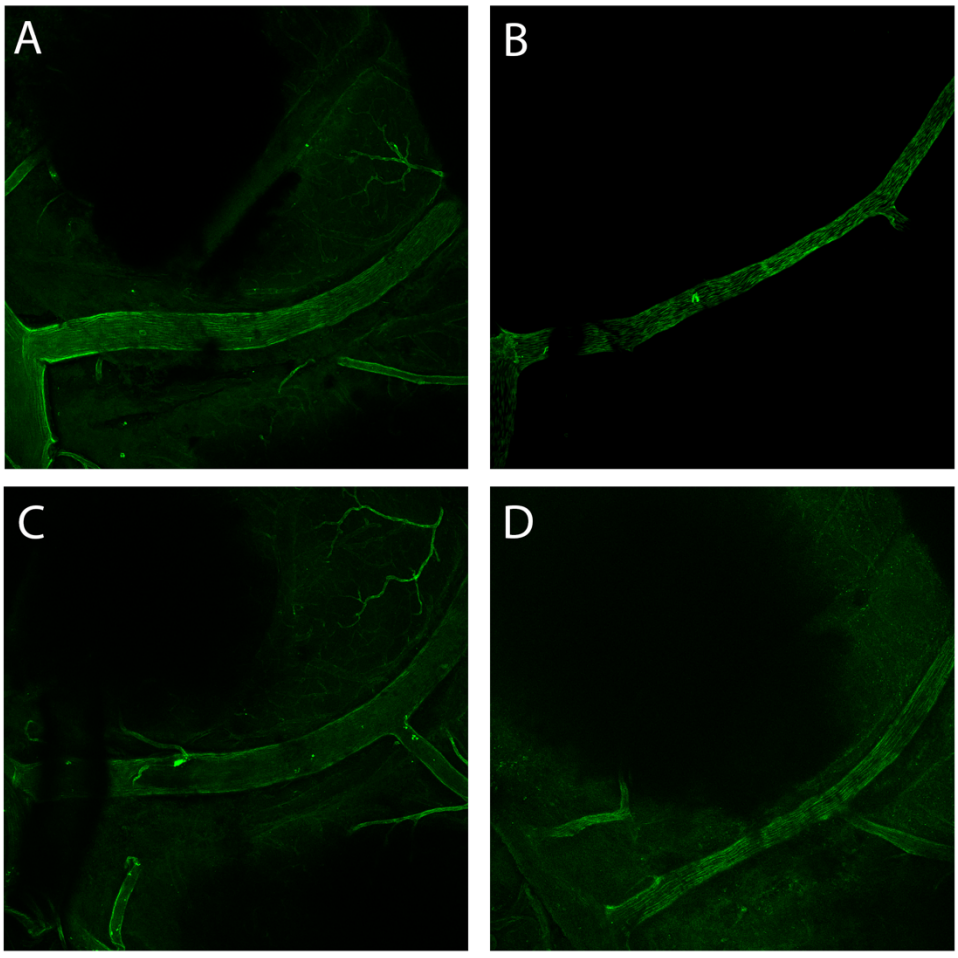

Figure 7.14 *Representative photomicrographs of the ROX SE perfused ipsilateral MCA during visual assessment of vasospasm in this refinement to the model, from* ***(A)*** *a saline injected animal without vasospasm,* ***(B)*** *a saline injected animal with vasospasm,* ***(C)*** *a blood injected animal without vasospasm, and* ***(D)*** *a blood injected animal with vasospasm.*

Blinded quantification of vessel diameters revealed that these two distinct populations of SAH mice (with and without vasospasm of the ipsilateral MCA, as assessed visually), had significantly different mean vessel diameters (p=0.0098, T test with Welch's correction for unequal SD). There was no statistically significant difference in vessel diameter between all SAH animals and all saline controls (ie all mice, with and without vasospasm). The saline animal with visual evidence of vasospasm had the smallest vessel diameter (lowest datapoint in the saline group, Figure 7.15), even narrower than SAH animals with vasospasm. The potential reason for vasospasm in saline animals is discussed later.

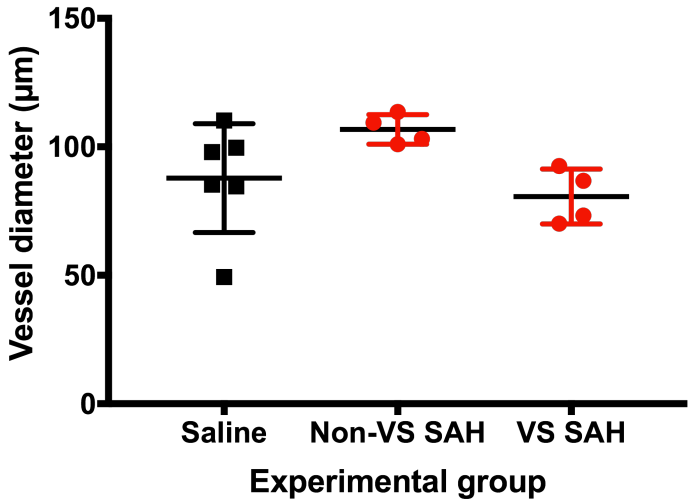

Figure 7.15 *Quantification of MCA ipsilateral to the injection in mice receiving an injection of 100 µL saline or blood at 200 µL/minute. Data are presented as mean ± SD. Within the SAH group there was a clear dichotomy between animals with and without vasospasm as assessed visually. Therefore, the SAH group in this figure has been split into those with and without vasospasm.*

7.2.3 Refinement of the model II

The mice in the previous experiments had been terminally anaesthetised with pentobarbital for perfusion fixation. In a study of isolated human cerebral arteries pentobarbital was found to cause vasorelaxation[189]. This was confirmed by other authors[190] who demonstrated that pentobarbital blocks Ca^{2+} channels thus inhibiting constriction. It was considered that the pentobarbital may be affecting vascular tone via its effects on smooth muscle, to cause vasodilatation or to increase variability in vascular tone. To test this hypothesis, two groups of naïve mice were perfused, using either pentobarbital or ketamine/xylazine to terminally anesthetise the mice. Vessel diameter was quantified in a blinded manner, as before. These data are shown in Figure 7.16, presented alongside data from the previous experiment (Figure 7.15) for comparison. Ketamine/xylazine during perfusion fixation reduced variability in vessel diameter,

compared with 1) pentobarbital in naïve mice, and 2) pentobarbital in previous saline/blood injected animals.

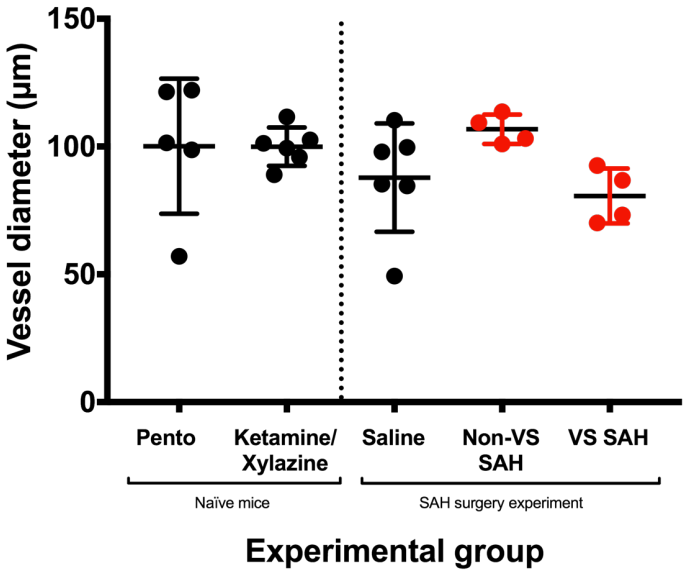

Figure 7.16 ***Left section:*** *Quantification of MCA diameter in naïve mice following perfusion fixation with anaesthesia by either pentobarbital or ketamine/xylazine. Data presented as mean ± SD. Variability of vessel wall diameter in the group anaesthetised with pentobarbital was higher compared to the ketamine/xylazine group.* ***Right section:*** *The data from the previous SAH vasospasm experiment (Figure 7.15) have been displayed here to facilitate comparison with the results of this experiment. Data are presented as mean ± SD.*

7.2.3.1 Ketamine perfusion

Based on the results of the ketamine/xylazine *vs* pentobarbital experiment (Figure 7.16), it was decided to repeat the experiment and perform perfusion fixation under ketamine/xylazine terminal anaesthesia, to reduce variability in vessel diameter. The mortality rate of all mice undergoing this modified surgery (saline n=7, SAH n=10) was 24% (4 of 17 animals, one saline animals, three SAH animals). In this experiment, vessel diameter was still not significantly different between saline and SAH animals, as shown in Figure 7.17 (p=0.608, t test).

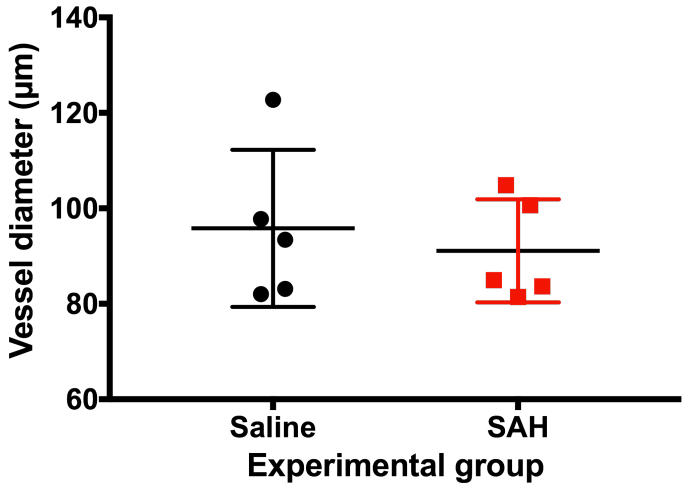

Figure 7.17 *Quantification of MCA ipsilateral to the injection in mice receiving an injection of 100 µL saline or blood at 200 µL/minute following perfusion fixation under ketamine/xylazine anaesthesia. Data are presented as mean ± SD.*

7.2.4 Refinement of the model III

Despite the above refinements to the model, vasospasm was not reliably seen, and mortality was around 25%, therefore a new approach was taken. A modified version of the Macdonald lab method[120] is used by Hanafy and colleageus[101,125]. In this protocol, a reduced injection volume of 60 µL is used in C57BL/6 mice, and the needle is left in place for five minutes after injection (previously it had been left for 60 seconds). Using this model, they show a significant effect of vasospasm at day three, as measured histologically in the posterior communicating artery. They controlled experiments with sham surgery, as opposed to saline injections. It was considered that the smaller injection volume might represent a refinement of the procedure by further reducing mortality rate. Leaving the needle in place for longer would possibly allow for better clot formation in the prechiasmatic cistern, enhancing clot placement around the circle of Willis, rather than extending up the needle tract. In summary, the Hanafy method was reproduced as below:

- 60 µL injection volume
- Leaving the needle in place for five minutes
- Ketamine/xylazine anaesthesia for surgery
- Avertin terminal anaesthesia for perfusion fixation

The mortality rate of this modified protocol was 6% (1 of 16 animals, a single SAH animal), significantly lower than the mortality rate of 24-26% seen previously. The single mouse that died

received an injection of blood. Vasospasm was measured in the brains of mice undergoing this revised protocol using the ROX SE fluorescent imaging technique as before. There was no significant difference in ipsilateral MCA diameter between SAH and saline control groups (Figure 7.18A). The ipsilateral posterior communicating artery diameter was measured as in the work by Hanafy *et al.*[101,125]; a visual trend towards reduced vessel diameter was not statistically significant (Figure 7.18B, p=0.399). ACA diameter measurement (Figure 7.18C) did not detect vasospasm in this artery.

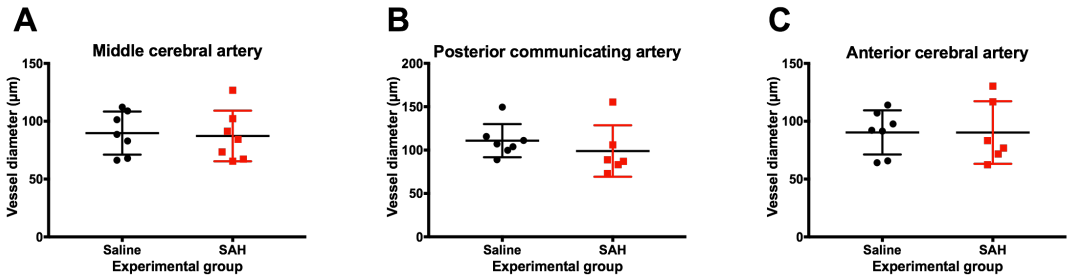

Figure 7.18 *Quantification of **A)** MCA, **B)** Posterior communicating artery and **C)** ACA, ipsilateral to the injection of 60 µL saline or blood. Data are presented as mean ± SD. Some data points are missing due to damaged or missing vessels.*

7.2.5 Histological characterisation of the SAH model

Histological analysis was performed to investigate iron deposition, microglial response and synaptic integrity. Animals from Section 7.2.2 (>3 months of age receiving 100 µL blood or saline injection at 200 µL/min rate) were selected since this was the most promising experiment in terms of vasospasm. Animals were perfused three days after surgery. Brains were embedded in wax and sectioned at 10 µm thickness in the coronal plane.

7.2.5.1 Iron deposition in the brain parenchyma

Iron deposition was assayed using Perls' histological stain. This stain detects ferric iron (Fe^{3+}) in tissue. Iron was quantified in the hemisphere ipsilateral to side of injection, at the level of the striatum, close to the site of injection in the prechiasmatic cistern.

Iron deposition was present in the parenchyma of saline injected control animals, where it localised to the basal surface of the brain, close to the site of injection (Figure 7.19A). In some cases, there was evidence of high intensity staining in lesions that appeared to be related to the needle tract (Figure 7.19B). In SAH animals, the staining was 1) more intense and, 2) more

widespread throughout the brain parenchyma (Figure 7.19B). In some SAH animals, there was intense staining close to the wall of the lateral ventricle.

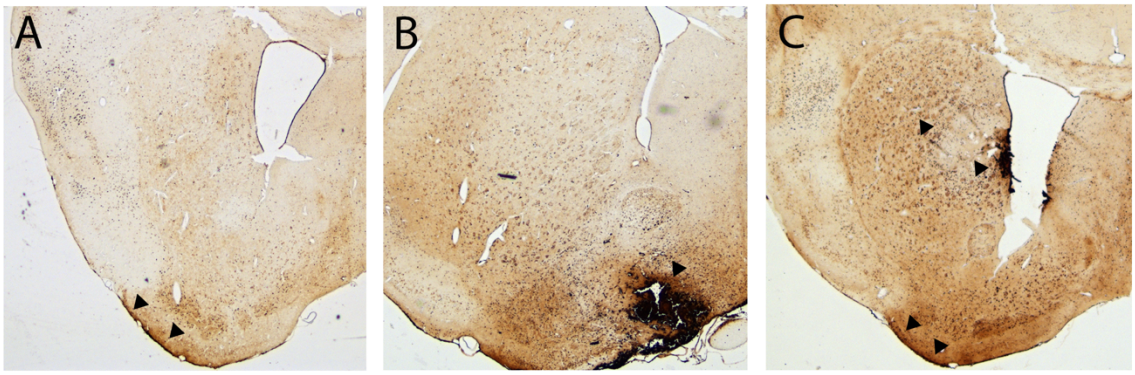

Figure 7.19 *Representative 20x magnification photomicrographs of Perls' staining for iron in brain sections from* ***(A)*** *saline control animals,* ***(B)*** *saline control animals showing intense staining around needle tract, and* ***(C)*** *SAH animals showing generally more intense staining in the parenchyma and staining close to the wall of the ventricle.*

Quantification was performed on the entire hemisphere ipsilateral to the blood clot and represented as a percentage of the tissue stained. These data are presented in Figure 7.20, and indicate that iron deposition is significantly higher in the parenchyma of SAH animals compared to controls (p=0.007, t test).

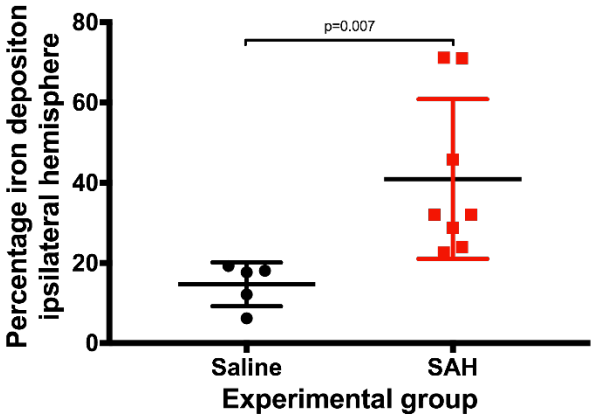

Figure 7.20 *Perls' stain for iron deposition at three days post-SAH, within the ipsilateral hemisphere at the level of the striatum, a region close to the blood clot in the prechiasmatic cistern. There was significantly increased deposition of iron within the parenchyma in the SAH group compared to saline controls (t test with Welch's correction for unequal SD). Data are presented as mean ± SD.*

7.2.5.2 Microglial response after SAH

Microglia were stained using an antibody against the ionized calcium binding adapter molecule 1 (Iba1). This is a microglial cytoplasmic protein which is upregulated when microglia are stimulated to increase their motility[191]. It was hypothesized that the mechanical, inflammatory and Hb-related injury would result in increased numbers of Iba1-positive microglia. A 10 mm reticule divided into a 10x10 grid was used to count Iba-1 positive cells. Two sections per animal were viewed at 20x magnification, and cells were manually counted in two non-overlapping regions: 1) the basal surface of the brain, encompassing the ventral striatum on the ipsilateral side of injection, ie a region close to the blood clot in the coronal plane, and 2) more superiorly, in a central region of the striatum, ie more distant from the blood clot in the coronal plane. There was no difference in Iba1-positive cell number between SAH and saline injected animals, in both regions (Figure 7.22).

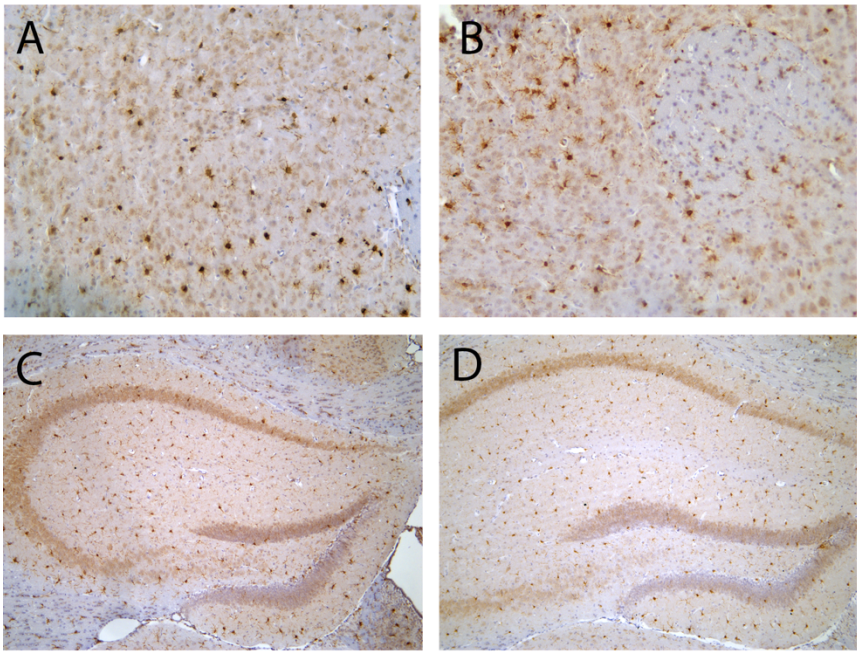

Figure 7.21 *Representative photomicrographs of Iba1 stained sections from **(A)** the striatum of a saline injected animal at 20x magnification, **(B)** the striatum of a blood injected animal at 20x magnification, **(C)** the hippocampus of a saline injected animal at 10x magnification, and **(D)** the hippocampus from a blood injected animal at 10x magnification. All photomicrographs were taken from the hemisphere ipsilateral to the injection.*

Iba1-positive cells were also counted in the ipsilateral hippocampus encompassing the molecular layers of the stratum radiatum and stratum lacunosum moleculare. These cell counts are

presented in Figure 7.22C; no difference in microglial number was observed in this region of the hippocampus between SAH and control saline injected animals.

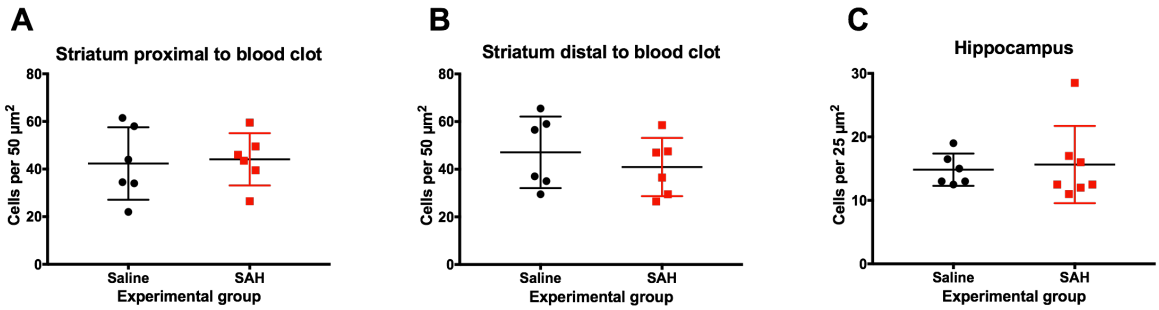

Figure 7.22 *Cell counts of Iba-1 positive microglia cells in **(A)** the ventral striatum on the basal surface of the brain, i.e. close to the blood clot in the coronal plane, **(B)** the central striatum, more distant from the blood clot in the coronal plane, and **(C)** the glial rich region of the molecular layers encompassing the stratum radiatum and stratum lacunosum moleculare of the ipsilateral hippocampus. Data are presented as mean ± SD.*

7.2.5.3 Synaptic integrity in the hippocampus

Synaptic integrity was assessed using Sy38, an antibody against the presynaptic protein synaptophysin (Figure 7.23). Sy38 staining was quantified using a published protocol to adjust for regional variation in staining[143]; in summary the ratio between the molecular layers of the stratum radiatum and stratum lacunosum was calculated, after adjusting the intensity of each region with an internal control region (the dentate gyrus). Sy38 quantification is presented in Figure 7.24; there was no synaptic loss in the SAH group, when compared to saline injected control animals (p=0.493, t test).

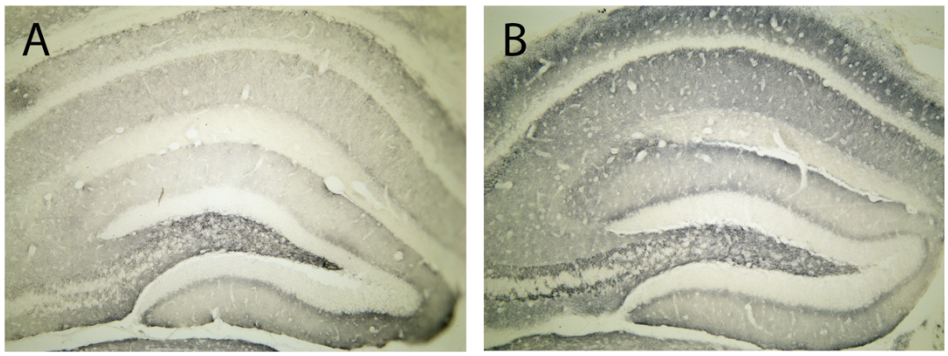

Figure 7.23 *Representative photomicrographs at 10x magnification of Sy38 staining for synaptophysin in the hippocampus ipsilateral to the site of injection. **(A)** a saline injected animal, and **(B)** a blood injected animal.*

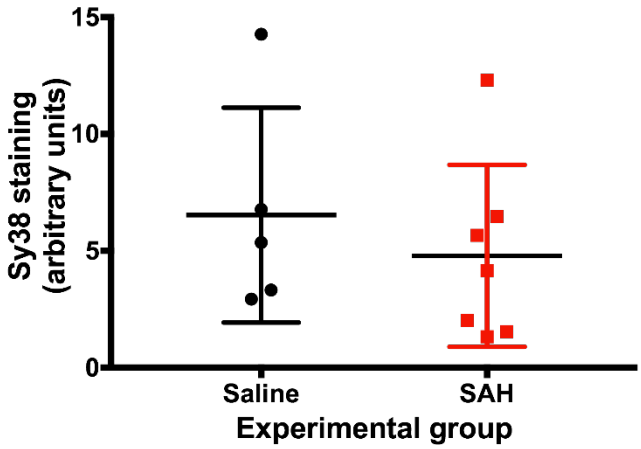

Figure 7.24 *Sy38 staining in the hippocampus, in the hemisphere ipsilateral to the injection. Data are presented as mean ± SD.*

7.3 Discussion

This work characterized and aimed to optimise an injection model of SAH in the mouse. The model was studied with respect to physiological response, behavioural deficits, vasospasm, iron deposition, neuronal integrity and microglial response in the brain.

A good animal model recapitulates the essential features of the human condition, to enable interrogation of mechanisms underlying the disease process, and test treatments. Hb neurotoxicity is only one aspect of SAH. During and after SAH, the brain is challenged by multiple insults including mechanical stress, raised ICP, hydrocephalus and ischaemia alongside Hb neurotoxicity. An animal model is therefore required that recreates all of these aspects of the human condition to ensure that targeting Hb toxicity with Hp therapy is clinically efficacious despite all of the other disease insults.

As discussed in the introduction to this thesis, a good animal model of SAH would possess the following attributes:

- Blood entering the subarachnoid space and subsequent clot formation.
- Clot retention in the subarachnoid space for several weeks.
- Increase in ICP.
- Lysis of clot and release of Hb.
- Hb neurotoxicity.
- Spasm of large cerebral arteries proximal to the clot.

- Behavioural and/or neurological deficits mirroring those in humans.
- Histopathological characteristics similar to those seen after human SAH.
- High repeatability and low variability between experimental animals.

Clearly this model recapitulated the gross characteristics of SAH, in that blood enters the subarachnoid space through the injection into the prechiasmatic cistern. Indeed post mortem examination at early time points (24-36 hours post ictus, data not shown) identified the presence of a blood clot.

Behavioural changes are important readouts from animal models when studying the efficacy of new pharmacological interventions. Behaviour assessments were made here to monitor locomotor activity, anxiety, photosensitivity, short term working memory, and innate behaviours. It was hypothesized that there would be behaviour deficits in this model, as SAH survivors experience cognitive, behavioural and emotional deficits[192]. Therefore, reproducing these functional outcomes in pre-clinical models of disease is important[193].

The open field paradigm was used in this work primarily to assess motor ability after induction of SAH. In both the mouse endovascular perforation and rat blood injection rodent models of SAH, the open field paradigm has shown significant changes in ambulation and anxiety[194,195]. Despite this, no effect was seen here between SAH and controls. The open field arena was also used to assess thigmotaxic behaviour as a measure of anxiety. No differences were observed between SAH and control groups. It is important to note that mice are ideally assessed when they first encounter the arena, to measure anxiety in a novel environment. Mice in these experiments were habituated to the open field arena prior to surgery, since open field locomotor activity was the pre-planned primary behavioural outcome measure.

Other labs, assessing perforation models of SAH in the open field have identified differences between SAH and sham controls with regard to speed and distance travelled, albeit at later timepoints (days 13 and 27)[194]. It is likely that either the perforation model 1) induces greater injury, or 2) the manifestation of changes in open field behaviour occur at a timepoint subsequent to that measured in this investigation.

Many SAH patients experience cognitive impairments such as deficits in attention, memory and learning. The T maze is a measure of working memory in which the mice are required to remember previous decisions when exploring new areas in the maze[139]. Using this behavioural assay, no evidence of a deficit in learning and memory was found in the original version of the model (before any refinements). The T maze was not performed in Refinement I, but there was no evidence of synaptic loss in the hippocampus after synaptophysin immunostaining in Refinement

I. In the literature, results from hippocampal dependent behavioural assays after experimental SAH have been conflicting. Some rodent models of SAH have displayed deficits in hippocampal dependent spatial learning tasks, for instance in an injection model of SAH in the rat, animals failed to learn the location of a submerged platform in the Morris water maze[196]. Others show no difference with this assay in the rat[197], and investigators using mouse models have not found an effect[198].

No difference in numbers of Iba1-positive microglia were observed at three days post-ictus, either proximal or distal to the blood clot in the subarachnoid space, between saline injected and SAH animals, while this has been observed after SAH[101,125,199]. It is entirely possible that one of the main drivers of the sterile inflammatory response after SAH is the increased ICP, and additionally in this model's case the tissue damage occurring from the needle tract – both these factors are present in the saline-injected animals. There is a known inflammatory response to Hb and haem after SAH, in a TLR 4 driven process[29,34,37,125], so it could be proposed that there has not been sufficient lysis of erythrocytes to release Hb into the CSF, at the time of my assessment (three days post-ictus). This is unlikely to be the case however, since 1) post mortem examination of the clot at three days showed evidence of clot reabsorption (data not shown), and 2) there is significant iron deposition in the brain parenchyma in SAH animals *vs* saline controls. Despite this, it would be useful to reassess Iba1 expression at a later time point. Iba1 is principally a marker of microglial motility, so other microglial activation markers such as morphology, MHC II or CD68 ought to be considered. It would be interesting to compare behavioural and histological data in SAH animals with vasospasm *vs* SAH animals without vasospasm. This was not possible in this thesis since subgroup sizes would have been too small.

It was intended to investigate the haemoglobin scavenger receptor CD163 via IHC in the brains of these mice. It was not possible however due to time constraints in this project, with much effort focussed on optimising the protocol. CD163 has an important role in clearance of Hb, particularly in the mouse, in which it is known that Hp is not required for CD163 mediated update[114] and there is a population of $CD163^{+}$ cells in the CNS that are active following SAH in humans[102]. It is known that scavenging of Hb by CD163 induces increased expression[200,201]. IHC examination of CD163 would have been of value in this work, providing insight into Hb handling following SAH, which may in turn relate to toxicity. However, in another model of *in vivo* intrathecal Hb exposure used in our laboratory, a two week infusion of Hb or HpHb did not elicit a change in CD163 expression as detected by IHC (Dr P Garland, manuscript under review), despite a clear therapeutic effect of Hp. Therefore the formation of HpHb complexes is sufficient to inhibit Hb's neurotoxicity, as predicted by biochemical studies and observed *in vitro* in the Chapter 6 of this thesis. While

clearance of HpHb complexes by CD163 would likely be beneficial, CD163 expression in the brain is very low such that HpHb complexes queue for clearance by CD163[102].

In the model, a substantial decrease in cerebral blood flow after injection of either blood or saline was observed. As the brain sits within the enclosed skull, the injection of blood or saline causes a dramatic increase in ICP[183] resulting in a reduction of CBF. This is not dissimilar to what occurs during ictus in human SAH; aneurysmal rupture releases blood under arterial pressure into the subarachnoid space causing a rise ICP[202]. The rise in ICP is associated with a reduction of CBF, due to the increased pressure within the non-expandable skull. This causes compression of the parenchyma and occlusion of the blood vessels, reducing blood flow to the brain[1]. Modifications to the model to 1) reduce the rate of injection and 2) reduce injection volume, still showed a substantial decrease in CBF. Thus these modifications still allowed for modelling this particular aspect of human SAH.

Refinement I involved reducing the injection rate (from 300 µL/min to 200 µL/min), employing older animals and using ketamine/xylazine instead of isoflurane for surgical plane anaesthesia. Initially, animals aged 8-10 weeks were used for the initial establishment and characterisation of the model in our lab. This was due to experience working with C57BL/6 mice of this age. The decision to use older mice was to make animals more representative of the human age at which SAH is likely to occur, but also to use animals with a larger cranium to reduce the rate of mortality. Therefore animals aged three months were selected based on availability of aged C57BL/6 mice in our Biomedical Research Facility. Three months of age is still relatively young for SAH, but is an improvement. Due to time and financial restrictions in this work, housing mice to reach an older age, specifically for the purpose of these experiments was not an option. These modifications did not affect mortality rate, but delivered the best vasospasm rates. Refinement III reduced mortality from 26% to 6%, which is in alignment with the principles of the 3R's. However it was offset by the fact that vasospasm was not observed. This demonstrates the difficult trade-off I was trying to achieve, reducing mortality in SAH animals while achieving a vasospasm rate that is significantly higher than control animals. Both mortality and vasospasm are clinical features of human SAH, and it may not be possible to reduce mortality without affecting vasospasm rate.

Since angiographic vasospasm is a common characteristic of human SAH (occurring in up to 60%[203] of cases), a large part of this optimisation focussed on producing vasospasm as an indicator of model performance. Previous work using the same model has shown that the 100 µL injection of blood into the prechiasmatic cistern induces vasospasm of both the MCA and ACA[120]. Work by others using the same model with a lower injection volume has shown that vasospasm is biphasic, peaking at days three and again at day seven[125]. Initial experiments using these protocols

failed to show vasospasm at three days. Modifying the protocol to include a slower injection rate and use of ketamine/xylazine anaesthesia for surgery induced vasospasm in 50% of the SAH group. A chi squared analysis of this experiment was non-significant, yet this experiment was underpowered. A *post-hoc* power calculation revealed this analysis had a power of 24%, and to achieve 80% power a sample size of 62 animals would be required (i.e. 31 animals per group). This is a large number of animals, especially when considering future experiments to test the efficacy of Hp against Hb-induced neurotoxicity using this SAH model.

Interestingly vasospasm was observed in two saline-injected animals, in the original model and in Refinement I. Vasospasm in the control group is undesirable since it reduces power. The aetiology of vasospasm after saline injection is uncertain, but several possibilities may be entertained. First, some of these animals may experience subarachnoid bleeding, as a result of surgery – this is illustrated by the presence of intense Perls' staining close to the needle tract in some saline-injected animals (Figure 7.19). Second, the use of saline may have induced a temporary drop in calcium and magnesium concentrations in the subarachnoid space, which may induce smooth muscle contraction. Third, the rise in ICP may, by itself, induce a series of responses leading to delayed vasospasm. It is possible that any of these three factors act in concert, for instance surgery and increased ICP may both cause inflammation which is a known inducer of vasospasm[49]. In most cases, vasospasm seemed to be a binary event, either present or absent, arguing against a predominant effect of temporary lowering of calcium and magnesium concentration in the subarachnoid space, which would occur in all animals. Also mice turnover their entire CSF volume in two hours[204], and vasospasm was assessed at day three. On the other hand, surgical trauma and CBF (Figure 7.1 and Figure 7.11) were variable between animals, and it is easy to see how in some animals, they could have colluded to cause vasospasm after saline injection.

Retention of the blood clot was not well modelled and this is a common feature of murine models of SAH. Blood clot resorption in humans takes about two weeks and can last up to one month[205] while blood clot only persisted for a few days in my model. The rate of CSF production in the mouse is greater than in humans with a rate of approximately 0.3 µl/min[204] compared to 0.4 ml/min in humans[206,207]. However the CSF volume of the mouse is 40 µL[204] and in humans it is 90-150 mL[207]. Thus the total CSF volume is turned over twice as fast in the mouse than in the human. It may well be hypothesized that this increased CSF turnover rate could be causing faster disruption of the blood clot and clearance of extracellular Hb in the mouse such that Hb does not linger within the CSF for sufficient time.

In addition to this, neuroanatomical differences between mouse and man may be responsible for discrepancies between this model and human SAH. The surface of the mouse cortex is relatively

smooth, whilst the human brain surface is extensively folded to increase the cortical surface area creating cerebral sulci which could trap the blood clot. In addition, it is likely that the blood clot within the sulci has a decreased rate of reabsorption due to a lower CSF flow in these areas. This in turn would result in the accumulation of higher concentrations of Hb in contact with the surface of the brain within sulci. A study using a swine model of SAH, as opposed to a murine model for this reason, to properly reconstruct the anatomical sulci of the human lacking in murine models[208] identified increased likelihood and recurrence of spreading cortical depolarisations and larger infarcts associated with sulcal clots[208]. It may also be true that the depth of tissue damage is extended by pooling within depths of sulci, as the Hb lingers in the CSF in close proximity to the brain surface. Magnetic resonance studies after human SAH have shown that iron deposition occurs deep within the brain, and this is accompanied by increased disintegration of white matter tracts colocalizing with iron overload and correlating with clinical cognitive dysfunction[209].

Further refinements could be made to the murine prechiasmatic model. One example of this could be replacing the saline control injections with artificial CSF, serum or plasma injections. While the use of serum or plasma would ensure that control injections are similar in terms of viscosity to blood in the SAH animals, a high concentration of blood-derived proteins is toxic to the central nervous system[210-214]. Other refinements could include the use of a smaller gauge needle for control saline injections, the use of sham surgery, older mice, different mouse strains and assessment of vasospasm, behavioural and histological features at later timepoints, such as days seven and fourteen.

The murine prechiasmatic model was established in our laboratory to test the hypothesis that **haptoglobin is therapeutic in an *in vivo* model of subarachnoid haemorrhage**, ie to translate the *in vitro* results to an *in vivo* model of SAH**.** Based on the experience detailed in this chapter, it may be time to re-consider the usefulness of this specific model as a tool to address this hypothesis. It might be beneficial to consider other SAH models, such as a rat injection model or a perforation model in the mouse. Whilst the perforation models are less desirable as the effect of increased ICP is not controlled for, and there is inherent variability in the size of the SAH produced, they may produce angiographic, behavioural and histological readouts suitable for testing the efficacy of Hp-based therapeutics against Hb neurotoxicity after SAH.

Chapter 8 General discussion

Subarachnoid haemorrhage is a complex haemorrhagic disease of the CNS resulting from the rupture of an intracranial aneurysm. This causes blood to enter the subarachnoid space and clot on the surface of the brain, in contact with the cerebral vasculature. Initially there is traumatic damage arising from the mechanical effects of blood injection under arterial pressure and the hydrocephalus that often develops. Then, erythrocyte lysis results in the release of a high concentration of free Hb in the CNS. Free Hb is directly neurotoxic via oxidative mechanisms[21] as reviewed in the introduction of this thesis.

Surgical management of SAH patients aims to secure the bleeding aneurysm; medical management is aimed at preventing vasospasm with triple H (hypertension, hypervolemia and haemodilution) therapy or prevention of DIND with nimodipine. Despite these interventions there is high morbidity in survivors, making the case for additional novel treatments to improve patient care and long term outcome. Despite the evidence supporting the involvement of Hb[102] in the pathophysiology of SAH, no treatments currently target this insult in the CNS. Along these lines, it is hypothesized in this thesis, that **haptoglobin affects the outcome after subarachnoid haemorrhage through its role in haemoglobin scavenging and its supplementation after SAH is of therapeutic benefit.**

8.1 Haptoglobin is important in modifying outcome

The HP gene duplication has resulted in the production of multiple isoforms of Hp in humans. Functional differences between Hp protein isoforms have been reported at multiple stages of the Hb scavenging pathway including: Hp circulating level[62,69,146-153] and HpHb complex affinity for CD163[55,84]. So far, previous work studying the relationship between the HP gene and SAH outcome has concentrated on short-term outcome, around six months or less, and the association between the HP2-2 genotype and vasospasm or outcome was not consistent[107-110,113]. An individual patient-level data meta-analysis of these studies disproved the prevailing hypothesis that the HP1 allele imparts a favourable prognosis as determined by the modified Rankin Scale[112].

Chapter 4 of this thesis presents novel data, looking at outcome after a significantly longer time after SAH, compared to previous studies – a median of 18 months, and up to 8 years. I identified a novel association of the HP1-1 genotype with unfavourable long term outcome after high grade SAH. The discrepancy between short-term and long-term outcome may be due to the overwhelming effect of early brain injury in the short-term, such that differences related to Hb scavenging take longer to become clinically apparent, after the early brain injury settles.

While previous studies have looked for associations of HP genotype and outcome, this study is the first to address the underlying mechanism. The SNP rs2000999 is the largest genetic contributor to Hp expression level[65], and this SNP did not associate with outcome after SAH. It was therefore concluded that the effect of the HP duplication on long term outcome was mediated by Hp isoform differences in Hb scavenging, not by the level of Hp expression.

It was hypothesised that the observed association of the HP2-2 genotype with favourable long term outcome in high grade SAH could be mediated by the higher valency of HP2-2 for Hb. Each molecule of Hp polymer can bind to, and therefore detoxify and clear more Hb, compared to Hp dimer, and this may deliver a higher level of protection. In Chapter 5, I provide evidence supporting the hypothesis that lower levels of complexed Hb occur in the CSF of HP2-2 individuals after SAH, *vs* HP1-1 individuals, due to greater removal from scavenging. In serial CSF samples after SAH, complexed Hb was significantly lower in HP2-2 patients and free Hb was associated with worse clinical outcome. The overarching hypothesis of this thesis is that **haptoglobin affects the clinical outcome after subarachnoid haemorrhage through its role in haemoglobin scavenging.** In combination, these data could be interpreted to mean that the lower levels of HpHb complexes observed in Hp2-2 individuals (with high Fisher grade) are a result of greater scavenging by CD163 of these complexes (compared to Hp1-1). This result may be driving the effect observed in Chapter 4 in that HP2-2 is associated with better long term outcome.

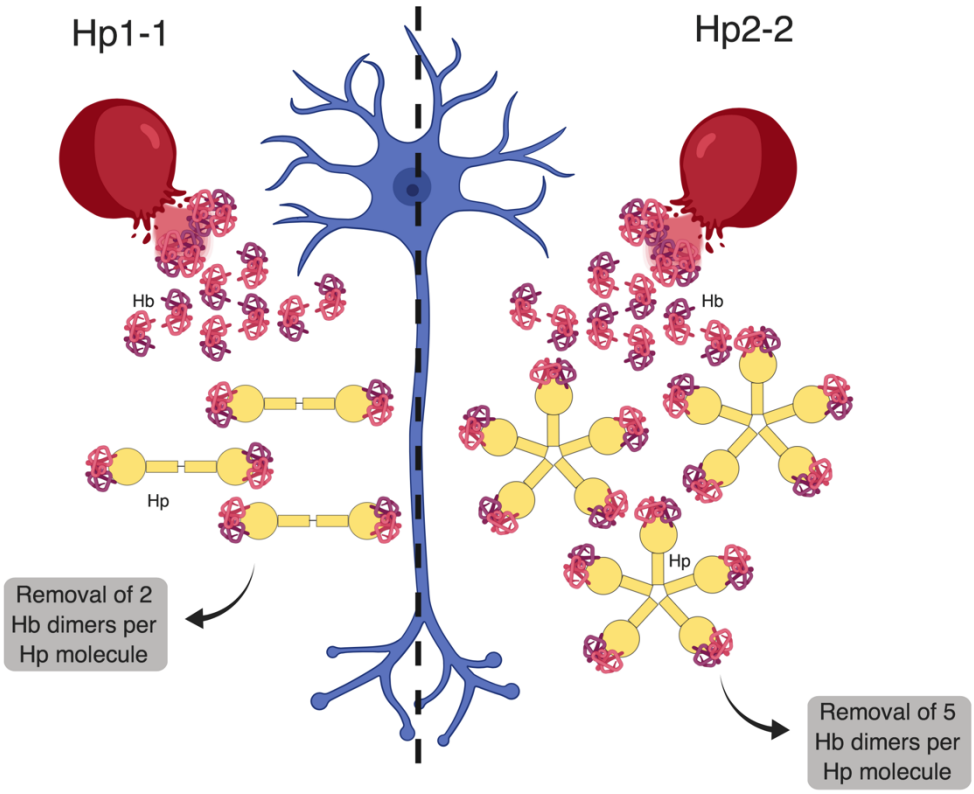

Figure 8.1 *The observations in Chapter 4, that patients with the HP2-2 genotype have better long term outcome may be explained by data from Chapter 5 in which Hp2-2 patients have lower levels of HpHb complexes in CSF. Here it is shown that each Hp2-2 molecule has a higher valency for Hb, therefore contributing to greater levels of Hb removal from the CSF (that is then subsequently scavenged by CD163). Figure created with BioRender.com.*

In summary, this work provides evidence that the Hb scavenging process is crucially important in determining outcome, especially in patients with larger bleeds (ie Fisher III & IV). This highlights Hp as a prime target for developing therapeutics for Hb toxicity after SAH, an area currently lacking in the management of SAH patients. With the knowledge that HP1-1 is a predictor of poor outcome in high Fisher grade patients, point-of-care HP genotyping or phenotyping would be of prognostic benefit to identify patients at risk of unfavourable long term outcome. This would help clinicians identify the patients who need higher level management, and it would help patients in making decisions and plans after SAH.

8.2 The resident haemoglobin scavenging system is overwhelmed

Following SAH, the clot in the subarachnoid space begins to degrade and the erythrocytes lyse, releasing Hb into the CSF. A Hp based therapeutic against Hb toxicity in SAH would aim to work by 1) detoxifying Hb, and 2) promoting scavenging and therefore eventual removal of HpHb

complexes from the CSF. Hence, the temporal profile of Hb release into the CSF and the Hb concentration is important, yet is currently unknown. Previous work often made observations in the CSF at a single time point[102]. Data presented in Chapter 6 show that complexation of Hb by Hp is by itself sufficient to inhibit neuronal death; clearance of HpHb complexes is likely to be of added benefit *in vivo*. Data presented in Chapter 5 show that the level of Hb in ventricular CSF reaches a peak of 10 μM within 13 days post-ictus. Free Hb in the CSF, in direct contact with the brain, is neurotoxic via the production of highly reactive oxidative species that cause DNA, protein and cell membrane damage. Hb surrounding the large cerebral arteries is a putative mediator of vasospasm which can lead to DINDs[7,46].

The Hp scavenging system of Hb is active in the brain after SAH[102]. Despite the high levels of Hb observed accumulating in the CSF, the capacity of Hp in the CSF to scavenge this Hb is low. Thus the resident Hb scavenger system in the CSF is overwhelmed by the Hb insult after SAH, and a high level of free Hb is present in the CSF after SAH. There is justification here therefore to support the hypothesis that **supplementing Hp in the CSF will augment Hb scavenging**. The temporal data presented in Chapter 5 also identify that there is a window of opportunity in the first 13 days post-ictus, proving that the free uncomplexed Hb in the CSF is still *scavengeable* by exogenous Hp; this is a novel observation of clinical translational importance. These advances were enabled by the development and application of a UPLC methodology to measure Hb species, with the ability to discriminate between free Hb and Hb in complex with Hp.

8.3 Haptoglobin can ameliorate haemoglobin toxicity

Experiments in Chapter 6 demonstrate the toxicity of Hb to neuronal cells. Hb toxicity is mediated by oxidative mechanisms[21], and necroptosis or ferroptosis[215] via an ERK1/2 pathway[215,216]. *In vitro* experiments in this thesis show that treatment with Hp ameliorates this toxicity, maintaining neuronal viability. While this work provides proof of principle within an *in vitro* system, translation to the *in vivo* setting is essential. Purification of human Hp to a pharmaceutical grade to render it safe for clinical use (GMP grade, or Good Manufacturing Practices grade) requires multiple harsh preparatory steps[217], so it was very important to show, for the first time, that a medicinal grade human Hp product retains the ability to neutralize Hb neurotoxicity *in vitro*.

Recently, work from our group has used an *in vivo* model that replicates the Hb insult of SAH by continuous intraventricular infusion of Hb via an osmotic minipump (manuscript under review). The infusion of Hb induced behavioural dysfunction as measured in the open field arena, characterised by a reduction in ambulatory activity and freezing behaviour in the peripheral zone;

this is often interpreted as an anxious phenotype[141]. Histological analysis revealed significant iron deposition in the brain, increased Iba1-positive microglial number and synaptic loss in the hippocampus. Concomitant infusion of Hp was able to reverse these behavioural deficits, iron deposition and tissue injury indicating Hp is able to reverse the toxicity of Hb, *in vivo*. Although these results are encouraging, the Hp delivery in this model is not equivalent to the clinical situation, since Hp was delivered at the same time as Hb. After human SAH, Hp would not able to be provided at the same time as the bleed occurs. Fortuitously, as shown in the observational data in Chapter 5, substantial accumulation of Hb occurs *after* the first three days post-ictus, such that Hp supplementation is clinically practical. Additionally, SAH is a highly complex condition, during which Hb exposure is one of several insults. Hp treatment for SAH must be demonstrated to have therapeutic potential in a model of SAH that encompasses other aspects of the disease such as increased ICP, global cerebral ischaemia and vasospasm.

To prepare for this task, I set up a murine model of SAH after a period of training at Loch Macdonald's lab[120] in Toronto. I aimed to characterize the model further, specifically addressing the issues of whether the model recapitulated all aspects of the human condition, principally increased ICP, vasospasm, cognitive deficits, neuronal injury and inflammation. The initial characterization of this SAH model showed it does not model SAH well. While previous work using the prechiasmatic model have identified some of these qualities[120], to date there has been no behavioural characterisation of the injection model of SAH in the mouse. The data presented in this thesis are in agreement with previous observations that the model clearly results in a rise in ICP and a fall in CBF, as occurs after human SAH. This was true even after modifications to the rate and volume of injected fluid to decrease the severity of the procedure. The occurrence of vasospasm was expected after experimental SAH since 50-70% of SAH patients develop vasospasm[203]. Vasospasm could be a target for Hp based therapy, to reduce the severity of vasospasm (ie reduce constriction of the artery) or prevent it. Instead it was found that vasospasm was not reliably detectable. Therefore, modifications were made to the model, and the best vasospasm rate achieved was 50% with Refinement I. Although the optimisation work on this model was heavily focussed on producing vasospasm since it is a core feature of human SAH, the relationship between vasospasm and long term outcome after SAH is uncertain or absent. For instance nimodipine has been shown to improve long term outcome without preventing vasospasm[14], and vasospasm is not a prerequisite for DIND[127]. Hence it may still be possible to model aspects of human SAH in the absence of vasospasm; certainly some SAH patients do not develop vasospasm, and a vasospasm-free SAH model would suffice to test treatments for this category of patients.

Behavioural dysfunction has been observed in rat models of SAH[193,195,197,218], yet much less studied in mouse models in the literature[198]. In this work dysfunction was not observed in a battery of tests addressing learning & memory, innate rodent behaviours, ambulation and anxiety. Some behavioural tests showed changes from baseline in both SAH and saline injected animals. In these cases, it is possible that a culmination of multiple insults common to both groups, for example the rise in ICP and needle tract injury, occluded any SAH-specific effects. Certainly authors who describe behavioural deficits in rodent models of SAH often do so using perforation models and controlling experiments with sham surgeries, as opposed to saline injections. It would be interesting to compare the prechiasmatic SAH model *vs* a sham surgery control; alternatively a perforation model with known behavioural deficits could be used.

The prechiasmatic injection model of SAH was selected to test the efficacy of Hp after SAH *in vivo* since it allowed the dissection of Hb toxicity from other mechanical effects of SAH. So far, the model has proven to be difficult to work with. A perforation model may be used to test Hp efficacy after experimental SAH in the future.

8.4 Haptoglobin as a novel treatment for SAH

Hp is currently commercially purified from human plasma. Work in this thesis has been done in collaboration with BPL, a plasma purification company. BPL have a Hp preparation that is enriched for the Hp dimer (approximately 60%) *vs* Hp polymer. Other companies also produce Hp solutions including CSL Behring (enriched for the Hp2-2 forms)[219] and Benesis Corporation in Japan (also enriched for Hp2-2 forms)[78]. Hp is used clinically in Japan and in line with this, the Benesis product has been subjected to most clinical trials, including for renal failure prevention following cardiopulmonary bypass surgery[220], haemolysis after massive transfusion[221] and haemolysis elevated liver enzymes and low platelet count syndrome[222].

The use of Hp to target Hb toxicity following SAH represents another market for Hp preparations. Early pilot experiments found that BPL's current Hp preparation (Hp5911) produced neuroinflammation *in vivo* (Dr Patrick Garland, unpublished data) and was neurotoxic *in vitro* as presented in Chapter 6. It was found that toxicity was reversed by dialysis with a 20 kDa cut off. Similar results can be achieved on a large scale using an optimised diafiltration process – a method for filtering impurities by size (Dr Zuby Okemefuna & Dr John More, BPL, personal communication), indicating a preparation close to being ready for medicinal use.

In 1979, a small Japanese case series of Hp therapy after SAH was published[126]. Here Hp was applied to arteries during an aneurysm clipping procedure to prevent vasospasm. This small study of 27 patients was complicated by further subgroupings and no control group, which makes it

difficult to draw conclusions. As my data in Chapter 5 show, the Hb scavenging deficit is large, so while the topical application of Hp to arteries during surgery will indeed scavenge Hb, it is unlikely to detoxify sufficient amounts of Hb to be clinically beneficial. More realistically a prolonged delivery of Hp will be required, especially as the Hb levels in the CSF are observed to build up from day three and persist for at least two weeks after SAH.

SAH is a multifaceted disease with inflammatory, ischaemic and mechanical insults in addition to Hb toxicity. A widely used treatment regime in SAH is daily oral nimodipine, which confers neuroprotection from ischaemic events[14]. Combination treatment with Hp and nimodipine could be more effective than nimodipine alone. Triple H (hypertension, hypervolaemia and haemodilution) therapy is used to improve cerebral blood flow and cerebral perfusion pressure, in an effort to prevent DIND[15]. Again, it is likely that a multimodal approach to treatment would be beneficial.

While adverse reactions to endogenous proteins are unlikely, the existence of multiple Hp isoforms raises the possibility of an immune reaction since HP1-1 patients will not naturally produce Hp2 polymers, so the latter may be seen by the immune system as foreign proteins. This is of particular concern in the CSF, which is not an immune privileged compartment of the CNS[172]. In our group, we have challenged mice with intrathecal infusion of human Hp for up to two weeks, and this was surprisingly well tolerated by the mice. Sickness behaviour was not observed, mice gained weight as expected for their age, and there was no evidence of inflammation in the brain. This is encouraging because 1) the Hp infused was human, and therefore of a foreign species to the mouse and 2) mice only express HP1-1, while the Hp infusion consisted of both Hp1 dimers and Hp2 polymers. However it is difficult to be sure that a mixed preparation would be safe in humans. Hp purified from pooled plasma (as is current practice in industry) can be purified into fractions containing specific isomers (as discussed in Chapter 6). Alternatively, procedures may need to be developed to enable purification of Hp from plasma of donors whose Hp genotype is known to be HP1-1 or HP2-1.

Hp's primary binding partner is Hb, however it is known to bind a small number of other ligands. HMGB 1 is a nuclear protein that is released into the cytosol or extracellularly, and acts as a DAMP, activating TLR 4 dependant inflammatory signalling[223]. HMGB-1 has been identified in cytosolic fractions following experimental SAH[224] and in the CSF of SAH patients[225,226]. Here, it was found to be associated with increased inflammation[226] inducing IL-1β production[224], and was associated with poor outcome[225]. Hp has been shown to bind to HMGB-1 through Hp's β chain[117,118], and in doing so has been shown to have an anti-inflammatory effect, attenuating systemic inflammation in mouse models[118]. HMGB-1 is unlikely to compete with Hb for Hp, since

HpHb affinity is in the pico- to femtomolar scale[227], whereas HMGB-Hp affinity is on the nanomolar scale[117]. Supplementation of Hp in amounts to oversaturate Hb may harness the anti-inflammatory signalling induced by Hp-HMGB complexes. Indeed targeting HMGB-1 to supress neuroinflammation has shown to be neuroprotective in murine models of inflammatory CNS disease (experimental autoimmune encephalitis)[228].

Hp has also been demonstrated to bind to Apolipoproteins A-1[229] and E[230]. Within the context of Alzheimer's disease (AD), in which there are links with Apolipoprotein E and amyloid β, Hp may also bind amyloid β and influence their interaction[231]. Apolipoproteins are involved in cholesterol metabolism; ApoA-1 is the major protein in high density lipoprotein and a cofactor for the enzyme lecithin:cholesterol acyltransferase and Apolipoprotein E is the major lipoprotein in the brain[232] involved in lipid metabolism. While Hp binding to both forms of apolipoprotein impairs their interaction with lecithin:cholesterol acyltransferase and inhibits cholesterol homeostastis[230], it is thought that Hp binding protects the cholesterol transport system from damage during oxidative stress[230]. It has been demonstrated that at concentrations above 0.7 μM, Hb displaces Apolipoprotein E from Hp[230] (and this is likely the case for Apolipoprotein A-1). Although Apolipoprotein E is present in the CSF[232], it is unlikely that the apolipoproteins compete for Hp and therefore saturate binding sites for Hb, since the levels of free Hb in the CSF after SAH are observed to be much greater than this (Chapter 5).

In SAH patients, Hp-based therapy can be achieved in a number of ways: systemic supplementation, intrathecal supplementation and pharmacological augmentation. These will now be discussed in turn.

8.4.1 Systemic delivery of Hp

The most practical way to deliver Hp would be systemically, via intravenous infusion. However under normal conditions Hp enters the CNS in small quantities, in a pattern that suggests *leakage* across the BBB, ie with Hp dimer and smaller polymers being more prominent than larger polymers in the CSF[233,234]. However, during SAH there is increased permeability of the BBB, as described in Chapter 5. This may be sufficient to allow entry of Hp from the circulation into the CSF. While calculations show that systemic Hp administration would not result in sufficient Hp entry into the CNS to bind the high Hb concentration in the CSF of high grade SAH patients, it may be enough for patients with low grade SAH (personal communication, Dr I Galea). The latter is an interesting observation since low grade SAH patients would not usually need insertion of an EVD, the most practical way for intrathecal delivery of Hp (see below). Moreover, increased BBB permeability facilitates increased *leakage* of Hb down a concentration gradient and out of the CSF

into the circulation[102]. Systemic administration of Hp may help maintain a steep concentration gradient for Hb across the BBB.

8.4.2 Intrathecal delivery of Hp

The most direct method is to deliver Hp into the CSF. The majority of high grade SAH patients have an EVD inserted to manage hydrocephalus. This drain is also used for direct delivery of compounds to the CNS, such as antibiotics when ventriculitis occurs[173]. This route presents an ideal opportunity to quickly target Hb in the CSF. The relative ease and frequency by which CSF can be non-invasively obtained from an EVD allows for daily assays of CSF Hb and Hp concentrations. This may be used to calculate a *personalized* dose of Hp that would be required to specifically target the patient's Hb burden on that day. While an EVD would only be usually inserted in high grade SAH patients, these are the patients who need Hp most.

8.4.3 Pharmacological induction of Hp synthesis

It is possible to upregulate the synthesis of Hp through the activation of the transcription factor Nuclear factor erythroid 2-related factor 2 (Nrf2)[182]. Under basal conditions Nrf2 is found in the cytoplasm bound to its negative regulator Kelch-like ECH-associated protein-1 (Keap1)[235,236]. However oxidative stress initiates the oxidation of the thiol groups on two cysteine residues of Keap1, which inhibits its interaction with Nrf2[237,238]. Free from its negative regulation, Nrf2 translocates to the nucleus where an accumulation of the transcription factor is observed[237,238]. Heterodimer formation with small Maf proteins initiates gene transcription by binding to an Antioxidant Response Element (ARE)[235,237,238] upstream of genes involved in the cytoprotective response to oxidative stress.

While Hp is normally present in the CSF in very low amounts[233,234], CNS synthesis has been reported during inflammatory conditions in ischaemia[239] and intracranial haemorrhage[58]. I have not detected intrathecal Hp synthesis after human SAH in HP1-1 individuals, however the Nrf2 system can be pharmacologically upregulated by compounds such as sulforaphane[236], resulting in higher expression of Hp in the CNS [58] via the Nrf2-ARE pathway[236].

Sulforaphane has been shown to have positive effects following experimental ICH[240], but its efficacy in SAH has not been tested. Both ICH and SAH are haemorrhagic diseases of the CNS, but the localisation of the blood clot is markedly different and this impacts of the accessibility of cells expressing Hp and CD163. A Phase II clinical trial of an α-cyclodextrin-stabilized form of sulforaphane is currently underway in Fisher grade III & IV patients[241]. Sulforaphane may be an

effective treatment for Hb toxicity in low grade SAH patients without an EVD, in whom direct intrathecal Hp delivery is not an option.

8.5 Summary

In summary I have shown the importance of the Hp scavenging system on long term outcome after SAH, and a beneficial effect of the HP2-2 genotype at high Fisher grades. The Hp scavenging system is overwhelmed by high concentrations of Hb in the CSF after SAH. Despite this, the Hb in the CSF remains scavengeable by Hp, providing a window of opportunity for treatment with Hp in the first two weeks post-ictus.

In proof of principle experiments *in vitro*, I have shown that Hp reverses Hb-mediated neurotoxicity. An *in vivo* model of SAH has been optimised but this is not yet at a stage to be used to test the efficacy of Hp after SAH *in vivo*.

Future directions would need to primarily concentrate on further developing the SAH model, with consideration given to the use of different controls or of a perforation SAH model. As fractions of Hp containing different isoforms have been obtained, it would be of interest to test these individually in their ability to reverse Hb neurotoxicity *in vitro* and *in vivo*.

Appendix A Clinical grading scales

Table 8.1 *The modified Rankin Scale.*

Score	Description
0	No symptoms at all.
1	No significant disability despite symptoms; able to carry out all usual duties and activities.
2	Slight disability; unable to carry out all previous activities, but able to look after own affairs without assistance.
3	Moderate disability; requiring some help, but able to walk without assistance.
4	Moderately sever disability; unable to walk without assistance and unable to attend to own bodily needs without assistance.
5	Severe disability; bedridden, incontinent and requiring constant nursing care and attention.
6	Dead.

Table 8.2 *The Glasgow outcome scale.*

Score	Description
1	Dead.
2	Persistent vegetative state.
3	Severe disability (conscious but disabled).
4	Moderate disability (disabled but independent).
5	Good recovery.

Table 8.3 *The Glasgow coma score.*

Score	Description
Motor response	
1	No response to pain.
2	Extensor posturing to pain: stimulus causes limb extension.
3	Abnormal flexor: stimulus causes abnormal flexion of limbs.
4	Withdraws to pain: pulls limb away from painful stimulus.
5	Localising response to pain: able to localise specific stimuli and alters behaviour to prevent it.
6	Obeying command: the patient is able to do simple tasks when asked.
Verbal response	
1	No verbal response.
2	Incomprehensible speech: moaning but no words.
3	Inappropriate speech: random or exclamatory articulated speech but no conversation exchange.
4	Confused conversation: the patient responds to questions in a conversational manner but some disorientation and confusion is present.
5	Orientated: the patient knows who he/she is, where he/she is and why, the current year, current season and month.
Eye response	
1	No eye opening.
2	Eye opening in response to pain.
3	Eye opening in response to any speech.
4	Spontaneous eye opening.
Interpretation of score	
<8	Severe.
9-12	Moderate.
>13	Mild.

Table 8.4 *World Federation of Neurological Surgeons grade.*

Score	Description
1	GCS score of 15 without focal neurological deficit.
2	GCS score of 13 or 14 without focal neurological deficit.
3	GCS score of 13 or 14 with focal neurological deficit.
4	GCS score of 7-12.
5	GCS score of 3-6.

Table 8.5 *Fisher grade.*

Score	Description
1	No blood present.
2	Diffuse deposition of SAH without clots or layers of blood >1 mm.
3	Localised clots and/or vertical layers of blood 1 mm or greater thickness.
4	Diffuse or no subarachnoid blood but intracerebral or intraventricular clots.

Appendix B Functional differences between haptoglobin phenotypes

Table 8.6 *Studies investigating **Hb binding** of Hp phenotypes*

Study	Methods	Key finding
Okazaki *et al.* 1997[79]	Two-dimensional affinity electrophoresis.	Hp1-1 vs Hp2-1 vs Hp2-2. Hp2-2 lower affinity than Hp2-1 and Hp1-1.
Melamed-Frank *et al.* 2001[73]	Ultrafiltration assay of non-complexed equimolar amounts of Hb.	Hp1-1 vs Hp2-2. No significant difference between Hp1-1 and Hp2-2 for Hb binding.
Asleh *et al.* 2005[77]	Surface plasmon resonance.	Hp1-1 vs Hp2-2 No significant difference in binding affinity to Hb.
Lipiski *et al.* 2013[78]	Mass spec and surface plasmon resonance.	Hp1-1 vs Hp2-2. No significant differences in Hb binding capacity or affinity.
Mollan *et al.* 2014[80]	Monitored spectrophotometric change when Hp interacts with Hb.	Both dimeric and polymeric fractions of Hp form HpHb complexes at comparable rates *(in vitro)*.

Table 8.7 *Studies investigating the* ***inhibition of Hb mediated oxidation*** *by different Hp phenotypes*

Study	Methods	Key finding
Bamm *et al.* 2004[81]	Assayed Hb oxidation of protein and lipids.	Hp1-1 vs Hp2-2. Hp1-1 significantly better at inhibiting Hb mediated oxidation.
Melamed-Frank *et al.* 2001[73]	*In vitro* linolenic acid and LDL oxidation assays.	Hp1-1 vs Hp2-2. Hp1-1 significantly better at inhibiting Hb mediated oxidation.
Asleh *et al.* 2005[77]	*In vitro* assay of chelatable redox active iron from HpHb complexes. *In vivo* assay of redox active chelatable iron from serum of Hp1 and Hp2 transgenic mice.	Hp1-1 vs Hp2-2. Significantly greater levels of oxidative stress with Hp2-2:Hb complexes. Hp1-1 vs Hp2-2. Four-fold increase in redox active iron in serum of Hp2-2 mice.
Lipiski *et al.* 2013[78]	Spectrophotometric methods to monitor redox reactions in presence of HpHb complex.	Hp1-1 vs Hp2-2. No significant difference in the ability of either complex to inhibit the oxidation of LDL *(in vitro)*.
Mollan *et al.* 2014[80]	Spectrophotometric methods.	Dimeric and polymeric Hp exert similar effects in reducing Hb redox potential and similar effects in inhibiting H_2O_2 induced $HbFe^{4+}$ *(in vitro)*.

Table 8.8 *Studies investigating the* ***inhibition of haem release*** *by different Hp phenotypes*

Study	Methods	Key finding
Asleh *et al.* 2005[77]	Assayed redox active chelatable iron (as haem proxy) using kinetic fluorometric assay with dihydrorhodamine.	Hp1-1 vs Hp2-2. Greater Haem release from Hp2-2:Hb complexes.
Lipiski *et al.* 2013[78]	*In vitro*. Hb to Hpx assayed monitoring UV spectrum at regions of Hb and Haem to measure transfer.	Hp1-1 vs Hp2-2. No significant differences in rate of Haem release between Hp1-1:Hb and Hp2-2:Hb complexes.
Mollan *et al.* 2014[80]	Spectrophotometric methods.	Dimeric and polymeric Hp inhibited haem release to the same extent.

Table 8.9 *Studies investigating the* ***inhibition of NO scavenging*** *by complexes of Hb with different Hp phenotypes*

Study	Methods	Key finding
Azarov *et al.* 2008[48]	Monitored dioxygenation reaction by time resolved absorption and competition experiments deducing NO scavenging from amount of metHb formed in presence of NO.	No significant difference in the consumption of NO in either Hp1-1 vs Hp2-2 or even compared to Hb alone.
Lipiski *et al.* 2013[78]	Use of NO sensitive electrode after serial administration of Hp1-1 or Hp2-2 complexes.	Hp1-1 vs Hp2-2. No significant difference between either Hp1-1 or Hp2-2 or Hb alone *(in vitro).*

Table 8.10 *Studies investigating the **affinity of CD163** for complexes of Hb with different Hp phenotypes*

Study	Methods	Key finding
Kristiansen *et al.* 2001	Surface Plasmon resonance binding of Hp1-1 and Hp2-2 complex to CD163.	Hp1-1 vs Hp2-2. Hp 2-2 Higher affinity for CD163 (surface plasmon resonance).
Asleh *et al.* 2003[84]	*In vitro* uptake assays using CHO cells constitutively expressing CD163.	Hp1-1 vs Hp2-2. Hp2-2 eight-fold greater binding affinity for CD163 *(in vitro)*.

Table 8.11 *Studies investigating the **uptake of Hb in complex with** different Hp phenotypes by $CD163^{+}$ macrophages*

Study	Methods	Key finding
Asleh *et al.* 2003[84]	*In vitro* Rhodamine-tagged Hp1-1 and Hp2-2 complexes in CHO-CD163 cells.	Hp1-1 vs Hp2-2. Greater uptake by CD163 expressing macrophages *(in vitro)*. Hp2-2 greater activation of CD163 signalling (IP_3 production and Ca^{2+} mobilisation).
Lipiski *et al.*2013	*In* vivo monitoring of clearance of HpHb complex from the serum.	Hp1-1 vs Hp2-2 comparable half life of Hp1-1:Hb and Hp2-2:Hb complexes in serum of Guinea pig.

Table 8.12 *Publications demonstrating circulating Hp levels between HP genotypes.*

Study	Notes and findings
Louagie *et al*. 1993[146]	Hp1-1 levels higher. (Hp1-1>Hp2-1>Hp2-2). Study of Caucasian adults.
Langlois *et al.* 1996[147]	Hp1-1 levels higher. (Hp1-1>Hp2-1>Hp2-2). Study of Caucasian adults.
Langlois and Delanghe 1996[62]	Seminal review of biological and clinical aspects of Haptoglobin. Provides reference ranges of serum levels for each genotype in Caucasians: Hp1-1 levels higher. (Hp1-1>Hp2-1>Hp2-2 circulating levels).
Kasvosve *et al.* 2000[148]	Hp1-1 higher than Hp2-2. (Hp1-1 + Hp2-1 > Hp2-2). Hp2-1 not different to Hp1-1 levels. Study in Black Zimbabwean adult population. Reference ranges identified lower than Caucasian populations.
Park *et al.* 2004[149]	Hp1-1 levels higher. (Hp1-1>Hp2-1>Hp2-2 circulating levels). Study of Korean adults.
Na *et al*. 2005[150]	Hp1-1 levels higher than Hp2-2. (Hp1-1>Hp2-1+Hp2-2. Hp 2-1 levels similar to Hp2-2). Age and ethnicity not stated.
Fowkes *et al.* 2006[151]	Hp1-1 levels higher. (Hp1-1>Hp2-1>Hp2-2 circulating levels). Study of African children (aged 1-12 years).
Imrie *et al.* 2006[152]	Hp1-1 levels higher. (Hp1-1>Hp2-1>Hp2-2 circulating levels). Study of children in Papua New Guinea (aged 1-17).
Marquez *et al.*2011[153]	Hp1-1 levels higher. (Hp1-1+Hp2-1>Hp2-2. Hp2-1 levels similar to Hp1-1). Study of adults, unstated ethnicity.
Soejima *et al.* 2014[69]	Hp1-1 levels higher than Hp2-2 in a Japanese population.

List of References

1. Macdonald RL, Diringer M, Citerio G. Understanding the disease: aneurysmal subarachnoid hemorrhage. *Intensive Care Medicine* 2014: 1-4.
2. Chalouhi N, Hoh BL, Hasan D. Review of Cerebral Aneurysm Formation, Growth, and Rupture. *Stroke* 2013; **44**(12): 3613-22.
3. Hall JE. Textbook of Medical Physiology. 12th ed: Elsevier Health Sciences; 2010.
4. de Oliveira Manoel AL, Goffi A, Marotta TR, Schweizer TA, Abrahamson S, Macdonald RL. The critical care management of poor-grade subarachnoid haemorrhage. *Critical Care* 2016; **20**(1): 21.
5. Barrows LJ, Hunter FT, Banker BQ. THE NATURE AND CLINICAL SIGNIFICANCE OF PIGMENTS IN THE CEREBROSPINAL FLUID. *Brain* 1955; **78**(1): 59-80.
6. Vergouwen MDI, Vermeulen M, van Gijn J, et al. Definition of Delayed Cerebral Ischemia After Aneurysmal Subarachnoid Hemorrhage as an Outcome Event in Clinical Trials and Observational Studies: Proposal of a Multidisciplinary Research Group. *Stroke* 2010; **41**(10): 2391-5.
7. Macdonald RL, Weir BK. A review of hemoglobin and the pathogenesis of cerebral vasospasm. *Stroke* 1991; **22**(8): 971-82.
8. Pluta RM, Hansen-Schwartz J, Dreier J, et al. Cerebral vasospasm following subarachnoid hemorrhage: time for a new world of thought. *Neurological research* 2009; **31**(2): 151-8.
9. Keedy A. An overview of intracranial aneurysms. *McGill Journal of Medicine : MJM* 2006; **9**(2): 141-6.
10. de Rooij NK, Linn FH, van der Plas JA, Algra A, Rinkel GJ. Incidence of subarachnoid haemorrhage: a systematic review with emphasis on region, age, gender and time trends. *J Neurol Neurosurg Psychiatry* 2007; **78**(12): 1365-72.
11. Galea JP, Dulhanty L, Patel HC, Uk, Ireland Subarachnoid Hemorrhage Database C. Predictors of Outcome in Aneurysmal Subarachnoid Hemorrhage Patients: Observations From a Multicenter Data Set. *Stroke* 2017; **48**(11): 2958-63.
12. Chang SD, Steinberg GK. Management of intracranial aneurysms. *Vasc Med* 1998; **3**(4): 315-26.
13. Dandy WE. INTRACRANIAL ANEURYSM OF THE INTERNAL CAROTID ARTERY: CURED BY OPERATION. *Ann Surg* 1938; **107**(5): 654-9.
14. Pickard JD, Murray GD, Illingworth R, et al. Effect of oral nimodipine on cerebral infarction and outcome after subarachnoid haemorrhage: British aneurysm nimodipine trial. *BMJ : British Medical Journal* 1989; **298**(6674): 636-42.
15. Luoma A, Reddy U. Acute management of aneurysmal subarachnoid haemorrhage. *Continuing Education in Anaesthesia Critical Care & Pain* 2013; **13**(2): 52-8.
16. Dorhout Mees SM, Rinkel GJ, Feigin VL, et al. Calcium antagonists for aneurysmal subarachnoid haemorrhage. *Cochrane Database Syst Rev* 2007; (3): Cd000277.
17. Atha DH, Riggs A. Tetramer-dimer dissociation in hemoglobin and the Bohr effect. *J Biol Chem* 1976; **251**(18): 5537-43.
18. Shaeffer JR, McDonald MJ, Turci SM, Dinda DM, Bunn HF. Dimer-monomer dissociation of human hemoglobin A. *J Biol Chem* 1984; **259**(23): 14544-7.
19. Riccio A, Vitagliano L, di Prisco G, Zagari A, Mazzarella L. The crystal structure of a tetrameric hemoglobin in a partial hemichrome state. *Proceedings of the National Academy of Sciences* 2002; **99**(15): 9801-6.
20. Reeder BJ, Svistunenko DA, Cooper CE, Wilson MT. The radical and redox chemistry of myoglobin and hemoglobin: from in vitro studies to human pathology. *Antioxid Redox Signal* 2004; **6**(6): 954-66.
21. Regan RF, Panter SS. Neurotoxicity of hemoglobin in cortical cell culture. *Neuroscience letters* 1993; **153**(2): 219-22.

22. Jaremko KM, Chen-Roetling J, Chen L, Regan RF. Accelerated hemolysis and neurotoxicity in neuron-glia-blood clot co-cultures. *Journal of neurochemistry* 2010; **114**(4): 1063-73.
23. Chen-Roetling J, Regan RF. Effect of heme oxygenase-1 on the vulnerability of astrocytes and neurons to hemoglobin. *Biochem Biophys Res Commun* 2006; **350**(1): 233-7.
24. Regan RF, Rogers B. Delayed Treatment of Hemoglobin Neurotoxicity. *Journal of Neurotrauma* 2003; **20**(1): 111-20.
25. Rogers B, Yakopson V, Teng Z-P, Guo Y, Regan RF. Heme oxygenase-2 knockout neurons are less vulnerable to hemoglobin toxicity. *Free Radical Biology and Medicine* 2003; **35**(8): 872-81.
26. Bunn HF, Jandl JH. Exchange of Heme among Hemoglobins and between Hemoglobin and Albumin. *Journal of Biological Chemistry* 1968; **243**(3): 465-75.
27. Gutteridge JMC. Iron promoters of the Fenton reaction and lipid peroxidation can be released from haemoglobin by peroxides. *FEBS Letters* 1986; **201**(2): 291-5.
28. Faivre B, Menu P, Labrude P, Vigneron C. Hemoglobin Autooxidation/Oxidation Mechanisms and Methemoglobin Prevention or Reduction Processes in the Bloodstream Literature review and outline of autooxidation reaction. *Artificial Cells, Blood Substitutes, and Biotechnology* 2009; **26**(1): 17-26.
29. Greenhalgh AD, Brough D, Robinson EM, Girard S, Rothwell NJ, Allan SM. Interleukin-1 receptor antagonist is beneficial after subarachnoid haemorrhage in rat by blocking haem-driven inflammatory pathology. *Dis Model Mech* 2012; **5**(6): 823-33.
30. Lunnon K, Teeling JL, Tutt AL, Cragg MS, Glennie MJ, Perry VH. Systemic Inflammation Modulates Fc Receptor Expression on Microglia during Chronic Neurodegeneration. *The Journal of Immunology* 2011; **186**(12): 7215.
31. Perry VH, Crocker PR, Gordon S. The blood-brain barrier regulates the expression of a macrophage sialic acid-binding receptor on microglia. *Journal of Cell Science* 1992; **101**(1): 201.
32. Cox KH, Cox ME, Woo-Rasberry V, Hasty DL. Pathways Involved in the Synergistic Activation of Macrophages by Lipoteichoic Acid and Hemoglobin. *PLoS ONE* 2012; **7**(10): e47333.
33. Figueiredo RT, Fernandez PL, Mourao-Sa DS, et al. Characterization of heme as activator of Toll-like receptor 4. *J Biol Chem* 2007; **282**(28): 20221-9.
34. Belcher JD, Chen C, Nguyen J, et al. Heme triggers TLR4 signaling leading to endothelial cell activation and vaso-occlusion in murine sickle cell disease. *Blood* 2014; **123**(3): 377-90.
35. Piazza M, Damore G, Costa B, Gioannini TL, Weiss JP, Peri F. Hemin and a metabolic derivative coprohemin modulate the TLR4 pathway differently through different molecular targets. *Innate immunity* 2011; **17**(3): 293-301.
36. Kwon MS, Woo SK, Kurland DB, et al. Methemoglobin is an endogenous toll-like receptor 4 ligand-relevance to subarachnoid hemorrhage. *Int J Mol Sci* 2015; **16**(3): 5028-46.
37. Lin S, Yin Q, Zhong Q, et al. Heme activates TLR4-mediated inflammatory injury via MyD88/TRIF signaling pathway in intracerebral hemorrhage. *J Neuroinflammation* 2012; **9**: 46.
38. Tschopp J, Schroder K. NLRP3 inflammasome activation: The convergence of multiple signalling pathways on ROS production? *Nat Rev Immunol* 2010; **10**(3): 210-5.
39. Viviani B, Bartesaghi S, Gardoni F, et al. Interleukin-1beta enhances NMDA receptor-mediated intracellular calcium increase through activation of the Src family of kinases. *J Neurosci* 2003; **23**(25): 8692-700.
40. Thornton P, Pinteaux E, Gibson RM, Allan SM, Rothwell NJ. Interleukin-1-induced neurotoxicity is mediated by glia and requires caspase activation and free radical release. *Journal of neurochemistry* 2006; **98**(1): 258-66.
41. Thornton P, Pinteaux E, Allan SM, Rothwell NJ. Matrix metalloproteinase-9 and urokinase plasminogen activator mediate interleukin-1-induced neurotoxicity. *Mol Cell Neurosci* 2008; **37**(1): 135-42.
42. McColl BW, Rothwell NJ, Allan SM. Systemic inflammatory stimulus potentiates the acute phase and CXC chemokine responses to experimental stroke and exacerbates brain damage via interleukin-1- and neutrophil-dependent mechanisms. *J Neurosci* 2007; **27**(16): 4403-12.
43. McColl BW, Rothwell NJ, Allan SM. Systemic inflammation alters the kinetics of cerebrovascular tight junction disruption after experimental stroke in mice. *J Neurosci* 2008; **28**(38): 9451-62.

44. Allen C, Thornton P, Denes A, et al. Neutrophil cerebrovascular transmigration triggers rapid neurotoxicity through release of proteases associated with decondensed DNA. *J Immunol* 2012; **189**(1): 381-92.
45. Nguyen HX, O'Barr TJ, Anderson AJ. Polymorphonuclear leukocytes promote neurotoxicity through release of matrix metalloproteinases, reactive oxygen species, and TNF-alpha. *Journal of neurochemistry* 2007; **102**(3): 900-12.
46. Pluta RM. Delayed cerebral vasospasm and nitric oxide: review, new hypothesis, and proposed treatment. *Pharmacol Ther* 2005; **105**(1): 23-56.
47. Eich RF, Li T, Lemon DD, et al. Mechanism of NO-induced oxidation of myoglobin and hemoglobin. *Biochemistry* 1996; **35**(22): 6976-83.
48. Azarov I, He X, Jeffers A, et al. Rate of nitric oxide scavenging by hemoglobin bound to haptoglobin. *Nitric Oxide* 2008; **18**(4): 296-302.
49. Eisenhut M. Vasospasm in cerebral inflammation. *Int J Inflam* 2014; **2014**: 509707.
50. Compeer MG, Janssen GM, De Mey JG. Endothelin-1 and endothelin-2 initiate and maintain contractile responses by different mechanisms in rat mesenteric and cerebral arteries. *Br J Pharmacol* 2013; **170**(6): 1199-209.
51. Pluta RM, Boock RJ, Afshar JK, et al. Source and cause of endothelin-1 release into cerebrospinal fluid after subarachnoid hemorrhage. *Journal of neurosurgery* 1997; **87**(2): 287-93.
52. Reeder BJ. The redox activity of hemoglobins: from physiologic functions to pathologic mechanisms. *Antioxid Redox Signal* 2010; **13**(7): 1087-123.
53. Sakamoto M, Takaki E, Yamashita K, et al. Nonenzymatic derived lipid peroxide, 8-iso-PGF2 alpha, participates in the pathogenesis of delayed cerebral vasospasm in a canine SAH model. *Neurol Res* 2002; **24**(3): 301-6.
54. Lin CL, Hsu YT, Lin TK, et al. Increased levels of F2-isoprostanes following aneurysmal subarachnoid hemorrhage in humans. *Free Radic Biol Med* 2006; **40**(8): 1466-73.
55. Kristiansen M, Graversen JH, Jacobsen C, et al. Identification of the haemoglobin scavenger receptor. *Nature* 2001; **409**(6817): 198-201.
56. Theilgaard-Monch K, Jacobsen LC, Nielsen MJ, et al. Haptoglobin is synthesized during granulocyte differentiation, stored in specific granules, and released by neutrophils in response to activation. *Blood* 2006; **108**(1): 353-61.
57. Oliviero S, Morrone G, Cortese R. The human haptoglobin gene: transcriptional regulation during development and acute phase induction. *Embo j* 1987; **6**(7): 1905-12.
58. Zhao X, Song S, Sun G, et al. Neuroprotective role of haptoglobin after intracerebral hemorrhage. *J Neurosci* 2009; **29**(50): 15819-27.
59. Andersen CB, Torvund-Jensen M, Nielsen MJ, et al. Structure of the haptoglobin-haemoglobin complex. *Nature* 2012; **489**(7416): 456-9.
60. Maeda N, Yang F, Barnett DR, Bowman BH, Smithies O. Duplication within the haptoglobin Hp2 gene. *Nature* 1984; **309**(5964): 131-5.
61. Smithies O. Zone electrophoresis in starch gels: group variations in the serum proteins of normal human adults. *Biochem J* 1955; **61**(4): 629-41.
62. Langlois MR, Delanghe JR. Biological and clinical significance of haptoglobin polymorphism in humans. *Clin Chem* 1996; **42**(10): 1589-600.
63. Boettger LM, Salem RM, Handsaker RE, et al. Recurring exon deletions in the HP (haptoglobin) gene contribute to lower blood cholesterol levels. *Nature genetics* 2016; **48**(4): 359-66.
64. Koda Y, Soejima M, Yoshioka N, Kimura H. The Haptoglobin-Gene Deletion Responsible for Anhaptoglobinemia. *The American Journal of Human Genetics* 1998; **62**(2): 245-52.
65. Froguel P, Ndiaye NC, Bonnefond A, et al. A genome-wide association study identifies rs2000999 as a strong genetic determinant of circulating haptoglobin levels. *PLoS One* 2012; **7**(3): e32327.
66. Maeda N. DNA polymorphisms in the controlling region of the human haptoglobin genes: a molecular explanation for the haptoglobin 2-1 modified phenotype. *Am J Hum Genet* 1991; **49**(1): 158-66.

67. Teye K, Quaye IK, Koda Y, et al. A-61C and C-101G Hp gene promoter polymorphisms are, respectively, associated with ahaptoglobinaemia and hypohaptoglobinaemia in Ghana. *Clin Genet* 2003; **64**(5): 439-43.
68. Grant DJ, Maeda N. A base substitution in the promoter associated with the human haptoglobin 2-1 modified phenotype decreases transcriptional activity and responsiveness to interleukin-6 in human hepatoma cells. *Am J Hum Genet* 1993; **52**(5): 974-80.
69. Soejima M, Sagata N, Komatsu N, et al. Genetic factors associated with serum haptoglobin level in a Japanese population. *Clin Chim Acta* 2014; **433**: 54-7.
70. Connell GE, Smithies O. Human haptoglobins: estimation and purification. *Biochem J* 1959; **72**(1): 115-21.
71. Gutteridge JM. The antioxidant activity of haptoglobin towards haemoglobin-stimulated lipid peroxidation. *Biochim Biophys Acta* 1987; **917**(2): 219-23.
72. Banerjee S, Jia Y, Siburt CJ, et al. Haptoglobin alters oxygenation and oxidation of hemoglobin and decreases propagation of peroxide-induced oxidative reactions. *Free Radic Biol Med* 2012; **53**(6): 1317-26.
73. Melamed-Frank M, Lache O, Enav BI, et al. Structure-function analysis of the antioxidant properties of haptoglobin. *Blood* 2001; **98**(13): 3693-8.
74. Cooper CE, Schaer DJ, Buehler PW, et al. Haptoglobin binding stabilizes hemoglobin ferryl iron and the globin radical on tyrosine beta145. *Antioxid Redox Signal* 2013; **18**(17): 2264-73.
75. Buehler PW, Abraham B, Vallelian F, et al. Haptoglobin preserves the CD163 hemoglobin scavenger pathway by shielding hemoglobin from peroxidative modification. *Blood* 2009; **113**(11): 2578-86.
76. Bowman BH, Kurosky A. Haptoglobin: the evolutionary product of duplication, unequal crossing over, and point mutation. *Adv Hum Genet* 1982; **12**: 189-261, 453-4.
77. Asleh R, Guetta J, Kalet-Litman S, Miller-Lotan R, Levy AP. Haptoglobin genotype- and diabetes-dependent differences in iron-mediated oxidative stress in vitro and in vivo. *Circ Res* 2005; **96**(4): 435-41.
78. Lipiski M, Deuel JW, Baek JH, Engelsberger WR, Buehler PW, Schaer DJ. Human Hp1-1 and Hp2-2 Phenotype-Specific Haptoglobin Therapeutics Are Both Effective In Vitro and in Guinea Pigs to Attenuate Hemoglobin Toxicity. *Antioxidants & Redox Signaling* 2013; **19**(14): 1619-33.
79. Okazakia T, Yanagisawa Y, Nagai T. Analysis of the affinity of each haptoglobin polymer for hemoglobin by two-dimensional affinity electrophoresis. *Clinica Chimica Acta* 1997; **258**(2): 137-44.
80. Mollan TL, Jia Y, Banerjee S, et al. Redox properties of human hemoglobin in complex with fractionated dimeric and polymeric human haptoglobin. *Free Radical Biology and Medicine* 2014; **69**(0): 265-77.
81. Bamm VV, Tsemakhovich VA, Shaklai M, Shaklai N. Haptoglobin Phenotypes Differ in Their Ability To Inhibit Heme Transfer from Hemoglobin to LDL. *Biochemistry* 2004; **43**(13): 3899-906.
82. Schaer CA, Vallelian F, Imhof A, Schoedon G, Schaer DJ. CD163-expressing monocytes constitute an endotoxin-sensitive Hb clearance compartment within the vascular system. *J Leukoc Biol* 2007; **82**(1): 106-10.
83. Van den Heuvel MM, Tensen CP, van As JH, et al. Regulation of CD 163 on human macrophages: cross-linking of CD163 induces signaling and activation. *Journal of Leukocyte Biology* 1999; **66**(5): 858-66.
84. Asleh R, Marsh S, Shilkrut M, et al. Genetically determined heterogeneity in hemoglobin scavenging and susceptibility to diabetic cardiovascular disease. *Circ Res* 2003; **92**(11): 1193-200.
85. Philippidis P, Mason JC, Evans BJ, et al. Hemoglobin scavenger receptor CD163 mediates interleukin-10 release and heme oxygenase-1 synthesis: antiinflammatory monocyte-macrophage responses in vitro, in resolving skin blisters in vivo, and after cardiopulmonary bypass surgery. *Circ Res* 2004; **94**(1): 119-26.
86. Schaer CA, Schoedon G, Imhof A, Kurrer MO, Schaer DJ. Constitutive Endocytosis of CD163 Mediates Hemoglobin-Heme Uptake and Determines the Noninflammatory and Protective Transcriptional Response of Macrophages to Hemoglobin. *Circulation Research* 2006; **99**(9): 943-50.

87. Kumar S, Bandyopadhyay U. Free heme toxicity and its detoxification systems in human. *Toxicol Lett* 2005; **157**(3): 175-88.
88. Morgan WT, Liem HH, Sutor RP, Muller-Ebergard U. Transfer of heme from heme-albumin to hemopexin. *Biochim Biophys Acta* 1976; **444**(2): 435-45.
89. Hrkal Z, Muller-Eberhard U. Partial characterization of the heme-binding serum glycoproteins rabbit and human hemopexin. *Biochemistry* 1971; **10**(10): 1746-50.
90. Smith A, Hunt RC. Hemopexin joins transferrin as representative members of a distinct class of receptor-mediated endocytic transport systems. *Eur J Cell Biol* 1990; **53**(2): 234-45.
91. Hvidberg V, Maniecki MB, Jacobsen C, Hojrup P, Moller HJ, Moestrup SK. Identification of the receptor scavenging hemopexin-heme complexes. *Blood* 2005; **106**(7): 2572-9.
92. Paoli M, Anderson BF, Baker HM, Morgan WT, Smith A, Baker EN. Crystal structure of hemopexin reveals a novel high-affinity heme site formed between two beta-propeller domains. *Nat Struct Biol* 1999; **6**(10): 926-31.
93. Gutteridge JM, Smith A. Antioxidant protection by haemopexin of haem-stimulated lipid peroxidation. *Biochem J* 1988; **256**(3): 861-5.
94. Li RC, Saleem S, Zhen G, et al. Heme-hemopexin complex attenuates neuronal cell death and stroke damage. *Journal of cerebral blood flow and metabolism : official journal of the International Society of Cerebral Blood Flow and Metabolism* 2009; **29**(5): 953-64.
95. Morris CM, Candy JM, Edwardson JA, Bloxham CA, Smith A. Evidence for the localization of haemopexin immunoreactivity in neurones in the human brain. *Neuroscience letters* 1993; **149**(2): 141-4.
96. Tolosano E, Cutufia MA, Hirsch E, Silengo L, Altruda F. Specific expression in brain and liver driven by the hemopexin promoter in transgenic mice. *Biochem Biophys Res Commun* 1996; **218**(3): 694-703.
97. Herz J, Strickland DK. LRP: a multifunctional scavenger and signaling receptor. *The Journal of clinical investigation* 2001; **108**(6): 779-84.
98. Chen-Roetling J, Li Z, Regan RF. Hemoglobin neurotoxicity is attenuated by inhibitors of the protein kinase CK2 independent of heme oxygenase activity. *Current neurovascular research* 2008; **5**(3): 193-8.
99. Ono S, Komuro T, Macdonald RL. Heme oxygenase-1 gene therapy for prevention of vasospasm in rats. *Journal of neurosurgery* 2002; **96**(6): 1094-102.
100. Suzuki H, Kanamaru K, Tsunoda H, et al. Heme oxygenase-1 gene induction as an intrinsic regulation against delayed cerebral vasospasm in rats. *The Journal of clinical investigation* 1999; **104**(1): 59-66.
101. Schallner N, Pandit R, LeBlanc R, 3rd, et al. Microglia regulate blood clearance in subarachnoid hemorrhage by heme oxygenase-1. *The Journal of clinical investigation* 2015; **125**(7): 2609-25.
102. Galea J, Cruickshank G, Teeling JL, et al. The intrathecal CD163-haptoglobin–hemoglobin scavenging system in subarachnoid hemorrhage. *Journal of neurochemistry* 2012; **121**(5): 785-92.
103. Galea I, Felton LM, Waters S, van Rooijen N, Perry VH, Newman TA. Immune-to-brain signalling: the role of cerebral CD163-positive macrophages. *Neuroscience letters* 2008; **448**(1): 41-6.
104. Galea I, Palin K, Newman TA, Van Rooijen N, Perry VH, Boche D. Mannose receptor expression specifically reveals perivascular macrophages in normal, injured, and diseased mouse brain. *Glia* 2005; **49**(3): 375-84.
105. Etzerodt A, Rasmussen MR, Svendsen P, et al. Structural basis for inflammation-driven shedding of CD163 ectodomain and tumor necrosis factor-alpha in macrophages. *J Biol Chem* 2014; **289**(2): 778-88.
106. Garland P, Durnford AJ, Okemefuna AI, et al. Heme-Hemopexin Scavenging Is Active in the Brain and Associates With Outcome After Subarachnoid Hemorrhage. *Stroke* 2016; **47**(3): 872-6.
107. Borsody M, Burke A, Coplin W, Miller-Lotan R, Levy A. Haptoglobin and the development of cerebral artery vasospasm after subarachnoid hemorrhage. *Neurology* 2006; **66**(5): 634-40.

108. Ohnishi H, Iihara K, Kaku Y, et al. Haptoglobin phenotype predicts cerebral vasospasm and clinical deterioration after aneurysmal subarachnoid hemorrhage. *J Stroke Cerebrovasc Dis* 2013; **22**(4): 520-6.
109. Kantor E, Bayir H, Ren D, et al. Haptoglobin genotype and functional outcome after aneurysmal subarachnoid hemorrhage. *Journal of neurosurgery* 2014; **120**(2): 386-90.
110. Leclerc JL, Blackburn S, Neal D, et al. Haptoglobin phenotype predicts the development of focal and global cerebral vasospasm and may influence outcomes after aneurysmal subarachnoid hemorrhage. *Proc Natl Acad Sci U S A* 2015.
111. Murthy SB, Caplan J, Levy AP, et al. Haptoglobin 2-2 Genotype Is Associated With Cerebral Salt Wasting Syndrome in Aneurysmal Subarachnoid Hemorrhage. *Neurosurgery* 2016; **78**(1): 71-6.
112. Gaastra B, Glazier J, Bulters D, Galea I. Haptoglobin Genotype and Outcome after Subarachnoid Haemorrhage: New Insights from a Meta-Analysis. *Oxid Med Cell Longev* 2017; **2017**: 6747940.
113. Kim BJ, Kim Y, Kim SE, Jeon JP. Study of correlation between Hp alpha1 expression of haptoglobin2-1 and clinical course in aneurysmal subarachnoid hemorrhage. *World Neurosurg* 2018.
114. Etzerodt A, Kjolby M, Nielsen MJ, Maniecki M, Svendsen P, Moestrup SK. Plasma clearance of hemoglobin and haptoglobin in mice and effect of CD163 gene targeting disruption. *Antioxid Redox Signal* 2013; **18**(17): 2254-63.
115. Chaichana KL, Levy AP, Miller-Lotan R, Shakur S, Tamargo RJ. Haptoglobin 2-2 genotype determines chronic vasospasm after experimental subarachnoid hemorrhage. *Stroke* 2007; **38**(12): 3266-71.
116. Guetta J, Strauss M, Levy NS, Fahoum L, Levy AP. Haptoglobin genotype modulates the balance of Th1/Th2 cytokines produced by macrophages exposed to free hemoglobin. *Atherosclerosis* 2007; **191**(1): 48-53.
117. Yang H, Wang H, Wang Y, et al. The haptoglobin beta subunit sequesters HMGB1 toxicity in sterile and infectious inflammation. *Journal of Internal Medicine* 2017; **282**(1): 76-93.
118. Yang H, Wang H, Levine YA, et al. Identification of CD163 as an antiinflammatory receptor for HMGB1-haptoglobin complexes. *JCI Insight* 2016; **1**(7).
119. Titova E, Ostrowski RP, Zhang JH, Tang J. Experimental models of subarachnoid hemorrhage for studies of cerebral vasospasm. *Neurol Res* 2009; **31**(6): 568-81.
120. Sabri M, Jeon H, Ai J, et al. Anterior circulation mouse model of subarachnoid hemorrhage. *Brain research* 2009; **1295**(0): 179-85.
121. Kamii H, Kato I, Kinouchi H, et al. Amelioration of vasospasm after subarachnoid hemorrhage in transgenic mice overexpressing CuZn-superoxide dismutase. *Stroke* 1999; **30**(4): 867-71; discussion 72.
122. Parra A, McGirt MJ, Sheng H, Laskowitz DT, Pearlstein RD, Warner DS. Mouse model of subarachnoid hemorrhage associated cerebral vasospasm: methodological analysis. *Neurol Res* 2002; **24**(5): 510-6.
123. Matz PG, Fujimura M, Chan PH. Subarachnoid hemolysate produces DNA fragmentation in a pattern similar to apoptosis in mouse brain. *Brain research* 2000; **858**(2): 312-9.
124. Lin CL, Calisaneller T, Ukita N, Dumont AS, Kassell NF, Lee KS. A murine model of subarachnoid hemorrhage-induced cerebral vasospasm. *Journal of neuroscience methods* 2003; **123**(1): 89-97.
125. Hanafy KA. The role of microglia and the TLR4 pathway in neuronal apoptosis and vasospasm after subarachnoid hemorrhage. *Journal of Neuroinflammation* 2013; **10**: 83-.
126. Nonaka T, Watanabe S, Chigasaki H, Miyaoka M, Ishii S. Etiology and Treatment of Vasospasm following Subarachnoid Hemorrhage. *Neurologia medico-chirurgica* 1979; **19**(1): 53-60.
127. Cossu G, Messerer M, Oddo M, Daniel RT. To look beyond vasospasm in aneurysmal subarachnoid haemorrhage. *BioMed Research International* 2014; **2014**.

128. Boretti FS, Buehler PW, D'Agnillo F, et al. Sequestration of extracellular hemoglobin within a haptoglobin complex decreases its hypertensive and oxidative effects in dogs and guinea pigs. *The Journal of clinical investigation* 2009; **119**(8): 2271-80.
129. Fisher CM, Kistler JP, Davis JM. Relation of cerebral vasospasm to subarachnoid hemorrhage visualized by computerized tomographic scanning. *Neurosurgery* 1980; **6**(1): 1-9.
130. Teasdale G, Jennett B. ASSESSMENT OF COMA AND IMPAIRED CONSCIOUSNESS. *The Lancet* 1974; **304**(7872): 81-4.
131. Jennett B, Bond M. ASSESSMENT OF OUTCOME AFTER SEVERE BRAIN DAMAGE: A Practical Scale. *The Lancet* 1975; **305**(7905): 480-4.
132. Farrell B, Godwin J, Richards S, Warlow C. The United Kingdom transient ischaemic attack (UK-TIA) aspirin trial: final results. *J Neurol Neurosurg Psychiatry* 1991; **54**(12): 1044-54.
133. Rankin J. Cerebral vascular accidents in patients over the age of 60. II. Prognosis. *Scott Med J* 1957; **2**(5): 200-15.
134. Quinn TJ, Dawson J, Walters MR, Lees KR. Reliability of the modified Rankin Scale: a systematic review. *Stroke* 2009; **40**(10): 3393-5.
135. Vora YY, Suarez-Almazor M, Steinke DE, Martin ML, Findlay JM. Role of transcranial Doppler monitoring in the diagnosis of cerebral vasospasm after subarachnoid hemorrhage. *Neurosurgery* 1999; **44**(6): 1237-47; discussion 47-8.
136. Teasdale GM, Drake CG, Hunt W, et al. A universal subarachnoid hemorrhage scale: report of a committee of the World Federation of Neurosurgical Societies. *J Neurol Neurosurg Psychiatry* 1988; **51**(11): 1457.
137. Koch W, Latz W, Eichinger M, et al. Genotyping of the Common Haptoglobin Hp 1/2 Polymorphism Based on PCR. *Clinical Chemistry* 2002; **48**(9): 1377-82.
138. Soejima M, Koda Y. TaqMan-based real-time PCR for genotyping common polymorphisms of haptoglobin (HP1 and HP2). *Clin Chem* 2008; **54**(11): 1908-13.
139. Deacon RM, Rawlins JN. T-maze alternation in the rodent. *Nat Protoc* 2006; **1**(1): 7-12.
140. Deacon RM. Burrowing in rodents: a sensitive method for detecting behavioral dysfunction. *Nat Protoc* 2006; **1**(1): 118-21.
141. Simon P, Dupuis R, Costentin J. Thigmotaxis as an index of anxiety in mice. Influence of dopaminergic transmissions. *Behav Brain Res* 1994; **61**(1): 59-64.
142. Aum DJ, Vellimana AK, Singh I, et al. A novel fluorescent imaging technique for assessment of cerebral vasospasm after experimental subarachnoid hemorrhage. *Sci Rep* 2017; **7**(1): 9126.
143. Cunningham C, Deacon R, Wells H, et al. Synaptic changes characterize early behavioural signs in the ME7 model of murine prion disease. *The European journal of neuroscience* 2003; **17**(10): 2147-55.
144. Gruys E, Toussaint MJM, Niewold TA, Koopmans SJ. Acute phase reaction and acute phase proteins. *Journal of Zhejiang University Science B* 2005; **6**(11): 1045-56.
145. Rodriguez S, Williams DM, Guthrie PA, et al. Molecular and population analysis of natural selection on the human haptoglobin duplication. *Ann Hum Genet* 2012; **76**(5): 352-62.
146. Louagie H, Delanghe J, Desombere I, De Buyzere M, Hauser P, Leroux-Roels G. Haptoglobin polymorphism and the immune response after hepatitis B vaccination. *Vaccine* 1993; **11**(12): 1188-90.
147. Langlois M, Delanghe J, De Buyzere M. Relation between serum IgA concentration and haptoglobin type. *Clinical Chemistry* 1996; **42**(10): 1722.
148. Kasvosve I, Gomo ZAR, Gangaidzo IT, et al. Reference range of serum haptoglobin is haptoglobin phenotype-dependent in blacks. *Clinica Chimica Acta* 2000; **296**(1–2): 163-70.
149. Park KU, Song J, Kim JQ. Haptoglobin genotypic distribution (including Hp0 allele) and associated serum haptoglobin concentrations in Koreans. *J Clin Pathol* 2004; **57**(10): 1094-5.
150. Na N, Ouyang J, Taes YE, Delanghe JR. Serum free hemoglobin concentrations in healthy individuals are related to haptoglobin type. *Clin Chem* 2005; **51**(9): 1754-5.
151. Fowkes FJ, Imrie H, Migot-Nabias F, et al. Association of haptoglobin levels with age, parasite density, and haptoglobin genotype in a malaria-endemic area of Gabon. *Am J Trop Med Hyg* 2006; **74**(1): 26-30.

152. Imrie H, Fowkes FJ, Michon P, et al. Haptoglobin levels are associated with haptoglobin genotype and alpha+ -Thalassemia in a malaria-endemic area. *Am J Trop Med Hyg* 2006; **74**(6): 965-71.
153. Márquez L, Shen C, Cleynen I, et al. Effects of haptoglobin polymorphisms and deficiency on susceptibility to inflammatory bowel disease and on severity of murine colitis. *Gut* 2012; **61**(4): 528-34.
154. Bjornsson E, Helgason H, Halldorsson G, et al. A rare splice donor mutation in the haptoglobin gene associates with blood lipid levels and coronary artery disease. *Human molecular genetics* 2017; **26**(12): 2364-76.
155. von Elm E, Altman DG, Egger M, Pocock SJ, Gøtzsche PC, Vandenbroucke JP. The Strengthening the Reporting of Observational Studies in Epidemiology (STROBE) statement: guidelines for reporting observational studies. *The Lancet* 2007; **370**(9596): 1453-7.
156. Kirkpatrick PJ, Turner CL, Smith C, Hutchinson PJ, Murray GD. Simvastatin in aneurysmal subarachnoid haemorrhage (STASH): a multicentre randomised phase 3 trial. *Lancet Neurol* 2014; **13**(7): 666-75.
157. Lantigua H, Ortega-Gutierrez S, Schmidt JM, et al. Subarachnoid hemorrhage: who dies, and why? *Critical Care* 2015; **19**(1): 309.
158. Lai L, Morgan MK. Incidence of subarachnoid haemorrhage: an Australian national hospital morbidity database analysis. *Journal of clinical neuroscience : official journal of the Neurosurgical Society of Australasia* 2012; **19**(5): 733-9.
159. Brilstra EH, Rinkel GJ, Algra A, van Gijn J. Rebleeding, secondary ischemia, and timing of operation in patients with subarachnoid hemorrhage. *Neurology* 2000; **55**(11): 1656-60.
160. Germanwala AV, Huang J, Tamargo RJ. Hydrocephalus after aneurysmal subarachnoid hemorrhage. *Neurosurgery clinics of North America* 2010; **21**(2): 263-70.
161. Khan AU, Dulhanty L, Vail A, Tyrrell P, Galea J, Patel HC. Impact of specialist neurovascular care in subarachnoid haemorrhage. *Clinical neurology and neurosurgery* 2015; **133**: 55-60.
162. Molyneux AJ, Birks J, Clarke A, Sneade M, Kerr RSC. The durability of endovascular coiling versus neurosurgical clipping of ruptured cerebral aneurysms: 18 year follow-up of the UK cohort of the International Subarachnoid Aneurysm Trial (ISAT). *Lancet* 2015; **385**(9969): 691-7.
163. Zacharia BE, Hickman ZL, Grobelny BT, et al. Epidemiology of aneurysmal subarachnoid hemorrhage. *Neurosurg Clin N Am* 2010; **21**(2): 221-33.
164. Schmidt JM, Wartenberg KE, Fernandez A, et al. Frequency and clinical impact of asymptomatic cerebral infarction due to vasospasm after subarachnoid hemorrhage. *J Neurosurg* 2008; **109**(6): 1052-9.
165. Rodriguez S, Gaunt TR, Day IN. Hardy-Weinberg equilibrium testing of biological ascertainment for Mendelian randomization studies. *Am J Epidemiol* 2009; **169**(4): 505-14.
166. Gaunt TR, Rodriguez S, Day IN. Cubic exact solutions for the estimation of pairwise haplotype frequencies: implications for linkage disequilibrium analyses and a web tool 'CubeX'. *BMC Bioinformatics* 2007; **8**: 428.
167. Asleh R, Marsh S, Shilkrut M, et al. Genetically determined heterogeneity in hemoglobin scavenging and susceptibility to diabetic cardiovascular disease. *Circulation research* 2003; **92**(11): 1193-200.
168. Kristiansen M, Graversen JH, Jacobsen C, et al. Identification of the haemoglobin scavenger receptor. *Nature* 2001; **409**(6817): 198-201.
169. Lipiski M, Deuel JW, Baek JH, Engelsberger WR, Buehler PW, Schaer DJ. Human Hp1-1 and Hp2-2 phenotype-specific haptoglobin therapeutics are both effective in vitro and in guinea pigs to attenuate hemoglobin toxicity. *Antioxid Redox Signal* 2013; **19**(14): 1619-33.
170. Galea J, Cruickshank G, Teeling JL, et al. The intrathecal CD163-haptoglobin-hemoglobin scavenging system in subarachnoid hemorrhage. *J Neurochem* 2012; **121**(5): 785-92.
171. Durnford A, Dunbar J, Galea J, et al. Haemoglobin scavenging after subarachnoid haemorrhage. *Acta Neurochir Suppl* 2015; **120**: 51-4.
172. Andersson PB, Perry VH, Gordon† S. The acute inflammatory response to lipopolysaccharide in cns parenchyma differs from that in other body tissues. *Neuroscience* 1992; **48**(1): 169-86.

173. Muralidharan R. External ventricular drains: Management and complications. *Surgical Neurology International* 2015; **6**(Suppl 6): S271-S4.
174. Vallelian F, Pimenova T, Pereira CP, et al. The reaction of hydrogen peroxide with hemoglobin induces extensive alpha-globin crosslinking and impairs the interaction of hemoglobin with endogenous scavenger pathways. *Free Radic Biol Med* 2008; **45**(8): 1150-8.
175. Dóczi T. The pathogenetic and prognostic significance of blood-brain barrier damage at the acute stage of aneurysmal subarachnoid haemorrhage. Clinical and experimental studies. *Acta neurochirurgica* 1985; **77**(3): 110-32.
176. Germano A, d'Avella D, Imperatore C, Caruso G, Tomasello F. Time-course of blood-brain barrier permeability changes after experimental subarachnoid haemorrhage. *Acta neurochirurgica* 2000; **142**(5): 575-80; discussion 80-1.
177. Scholler K, Trinkl A, Klopotowski M, et al. Characterization of microvascular basal lamina damage and blood-brain barrier dysfunction following subarachnoid hemorrhage in rats. *Brain Res* 2007; **1142**: 237-46.
178. Link H, Tibbling G. Principles of albumin and IgG analyses in neurological disorders. II. Relation of the concentration of the proteins in serum and cerebrospinal fluid. *Scandinavian Journal of Clinical and Laboratory Investigation* 1977; **37**(5): 391-6.
179. Jia Y, Buehler PW, Boykins RA, Venable RM, Alayash AI. Structural basis of peroxide-mediated changes in human hemoglobin: a novel oxidative pathway. *J Biol Chem* 2007; **282**(7): 4894-907.
180. Garton TP, He Y, Garton HJ, Keep RF, Xi G, Strahle JM. Hemoglobin-induced neuronal degeneration in the hippocampus after neonatal intraventricular hemorrhage. *Brain research* 2016; **1635**: 86-94.
181. Zolnourian A, Galea I, Bulters D. Neuroprotective Role of the Nrf2 Pathway in Subarachnoid Haemorrhage and Its Therapeutic Potential. *Oxidative Medicine and Cellular Longevity* 2019; **2019**: 21.
182. Thimmulappa RK, Mai KH, Srisuma S, Kensler TW, Yamamoto M, Biswal S. Identification of Nrf2-regulated genes induced by the chemopreventive agent sulforaphane by oligonucleotide microarray. *Cancer Res* 2002; **62**(18): 5196-203.
183. Prunell GF, Mathiesen T, Diemer NH, Svendgaard NA. Experimental subarachnoid hemorrhage: subarachnoid blood volume, mortality rate, neuronal death, cerebral blood flow, and perfusion pressure in three different rat models. *Neurosurgery* 2003; **52**(1): 165-75; discussion 75-6.
184. Weller RO, Sharp MM, Christodoulides M, Carare RO, Mollgard K. The meninges as barriers and facilitators for the movement of fluid, cells and pathogens related to the rodent and human CNS. *Acta Neuropathol* 2018; **135**(3): 363-85.
185. Coles JA, Myburgh E, Brewer JM, McMenamin PG. Where are we? The anatomy of the murine cortical meninges revisited for intravital imaging, immunology, and clearance of waste from the brain. *Progress in Neurobiology* 2017; **156**: 107-48.
186. Barkus C, Dawson LA, Sharp T, Bannerman DM. GluN1 hypomorph mice exhibit wide-ranging behavioral alterations. *Genes Brain Behav* 2012; **11**(3): 342-51.
187. Digre KB, Brennan KC. Shedding Light on Photophobia. *Journal of neuro-ophthalmology : the official journal of the North American Neuro-Ophthalmology Society* 2012; **32**(1): 68-81.
188. Milner E, Johnson AW, Nelson JW, et al. HIF-1alpha Mediates Isoflurane-Induced Vascular Protection in Subarachnoid Hemorrhage. *Annals of clinical and translational neurology* 2015; **2**(4): 325-37.
189. Marin J, Lobato RD, Rico ML, Salaices M, Benitez J. Effect of pentobarbital on the reactivity of isolated human cerebral arteries. *Journal of neurosurgery* 1981; **54**(4): 521-4.
190. Nishiwada M, Nakamura K, Hatano Y, Mori K. The relaxing effects of barbiturates in vascular smooth muscle of rat aorta. *J Anesth* 1991; **5**(4): 380-7.
191. Ohsawa K, Imai Y, Sasaki Y, Kohsaka S. Microglia/macrophage-specific protein Iba1 binds to fimbrin and enhances its actin-bundling activity. *Journal of neurochemistry* 2004; **88**(4): 844-56.
192. Al-Khindi T, Macdonald RL, Schweizer TA. Cognitive and functional outcome after aneurysmal subarachnoid hemorrhage. *Stroke* 2010; **41**(8): e519-36.

193. Turan N, Miller BA, Heider RA, et al. Neurobehavioral testing in subarachnoid hemorrhage: A review of methods and current findings in rodents. *J Cereb Blood Flow Metab* 2017; **37**(11): 3461-74.
194. Fanizzi C, Sauerbeck AD, Gangolli M, Zipfel GJ, Brody DL, Kummer TT. Minimal Long-Term Neurobehavioral Impairments after Endovascular Perforation Subarachnoid Hemorrhage in Mice. *Sci Rep* 2017; **7**(1): 7569.
195. Boyko M, Azab AN, Kuts R, et al. The neuro-behavioral profile in rats after subarachnoid hemorrhage. *Brain Res* 2013; **1491**: 109-16.
196. Liu Y, Qiu J, Wang Z, et al. Dimethylfumarate alleviates early brain injury and secondary cognitive deficits after experimental subarachnoid hemorrhage via activation of Keap1-Nrf2-ARE system. *Journal of neurosurgery* 2015; **123**(4): 915-23.
197. Jeon H, Ai J, Sabri M, Tariq A, Macdonald RL. Learning deficits after experimental subarachnoid hemorrhage in rats. *Neuroscience* 2010; **169**(4): 1805-14.
198. Milner E, Holtzman JC, Friess S, et al. Endovascular perforation subarachnoid hemorrhage fails to cause Morris water maze deficits in the mouse. *Journal of cerebral blood flow and metabolism : official journal of the International Society of Cerebral Blood Flow and Metabolism* 2014; **34**(9).
199. Kooijman E, Nijboer CH, van Velthoven CT, et al. Long-term functional consequences and ongoing cerebral inflammation after subarachnoid hemorrhage in the rat. *PLoS One* 2014; **9**(6): e90584.
200. Liu R, Cao S, Hua Y, Keep RF, Huang Y, Xi G. CD163 Expression in Neurons After Experimental Intracerebral Hemorrhage. *Stroke* 2017; **48**(5): 1369-75.
201. Boyle JJ, Harrington HA, Piper E, et al. Coronary intraplaque hemorrhage evokes a novel atheroprotective macrophage phenotype. *The American journal of pathology* 2009; **174**(3): 1097-108.
202. Bo Voldby, Erna M. Enevoldsen. Intracranial pressure changes following aneurysm rupture. *Journal of neurosurgery* 1982; **56**(2): 186-96.
203. Macdonald RL, Kassell NF, Mayer S, et al. Clazosentan to overcome neurological ischemia and infarction occurring after subarachnoid hemorrhage (CONSCIOUS-1): randomized, double-blind, placebo-controlled phase 2 dose-finding trial. *Stroke* 2008; **39**(11): 3015-21.
204. Rudick RA, Zirretta DK, Herndon RM. Clearance of albumin from mouse subarachnoid space: a measure of CSF bulk flow. *Journal of neuroscience methods* 1982; **6**(3): 253-9.
205. Naff NJ, Williams MA, Rigamonti D, Keyl PM, Hanley DF. Blood clot resolution in human cerebrospinal fluid: evidence of first-order kinetics. *Neurosurgery* 2001; **49**(3): 614-9; discussion 9-21.
206. Johanson CE, Duncan JA, Klinge PM, Brinker T, Stopa EG, Silverberg GD. Multiplicity of cerebrospinal fluid functions: New challenges in health and disease. *Cerebrospinal Fluid Research* 2008; **5**: 10-.
207. Brinker T, Stopa E, Morrison J, Klinge P. A new look at cerebrospinal fluid circulation. *Fluids and Barriers of the CNS* 2014; **11**: 10-.
208. Krueger B, Carroll CP, Mahoney E, et al. Subarachnoid blood acutely induces spreading depolarizations and early cortical infarction. *Brain* 2017; **140**(10): 2673-90.
209. Scherfler C, Schiefecker AJ, Delazer M, et al. Longitudinal profile of iron accumulation in good-grade subarachnoid hemorrhage. *Annals of clinical and translational neurology* 2016; **3**(10): 781-90.
210. Hassel B, Iversen EG, Fonnum F. Neurotoxicity of albumin in vivo. *Neuroscience letters* 1994; **167**(1-2): 29-32.
211. Kadota E, Nonaka K, Karasuno M, Nishi K, Teramura K, Hashimoto S. Neurotoxicity of serum components, comparison between CA1 and striatum. *Acta neurochirurgica Supplement* 1997; **70**: 141-3.
212. Frigerio F, Frasca A, Weissberg I, et al. Long-lasting pro-ictogenic effects induced in vivo by rat brain exposure to serum albumin in the absence of concomitant pathology. *Epilepsia* 2012; **53**(11): 1887-97.

213. Ralay Ranaivo H, Wainwright MS. Albumin activates astrocytes and microglia through mitogen-activated protein kinase pathways. *Brain research* 2010; **1313**: 222-31.
214. Hooper C, Taylor DL, Pocock JM. Pure albumin is a potent trigger of calcium signalling and proliferation in microglia but not macrophages or astrocytes. *Journal of neurochemistry* 2005; **92**(6): 1363-76.
215. Zille M, Karuppagounder SS, Chen Y, et al. Neuronal Death After Hemorrhagic Stroke In Vitro and In Vivo Shares Features of Ferroptosis and Necroptosis. *Stroke* 2017; **48**(4): 1033-43.
216. Chen-Roetling J, Li Z, Chen M, Awe OO, Regan RF. Heme oxygenase activity and hemoglobin neurotoxicity are attenuated by inhibitors of the MEK/ERK pathway. *Neuropharmacology* 2009; **56**(5): 922-8.
217. Dalton J, Okemefuna A. Haptoglobin. 2012: 321-36.
218. Sasaki T, Hoffmann U, Kobayashi M, et al. Long-Term Cognitive Deficits After Subarachnoid Hemorrhage in Rats. *Neurocritical care* 2016; **25**(2): 293-305.
219. Schaer CA, Deuel JW, Schildknecht D, et al. Haptoglobin Preserves Vascular Nitric Oxide Signaling during Hemolysis. *Am J Respir Crit Care Med* 2016; **193**(10): 1111-22.
220. Hashimoto K, Nomura K, Nakano M, Sasaki T, Kurosawa H. Pharmacological intervention for renal protection during cardiopulmonary bypass. *Heart Vessels* 1993; **8**(4): 203-10.
221. Gando S, Tedo I. The effects of massive transfusion and haptoglobin therapy on hemolysis in trauma patients. *Surg Today* 1994; **24**(9): 785-90.
222. Yamamoto H, Nishikawa S, Yamazaki K, Kudo R. Efficacy of haptoglobin administration in the early postoperative course of patients with a diagnosis of HELLP syndrome. *J Obstet Gynaecol* 2000; **20**(6): 610-1.
223. Andersson U, Tracey KJ. HMGB1 Is a Therapeutic Target for Sterile Inflammation and Infection. *Annual Review of Immunology* 2011; **29**(1): 139-62.
224. Sun Q, Wu W, Hu YC, et al. Early release of high-mobility group box 1 (HMGB1) from neurons in experimental subarachnoid hemorrhage in vivo and in vitro. *J Neuroinflammation* 2014; **11**: 106.
225. Sokol B, Wozniak A, Jankowski R, et al. HMGB1 Level in Cerebrospinal Fluid as a Marker of Treatment Outcome in Patients with Acute Hydrocephalus Following Aneurysmal Subarachnoid Hemorrhage. *J Stroke Cerebrovasc Dis* 2015; **24**(8): 1897-904.
226. Nakahara T, Tsuruta R, Kaneko T, et al. High-Mobility Group Box 1 Protein in CSF of Patients with Subarachnoid Hemorrhage. *Neurocritical care* 2009; **11**(3): 362.
227. Hwang PK, Greer J. Interaction between hemoglobin subunits in the hemoglobin . haptoglobin complex. *J Biol Chem* 1980; **255**(7): 3038-41.
228. Lee S, Nam Y, Koo JY, et al. A small molecule binding HMGB1 and HMGB2 inhibits microglia-mediated neuroinflammation. *Nat Chem Biol* 2014; **10**(12): 1055-60.
229. Spagnuolo MS, Cigliano L, D'Andrea LD, Pedone C, Abrescia P. Assignment of the binding site for haptoglobin on apolipoprotein A-I. *J Biol Chem* 2005; **280**(2): 1193-8.
230. Cigliano L, Pugliese CR, Spagnuolo MS, Palumbo R, Abrescia P. Haptoglobin binds the antiatherogenic protein apolipoprotein E - impairment of apolipoprotein E stimulation of both lecithin:cholesterol acyltransferase activity and cholesterol uptake by hepatocytes. *Febs j* 2009; **276**(21): 6158-71.
231. Spagnuolo MS, Maresca B, La Marca V, et al. Haptoglobin Interacts with Apolipoprotein E and Beta-Amyloid and Influences Their Crosstalk. *ACS Chemical Neuroscience* 2014; **5**(9): 837-47.
232. Mahley RW, Weisgraber KH, Huang Y. Apolipoprotein E: structure determines function, from atherosclerosis to Alzheimer's disease to AIDS. *J Lipid Res* 2009; **50 Suppl**: S183-8.
233. Blau JN, Harris H, Robson EB. Haptoglobins in cerebrospinal fluid. *Clin Chim Acta* 1963; **8**: 202-6.
234. Chamoun V, Zeman A, Blennow K, et al. Haptoglobins as markers of blood–CSF barrier dysfunction: the findings in normal CSF. *Journal of the neurological sciences* 2001; **182**(2): 117-21.
235. Itoh K, Wakabayashi N, Katoh Y, et al. Keap1 represses nuclear activation of antioxidant responsive elements by Nrf2 through binding to the amino-terminal Neh2 domain. *Genes & Development* 1999; **13**(1): 76-86.

236. Zhao XD, Zhou YT, Lu XJ. Sulforaphane enhances the activity of the Nrf2–ARE pathway and attenuates inflammation in OxyHb-induced rat vascular smooth muscle cells. *Inflammation Research* 2013; **62**(9): 857-63.
237. Dinkova-Kostova AT, Holtzclaw WD, Cole RN, et al. Direct evidence that sulfhydryl groups of Keap1 are the sensors regulating induction of phase 2 enzymes that protect against carcinogens and oxidants. *Proc Natl Acad Sci U S A* 2002; **99**(18): 11908-13.
238. Zhang DD, Lo SC, Cross JV, Templeton DJ, Hannink M. Keap1 is a redox-regulated substrate adaptor protein for a Cul3-dependent ubiquitin ligase complex. *Mol Cell Biol* 2004; **24**(24): 10941-53.
239. Lee MY, Kim SY, Choi JS, et al. Upregulation of haptoglobin in reactive astrocytes after transient forebrain ischemia in rats. *Journal of cerebral blood flow and metabolism : official journal of the International Society of Cerebral Blood Flow and Metabolism* 2002; **22**(10): 1176-80.
240. Zhao X, Sun G, Zhang J, et al. Transcription factor Nrf2 protects the brain from damage produced by intracerebral hemorrhage. *Stroke* 2007; **38**(12): 3280-6.
241. Medicine UNLo. clinicaltrials.gov/ct2/show/NCT02614742. ClinicalTrials.gov: US National Library of Medicine; 2017.